

**A STUDY ON REMOVAL OF FLUORIDE AND ARSENIC  
PRESENT IN GROUND WATER OF GOLAGHAT DISTRICT  
OF ASSAM AND ITS PERIPHERAL AREAS**

*by*

**CHAMPA GOGOI**



*Submitted to*

**NAGALAND UNIVERSITY**

*In Partial Fulfillment of the Requirements for Award of the Degree*

*of*

**DOCTOR OF PHILOSOPHY IN CHEMISTRY**

**DEPARTMENT OF CHEMISTRY**

**NAGALAND UNIVERSITY**

**LUMAMI-798627**

**NAGALAND, INDIA**

**2020**

## **DEDICATION**

**To**

**My Beloved Parents**

**Mr. Thaneswar Gogoi (father), Mrs. Bulbuli Gogoi (mother),  
Mr. Tokheswar Neog (father-in-law) & Mrs. Kusum Neog (mother-in-law)**

Who are eagerly waiting for the result of my research work.

## DECLARATION

I, Champa Gogoi, bearing registration No. 711/2016 hereby declare that the content of the thesis entitled ***“A STUDY ON REMOVAL OF FLUORIDE AND ARSENIC PRESENT IN GROUND WATER OF GOLAGHAT DISTRICT OF ASSAM AND ITS PERIPHERAL AREAS”*** is the result of my own research on the subject. I also declare that the contents of this thesis has not been submitted to any other University or Institution in part or full for the award of any degree or diploma.

This is being submitted to Nagaland University for the degree of Doctor of Philosophy in Chemistry.

Place: CSIR-NEIST, Jorhat  
Date:

(Champa Gogoi)

**Dr. Rajib Lochan Goswamee**  
(Former alumni DAAD Germany & CNRS France)  
Senior Principal Scientist & HoD  
Advanced Materials Group, Materials Science and  
Technology Division  
Email: [goswamirl@neist.res.in](mailto:goswamirl@neist.res.in)

## CERTIFICATE

This is to certify that **Mrs Champa Gogoi** was registered as a Research Scholar for Ph.D. (Science) degree in Chemistry in Nagaland University and has been working under my supervision. Her thesis entitled ***“A STUDY ON REMOVAL OF FLUORIDE AND ARSENIC PRESENT IN GROUND WATER OF GOLAGHAT DISTRICT OF ASSAM AND ITS PERIPHERAL AREAS”*** is being forwarded for submission for the Ph.D. (Science) degree of this University. It is certified that she has fulfilled all the requirements according to the rules of Nagaland University regarding investigations embodied in her thesis and I further certify that the contents of this thesis has not been submitted to any other University or Institution in part or full for the award of any degree or diploma.

Place: CSIR-NEIST, Jorhat  
Date:

(**Dr. Rajib Lochan Goswamee**)  
Supervisor



**NAGALAND**



**UNIVERSITY**

*(A Central University Estd. By the Act of Parliament No. 35 of 1989)*

**DEPARTMENT OF CHEMISTRY**

Headquarters: LUMAMI, ZUNHEBOTO DISTRICT-798627 NAGALAND, INDIA

**Prof. Dipak Sinha**

**Email:** [dipaksinha@nagalanduniversity.ac.in](mailto:dipaksinha@nagalanduniversity.ac.in)

---

**CERTIFICATE**

This is to certify that **Mrs Champa Gogoi** was registered as a Research Scholar for Ph.D. (Science) degree in Chemistry in Nagaland University and has been working under my co-supervision. Her thesis entitled “***A STUDY ON REMOVAL OF FLUORIDE AND ARSENIC PRESENT IN GROUND WATER OF GOLAGHAT DISTRICT OF ASSAM AND ITS PERIPHERAL AREAS***” is being forwarded for submission for the Ph.D. (Science) degree of this University. It is certified that she has fulfilled all the requirements according to the rules of Nagaland University regarding investigations embodied in her thesis and I further certify that this work has not been submitted to any other University or Institution in part or full for the award of any degree or diploma.

Place: Nagaland University

(Dr. Dipak Sinha)

Date:

Co-supervisor



## HEADQUARTERS: LUMAMI

# Ph. D COURSE WORK EXAMINATION

This is to certify that Mr/Ms.....  
CHAMPA GOGOI.....  
02/14..... is qualified in the Ph. D Course Work Examination  
of Nagaland University bearing Roll No.....  
CHEMISTRY.....  
in the Department of..... Nagaland University held in the Year 2015.....

Head of Department  
15/5/15  
D B S. H.

Department of Chemistry  
Nagaland University.

Dr. S. S. Kulkarni  
Dean  
School of Sciences  
K. J. Somaiya Institute of Technology  
Mumbai-400 075

## ACKNOWLEDGEMENTS

At first I offer my humble “Pranam” and heartiest thanks at the lotus feet of God for his grace upon me.

I take this opportunity to express my deep sense of gratitude and indebtedness to a lot of people whose contribution is immense without whom this work would not have been possible.

I express my deep sense of respect and gratitude to my supervisor, Dr. Rajib Lochan Goswamee, Senior Principal Scientist & HoD, Materials Science and Technology Division, CSIR-NEIST, Jorhat, Assam, for providing inspring and valuable guidance throughout the course of this investigation. I am indebted to him for his constant suggestion and encouragement. He has not only been a mentor and a guide but also acted as a support anchor throughout my research work. Thank you sir, thank you for accepting me as your research student.

I wish to express my honest gratitude to my co-supervisor, Dr. Dipak Sinha, Professor, Department of Chemistry, Nagaland University, who gave me very nice opportunity to admit at his department in Ph. D. course work and his thoughtful advice.

I do express my thanks particularly to Dr. Balin Konwer, ex-vice Chancellor, Prof. G. T. Thong, ex-Dean of Research Development & Consultancy, Nagaland University for their helping steps in making an MoU with CSIR-NEIST, Jorhat, due to which I got the permission to do my research work in CSIR-NEIST, Jorhat, Assam.

I would also like to acknowledge to Dr. D. Ramaiah, ex-Director, CSIR-NEIST, Jorhat, for giving me the opportunity to work in this reputed institute and making all the facilities available for my research work.

I would like to acknowledge Dr. G. Narahari, present director, CSIR-NEIST, Jorhat, for allowing me to submit my Ph.D. thesis.

On this occasion, I also would like to thank Mr. Sarat Chandra Dutta, Principal, C.N.B. College, Bokakhat, for giving me the permission to carry out my research work.

I would like to acknowledge Prof. Pardeshi Lal, the present vice-Chancellor of Nagaland University for allowing me to submit my Ph. D. thesis.

I acknowledge with thanks the help rendered by Dr. Jonali Goswami, ex-Women Scientist, CSIR-NEIST, Jorhat; Dr. Ramesh Baruah FNA, ex-Chief Scientist, CSIR-NEIST, Jorhat, Dr Aradhana Goswami former Sr Principal Scientist CSIR-NEIST Jorhat for giving me the necessary permission to carry out my research work in this institute.

I would also like to thank Dr. Upasana Bora Sinha, Associate Professor, Department of Chemistry, Nagaland University, for her useful suggestion and mental support all through.

Sincere gratitude shall be also paid to all the teaching faculties of Chemistry Department, Nagaland University; Prof. M.Indira Devi, Head of Department, Dr. I. Tavishe Phucho, Dr. Nurul Alam Choudhury, and Dr. Seram Dushila Devi, for their support and valuable discussions.

My deepest thanks goes to my husband Mr. Simanta Neog, my father in-law, mother in-law, father, mother, my sisters, my sons and daughter and my nephew for their blessing, constant support, encouragement and love throughout the period of my Ph.D. work.

I also express my thanks Dr. Pinaki Sengupta, ex-Chief Scientist & HoD Materials Science and Technology Division; Dr. Manab Jyoti Bordoloi, Chief Scientist; Dr. Binoy K Saikia, Scientist; Dr. Lakshi Saikia, Senior Scientist; Dr. Manash R. Das, Senior Scientist; Dr. Prashenjit Saikia, Scientist, Dr. Biswajit Saha, Scientist; Dr. Dipak Kumar Dutta, Emeritus Scientist, MSTD; Dr. Chubaakum Pongener, Research Associate, MSTD; Mr. Dipak Kumar Bordoloi, ex-Principal Technical Officer, MSTD; Dr, Ankana Saikia; Mr. Nagen Gogoi; Mrs Dipa Rajbongshi Kachari; Mr. Priyam Jyoti Bora; Mr. Paran Jyoti Kalita; Mr. Tonkeswar Das, Mr. Krishna Prasad Sharma and all staff members of Advanced Materials Group, MSTD, for their valuable help.

I would also like to thank Mr. J. Bori, FESEM operator, CSIR-NEIST, Jorhat, for his helping, support, love, and friendship.

I also wish to express my appreciation to my fellow research scholars from my department MSTD, CSIR-NEIST, Ms. Pinky Saikia, Mr. Jitu Saikia, Ms. Susmita Sarmah, Mr. N'guadi Blaise Allou, Mr. Purna Boruah, Ms. Priyakshree Borthakur, Ms. Gitashree Darabdhara, for their vital inputs, helping hand, support, love, and friendship.

I would also like to express my heartfelt gratitude to my research scholar friends at Chemistry Department of Nagaland University, Mr. Parimal Chandra Bhomick, Ms. Ruokuosenuo Zatsu, Ms. Thechano Merry, Ms. Bernadette Kuotsu, Ms. I. Narola Imchen,

Ms. Aola Supong, Ms. Rituparna Karmaker, and Ms. Mridushmita Baruah for their valuable assistance, love and friendship.

I would also like to express my thanks to all non teaching staff of Chemistry Department of Nagaland University, Ms. S. Bendangtemsu, Ms. T. Amer, Mr. Johnny Yanthan, Mr. P. Patton, Ms. Sunepjungla and Ms. Mughato for their help and love.

My thanks go to Mr. Pallab Handique and Mr. Lusan Gogoi for their valuable help.

My special thanks should be dedicated to Shri Temsu Wathi Ao, DIO, Scientist-F, Mokokchung, Nagaland; Dr. Chandra Kanta Gogoi, ex-Guest Professor of Sociology department, Nagaland University, for their invaluable help, advice, encouragement and support.

I am very much grateful to Dr. Mridul Chetia, Assistant Professor, D.R. College, Golaghat, for his helping hand and advice.

On this occasion, I also would like to thank the whole family of C.N.B. College, Bokakhat, for their constant support and love.

Last but not least, my sincerest thanks go to all who helped me in the collection of groundwater and who have contributed in some way for the realization of this work.

(Champa Gogoi)

# Contents

<i>List of Figures</i>	<b>xv</b>
<i>List of Tables</i>	<b>xix</b>
<b>CHAPTER – 1: GENERAL INTRODUCTION</b>	<b>1-31</b>
1.1 Introduction	2
1.2 Fluoride	3
1.2.1 Global and Indian scenario of fluoride polluted ground water	5
1.3 Arsenic	7
1.3.1 Global and Indian scenario of arsenic polluted ground water	9
1.4 Inorganic Quality parameters of drinking water	11
1.4.1 pH	11
1.4.2 Electrical conductivity (EC)	11
1.4.3 Total dissolved solids (TDS)	11
1.4.4 Total alkalinity(TA)	11
1.4.5 Total Hardness(TH)	12
1.4.6 Bicarbonate	12
1.4.7 Sodium	12
1.4.8 Potassium	12
1.4.9 Calcium	12
1.4.10 Magnesium	13
1.4.11 Iron	13
1.4.12 Arsenic	13
1.4.13 Fluoride	13
1.4.14 Chloride	13
1.4.15 Nitrate	14
1.4.16 Phosphate	14
1.4.17 Sulfate	14
1.5 Different practices adopted for removal of Fluoride and Arsenic	14
1.5.1 Adsorption phenomena of fluoride and arsenic from water	14
1.5.1.a Adsorption kinetics	15
Pseudo-first-order kinetic	15
Pseudo-second-order kinetic	16

Elovich model	16
Intra-particle diffusion model	16
1.5.1.b Adsorption isotherms	17
Langmuir adsorption isotherm	17
Freundlich adsorption isotherm	18
Temkin adsorption isotherm	18
1.5.1.c Fitness of the adsorption model	18
Chi-square analysis	18
Coefficient of determination ( $R^2$ )	19
1.5.1.d Thermodynamic study	19
1.6 Importance of the study	19
1.7 Aim and objectives of the work	22
References	23
 <b>CHAPTER - 2: ASSESSMENT OF GROUNDWATER QUALITY OF THE GOLAGHAT DISTRICT OF ASSAM, INDIA AND ITS PERIPHERAL AREAS USING MULTIVARIATE STATISTICAL TECHNIQUE WITH SPECIAL REFERENCE TO THE PRESENCE OF HIGHER LEVELS OF FLUORIDE AND ARSENIC</b>	 <b>32-63</b>
2.1 Introduction	33
2.2 Materials and methods	33
2.2.1 Study Area	33
2.2.2 Sampling methodology	35
2.2.3 Sample analysis	37
2.2.4 Statistical analysis	38
2.2.5 Piper diagram analysis	38
2.3 Results and discussion	38
2.4 Conclusion	58
References	60

<b>CHAPTER-3:MITIGATION APPROACH OF FLUORIDE AND</b>	<b>64-90</b>
<b>ARSENIC- PRESENT STATE OF THE ART, THE GLOBAL SOLUTIONS</b>	
<b>VIS A VIS LOCAL CONDITIONS AND THE NEED FOR LOCAL SOLUTIONS</b>	
3.1 Introduction	65
3.2 Existing process for the removal of fluoride and arsenic from water	65
3.2.1 Precipitation-Coagulation	65
3.2.2 Membrane based process	66
3.2.3 Ion Exchange Processes	67
3.2.4 Subterranean Arsenic Removal (SAR) Technology	68
3.2.5 Adsorption	68
3.2.5.a Adsorbents for fluoride removal	70
3.2.5.b Adsorbent for arsenic removal	74
References	79
 <b>CHAPTER- 4: PREPARATION OF FLUORIDE AND ARSENIC</b>	 <b>91-132</b>
<b>ADSORBENTS (CBP AND IOCS) FROM LOCALLY AVAILABLE</b>	
<b>RAW MATERIALS AND THEIR CHARACTERIZATION</b>	
4.1 Introduction	92
4.2 Activated carbon as adsorbent	92
4.2.1 Carbon of banana plant as adsorbent	95
4.3 Sand as adsorbent	97
4.3.1 Selection of Kanaighat sand as local raw material for preparation of adsorbent	98
SECTION A: PREPARATION AND CHARACTERIZATION OF CARBON OF BANANA PLANT (CBP)	101
4.4 Experimental	101
4.4.1 Preparation of the adsorbent (carbon from Banana plant, <i>Musa     balbisiana</i> )	101
4.4.2 Physico-chemical characterization of CBP	102
a) Moisture content of CBP	102



b) Volatile matter of CBP	102
c) Water soluble matter of CBP	103
d) Ash content of CBP	103
e) Acid soluble matter of CBP	103
f) Fixed carbon of CBP	103
g) Bulk density of CBP	104
h) The pH and conductivity of the adsorbent CBP	104
i) Zeta potential of CBP	104
j) Zero point charge ( $\text{pH}_{\text{ZPC}}$ ) of CBP	104
k) Oxygen containing functional groups (Boehm's titration) present in CBP	105
l) Pore volume and surface area of CBP (BET method)	105
m) Field Emission Scanning Electron Microscopy (FESEM) study of CBP	106
n) FT-IR study of CBP	107
o) Thermo Gravimetric Analysis (TGA) of CBP	107
p) Powder X-ray Diffraction (PXRD) study of CBP	107
4.5 Results and discussion	107
SECTION B: PREPARATION AND CHARACTERIZATION OF IRON OXIDE COATED SAND (IOCS)	116
4.6 Experimental	116
4.6.1 Preparation of the adsorbent iron oxide coated sand, IOCS (surface modification of Kanaighat sand)	116
4.6.2 Physico-chemical characterization of the adsorbent (IOCS) prepared	117
a) Chemical composition of raw Kanaighat sand and iron content of prepared IOCS	117
b) pH and conductivity of the IOCS	117
c) Zeta Potential of the adsorbent IOCS	117
d) Zero point charge ( $\text{pH}_{\text{zpc}}$ ) of IOCS	118
e) Pore volume and BET surface area of OCS	118

f) Scanning Electron Microscopy (SEM) study of IOCS	118
g) FT-IR study of IOCS	118
h) Thermo gravimetric analysis (TGA) of IOCS	118
i) Powder X-ray Diffraction (PXRD) study and IOCS	118
4.7 Results and discussion	119
4.8 Conclusions	126
References	127
 <b>CHAPTER – 5: REMOVAL OF FLUORIDE FROM CONTAMINATED</b>	<b>133-165</b>
<b>WATER BY USING TWO LOCALLY AVAILABLE MATERIALS</b>	
<b>SECTION A-CBP &amp; SECTION B-IOCS</b>	
5.1 Introduction	134
5.2 Materials and methods	134
5.2.1 Preparation of standard fluoride stock solution	134
5.2.2 Determination of fluoride concentration	134
5.2.3 Batch mode adsorption study	135
5.3 Results and discussions	135
<b>SECTION A: CBP AS AN ADSORBENT</b>	135
5.3.A.1 Results and discussion of fluoride adsorption studies using CBP	135
a) Effect of adsorbent dose	135
b) Effect of initial concentration of fluoride solution	136
c) Effect of pH of fluoride solution on defluoridation	137
d) Effect of contact time	138
e) Adsorption isotherms study	139
f) Adsorption kinetics study	143
g) Effect of competitive anions on defluoridation	146
5.3.A.2: Studies on CBP after adsorption of fluoride	147
a) Study of FESEM images & EDX spectra	147
b) Study of FT-IR spectra	148
5.3.A.3: Mechanism of adsorption of fluoride	148

SECTION B: IOCS AS AN ADSORBENT	149
5.3.B.1 Results and discussion of fluoride adsorption studies using IOCS	149
a) Effect of adsorbent dose	149
b) Effect of contact time	149
c) Effect of initial concentration of fluoride solution	150
d) Effect of pH on defluoridation	151
e) Adsorption isotherms Study	152
f) Adsorption Kinetic Study	155
g) Thermodynamic Analysis	158
h) Effect of other anions on defluoridation	159
5.3.B.2: Studies on IOCS after adsorption of fluoride	160
a) Study of FESEM images & EDX spectra	160
b) Study of FT-IR spectra	161
5.4: Conclusion	162
References	163
 <b>CHAPTER – 6: REMOVAL OF ARSENIC FROM CONTAMINATED WATER BY USING TWO LOCALLY AVAILABLE MATERIALS</b>	 <b>166-205</b>
<b>SECTION A-CBP &amp; SECTION B-IOCS</b>	
6.1 Introduction	167
6.2 Materials and methods	167
6.2.1 Preparation of standard arsenic stock solution	167
6.2.2 Determination of As (V) (arsenate, $\text{H}_2\text{AsO}_4^-$ ) concentration	167
6.2.3 Batch mode adsorption study	168
6.3: Results and discussions	168
 SECTION A: CBP AS AN ADSORBENT	 168
6.3.A.1 Results and discussion of arsenic adsorption studies using CBP	168
a) Effect of adsorbent dosage	168
b) Effect of initial concentration of arsenic solution	169
c) Effect of pH on As (V) adsorption	170
d) Effect of contact time	171

e) Adsorption kinetics study	172
f) Adsorption isotherms Study	175
g) Effect of temperature on arsenic adsorption	178
h) Effect of other anions on arsenic adsorption	179
6.3.A.2: Simultaneous adsorption of fluoride and arsenic from real ground water	180
6.3.A.3: Characterization of CBP after arsenic adsorption	182
a) Study of FESEM images & EDX spectra	182
b) Study of FT-IR spectra	183
6.3.A.4: Mechanism of adsorption of arsenic on CBP	184
 SECTION B: IOCS AS AN ADSORBENT	184
6.3.B.1: Results and discussion of Arsenic adsorption studies using IOCS	184
a) Effect of adsorbent dosage	184
b) Effect of initial concentration of arsenic solution	185
c) Effect of pH on As (V) adsorption	186
d) Effect of contact time	187
e) Adsorption kinetics study	188
f) Adsorption isotherms Study	191
g) Effect of temperature on arsenic adsorption	194
h) Effect of other anions on adsorption of arsenic	196
6.3.B.2: Simultaneous adsorption of fluoride and arsenic from real ground water by IOCS	197
6.3.B.3: Some study of IOCS after adsorption of arsenic	199
a) Study of FESEM images & EDX spectra	199
b) Study of FT-IR spectra	200
6.3.B.4: Mechanism of As adsorption on IOCS	200
6.4 Conclusion	201
References	202
 <b>CHAPTER – 7: SUMMARY AND CONCLUSIONS</b>	<b>206-210</b>

## List of figures

Fig 1.1 Dental and skeletal fluorosis	4
Fig 1.2 Current fluoride contamination scenarios around the world	5
Fig 1.3 Map of India showing state wise fluoride distribution	6
Fig 1.4 Danger of Arsenic Poisoning	8
Fig 1.5 Current arsenic contamination scenarios around the world	9
Fig 1.6 Arsenic affected areas of India	10
Fig 1.7 Study sites showing six blocks of Golaghat district, Assam	21
Fig 2.1 Study sites of Golaghat district with its peripheral areas (1-27), Assam	35
Fig 2.2 Some water collection point of study area	37
Fig 2.3 Graphical representation of block wise distribution of fluoride in Dergaon as F-Dg, in Kathalguri as F-Kt, in Podumoni as F-Pd, in Kakodonga as F-Kd, in Morangi as F-Mn, in Gamariguri as F-Gg, in Sorupathar as F-Sp and in Bokakhat as F-Bkt.	49
Fig 2.4 Graphical representation of block wise distribution of arsenic in Dergaon as As-Dg, in Kathalguri as As-Kt, in Podumoni as As-Pd, in Kakodonga as As-Kd, in Morangi as As-Mn, in Gamariguri as As-Gg, in Sorupathar as As-Sp and in Bokakhat as As-Bkt	50
Fig 2.5 Graphical representation of distribution of fluoride and arsenic in peripheral areas of Golaghat district (Jorhat, Karbi-Anglong and Nagaon district) as JHT-F, JHT-As, KAL-F, KAL-As and NGN-F, NGN-As.	51
Fig 2.6 Principal component analysis by (A) Scree plot of the eigenvalues and (B) component plot in rotated space	57
Fig 2.7 Piper diagram of groundwater samples of Golaghat district	58
Fig 4.1: Some important functional groups present on the surface of carbon	93
Fig 4.2 Various pores present in a porous solid O-open pores; C-closed pores; t-transport pores; b-blind pores.	94
Fig 4.3: Different surface functional groups present on carbon	95
Fig 4.4 Assamese traditional kitchen fire place containing dry banana peel and stem for the preparation of <i>Kolkhar</i>	96
Fig 4.5 <i>Musa balbisiana</i> plant	97
Fig 4.6 Site map of sand collection area	99

Fig 4.7 Photo of Kanaighat sandbar on the banks of river Kaliani	100
Fig 4.8 Graphical abstract of preparation of CBP	101
Fig 4.9 Plot of $pH_i$ vs $pH_f$ - $pH_f$	110
Fig 4.10 (A) and (B) are FESEM images (A & B) of CBP	111
Fig 4.11 EDX spectra for elemental composition of CBP	112
Fig 4.12 FTIR Spectra of CBP	112
Fig 4.13 Thermogram of CBP	114
Fig 4.14 XRD Spectra of CBP	115
Fig 4.15 Plot of Zeta potential vs pH of IOCS	120
Fig 4.16 (A) & (B) are FESEM images of raw Kanaighat sand (KS)	121
Fig 4.17 (A), (B), (C) & (D) are FESEM images of Iron Oxide Coated Sand (IOCS)	122
Fig 4.18 EDX Spectrum of (A) KS and (B) IOCS	122
Fig 4.19 FTIR Spectra of (A) KS and (B) IOCS	123
Fig 4.20 XRD Spectra of KS (A) and IOCS (B)	125
Fig 4.21 TGA curve of KS and IOCS	126
Fig 5.1 Effect of adsorbents dose on the (A) percent removal of fluoride (B) removal capacity ( $q_e$ ) at 30°C at the pH of 6.1 and 3 hours of stirring.	136
Fig 5.2 Effect of initial concentration of fluoride solution on defluoridation by CBP at 30°C in a pH of 6.1 with 3 hours stirring	137
Fig 5.3 Graph of effect of pH of fluoride solution on defluoridation by CBP	138
Fig 5.4 Effect of contact time on the adsorption of fluoride at 30°C in a pH of 6.1 with adsorbent dose of 14 g/L	139
Fig 5.5 (A) Langmuir, (B) Freundlich, (C) Temkin adsorption isotherm of CBP and (D) graph of $R_L$ vs $C_o$	142
Fig 5.6 Graph (A), (B), (C) and (D) are the Psuedo first order, psuedo second order, Elovich model and Intra Particle Diffusion of kinetics study.	145
Fig 5.7 Bar diagram showing the effect of competitive anions on defluoridation	146
Fig 5.8 Various magnifying FESEM photograph (A & B) of CBP after Adsorption of fluoride	147
Fig 5.9 EDX spectra of CBP after adsorption of fluoride	147

Fig 5.10 FT-IR spectra of CBP after adsorption of fluoride	148
Fig 5.11 A plausible mechanism of fluoride adsorption onto CBP	149
Fig 5.12 (a)- Effect of adsorbent dose on the adsorption of fluoride at 30°C in a pH of 6.1 with 3 hour stirring. (b)- Effect of contact time on the adsorption of fluoride at 30°C in a pH of 6.1 with an adsorbent of 10 g/L. (c)- Effect of initial concentration of fluoride solution on defluoridation at 30°C in a pH of 6.1 with an adsorbent of 10 g/L.	151
Fig 5.13 Effect of pH of fluoride solution on % removal of fluoride by IOCS at 30°C	152
Fig 5.14 (a) Langmuir, (b) Freundlich, (c) Temkin adsorption isotherm of IOCS and (d) graph of $R_L$ vs $C_o$	155
Fig 5.15 Plots of (a) pseudo-first-order (b) pseudo second- order (c) Intra particle diffusion model and (d) Elovich model.	158
Fig 5.16 van't Hoff plots of fluoride adsorption onto IOCS	159
Fig 5.17 Bar diagram showing the effect of competitive anions on defluoridation	160
Fig 5.18 (A), (B) & (C) are FESEM photograph of IOCS after adsorption of fluoride	160
Fig 5.19 EDX spectra of Iron Oxide Coated sand (IOCS) after adsorption of fluoride	161
Fig 5.20 FT-IR spectra of IOCS before and after adsorption of fluoride	161
Fig 6.1 Effect of adsorbents dosage on the % removal of arsenic at 30°C in pH- 7 with 3 hours stirring	169
Fig 6.2 Effect of initial concentration of arsenic solution on adsorption of arsenic by CBP at 30°C in a pH of 7 with 3 hours stirring	170
Fig 6.3 Effect of pH on adsorption of As (V)	171
Fig 6.4 Effect of contact time on the adsorption of arsenic at 30°C in a pH of 7 with adsorbent dose of 14 g/L	172
Fig 6.5 Graph (A), (B), (C) and (D) are the Psuedo first order, pseudo second order, Elovich model and Intra Particle diffusion of kinetics study	175

Fig 6.6 (A) Langmuir, (B) Freundlich, (C) Temkin adsorption isotherm of CBP and (D) graph of $R_L$ vs $C_o$	178
Fig 6.7 Effect of temperature on arsenic adsorption by CBP	179
Fig 6.8 Bar diagram showing the effect of competitive anions on adsorption of arsenic by CBP	179
Fig 6.9 Bar diagram of concentration of fluoride (A) and arsenic (B) in natural water before and after adsorption by CBP	182
Fig 6.10 FESEM images of CBP (A) & (B) after adsorption of arsenic at various magnification	182
Fig 6.11 EDX spectra of CBP after adsorption of arsenic	183
Fig 6.12 FT-IR spectra of CBP after adsorption of arsenic	183
Fig 6.13 Effect of adsorbents dose on % removal of As (V) at 30°C in the pH of 7 with 3 hours stirring.	185
Fig 6.14 Effect of initial concentration of arsenic solution on % removal by IOCS at 30°C in a pH of 7 with 45 minutes stirring	186
Fig 6.15 Effect of pH of arsenic solution on % removal of arsenic by IOCS at 30°C	187
Fig 6.16 Effect of contact time on the adsorption of arsenic at 30°C in a pH of 7 with adsorbent dose of 14 g/L	188
Fig 6.17 Plot (A) pseudo-first-order kinetic model; (B) pseudo second- order kinetic model; (C) Elovich model; (D) Linear plot of intra particle diffusion model and (E) Non linear plot of intra particle diffusion model	191
Fig 6.18 (A) Langmuir, (B) Freundlich, (C) Temkin isotherms of arsenic adsorption by IOCS and (D) graph of $R_L$ vs $C_o$	194
Fig 6.19 Effect of temperature on arsenic adsorption by IOCS	195
Fig 6.20 Plot of $\ln K_d$ versus $1/T$	195
Fig 6.21 Bar diagram showing the effect of competitive anions on adsorption of arsenic by IOCS	196
Fig 6.22 (A) Bar diagram of concentration of fluoride before and after adsorption. (B) Bar diagram of concentration of arsenic before and after adsorption	198



Fig 6.23 FESEM images of IOCS after adsorption of arsenic	199
Fig 6.24 EDX spectra of IOCS after adsorption of arsenic	199
Fig 6.25 FT-IR spectra of IOCS after adsorption of arsenic	200

## List of Tables

Table 1.1	Percentage of fluorine in various minerals	3
Table 1.2	Effect of prolonged use of drinking water on human body, related to fluoride content.	5
Table 2.1	Some water quality parameters of groundwater samples of Golaghat district	39
Table 2.2	Concentration of important cations in groundwater samples of Golaghat district	41
Table 2.3(a) & 3(b)	Some groundwater quality parameters of the peripheral areas	43
Table 2.4	Concentration of fluoride in groundwater samples of Golaghat district	46
Table 2.5	Concentration of arsenic in groundwater samples of Golaghat district	47
Table 2.6	Pearson correlation between chemical parameters of groundwater samples	53
Table 2.7	Rotated component matrix for data of groundwater samples	56
Table 3.1	The comparison of various technologies for the removal of fluoride and arsenic	69
Table 3.2	List of Carbon feedstocks	77
Table 4.1	Physico-chemical parameters of CBP	108
Table 4.2	pH of 0.01M NaCl solution before and after treatment with CBP	110
Table 4.3	Surface acidic groups and basic groups present in CBP, measured by Boehm titration method	111
Table 4.4	Elemental composition of CBP from EDS spectra	112
Table 4.5	Wave numbers and assignment of the principal bands in the FTIR spectra of CBP	113
Table 4.6	Composition of Kanaighat sand	119
Table 4.7	Values of zeta potential with corresponding pH values	120

Table 4.8	Values of BET surface area, pore size of KS and IOCS	121
Table 4.9	Wave numbers and assignment of the principal bands in the FTIR spectra of KS and IOCS	124
Table 5.1	Langmuir, Freundlich, and Temkin parameters along with correlation coefficients	141
Table 5.2	Comparison of pseudo first order, pseudo second order, intra particle diffusion and Elovich model rate constants and calculated $q_e$ values using CBP as adsorbent	144
Table 5.3	Langmuir, Freundlich, and Temkin parameters along with correlation coefficients	154
Table 5.4	Comparison of the various parameters obtained in Pseudo first order, Pseudo Second order, Intra particle diffusion model and Elovich model of adsorption of fluoride onto IOCS	156
Table 5.5	Thermodynamic parameters ( $\Delta G^\circ$ , $\Delta H^\circ$ and $\Delta S^\circ$ ) of fluoride adsorption on IOCS	159
Table 6.1	Comparison of pseudo first order, pseudo second order, intra Particle diffusion and Elovich model rate constants and calculated $q_e$ values using CBP as adsorbent	173
Table 6.2	Langmuir, Freundlich, and Temkin parameters along with correlation coefficients	177
Table 6.3	Chemical composition of real life ground water collected from different places of Golaghat district of Assam, India	180
Table 6.4	The residual amount of fluoride and arsenic of collected real life ground water after treatment with CBP	181
Table 6.5	Elemental composition of CBP from EDS spectra, after adsorption of arsenic	183
Table 6.6	Comparison of pseudo first order, pseudo second order, Elovich and intra particle diffusion model rate constants and calculated $q_e$ values using IOCS as adsorbent	189
Table 6.7	Langmuir, Freundlich, and Temkin parameters along with correlation coefficients	193
Table 6.8	Thermodynamic parameters ( $\Delta G^\circ$ , $\Delta H^\circ$ and $\Delta S^\circ$ ) of arsenic adsorption on IOCS	195

Table 6.9	The amount of fluoride and arsenic of collected real life groundwater before and after treatment with NIOCS	197
Table 6.10	Elemental composition of IOCS from EDX spectra, after adsorption of arsenic	200

# **CHAPTER - 1**

## **GENERAL INTRODUCTION**

*This chapter represents a brief discussion about the fluoride and arsenic contamination of groundwater and their health effect. Also, the different adsorptive techniques for the removal of these contaminants are discussed.*

## **1.1 Introduction**

No life can survive without water and water can be found in the form of rain, ice, snow and fog in nature. Human body contains 70-80% water. Three fourth of the earth is water. In spite of such abundances, all over the world the amount of drinking water is decreasing day by day. During the period from 1940 to 1950 India faced health problems due to the water-borne diseases. According to the report of Environmental Hygiene Committee (EHC) of India, from 1940 to 1950 more than 400,000 people died on cholera, dysentery, and diarrhoea [1]. As the ground water is relatively free from the contaminants than that of the surface water, so groundwater was considered more better than surface water for drinking as well as agricultural and industrial uses in India. At the global level, about one third of the population uses groundwater for domestic purposes. Nowadays, hand pumps or tube wells are most popular in both urban and rural areas for drinking and other domestic purposes [2].

As a result of fast development in industrialisation, urbanisation, unskilled utilization of water resources and expanding population, groundwater has become polluted in last few decades. In many areas, ground water is contaminated with toxic materials as well as heavy metals. Globally, as a result of rapid industrialization, water pollution have become a big challenge for the human beings as well as for the other organisms due to factors such as leaking of fuels and chemical tanks, industrial chemical spills, industrial emission, drainage of house hold chemicals and rapid growth of population throughout the world. It is noted that if groundwater once get contaminated, it becomes very challenging to recover the original quality. Due to some human activities like metal mining, discharge of industrial and municipal waste, use of arsenical pesticides [3,4,5] and natural activities such as geochemical reactions and volcanic emissions, ground water become polluted by toxic pollutants like arsenic and fluoride.

According to WHO, about 80% of all the diseases such as gastrointestinal diseases, reproductive problems, neurological disorders, and even cancer in human beings are caused by water [6,7]. Presence of chemical water pollutants in significant amount might lead to chronic long-term health effects. Specifically, excessive amount of fluoride and arsenic concentration in drinking water can cause crucial health impacts. As specified by World Health Organization [8], the maximum permissible limit of fluoride is 1.5 mg/L and for arsenic is 0.01 mg/L WHO [9] in drinking water. However, in India in the event of absence of alternate source, the highest permissible value for As in drinking water is relaxed to 0.05 mg/L by BIS [10].

## 1.2 Fluoride

Fluorine is a very reactive element that is why it can't be found in its elemental state. It always obtained in a combined form of minerals as fluoride. The fluoride occurs in nature in various minerals such as Sellaite, Fluorspar, Cryolite, Fluorapatite etc [11,12]. The following table gives the amount of fluorine (in %) present in various minerals.

**Table 1.1: Percentage of fluorine in various minerals**

Serial No	Name of the mineral	% fluorine (W/W)
1	Sellaite $\text{MgF}_2$	61
2	Villianmite $\text{NaF}$	55
3	Fluorite (Fluorspaar) $\text{CaF}_2$	49
4	Cryolite $\text{Na}_3\text{AlF}_6$	45
5	Bastnaesite (Ce,Ln) $(\text{CO}_3)\text{F}$	9
6	Fluorapatite $\text{Ca}_3(\text{PO}_4)_3\text{F}$	3-4

Natural and anthropogenic activities causes fluoride contamination in drinking water [13,14,15], which is an important health issue in different countries across the world. Since, Fluorspar is a sedimentary rock and Cryolite is an igneous rock, so these fluoride minerals are generally insoluble in water i.e. only under favoured conditions, fluorides will be released to ground water, when water moves through these rocks. The factors influencing the natural concentration of ground water are the geological, physico-chemical characteristics and depth of the aquifer [16]. Geogenic occurrence of fluoride is often linked to volcanic activity. It is seen that, in many countries elevation of fluoride concentration in water is due to discharging of fluoride polluted waste water from various industries. Such type of waste water containing fluoride as contaminant are generally created from the superphosphate fertilizer industry [17,18,19,20], glass and ceramic manufacturing process [21,22], aluminium and zinc smelters [23], photovoltaic solar cells industry [24,25], silicon based high tech-semiconductors production [26,27] and by burning of fluorinated plastic [28].

Fluorine has strong affinity to calcium present in our teeth and bone. Drinking water is the main source of fluoride into the human physiology. Whereas, fluoride concentration lower

than 1.0 ppm is considered beneficial for teeth and that can even prevent tooth decay. In this stage, the skeletal system becomes stable by increasing the size of the apatite crystal and reducing the solubility [29]. If the daily consumed drinking water contains fluoride more than 1.5 mg/L. It causes dental fluorosis and with prolonged exposure it progresses to skeletal fluorosis [30,11] as shown in the Fig 1.1. In this stage, teeth becomes harder and more brittle due to the transformation of large amount of hydroxyapatite into fluoroapatite. The bones becomes weaker and it damages the skeletal framework.



**Fig1.1: Dental and skeletal fluorosis (Sources: Farooqi [96])**

The adverse sequel of fluoride on human health are: dental fluorosis [30], skeletal fluorosis [11], cardiovascular effects, gastro intestinal disorder, endocrine effects, neurological effects, reproductive effects [31,32,33,34], enzyme inhibition, genetic damage, effect on the pineal gland. In addition to water other routes of fluoride contamination into the human system are through food, industrial exposure, drugs and cosmetics [31].

**Table 1.2: Effect of prolonged use of drinking water on human body and relation to fluoride content.**

Fluoride concentration (mg/L)	Health outcome
< 0.5	Dental caries
0.5-1.5	Optimum dental health
1.5-4.0	Dental fluorosis
4.0-10	Dental and skeletal fluorosis
>10.0	Crippling fluorosis

### 1.2.1 Global and Indian scenario of fluoride polluted ground water

Fluoride defilement of ground water is a global issue. The presence of fluoride has been reported by different countries like USA, Africa, China, India, Sri Lanka, Thailand, Indonesia, Yemen, Pakistan, Iraq, Turkey, Syria, Palestine, Bangladesh, Iran, Saudi Arabia, Kenya, Tanzania, Ghana [35,6,36], etc (shown in Fig 1.2). There are more than twenty developed and developing countries in which fluorosis is common problem.

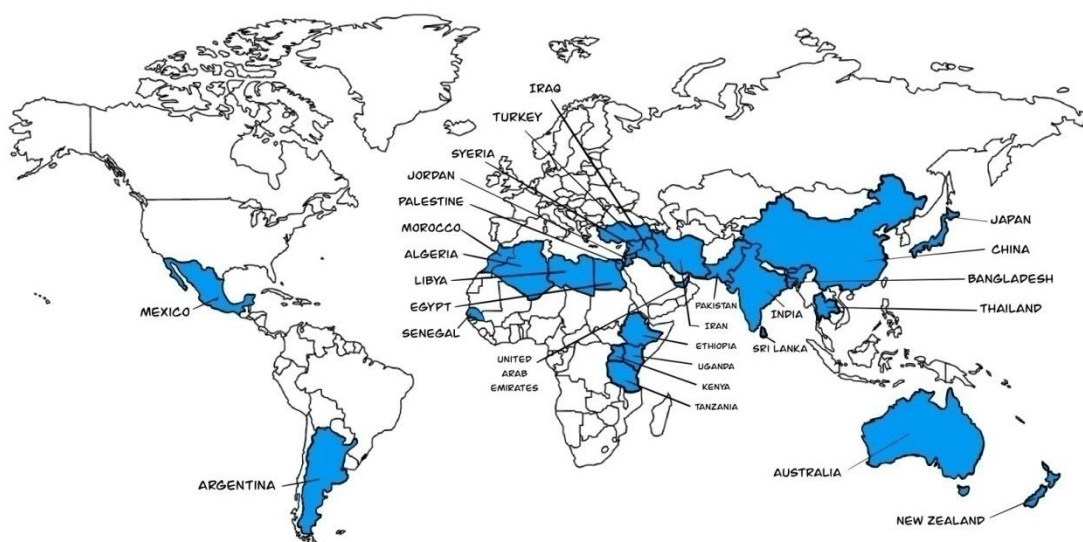


**Fig 1.2: Current fluoride contamination scenarios around the world (Source: Farooqi, 2015)**



In India many people suffer from fluorosis. Gujarat, Madhya Pradesh, Tamil Nadu, Andhra Pradesh, Rajasthan, Uttar Pradesh, Manipur, Assam etc [11,37,2] are the Indian states having fluoride contaminated ground water (as shown in Fig. 1.3). More than 62 million people are suffering from fluorosis in India [38]. In India in 1937, fluoride contamination of drinking water in Andhra Pradesh was first reported [38].

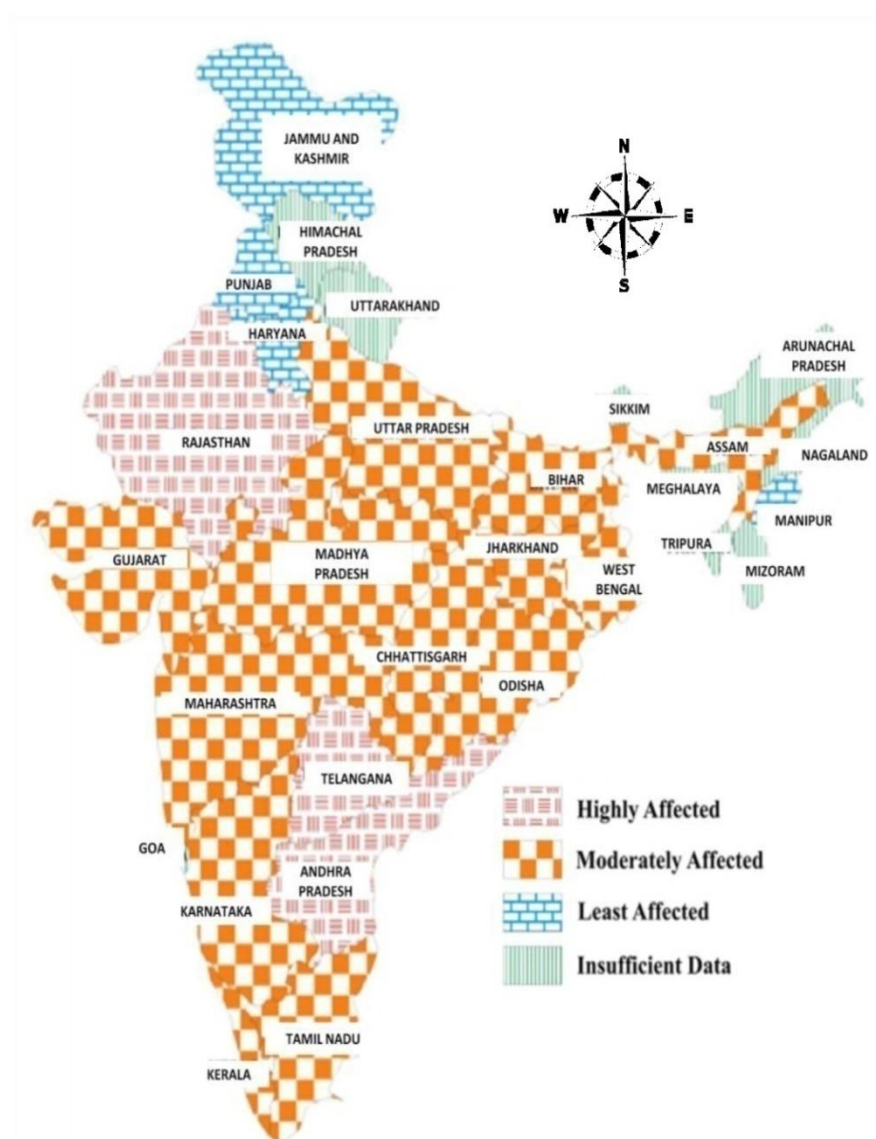


**Fig 1.3: Map of India showing state wise fluoride distribution (Source: Saikia [39])**

In Assam, groundwater of the districts Karbi-Anglong, Nagaon, Dhemaji, Goalpara, Kamrup, Golaghat [40,41,42] are also affected by fluoride. At many locations of Karbi-

Anglong and Nagaon districts of Assam, the level of fluoride in the ground water have been recorded above the upper limit of 1.5mg/L that is prescribed by BIS [10] [41,43]. Fluoride concentration in groundwater of Howraghat (zone II), Nopekling village and Ramsapather of Karbi-Anglong district are 23.5, 16.3 and 15.4 mg/L. Similarly the fluoride concentration at Akashiganga, Nij Parakhowa and Tapatjuri village of Nagaon district are 16, 15.5 and 13.5 mg/L. Many cases of fluorosis (both dental and skeletal) are confirmed in these two districts of Assam. Source of fluoride in these areas is reported as geogenic dissolution of fluoride bearing Precambrian granite [44].

### **1.3 Arsenic**

Presence of arsenic along with sulphide and iron pyrites is found in the earth's crust. Three arsenic compounds (i) Realgar or arsenic disulphide, (ii) Orpiment or arsenic trisulphide and (iii) Arsenopyrite or ferrous arsenic sulphide are the main ores of arsenic. Arsenic is poisonous to any multi-cellular organism, including humans. The toxicity of arsenic depends on its chemical composition and valency. Arsine gas ( $\text{AsH}_3$ ) is the most toxic form of arsenic compound. When arsenic compound reacts with acid, non irritant colour less arsine gas evolves. This gas is so toxic that it will take only 30 minute to cause death even if it enters into our body with concentration as low as 25-30 mg/L [45]. Due to its poisoning effect, in the first half of 20<sup>th</sup> century arsenic was used in chemical warfare agents [46]. Arsenic comes into water due to anthropogenic activities such as smelting of metals, pharmaceutical industry, pesticide manufacture, wood preservative like Chromated Copper Arsenate (CCA) which of course is now phased out, dye stuffs, glass industries, petroleum, coal, semiconductor manufacture, drilling wells, mineral extraction, processing wastes [5,47] and natural activities such as geochemical reactions and volcanic emissions. When the arsenic contaminated ground water is pumped out, one part of arsenic is consumed directly by human, one part by plant, due to which it enters our body through food chain and remaining part will remain along with other minerals in the topsoil.

According to BIS, highest acceptable limit of arsenic in drinking water is 50  $\mu\text{g/L}$  (0.05 mg/L) [48,10]. Daily consumption of drinking water with arsenic content more than 0.01 mg/L is toxic for health accordingly, headaches, confusion, diarrhea are the beginning symptoms of arsenic poisoning [49]. When the poisoning becomes acute, symptoms may include severe diarrhea, vomiting, vomiting of blood, blood in the urine, shutdown of the cardiovascular system and slowing down of the central nervous system and the final result of arsenic poisoning is coma and death [48].

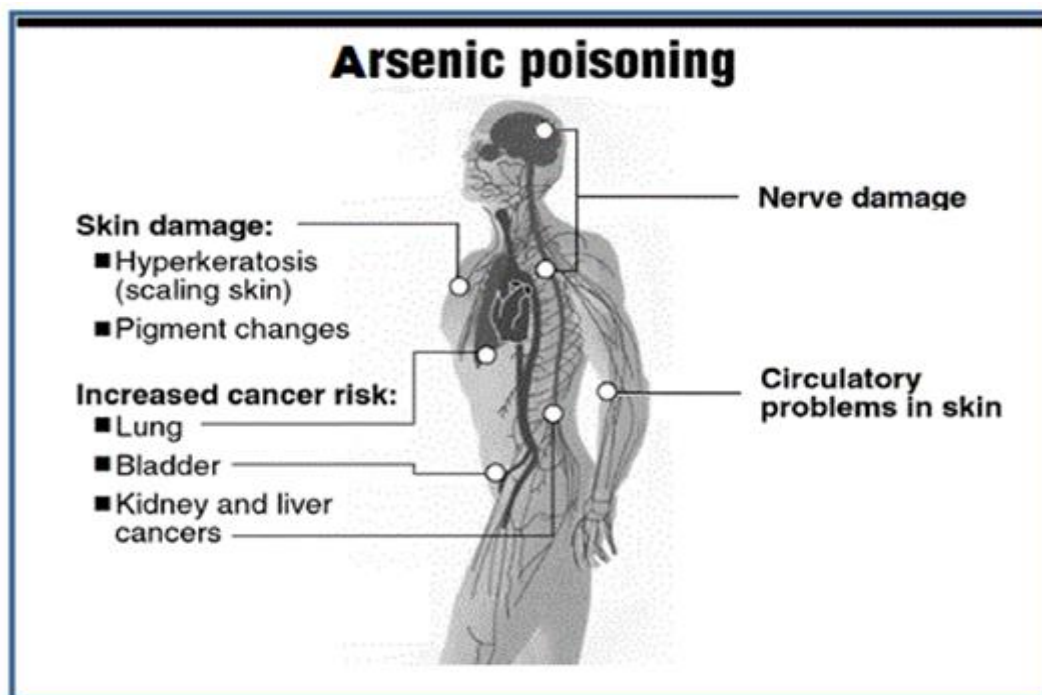


**Fig 1.4: Danger of Arsenic Poisoning (Khan [98])**

Apart from the above, arsenic act as human carcinogen i.e. can form cancer in skin, lung, and urinary bladder. Other health effects of arsenic includes high blood pressure, neurological disorder, cardiovascular disorder, reproductive disorders, diabetes, diseases of the blood vessels of the legs and feet etc [50,31,51] as given in the Fig 1.4. Skin lesions are the earliest nonmalignant effects of arsenicosis. As arsenic has an affinity towards sulfur so it get bind to the hydrogen sulfide group of proteins present in our body, and ultimately disrupts enzymatic activities [52,53].

Arsenic exists in multiple oxidation states (+5, +3, 0 and -3) and are stable in different redox condition [3]. Arsenite [As (+3)] is the dominant form under reducing condition whereas, Arsenate [As (+5)] is generally the stable form in oxygenated environments. Arsenite [As (+3)] and arsenate [As (+5)] are the most common state in which they are found in water [54,55]. Although both As(+3) and As(+5) states are toxic, As (+3) is much more toxic and mobile than As(+5). In natural water arsenic is present in both organic and inorganic form. Inorganic arsenic such as arsenic oxide ( $\text{As}_2\text{O}_3$ ) or realgar ( $\text{As}_4\text{S}_4$ ) is the result of dissolution from mineral phase [56]. Mono methyl arsenic acid (MMAA), dimethyl arsenic acid (DMAA), and arseno-sugars are the various forms of organic arsenic species. Organic arsenic is less toxic than inorganic arsenic.

### 1.3.1 Global and Indian scenario of arsenic polluted ground water

Arsenic in groundwater is world wide problem. Arsenic contamination of groundwater has been found in more than 105 countries including USA, Chile, Mexico, Argentina, Poland, Canada, Hungary, China, Cambodia, Brazil, India, Bangladesh, Nepal, Myanmar, Pakistan, Japan [57].



**Fig 1.5: Current arsenic contamination scenarios around the world (Source: Ahmed et al. [57])**

In India in early 1980s the arsenic contaminated groundwater was first discovered [58] in West Bengal and its health effects in the Bengal delta plain are now reasonably well documented. Groundwater of many states of India like Assam, Manipur, Arunachal Pradesh, Nagaland, Bihar, Jharkhand, Tripura, Uttar Pradesh etc. are contaminated by As [48,49,59]. Our neighbourhood country Bangladesh has suffered severe health effects due to use of highly arsenic contaminated water for drinking purpose [6,60,61]. Ground water of the Bengal Delta Plain is highly affected by arsenic which is drained by three important rivers – the Ganges, Brahmaputra and Meghna (G–B–M) – originating from the Himalayas. The Bengal Delta Plain covers the state of West Bengal, Northeastern states of India, the adjoining country of Bangladesh and the neighboring country of Nepal [62]. Arsenic-iron bearing minerals are the main source of arsenic in Bengal Delta Plain [59]. Fig 1.5 and Fig 1.6 gives the arsenic affected countries around the world and the arsenic affected areas of India.

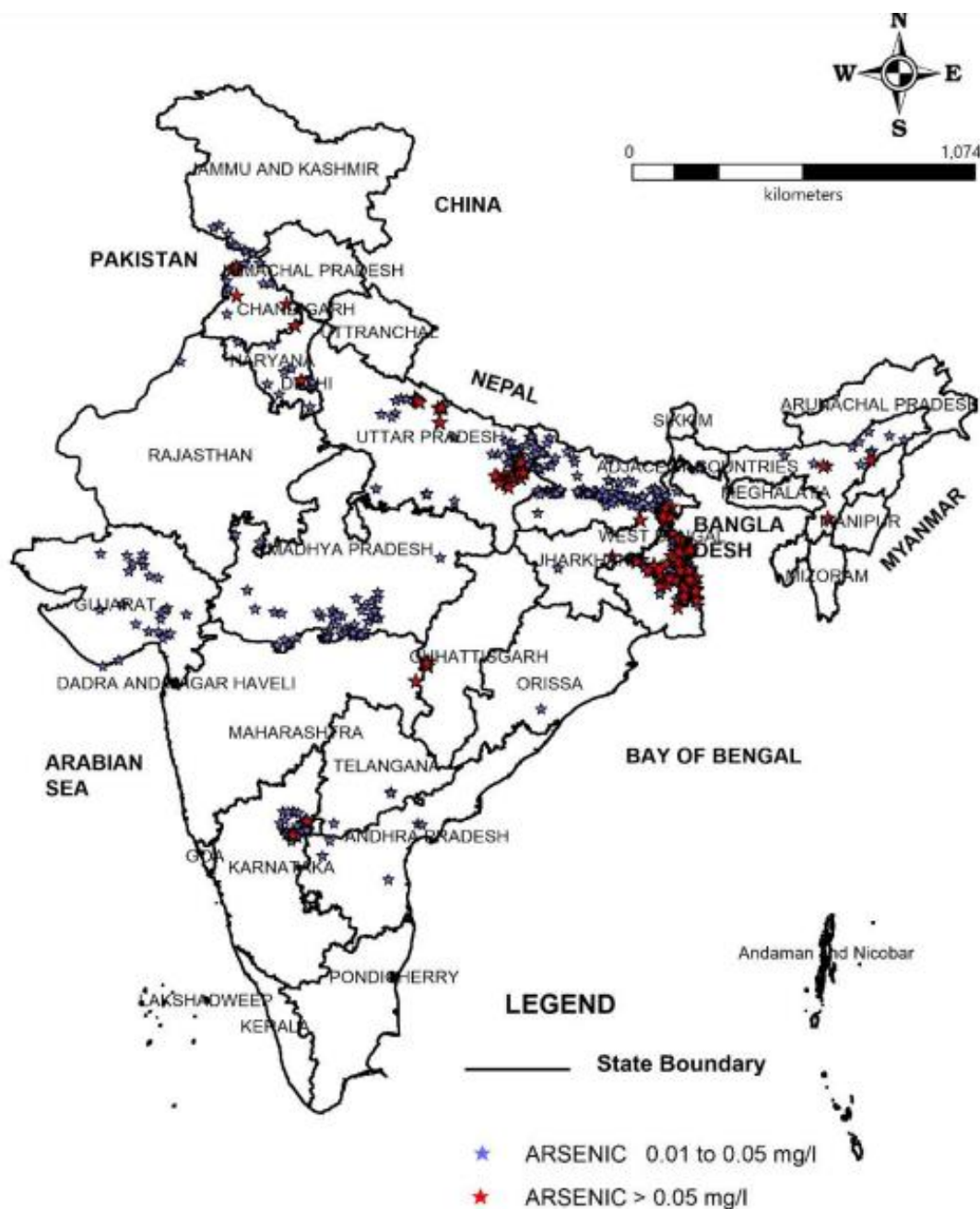


**Fig 1.6: Arsenic affected areas of India (Source: Reddy [97])**

Arsenic contamination of groundwater of Assam was reported in 2004 [63,59]. A survey by PHED during the period 2004-2005, supported by UNICEF, reported that ground water of 72 blocks of 18 districts of Assam had been contaminated by arsenic [48]. The state assembly of Assam in 2018 was informed that 24 districts of Assam such as Hailakandi, Karimganj, Goalpara, Kamrup, Sivasagar, Darrang, Lakhimpur, Dhemaji, Dibrugarh, Jorhat, Golaghat, Bongaigoan, Nagoan, Barpeta, Nalbari, Kokrajhar, Tinsukia are affected by arsenic. Among these the maximum arsenic was observed in Jorhat districts. Chakraborti et al. [63],

reported that Golaghat district which is situated in the upper Assam section of Brahmaputra river basin and is also a badly affected by arsenic. Chetia et al. also reported the same about ground water of Golaghat district [64].

Since, Jorhat is a recognized arsenic affected area and Karbi Anglong and Nagaon are two recognized fluoride affected areas therefore Golaghat district being a sandwiched zone in between these districts provides a good location for a detailed groundwater quality survey and analysis covering not only the arsenic and fluoride aspects but also other important parameters like pH, alkalinity, hardness, dissolved solids, nitrate, chloride, iron concentration emphasizing the overall quality of ground water especially with respect to drinking water parameters.

## **1.4 Inorganic Quality parameters of drinking water**

### **1.4.1 pH**

pH is the very important water quality parameter. The permitted limit of pH of drinking water is 6.5-8.5 [65]. pH can be measured by pocket meters, portable meters or bench top meters or pH test strips. In modern days low or high pH of groundwater are linked to the industrial and municipal sewage, use of chemical fertilizers, dissolution of carbon dioxide and organic soil and plant humus originated acids like fulvic and humic acids etc. [66].

### **1.4.2 Electrical Conductivity (EC)**

EC of groundwater measures the ability to conduct an electric current of all ions present in water. It can be measured by pocket conductivity meter or bench top conductivity meter. It is expressed in the unit mMho/cm or mS/cm

### **1.4.3 Total Dissolved Solids (TDS)**

It refers to the total amount of ions in dissolving states. It can be measured by pocket TDS meter. It is expressed in the unit mg/L.

### **1.4.4 Total alkalinity (TA)**

It is the capacity to neutralize acid. Alkalinity of groundwater is due to the presence of hydroxide compounds, bi-carbonates and carbonates of K, Mg, Na, and Ca. It is expressed in the unit mg/L. TA can be measured by titrimetric method [67].

### **1.4.5 Total Hardness (TH)**

TH is the total concentration of  $\text{Ca}^{2+}$  and  $\text{Mg}^{2+}$  ions present in groundwater and expressed as calcium carbonate.  $\text{Ca}^{2+}$  and  $\text{Mg}^{2+}$  ions react with soap to form an insoluble substance. The ability of water for destroying and reducing the lather of soap define its degree of hardness. Bicarbonate of Calcium and Magnesium gives the temporary hardness in water, whereas permanent hardness of water is obtained through chlorides, sulphates, nitrates of magnesium and calcium. TH can be measured by titrimetric method [67]. It is expressed in the unit mg/L.

### **1.4.6 Bicarbonate**

Bicarbonate is present in water as calcium and magnesium bicarbonate, which is a measure of temporary hardness of water. It is also measured by titrimetric method [67]. It is expressed in the unit mg/L.

### **1.4.7 Sodium**

The main source of sodium in groundwater is leaching of mineral. The role of sodium in the living organism is very important. High concentration of sodium is responsible for some serious health problems such as hypertension, kidney damage etc., while low value of sodium cause low blood pressure, mental apathy, and depression [68]. The concentration of sodium ion present in water can be measured by using ion chromatograph and flame photometer.

### **1.4.8 Potassium**

The main sources of potassium ions in water is weathering of mineral. Again, uses of potash fertilizers cause potassium contamination of water like sodium ion for normal body functions, potassium ion is also very important. Heart problem, hypertension are caused by low concentration of  $\text{K}^+$  [69]. The concentration of potassium ion present in water also can be measured by using ion chromatograph and flame photometer.

### **1.4.9 Calcium**

Drinking water should contain appropriate amount of calcium ions. Leaching of minerals present in soil and rocks is the main reason for the presence of calcium in ground water. Ion chromatograph, flame photometry and conventional titrimetry are used to measure

the concentration of calcium ion present in drinking water.

#### **1.4.10 Magnesium**

Magnesium in water causes hardness. The main source of magnesium in water is the leaching of magnesium containing rocks. Although  $Mg^{2+}$  is important for enzyme activation in living organism but it causes nausea, muscular neuropathy and paralysis in human body, when the concentration of  $Mg^{2+}$  is high [70]. Ion chromatograph, flame photometry and conventional titrimetry are used to measure the concentration of magnesium ion present in drinking water.

#### **1.4.11 Iron**

The role of iron in all living organisms is very important. The main source of iron in ground water is leaching of ferruginous minerals. The concentration of iron present in water can be measured by using UV-Visible spectrophotometer, atomic absorption spectroscopy, ion chromatography etc.

#### **1.4.12 Arsenic**

The impact and the source of arsenic in our body at higher concentration ( $>0.05$  mg/L) have already been discussed in this chapter. The concentration of arsenic in water can be measured by both ion chromatograph and atomic absorption spectrophotometer.

#### **1.4.13 Fluoride**

The impact and the source of fluoride in our body at higher concentration ( $>1.5$  mg/L) have already been discussed in this chapter. The concentration of fluoride in water can be measured by spectrophotometry, ion chromatograph and ion selective electrode.

#### **1.4.14 Chloride**

Chloride concentration in ground water is the measure of water pollution by sewage. Although sediments, sewages and industrial effluents are the main sources of chloride in river and sea water, another probable sources of chloride in ground water is the leaching of chloride containing minerals like apatite. The concentration of chloride in water can be measured by ion chromatograph.



**1.4.14 Nitrate**

Due to the excessive use of nitrogenous fertilizers as nitrate in soil to increase the production of agriculture ground water may become contaminated with nitrate [71]. In rainy seasons nitrate concentration in ground water increases because of loosely bound to soil and hence it is expected to be more in runoff. In higher concentrations, nitrate may produce a disease in infants known as methemoglobinemia [72]. The concentration of nitrate in water can be measured by ion chromatograph.

**1.4.15 Phosphate**

The main cause of phosphate contamination of groundwater is uses of phosphate containing fertilizers and detergents [73]. The concentration of phosphate in water can be measured by ion chromatograph [74,75] and gravimetry.

**1.4.16 Sulfate**

The main causes of sulfate contamination of groundwater are oxidation of sulfide minerals, farming and industrial sewage and human and animal waste [76]. The concentration of sulfate in water can be measured by ion chromatograph [74,75] and gravimetry.

**1.5 Different practices adopted for removal of Fluoride and Arsenic**

In case of fluoride and arsenic in drinking water, WHO and BIS have recommended the maximum permissible limits. So it is important to maintain fluoride and arsenic standard of drinking water. A variety of methods like coagulation and precipitation [77], adsorption [78], ion-exchange methods [52], reverse osmosis based membrane filtration, nanofiltration [52] etc have been adopted. Among these methods, adsorption process is the most promising for removal of fluoride and arsenic from drinking water due to greater accessibility, low cost, simple operation, availability of wide range of adsorbents.

**1.5.1 Adsorption phenomena of fluoride and arsenic from water**

Adsorption from aqueous solutions means the accumulation of solute by physical/chemical forces to the surface of an adsorbent. Adsorption may be physical or

chemical. If the adsorption interaction between solute-adsorbent is weak van der Waals forces then the adsorption is physical; but in case of chemical adsorption, there will be strong solute-adsorbent bonding. By adsorption process we can remove the contaminants like fluoride and arsenic from water through using suitable adsorbent. The amount of materials adsorbed by an adsorbent depends on some parameters such as temperature of the experiment, pH of the solution, concentration of solute, amount of adsorbent etc. The adsorption data obtained at equilibrium are analyzed with the help of the linear mathematical equations of various adsorption isotherms and kinetics models. The following equations (1) and (2) were used for calculation of percentage removal (E) and removal capacity ( $q_e$ ).

$$E = \frac{C_o - C_e}{C_o} \times 100 \quad (1)$$

$$q_e = \frac{C_o - C_e}{W_m} \times V \quad (2)$$

Where, initial and equilibrium concentrations are denoted by  $C_o$  and  $C_e$  respectively.  $W_m$  is the mass of adsorbent in gram and  $V$  is the volume of treated fluoride solution in litre.

### 1.5.1.a Adsorption kinetics

Adsorption kinetics study is an important study which gives us most valuable information about an adsorption process. From an adsorption study we can know about the rate at which a specific solute (adsorbate) is accumulated on the surface of the adsorbent, about the binding force between adsorbent and adsorbate i.e., whether the adsorption process is a physical or chemical. For the study of adsorption kinetics, the experimental system must have to reach equilibrium stage. There are four kinetics models namely pseudo-first order, pseudo-second order, Elovich model and Intra particle diffusion model to describe the adsorption process.

#### Pseudo-first order kinetic

Pseudo-first order reaction means a reaction which is not first-order naturally but made first order by increasing or decreasing the concentration of the other reactant. It is the earliest kinetic model for the adsorption of liquid-solid system. This model assumes physical process involving van der Waals forces of interactions [79]. Adsorbate uptake capacity ( $q$ ) of adsorbent is the basis of pseudo-first order kinetic rate equation [80]. The integrated form of pseudo first-order rate equation is:

$$\log(q_e - q_t) = \log q_e - k_1(t/2.303) \quad (3)$$

Where  $Q_e$ ,  $Q_t$  are the adsorbate adsorbed capacity at equilibrium and at time  $t$ . First order rate constant  $k_1$  can be calculated by plotting the value of  $\log(q_e - q_t)$  versus  $t$ . In case of pseudo first order kinetic equation, the parameter  $\log(q_e)$  may or may not be equal to the intercept of the plot of  $\log (q_e - q_t)$  versus  $t$  [81].

### **Pseudo-second order kinetic**

The pseudo-second order kinetic model [82] commonly describe the chemisorptions mechanism in which sharing or exchange of electrons takes place. This model assumes the proportionality between the rate constant and the occupied active adsorption sites

The integrated form of pseudo-second order rate equation is:

$$t/q_t = [1/(k_2 q_e^2)] + t/q_e \quad (4)$$

Here,  $k_2$  represent the second order rate constant.  $k_2$  and  $q_e$  can be determined from the linear of  $t/q_t$  vs  $t$ .

### **Elovich model**

Elovich model describes the chemical adsorption mechanism [83]. Elovich equation can be represented by the equation (5) and useful for energetically heterogeneous solid surface.

$$q_t = 1/b[\ln(ab)] + 1/b[\ln t] \quad (5)$$

Where  $b$  and  $a$  are the Elovich constant and initial adsorption rate respectively. If the adsorption follows Elovich model then a linear plot will be obtained from where  $b$  and  $a$  can be determined.

### **Intra-particle diffusion model**

In liquid-solid system, Weber and Morris proposed the “Intra Particle Diffusion” model to link the adsorption capacity  $q$  with time  $t$  and the boundary layer  $C$ . According to this model, intra particle diffusion is the only rate controlling step [84], as from the bulk of the solution, the solutes are transported into the surface of adsorbent. The kinetic equation for the intraparticle diffusion model is:

$$q_t = k_d t^{1/2} + C \quad (6)$$

Where  $k_d$  is the intra particle diffusion constant. From equation (6), a linear plot ( $q_t$  vs  $t^{1/2}$ ) will be obtained from where  $k_d$  and  $C$ , the thickness of boundary layer can be calculated [85,86,87].

### 1.5.1.b Adsorption isotherms

An adsorption isotherm is an equation which represent the relation between the amount of adsorbate adsorbed on the surface of the adsorbent and the equilibrium concentration of the adsorbate in the solution at a given temperature. In order to know the important information such as effectiveness of the adsorbent towards the specific solute, adsorption process etc., Langmuir isotherm model, Freundlich isotherm model and Tamkin isotherm model have been used.

#### Langmuir adsorption isotherm

In 1916, Irving Langmuir proposed a theoretical model for the adsorption of gaseous molecules onto solid surface at a fixed temperature and still retains in the same position for physisorption as well as chemisorptions process for both the adsorption of gases onto solid surfaces and solutes onto solid surfaces in solution systems. On the basis of some important assumptions, the American scientist I. Langmuir [88] derived an equation, which is called Langmuir adsorption isotherm. The important assumptions are:

1. Only a fixed number of adsorption sites are available on the adsorbent surface, all of which have the same energy, i.e., homogeneous surface energy.
2. Adsorption processes are homogeneous.
3. Adsorption is reversible.
4. Monolayer adsorption occurs.
5. No interaction between the adsorbate species.

The linear form of Langmuir equation is

$$C_e/q_e = C_e/q_m + 1/(bq_m) \quad (7)$$

Here, the concentration of solute (adsorbate) in the bulk solution after adsorption is  $C_e$  in mg/L and the adsorption capacity of the adsorbent is  $q_e$  in mg/g. The Langmuir maximum adsorption capacity  $q_m$  and equilibrium constant  $b$  can be calculated from the linear plot of  $C_e/q_e$  vs  $C_e$ . The favourability of Langmuir adsorption isotherm is determined from the dimensionless constant separation factor or equilibrium parameter  $R_L$ .  $R_L$  is expressed as the relation between the initial concentration of the solute  $C_o$  and the Langmuir constant  $b$  as follows:

$$R_L = 1/(1+bC_0) \quad (8)$$

The  $R_L$  value gives the information about the adsorption process [89]. When the value of  $R_L$  is in between 0 and 1 (i.e.,  $0 < R_L < 1$ ), the adsorption is Favourable; but the value of  $R_L > 1$  means the adsorption is Unfavourable.

### Freundlich adsorption isotherm

This adsorption isotherm was first suggested by Boedecker in 1895 and latter enhanced to account for simple adsorption isotherm by Freundlich [90]. This isotherm generally explains the adsorption behaviour of heterogeneous surface [91]. The linear form of Freundlich adsorption isotherm is

$$\text{Log } q_e = \text{log } K_f + (1/n) \text{log } C_e \quad (9)$$

From this linear equation, by plotting of  $\log q_e$  vs  $\log C_e$ , Freundlich adsorption constant i.e., the adsorption capacity of adsorbent  $K_f$  and the intensity of adsorption  $n$  have been calculated. For favourable adsorption, the values of  $n$  in between 1 and 10 [92].

### Temkin adsorption isotherm

Temkin and Pyzhev derived an adsorption isotherm by assuming that, the heat of adsorption normally decreases linearly rather than logarithmic with surface coverage from the Langmuir adsorption isotherm. That is, Temkin isotherm model considered the effects of indirect adsorbent-adsorbate interactions on adsorption [93,92,94].

The linear form of Temkin equation is:

$$q_e = B_T \ln A_T + B_T \ln C_e \quad (10)$$

The Temkin isotherm constant  $A_T$  (L/g) and  $B_T$  (where  $B_T = RT/b_T$ ,  $b_T$  is the Temkin constant and  $R$  is the gas constant) can be calculated from the intercept and the slope of the plot of  $q_e$  against  $\ln C_e$ .

### 1.5.1.c Fitness of the adsorption model

#### Chi-square analysis

A chi-square analysis ( $\chi^2$ ) test is a statistical hypothesis and is used to determine whether there is a significant difference between the expected frequencies and the observed frequencies. Thus to determine suitable adsorption model, the  $\chi^2$ -square analysis has been used. The mathematical statement for chi-square analysis is,

$$\chi^2 = \sum \frac{[q_e(\text{exp}) - q_e(\text{cal})]^2}{q_e(\text{exp})} \quad (11)$$

Here  $q_e$  is the adsorption capacity. Its experimental value [ $q_e(\text{exp})$ ] is obtained from the experimental adsorption capacity (mg/g) at equilibrium and calculated value [ $q_e(\text{cal})$ ] is obtained from the sorption model.  $\chi^2$  will be a small number, if the experimental adsorption

capacity and calculated adsorption capacity is almost same. A lower value of  $\chi^2$  generally indicate a good fit between experimental and calculated data [95].

### Coefficient of determination ( $R^2$ )

The coefficient determination ( $R^2$ ) is the square of a correlation coefficient. It explains the amount of variance accounted for in the relationship between two or more variables. The value of  $R^2$  is in between 0 and 1. If  $R^2 = 0$ , the line has no explanatory value and if  $R^2 = 1$ , the line variable explains 100% of the variation in the response variable.

#### 1.5.1.d Thermodynamic study

From the study of effect of temperature, we can able to know about the adsorption nature whether it is an exothermic or endothermic process. By using the following equations (12), (13) and (14), the thermodynamic parameters such as change of free energy ( $\Delta G^\circ$ ), change of entropy ( $\Delta S^\circ$ ) and change of enthalpy ( $\Delta H^\circ$ ) of the adsorption process have been determined.

$$\Delta G^\circ = -RT \ln K_d \quad (12)$$

Here the distribution coefficient  $K_d = q_e / C_e$  and R is the gas constant.

$$\ln K_d = \Delta S^\circ / R - \Delta H^\circ / RT \quad (13)$$

The equation (13) is linear one, so from the linear plot of  $\ln K_d$  versus  $1/T$ , the values of  $\Delta H^\circ$  and  $\Delta S^\circ$  have been calculated. The  $\Delta G^\circ$  value is calculated by the following equation:

$$\Delta G^\circ = \Delta H^\circ - T \Delta S^\circ \quad (14)$$

### 1.6 Importance of the study

As said earlier the presence of arsenic and fluoride in ground water is becoming a serious problem in all over the world. In India specially in the state of Assam, some districts are badly affected by only arsenic and while some are affected by fluoride. Golaghat district of Assam is in such a position that the eastern side is surrounded by recognized arsenic affected area especially Titabar area of Jorhat district and the west-south portion is surrounded

by recognized fluoride affected area of Nagaon and Karbi-Anglong district. Therefore a survey of ground water quality of entire Golaghat district is very essential to know how these contaminants may be distributed within the district. The study area of entire Golaghat district is shown in the Fig 1.7.

Side by side the development of processes for their cost effective removal is also equally important. One way of developing cost effective process is to look for local cheaper resources as suitable adsorbents. So in the present work, it has been tried to develop adsorbents from (i) the carbon produced at the time of preparation of banana based edible alkali (Assamese *Kol Khar*) from *Musa balbasiana* plant, a variety of indigenous banana plant and (ii) the surface modified Kanaighat sand obtained abundantly in the Kanaighat area of Golaghat district for adsorption of fluoride and arsenic from water and their respective systemic scientific study.

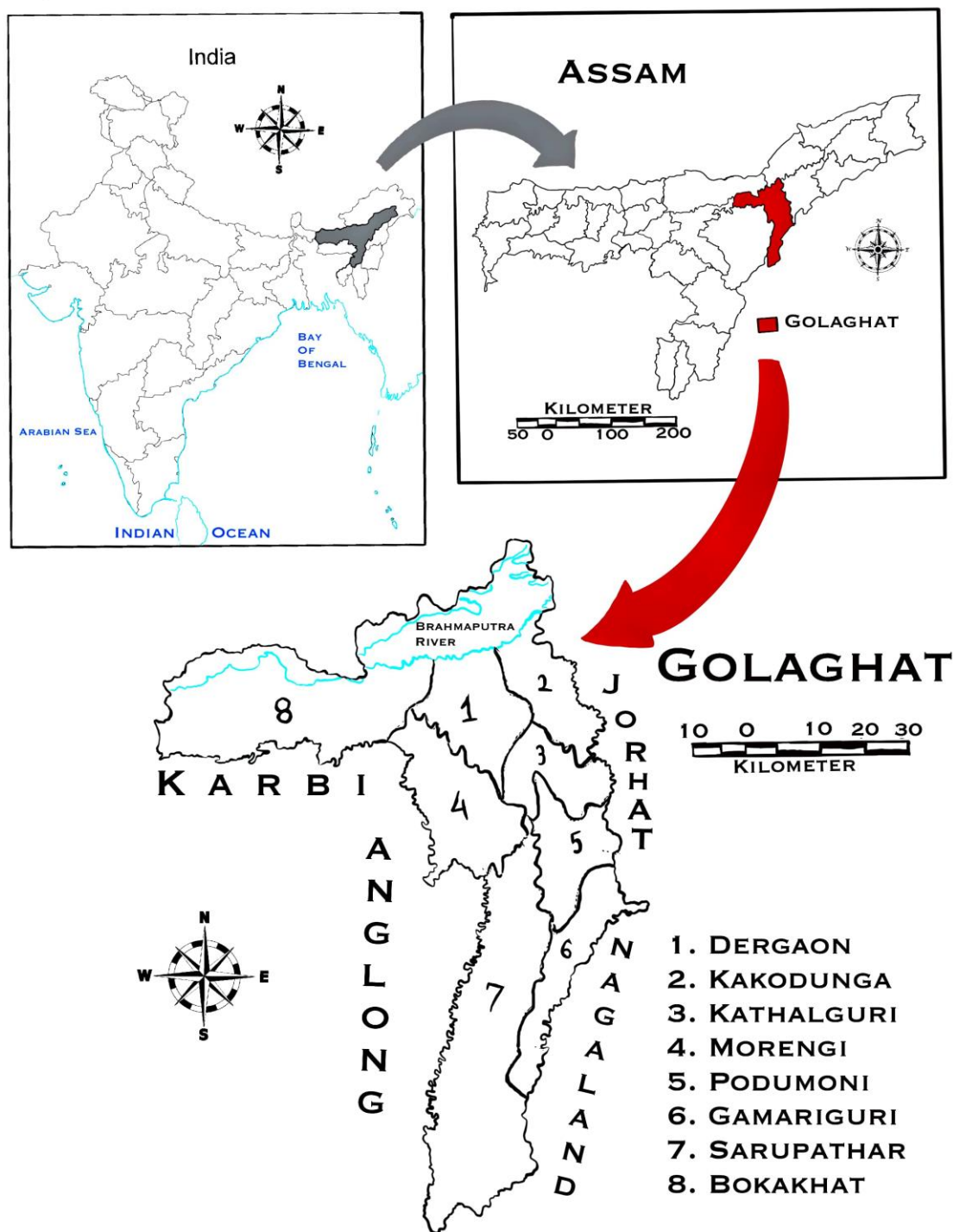


Fig 1.7: Study sites showing six blocks of Golaghat district, Assam



**1.7 Aim and objectives of the work:**

In this thesis, it is aimed to assess the groundwater quality of Golaghat district and its peripheral areas with reference to fluoride and arsenic and to develop a new method for fluoride and arsenic removal using local materials which may be very useful in laboratory and field condition in terms of economic and environmental points of view. The main objectives of the work can be divided as follows-

1. To find out the concentration of fluoride in the samples of ground water collected from peripheral areas of Golaghat district e.g. Burra Pahar and adjoining areas.
2. To find out the concentration of arsenic in the samples of ground water collected from different parts of Golaghat district e.g. Gamari Guri Block and adjoining areas.
3. To prepare and characterize the different adsorbents from local materials for Fluoride and Arsenic and their performance evaluation by using analytical techniques like AAS, SEM, FTIR, TGA/DTA/DSC etc.
4. To optimize the arsenic and fluoride removal capacity with such selected adsorbents.

**References**

- [1] Chakraborti D., Das B., and Murrill M.T. (2011) Examining India's groundwater quality management. *Environmental Science and Technology*. 45 (1) 27-33.
- [2] Paul R., Brindha K., Gowrisankar G., Tan M.L., and Singh M.K. (2019) Identification of hydrogeochemical processes controlling groundwater quality in Tripura, Northeast India using evaluation indices, GIS, and multivariate statistical methods. *Environmental Earth sciences*. 78: 470 <https://doi.org/10.1007/s12665-019-8479-6>.
- [3] Smedley P.L., and Kinniburgh D.G. (2002) A review of the source, behavior and distribution of arsenic in natural waters. *Applied Geochemistry*. 17(5), 517–568.
- [4] Bohrer D., Becker E., Nascimento P., Moerschbaecher V., Carvalho L. De, and Silva M.M. Da. (2006) Arsenic release from glass containers by action of intravenous nutrition formulation constituents. *International Journal of Pharmaceutics*. 315, 24-29.
- [5] Patel K.S., Shrivastava K., Brandt R., Jakubowski N., Corns W., and Hoffmann P. (2005) Arsenic contamination in water, soil, sediments and rice of India. *Environ Geochem Health*. 27:131–145.
- [6] Kimambo V., Bhattacharya P., Mtalo F., Mtamba J., and Ahmad A. (2019) Fluoride occurrence in groundwater systems at global scale and status of defluoridation – state of the art. *Groundw. Sustain. Dev.* 9, 100223. <https://doi.org/10.1016/j.gsd.2019.100223>.
- [7] International Agency for Research on Cancer (IARC) (2004). Summaries & evaluations: Arsenic in drinking-water (group 1) *Int. Agency Res. Cancer. IARC Monogr. Eval. Carcinog. Risk to Humans* vol. 84, p. 39. <http://www.inchem.org/documents/iarc/vol84/84-01-arsenic.html>, Accessed date: 23 August 2019.
- [8] World Health Organization (WHO) (2017) *Guidelines for Drinking-water Quality: Fourth Edition Incorporating the First Addendum*.
- [9] WHO (1993). *Guidelines for drinking water quality*. Geneva: World Health Organization <http://www.lenntech.com/WHO's-drinking-water-standards.htm>. Accessed 28 Feb 2010.
- [10] Bureau of Indian Standards (BIS) (1991). 10500:1991, Second Revision ICS No. 13.060.20. [http://www.bis.org.in/sf/fad/FAD25\(2047\)C.pdf](http://www.bis.org.in/sf/fad/FAD25(2047)C.pdf). Accessed 6 Jan 2010.

- [11] Jagtap, S., Yenkie, M. K., Labhsetwar, N., and Rayalu, S. (2012). Fluoride in drinking water and defluoridation of water. *Chemical Reviews*. 112, 2454–2466.
- [12] Singh R., and Maheswari R.C. (2001) Defluoridation of drinking water- a review, *Ind. J. Environ. Protec.* 21(11) 983-991.
- [13] Johnson A. C., and Bretzler A. (2015). *Water Resource Quality (WRQ)-Geogenic Contamination Handbook, Addressing Arsenic and Fluoride in Drinking Water (EAWAG)* Swiss Federal Institute of Aquatic Science and Technology Editors Johnson, A. C., & Bretzler, A.
- [14] Gandhi N., Sirisha D., Asthana S., Manjusha A. (2012) Adsorption studies of fluoride on multani matti and red soil. *Res. Journal of Chemical Sciences*. 2, 32–37.
- [15] Brindha K., and Elango L. (2011) Fluoride in groundwater: causes, implications and mitigation measures. In: Monroy, S.D.(Ed.), *Fluoride properties applications and environmental management*, 111–136. [https://www.novapublishers.com/catalog/product\\_info.php?products\\_id=15895](https://www.novapublishers.com/catalog/product_info.php?products_id=15895).
- [16] Feenstra L., Vasak L., and Griffioen J. (2007) Fluoride in groundwater: Overview and evaluation of removal Methods, *International Groundwater Resources Assessment Centre Report nr. SP 2007-1*, 1-21.
- [17] Bhatnagar A., Kumar E., and Sillanpaa M. (2011) Fluoride removal from water by adsorption: A review. *Chem. Eng. J.* 171, 811–840.
- [18] Khatibikamal V., Torabian A., Janpoor F., and Hoshyaripour G. (2010) Fluoride removal from industrial wastewater using electrocoagulation and its adsorption kinetics. *J. Hazard. Mater.* 179, 276–280.
- [19] Mourad N.M., Sharshar T., Elnimr T., and Mousa M.A. (2009) Radioactivity and fluoride contamination derived from a phosphate fertilizer plant in Egypt. *Appl. Radiat. Isot.* 67, 1259–1268.
- [20] Habuda-Stanić M., Ravancic M. E., and Flanagan A. (2014) A review on adsorption of fluoride from Aqueous solution. *Materials*. 7, 6317-6366.
- [21] Fan C.-S., AND Li K.-C. (2013) Production of insulating glass ceramics from thin film transistor-liquid crystal display (TFT-LCD) waste glass and calcium fluoride sludge. *J. Clean. Prod.* 57, 335–341.

- [22] Ponsot I., Falcone R., AND Bernardo E. (2013) Stabilization of fluorine-containing industrial waste by production of sintered glass-ceramics. *Ceram. Int.* 39, 6907–6915.
- [23] Shen F., Chen X., Gao P., Chen G. (2003) Electrochemical Removal of Fluoride Ions from Industrial Wastewater, *Chem. Eng. Sci.* 58(3), 987.
- [24] Drouiche N., Aoudj S., Hecini M., Ghaffour N., Lounici H., and Mameri N. (2009) Study on the treatment of photovoltaic wastewater using electrocoagulation: Fluoride removal with aluminium electrodes—Characteristics of products. *J. Hazard. Mater.* 169, 65–69.
- [25] Drouiche N., Djouadi-Belkada F., Ouslimane T., Kefaifi A., Fathi J., and Ahmetovic A. (2013) Photovoltaic solar cells industry wastewater treatment. *Desalin. Water Treat.* 51, 5965–5973.
- [26] Hu C. Y., Lo S. L., Kuan W. H., and Lee Y. D. (2005) Removal of fluoride from semiconductor wastewater by electrocoagulation-flotation. *Water Research.* 39, 895–901.
- [27] Warmadewanthi B., and Liu J. C. (2009) Selective separation of phosphate and fluoride from semiconductor wastewater. *Water Sci. Technol.* 59, 2047–2053.
- [28] Joint Research Centre (JRC): Seville, Spain , Best Available Techniques (BAT) Reference Document for Waste Incineration; European Integrated Pollution Prevention and Control Bureau (EIPPCB), Institute of Prospective Technological Studies (IPTS), 2006.
- [29] Rao, C. R. N. (2003) Fluoride and Environment—A Review. In *Proceedings of the Third International Conference on Environment and Health*, Chennai, India, 15–17 December 2003; pp. 386–399.
- [30] Kut K. M. K., Sarswat A., Srivastava A., Charles U., Pittman Jr C. U., and Mohan D. (2016). A review of fluoride in african groundwater and local remediation methods. *Groundwater for Sustainable Development.* 2-3, 190–212.
- [31] Khan S. A., Ali N., and Srivastava Y. (2015) Comparative Study of Defluoridation from Water using Waste Materials as Adsorbents— A Review. *IJIET.* 6, 159-164.
- [32] Jiménez L. V., Fregozo C. S., Beltrán M. L. M., Coronado O. G., and Vega M. I. P. (2011) Effects of the fluoride on the central nervous system. *Neurología.* 26, 297–300.

- [33] Mandinic Z., Curcic M., Antonijevic B., Lekic C.P., and Carevic M. (2009) Relationship between fluoride intake in Serbian children living in two areas with different natural levels of fluorides and occurrence of dental fluorosis. *Food and Chemical Toxicology*. 47, 1080 –1084.
- [34] Singh B., Gaur S., and Garg V.K. (2007) Fluoride in drinking water and human urine in Southern Haryana, India. *Journal of Hazardous Materials*. 144, 147 –151.
- [35] Shakoor M.B., Nawaz R., Hussain F., Raza M., Ali S., Rizwan M., Oh S.-E.E., and Ahmad S. (2017) Human health implications, risk assessment and remediation of ascontaminated water: a critical review. *Sci. Total Environ*. 601–602, 756–769.  
<https://doi.org/10.1016/j.scitotenv.2017.05.223>.
- [36] Mumtaz N., Pandey G., and Labhasetwar P.K. (2015) Global fluoride occurrence, Available technologies for fluoride removal, and electrolytic defluoridation: a review. *Crit. Rev. Environ. Sci. Technol*. 45, 2357–2389. <https://doi.org/10.1080/10643389.2015.1025638>.
- [37] Zhang J., Chen N., Tang Z., Yu Y., Hua Q., and Feng, C. (2015) A study of the mechanism of fluoride adsorption from aqueoussolutions onto Fe-impregnated chitosan. *Physical Chemistry Chemical Physics*. 17, 12041–12050.
- [38] Ayoob S., and Gupta A.K. (2006) Fluoride in Drinking Water: A Review on theStatus and Stress Effects, *Crit. Rev. Environ. Sci. Technol*. 36 (6),433.
- [39] Saikia J. (2019) Synthesis and coating of nano particle loaded carbon on ceramic barriers prepared from local resources for treatment of contaminated water.-Ph.D Thesis submitted to AcSIR.
- [40] Sushella A.K. (2001) A treatise on Fluorosis, Fluorosis Research and Rural Development Foundation, New Delhi. 15, 2001.
- [41] Dutta R. K., Saikia G., Das B., Bezboruah C., Das H. B., and Dube S. N. (2006) Fluoride contamination in ground water of Central Assam, India. *Asian Journal of Water Environment and Pollution* 2(3), 93–100.
- [42] Kakoty P., Barooah P.K., Baruah M.K., Goswami A., Borah G.C., Gogoi H.M., Ahmed F., Gogoi A., and Paul A.B. (2008) Fluoride and endemic fluorosis in Karbianglong district of Assam, India. *Fluoride*. 41, 42-45.
- [43] Nath S.K., Dutta R.K. (2010) Fluoride removal from water using crushed limestone. *Indian J. Chem. Technol*. 17:120–125.

- [44] Das D. P., Das J., and Parida K. (2003) Physicochemical characterization and adsorption behavior of calcined Zn/Al hydrotalcite-like compound (HTLc) towards removal of fluoride from aqueous solution. *Journal of Colloid and Interface Sci.* **261**: 213–220.
- [45] Temraz H.N.H.J. (2014) Slide share. <https://www.slideshare.net/BakrYou/arsenic-poisoning-43781240>.
- [46] Kruger T., Hollander H.M., Boochs P-W, Billib M., Stummeyer J., and Harazim B. (2007) In situ remediation of arsenic at a highly contaminated site in Northern Germany. In: GQ07: Securing Groundwater Quality in Urban and Industrial Environments. Proc. 6th International Groundwater Quality Conference held in Fremantle, Western Australia, 2–7 December 2007.
- [47] Wang Y., and Tsang D.C. (2013) Effects of solution chemistry on arsenic(V) removal by low-cost adsorbents. *J Environ Sci (China)*. 25(11): 2291 -8.
- [48] Nickson R., Sengupta C., Mitra P., Dave S. N., Banerjee A. K., Bhattacharya A., et al. (2007) Current knowledge on the distribution of arsenic in groundwater in five states of India. *Journal of Environmental Science and Health Part A*, 42, 1707–1718.
- [49] Mukherjee A., Sengupta M.K., Hossain M.A., Ahamed S., Das B., Nayak B., Lodh D., Rahman M.M., and Chakraborti D. (2006) Arsenic contamination in groundwater: a global perspective with emphasis on the Asian scenario. *J Health Populat Nutr*. 24:142–163.
- [50] Mohammadi A.A., Yousefi M., Yaseri M., Jalilzadeh M., and Mahvi A.H. (2017) Skeletal fluorosis in relation to drinking water in rural areas of West Azerbaijan, Iran. *Sci. Rep.* 7, 4–10. [https://doi.org/https://doi.org/10.1038/s41598-017-17328-8](https://doi.org/10.1038/s41598-017-17328-8).
- [51] Limon-Pacheco J.H., Jimenez-Cordova M.I., Cardenas-Gonzalez M., Sanchez Retana I.M., Gonsbatt M.E., and Del Razo, L.M. (2018) Potential co-exposure to arsenic and fluoride and biomonitoring equivalents for Mexican children. *Ann. Glob. Heal*, 84, 257–273.
- [52] Jana P. (2012) Removal of arsenic(III) from water with a new solid-supported thiol.- Thesis and Dissertations--Chemistry.
- [53] Shukla S.C. (2008) Development, safety evaluation and comparative studies of low cost adsorbent technology for arsenic removal from drinking water. Ph D thesis submitted to Hemwatinandan Bahuguna Garhwal University.

- [54] Kumari P., Sharma P., Srivastava S. and Srivastava M.M. (2005) Arsenic removal from the aqueous system using plant biomass: a bioremedial approach, *Journal of Industrial Microbiology and Biotechnology*. 32(11–12), 521–526.
- [55] Chiban M., Zerbet M., Carja G., and Sinan F. (2012) Application of low-cost adsorbents for arsenic removal: a review, *Journal of Environmental Chemistry and Ecotoxicology*, 4(5), 91–102.
- [56] Thakur J.K., Thakur R.K., Ramanathan A.L., Kumar M., and Singh S.K. (2011) Arsenic contamination of groundwater in Nepal-An overview. *Water*. 3, 1-20; doi:10.3390/w3010001.
- [57] Ahmed A., Wens P., Baken K., Waal L.de., Bhattacharya P., and Stuyfzand P. (2020) Arsenic reduction to < 1 µg/L in Dutch drinking water. *Environment International*. 134-105253.
- [58] Garai R., Chakraborti A. K., Dey S. B., and Saha K. C. (1984). Chronic arsenic poisoning from tubewell water. *Journal of Indian Medical Association*, 82, 34–35.
- [59] Singh A. K. (2004). Arsenic contamination in groundwater of North eastern India. In *Proceedings of 11th national symposium on hydrology with focal theme on water quality* (pp. 255–262). Roorkee: National Institute of Hydrology.
- [60] Pennesi C., Veglio F., Totti C., Romagnoli T., and Beolchini F. (2012) Nonliving biomass of marine macrophytes as arsenic(V) biosorbents, *Journal of Applied Phycology*. 24(6), 1495–1502.
- [61] Kamsonlian S., Suresh S., Majumder C.B., and Chand S. (2012) Biosorption of arsenic from contaminated water onto solid *Psidium guajava* leaf surface: equilibrium, kinetics, thermodynamics, and desorption study, *Bioremediation Journal*. 16(2), 97–112.
- [62] Singh A. K. (2006). Review article-Chemistry of arsenic in groundwater of Ganges–Brahmaputra river basin. *Current Science*. 91, 599–605.
- [63] Chakraborti D., Sengupta M.K., Rahman M.M., Ahamed S., Chowdhury U.K., Hossain M.A. (2004) Groundwater arsenic contamination and its health effects in the Ganga–Meghna–Brahmaputra plain, *J. Environ. Monit.* 6 (6) 74–83.
- [64] Chetia M., Chatterjee S., Banerjee S., Nath M.J., Singh L., and Srivastava R.B. (2011) Groundwater arsenic contamination in Brahmaputra river basin: A water quality assessment in Golaghat (Assam), India. *Environ Monit Assess.* 173, 371-85.

- [65] World Health Organization (WHO) (2011) Guidelines for drinkingwater quality, 4th edn. World Health Organization, Geneva.
- [66] Raghunath R., Sreedhara Murthy T.R., and Raghavan B.R. (2001) Spatial distribution of pH, EC and total dissolved solids of Nethravathi riverbasin, Karnataka state, India. *Pollut Res.* 20(3):413–418.
- [67] IS 3025 (Part 23): 1986 Methods of sampling and test (Physical and Chemical) for water and wastewater.
- [68] WHO Regional Office for Europe, Copenhagen. (1979) Sodium, chloride and conductivity in drinking water. EURO Reports and Studies No. 2 .
- [69] Gosselin R.E., Smith R.P., and Hodge H.C. (1984) Clinical toxicology of commercial products, 5<sup>th</sup> ed. Baltimore, MD, Williams & Wilkins. ISBN: 0-683-03632-7.
- [70] Alawi A.M.Al., Majoni S.W., and Falhammar H. (2018) Magnesium and human health: perspectives and research directions. *International Journal of Endocrinology* 2018: 9041694. Doi: 10.1155/2018/9041694.
- [71] Almasri M.N. (2007). Nitrate contamination of groundwater: A conceptual management framework. *Environmental Impact Assessment Review.* 27 (3) 220-242.
- [72] Johnson C.J., Bonrud P.A., Dosch T.L., Kilness A.W., Senger K.A., Busch D.C. and Meyer M.R. (1987) Fatal outcome of methemoglobinemia in an infant. *Journal of the American Medical Association.* 257, 2796-2797.
- [73] Metzner G. (2006) Phosphate aus Wasch-und Reinigungsmitteln im kommunalen Abwasser der Bundesrepublik Deutschland. <http://www.gdch.de/strukturen/fg/wasch/had/phosphaate.pdf>.
- [74] Viswanathan V.C. (2015) Effect of river restoration and hydrological changes on surface water quality – River reachscale to catchment-scale study. Ph D. Thesis- presented to the Faculty of Science of the University of Neuchâtel to satisfy the requirements of the degree of Doctor of Philosophy in Science.
- [75] Liu F., Song X., Yang L., Zhang Y., Han D., Ma Y., Bu H. (2015) Identifying the origin and geochemical evolution of groundwater using hydrochemistry and stable isotopes in the Subei Lake basin, Ordos energy base, Northwestern China. *Hydrol. Earth Syst. Sci.* 19, 551–565.
- [76] Miao Z., Brusseau M.L., and Johnson B. (2012) Sulfate reduction in groundwater: characterization and applications for remediartion. *Environmental geochemistry and health.* 34(4), 539-550.



- [77] Waghmare S. S., and Arfin T. (2015) Fluoride Removal from Water By Calcium Materials: A State-Of-The-Art Review. *Intl J of Innovative Res in Sci, Engg and Technol*, 4(9):2347-6710.
- [78] Loganathan P., Vigneswaran S., Kandasamy J., and Naidu R. (2013) Defluoridation of drinking water using adsorption processes. *J Hazard Mater*, 248–249, 1–19.
- [79] Chang J., Ma J., Ma Q., Zhang D., Qiao N., Hu M., and Ma H. (2015) Adsorption of methylene blue onto Fe<sub>3</sub>O<sub>4</sub>/activated montmorillonite nanocomposite, *Appl. Clay Sci.* 119, 132-140. Doi:10.1016/j.clay.2015.06.038.
- [80] Lagergren S. (1898). About the theory of so called adsorption of soluble substances. *Kungliga Svenska Vetenskapsakademiens Handlingar*, 24, 1–39.
- [81] Gandhi N., Sirisha D., and Sekhar K.B.C. (2016) Adsorption of fluoride (F-) from aqueous solution by using pineapple (*Ananas comosus*) peel and orange (*Citrus sinensis*) peel powders. *International Journal of Environmental Bioremediation & Biodegradation*, 4(2):55-67.
- [82] Ho Y. S., and McKay G. (1999) Pseudo-second order model for sorption processes. *Process Biochemistry*. 34(5), 451–465.
- [83] Wu F.C., Tseng R.L. and Juang R.S. (2009) Characteristics of Elovich equation used for the analysis of adsorption kinetics in dye-chitosan systems. *Chemical Engineering Journal*. 150 (2-3), 366-373.
- [84] Rudzinski W., and Plazinski W. (2007) Studies of the kinetics of solute adsorption at solid/solution interfaces: on the possibility of distinguishing between the diffusional and the surface reaction kinetic models by studying the pseudo-first-order kinetics. *Journal of Physical Chemistry C*, 111(41), 15100–15110.
- [85] Khal H.E., and Batis N.H. (2015) Effects of temperature on the preparation and characteristics of hydroxyapatite and its adsorptive properties toward lead. *New J Chem*. 39:3597–3607.
- [86] Saikia J., Sarmah S., Ahmed T.H., Kalita P.J., and Goswamee R.L. (2017) Removal of toxic fluoride ion from water using low cost ceramic nodules prepared from some locally available raw materials of Assam, India. *Journal of Environmental Chemical Engineering*. 5:2488–2497.
- [87] Daifullah A., Yakout S., and Elreefy S. (2007) Adsorption of fluoride in aqueous solutions using KMnO<sub>4</sub>-modified activated carbon derived from steam pyrolysis of rice straw. *Journal of Hazardous Materials*. 147(1-2), 633–643.

- [88] Langmuir I. (1918) The adsorption of gases on plane surfaces of glass, mica and platinum. *J Am Chem Soc.* 40:1361–1403.
- [89] Hameed B.H. (2009) Removal of cationic dye from aqueous solution using jackfruit peel as non-conventional low-cost adsorbent. *J Hazard Mater.* 162:344–350.
- [90] Freundlich H.M.F. (1906) Uber die adsorption in Losungen. *Z fur PhysChem (Leipzig)* 57A:385–470.
- [91] Dada A.O., Olalekan A.P., Olatunya A.M., Dada O. (2012) Langmuir, Freundlich, Temkin and Dubinin-Radushkevich Isotherms studies of equilibrium sorption of  $Zn^{2+}$  onto phosphoric acid modified rice husk. *J Appl Chem.* 3(1) 38-45.
- [92] Tan I.A.W., Ahmad A.L. and Hameed B.H. (2008) Adsorption of basic dye on high– surface–area activated carbon prepared from coconut husk: equilibrium, kinetic and thermodynamic studies, *Journal of Hazardous Materials.* 154(1– 3), 337–346.
- [93] Temkin M., and Pyzhev V. (1940) Kinetics of ammonia synthesis on promoted iron catalysts. *Acta Physicochimica URSS.* 12, 217-222.
- [94] Chiban M., Carja G., Lehotu G, and Sinan F. (2012.b) Equilibrium and thermodynamic studies for the removal of As(V) ions from aqueous solution using dried plants as adsorbents, *Arabian Journal of Chemistry.* doi: 10.1016/j.arabjc.2011.10.002.
- [95] Bhomick P.C., Supong A., Baruah M., Pongener C., Gogoi C., and Sinha D. (2019) Alizarin Red S adsorption onto biomass-based activated carbon: optimization of adsorption process parameters using Taguchi experimental design. *International Journal of Environmental Science and Technology.* Doi. Org/10.1007/s13762-019-02389-1.
- [96] Farooqi A. (2015) Arsenic and fluoride contamination - A Pakistan Perspective, Springer, ISBN 978-81-322-2297-2 (e-Book); DOI 10.1007/978-81-322-2298-9\_1.
- [97] Reddy S. (2019) Arsenic contamination in groundwater in India. *Vikaspedia (Environment).* <http://vikaspedia.in/energy/environment/known-your-environment/water/arsenic-hot-spot-in-ground-water-in-india>].
- [98] Khan K. (2016) Arsenic poisoning. Slide share. <https://www.slideshare.net/Kaleem7/arsenic-poisoning-acute-subacute-and-chronic>. Aug 23-2016.

## **CHAPTER – 2**

**Assessment of groundwater quality of the Golaghat district of Assam, India and its peripheral areas using multivariate statistical technique with special reference to the presence of higher levels of fluoride and arsenic**

## **2.1 Introduction**

Several recent reports describe that, the groundwater sources of various part of Assam state of India are contaminated by arsenic (As) and fluoride ( $F^-$ ). While, the groundwater of lower part of Assam covering mainly areas under the districts such as amalgamated Kamrup, Nagaon, Bongaigoan, Kokrajhar, Borpeta, Nalbari are contaminated by both fluoride and arsenic [1,2,3,4] the groundwater of upper part of Assam such as Sivasagar, Dibrugarh, Jorhat, Lakhimpur, Majuli and Tinsukia are contaminated by arsenic. Karbi-Anglong district of Assam is relatively free from arsenic but is highly affected by fluoride. Such an area wise categorization was done by considering the bench mark of lethality of contamination as per the scale recommended by World Health Organization where a maximum permissibility level of 1.5 mg/L is set for  $F^-$  [5] and 0.01 mg/L for As [6], in drinking water. The health effects caused by arsenic and fluoride were discussed separately in the Chapter-1. Recent publications report that, co-contamination of fluoride and arsenic in drinking water can affect the Intelligence Quotient levels leading to the decrease of intellectual functionality among children [7,8,9,10].

Since, Golaghat district in Assam is sandwiched between  $F^-$  affected Karbi-Anglong and As affected Jorhat district, the assessment of groundwater quality with special reference to these two contaminants in Golaghat district and its peripheral area in the state of Assam has been thoroughly investigated, attempts were also made to locate places where both As and  $F^-$  could be simultaneously present.

## **2.2 Materials and methods**

### **2.2.1 Study Area**

As stated above Golaghat is a district with an area of 3,502 km<sup>2</sup>, situated in the upper side of state of Assam along the southern bank of river Brahmaputra and forms a part of the vast alluvial plains of the state [11]. The Kakodonga tributary of Brahmaputra is the eastern border of Golaghat district and sharing with Jorhat district. Dhansiri is a southern tributaries of Brahmaputra flowing from south to north in the Golaghat district, constitutes the main surface water runoff routes of the district. Dhansiri originate from Laisang peak of nearby Nagaland and falls in the river Brahmaputra near Kaziranga national park.

The district has a sub-tropical humid climate. There is a variation in the intensity of rainfall from east to west and from north to south part of the district. During winter season, the average temperature varies from 6° to 14° C and during summer season, it varies from 29° to 36°C [12].

There is a prosperous ecological environment in the district. As per Groundwater Information Booklet 2008, percentage of total area occupied by forest, cultivated land and fallow land in the district is 40% cultivated land, 20% fallow land and 40% forest area. Golaghat is home to the one-horned rhinoceros which is found exclusively in this part of the world. The district shares the world-famous Kaziranga National Park with Nagaon district. The Nambor Wildlife Sanctuary is also situated in Golaghat.

The population of the district is approximately 1.1 million and constitutes 3.4% of the population of the state. The district head quarter also called Golaghat, is a town located at coordinates of 26.0° N to 27.1° N and 93.0° E to 94.18° E. It has an average elevation of 95 metres above sea level. The urban to rural population ratio in the district is 90.8:9.2. There are 8 rural block development areas namely Dergaon, Kathalguri, Podumoni, Kakodonga, Morongi, Gomariguri, Sorupathar and Bokakhat. The maps of relevant rural development blocks with respect to the larger maps of the state and the country are shown in the Figure 1.8 of the chapter 1.

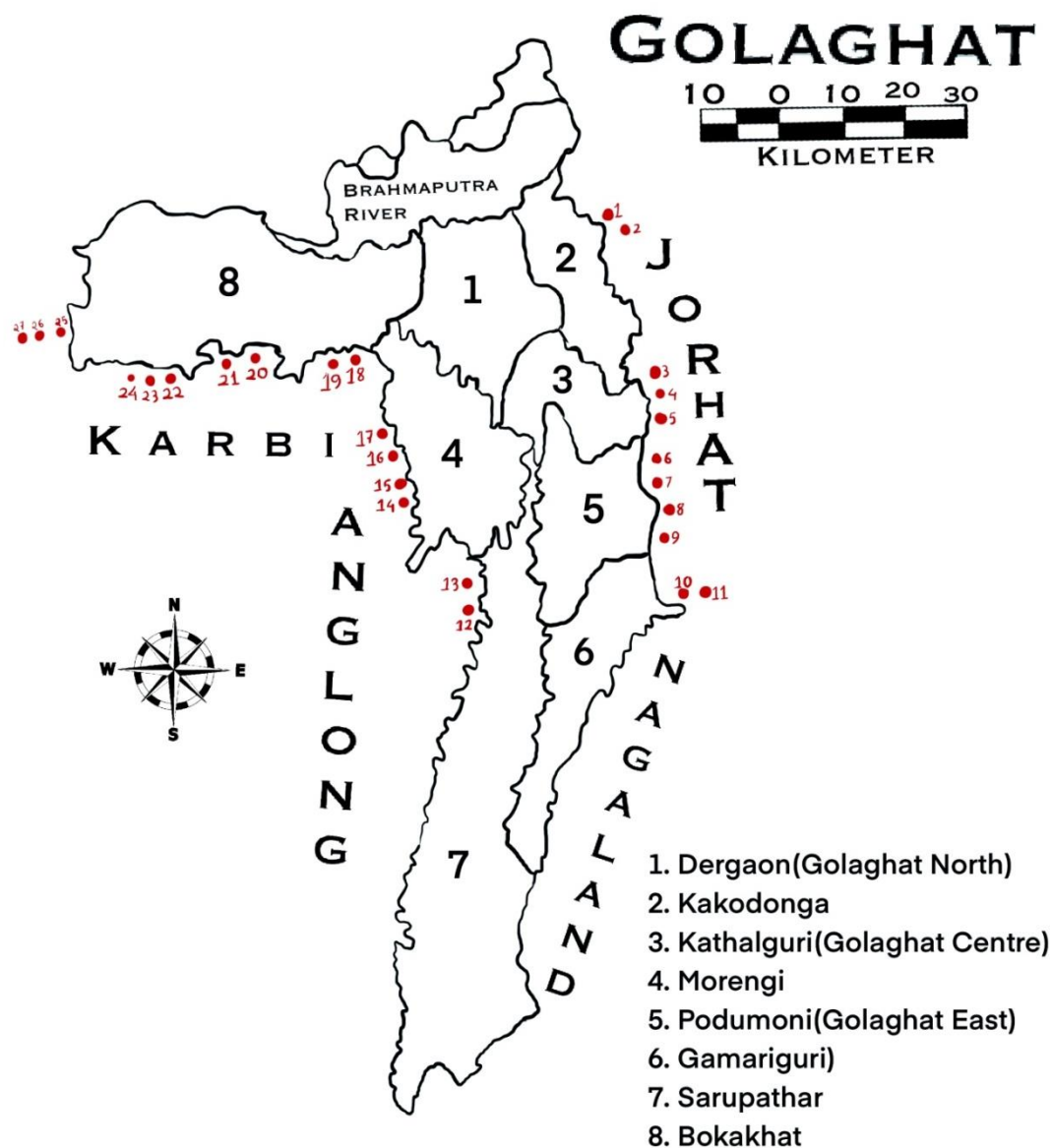


**Fig 2.1: Study sites of Golaghat district with its peripheral areas (1-27), Assam**

### 2.2.2 Sampling methodology

In Golaghat district, depending on the depth of water tables, people uses shallow hand tubewells (20-60ft depth) and deep tubewells like Tara pump (up to 180 ft depth) and Mark-II tubewells (180 ft -300 ft). The groundwater samples were collected from 247 numbers of existing tubewells of different depth (from 20 ft to 300 ft), in eight development blocks of Golaghat district just after the flood season mainly during the months of September to

November, 2017. At this time of the year water level in most of the wells are comfortably high enough to draw easily by hand or electrical pumps. Some photographs of three types of hand tubewell from which groundwater samples were collected are given in the Fig 2.2.

During sampling for washing out the stagnant water inside the tube, tube wells were operated 4-5 minutes before collection. Two sets of water samples were collected from each location in poly propylene bottles. The bottles were previously washed by 8 M nitric acid and scrupulously washed with distilled water. At the time of collection of water samples, the bottles were rinsed repeatedly with the sample water [13] again. For metal analysis the collected water samples were acidified by using 1:1 HNO<sub>3</sub> acid solution to decrease the pH below 2. Among eight development blocks of Golaghat district, 72 samples were collected from Bokakhat, 50 samples from Padumoni, 30 samples from Gamariguri, 27 samples from Morongi, 20 samples from Kakodonga, 19 samples from Kathalguri, 15 samples from Dergaon and 14 samples from Sorupathar block development area.

At the same time, 27 groundwater samples were also collected from the peripheral areas of Golaghat district (Jorhat, Karbi-Anglong and Nagaon districts). Among 27 groundwater samples collected from the peripheral areas, 11 samples were from Jorhat district, 13 samples from Karbi-Anglong district and 3 samples from Nagaon district. The different location of these points of sample collection from the peripheral areas are shown in the Fig. 2.1.



**(A). A hand tubewell pump (Mark-II); (B). A hand tubewell pump (Tara pump)**



(C). A hand tubewell of Padumoni block; (D). A hand tubewell of Bokakhat block

**Fig 2.2: Some water collection point of study area**

### 2.2.3 Sample analysis

The groundwater quality parameters such as pH, Total Hardness (TH), Bicarbonate ( $\text{HCO}_3^-$ ), Total Dissolved Solids (TDS), Electrical Conductivity (EC), concentration of various cations and anions with total arsenic and iron were determined. A previously calibrated pocket pH meter (HANNA Co) was used to measure the pH of collected water samples at the spots. Similarly, TDS and EC of water samples were also measured immediately by using pocket TDS meter (HANNA Co) and Systronics digital conductivity meter type 304 which was previously standardized by standard potassium chloride solution. The cations  $\text{NH}_4^+$ ,  $\text{Na}^+$ ,  $\text{K}^+$ ,  $\text{Ca}^{2+}$ ,  $\text{Mg}^{2+}$  were determined by Ion Chromatograph (IC, Metrohm and column Metrosep C4-150). The anions  $\text{F}^-$ ,  $\text{Cl}^-$ ,  $\text{NO}_3^-$ ,  $\text{SO}_4^{2-}$  and  $\text{PO}_4^{3-}$  were also determined by Ion Chromatograph (IC, Metrohm and column MetrosepA Supp 5) [14,15]. Standard methods [13] were followed for determination of other quality parameters.  $\text{F}^-$  was measured by both Ion Chromatograph and Ion Selective Electrode (Orion 4 star-pH/ISE). Atomic Absorption Spectrophotometer (Perkin Elmer, USA) was used for determination of Concentration of arsenic. All the required reagents were of analytical grade (Merck, India). For Atomic Absorption Spectrometry (AAS), the standard arsenic solution was procured from Perkin Elmer, USA. In this method,  $\text{As}^{5+}$  was pre-reduced to  $\text{As}^{3+}$  using standard potassium iodide solution, ascorbic acid solution and hydrochloric acid solution [16].



**2.2.4 Statistical analysis**

By using Statistical Package for Social Science version: 25, Pearson's correlation coefficient analysis and Principal Component Analysis (PCA) were used for the assessment of groundwater quality. This study helped to infer the possible factors or sources which affect the quality of groundwater of Golaghat district [15,17,18]. The Pearson's correlation coefficient analysis provides the values of correlation coefficients ( $r$ ) [18,19], that indicate the strength of inter-relationship between two chemical parameters. The value of correlation coefficient ( $r$ ) may be in between +1 and -1. Positive and negative sign of  $r$  value indicates the inter-relationship between two parameters positively and negatively. For strong correlation  $r > 0.50$ , for good correlation  $r = 0.50$  and for poor correlation  $r < 0.50$  [20].

**2.2.5 Piper diagram analysis**

To identify the hydrochemistry of collected groundwater samples Piper diagram analysis was performed [21]. The Piper trilinear diagram [22] was drawn by using the value of groundwater quality parameters of samples. The diagram is highly useful to infer the hydro geochemistry of water [21]. In the Piper diagram, we obtain two lower triangles and one quadrilateral shape. One of these triangles is for the cations ( $\text{Na}^+$ ,  $\text{K}^+$ ,  $\text{Ca}^{2+}$  and  $\text{Mg}^{2+}$ ), another triangle is for the anions ( $\text{Cl}^-$ ,  $\text{SO}_4^{2-}$ ,  $\text{CO}_3^{2-}$  and  $\text{HCO}_3^-$ ) and the quadrilateral shape indicates the combined distribution of both cations and anions i.e., the final water type of the sources.

**2.3 Results and discussion**

The analysed physico-chemical parameters of collected groundwater samples from entire Golaghat district and its peripheral areas have been compared with WHO [6] and BIS [23] recommended specifications. The water quality data of block wise collected samples along with their minimum, maximum values and standard deviations are given in Table 2.1, 2.2 and 2.3.

Table 2.1: Some water quality parameters of groundwater samples of Golaghat district

Name of the Block Development area (depth of water samples in ft)		pH	TDS (mg/L)	EC (mS/cm)	TH (mg/L)	F <sup>-</sup> (mg/L)	Cl <sup>-</sup> (mg/L)	NO <sub>3</sub> <sup>-</sup> (mg/L)	PO <sub>4</sub> <sup>3-</sup> (mg/L)	SO <sub>4</sub> <sup>2-</sup> (mg/L)	HCO <sub>3</sub> <sup>-</sup> (mg/L)
<b>Dergaon</b> (40ft-260ft)	Min- Max	6.5- 7.8	58- 59.5	0.03- 0.06	66- 240	0.07- 0.45	1.27- 5.98	0.01- 4.75	0.23- 0.26	1.72- 11.6	54.88- 350.42
	Mean	6.97	58.8	0.05	92.71	0.28	3.43	1.58	0.25	3.42	104.1
	Stnd dev	0.38	0.51	0.02	64.96	0.11	1.36	1.47	0.01	3.60	108.9
<b>Kathalguri</b> (40ft-300ft)	Min- Max	6.5- 8.5	109- 232	0.1- 0.28	54- 110	0.09- 0.87	0.32- 4.94	0.53- 5.09	0.19- 1.71	0.05- 0.19	108.4- 238.4
	Mean	7.366	165	0.20	81.77	0.47	2.71	1.52	1.71	0.08	179.29
	Stnd dev	0.70	46.88	0.13	23.3	0.21	2.02	1.41	0.8	0.04	38.4
<b>Podumoni</b> (60ft-300ft)	Min- Max	6.7- 8.4	164- 610	0.02- 0.68	90- 186	0.16- 1.69	0.09- 3.19	0.95- 32.8	1.11- 6.28	0.02- 39.83	213.5- 528.6
	Mean	7.44	364.52	0.19	151.22	0.76	0.86	14.29	2.52	2.04	338.98
	Stnd dev	0.41	109.69	0.46	29.32	0.40	0.78	7.01	1.52	8.44	114.22
<b>Kakodonga</b> (60ft-220ft)	Min- Max	6.3- 8.2	171- 262	0.18- 0.37	90- 170	0.10- 0.54	0.11- 9.56	0.06- 16.44	0.03- 1.46	0.11- 2.01	220.34- 247.28
	Mean	7.64	206.6	0.24	140.80	0.34	2.13	2.73	0.37	0.96	239.79
	Stnd dev	0.50	37.99	0.13	34.11	0.12	2.78	4.39	0.62	0.51	7.71
<b>Morangi</b> (20ft-180ft)	Min- Max	6-7.6	78.4- 349	0.01- 0.39	44- 150	0.08- 0.46	0.42- 5.31	0.10- 32.8	0.2- 1.72	0.08- 5.21	34.68- 54.9
	Mean	6.68	183.33	0.07	90	0.23	2.09	12	0.74	1.83	46.12
	Stnd dev	0.58	145.16	0.26	54.36	0.10	2.79	18.07	0.84	2.92	10.37

**Chapter-2****Ground water quality of Golaghat**

<b>Gamariguri</b> <b>(60ft-300ft)</b>	Min-	6.3-	222-	0.04-	50-	0.25-	0.34-	1.669-	0.402-	0.04-	252.2-
	Max	8.4	502	0.54	123	2.92	4.40	16.85	2.831	1.50	457.5
	Mean	7.18	344.66	0.13	96	0.95	1.91	10.11	1.95	0.47	319.5
	Stnd dev	0.60	116.25	0.35	24.93	0.52	1.43	5.472	0.905	0.55	86.86
<b>Sorupathar</b> <b>(40ft-260ft)</b>	Min-	6-7.7	210-	0.003-	100-	0.11-	0.75-	2.14-	0.40-	0.06-	234.8-
	Max		359	0.41	200	1.83	9.97	4.12	3.23	3.23	323.3
	Mean	7.15	295	0.15	143	0.78	5.75	3.06	1.97	0.76	279.5
	Stnd dev	0.53	5.01	0.29	28.67	0.57	3.13	0.73	0.91	1.03	28.77
<b>Bokakhat</b> <b>(20ft-260ft)</b>	Min-	6.1-	47.7-	0.001-	35-	0.09-	0.47-	0.16-	0.18-	0.25-	21.25-
	Max	7.7	217	0.31	170	0.85	43.26	23.58	3.68	42.27	330.4
	Mean	7.01	120.51	0.07	107.2	0.33	10.68	5.04	0.67	7.99	181.17
	Stnd dev	0.43	51.52	0.22	41.69	0.17	12.14	6.46	1.13	10.99	104.36
<b>WHO/BIS standard</b>		<b>6.5-8.5</b>	<b>500</b>	<b>0.2</b>	<b>200</b>	<b>1.0</b>	<b>250</b>	<b>45</b>	<b>-</b>	<b>200</b>	<b>-</b>
<b>Desirable limit</b>											
<b>WHO/BIS standard</b>			<b>2000</b>	<b>1.5</b>	<b>600</b>	<b>1.5</b>	<b>1000</b>	<b>100</b>	<b>-</b>	<b>400</b>	<b>500</b>
<b>Permissible limit</b>											

Table 2.2: Concentration of important cations in groundwater samples of Golaghat district

Name of the Block Development area		Na <sup>+</sup> (mg/L)	NH <sub>4</sub> <sup>+</sup> (mg/L)	K <sup>+</sup> (mg/L)	Ca <sup>2+</sup> (mg/L)	Mg <sup>2+</sup> (mg/L)	As (mg/L)	Fe (mg/L)
<b>Dergaon</b>	Min-Max	4.46-33.42	0.01-2.3	0.04- 0.40	0.48- 33.98	0.74- 12.44	0.001- 0.028	3.28-4.4
	Mean	10.96	0.36	0.56	5.65	2.77	0.010	4.15
	Std dev	9.97	0.85	1.08	12.49	4.27	0.012	0.4
<b>Kathalguri</b>	Min-Max	12.2-51.6	1.36-6	1.94- 25.2	16.44- 31.48	4.56- 9.66	0.001- 0.077	1.4-4.01
	Mean	25.24	3.09	5.9	23.03	6.86	0.017	2.9
	Std dev	15.77	1.71	7.41	5.82	1.71	0.029	0.80
<b>Podumoni</b>	Min-Max	11.15- 191.64	1.48-4.2	1.98- 26.2	18.9- 48.5	8.92- 17.2	0.001- 0.450	0.125- 4.8
	Mean	75.28	3.5	5.23	30.71	12.66	0.117	3.92
	Std dev	48.94	4.69	4.83	8.47	2.14	0.107	0.72
<b>Kakodonga</b>	Min-Max	16.88- 61.38	1.76-2.11	1.35- 8.07	19.46- 25.69	6.77- 12.54	0.001- 0.186	1.5-2.3
	Mean	31.9	1.97	3.21	23.72	10.48	0.105	1.86
	Std dev	14.08	0.18	2.30	1.90	1.56	0.075	0.40
<b>Morangi</b>	Min-Max	12.84- 68.94	1.78-7.41	1.69- 3.02	19.14- 74.36	5.82- 12.96	0.001- 0.444	1.1-1.67
	Mean	32.22	3.91	2.31	41.94	9.51	0.026	1.42
	Std dev	31.81	3.05	0.66	28.83	3.57	0.084	0.29
<b>Gamariguri</b>	Min-Max	3.14- 186.76	2.02-3.43	2.26- 6.56	19.94- 34.4	6.08- 11.65	0.001- 0.460	0.1-3.2

**Chapter-2****Ground water quality of Golaghat**

	Mean	84.18	2.69	4.35	26.83	9.13	0.082	2.38
	Std dev	75.04	0.63	1.60	5.50	1.82	0.121	0.72
<b>Sorupathar</b>	Min-Max	31.18-90	1.48-4.08	2.5-4.14	22.6-35.8	7.3-15.18	0.001-0.175	2.8-4.5
	Mean	65.61	3.34	3.07	28.00	10.59	0.002	3.78
	Std dev	18.77	0.54	0.54	4.37	2.26	0.045	0.60
<b>Bokakhat</b>	Min-Max	7.6-21.6	0.64-4.8	1.76-5.92	13.24-59.14	2.66-15.24	0.001-0.024	0.8-3.8
	Mean	13.12	2.08	3.21	24.53	6.89	0.002	1.23
	Std dev	4.12	1.10	1.27	12.13	3.7	0.003	0.87
<b>WHO/BIS Standards</b>		<b>200</b>	<b>0.5 mg/L</b>	<b>--</b>	<b>75</b>	<b>30</b>	<b>0.01 mg/L</b>	<b>0.3</b>
<b>Desirable limit</b>								
<b>WHO/BIS Standards</b>		<b>No relaxation</b>	<b>No relaxation</b>	<b>--</b>	<b>200</b>	<b>100</b>	<b>0.05 mg/L</b>	<b>1.0</b>
<b>Permissible limit</b>								

Table 2.3(a) &amp; 3(b): Some groundwater quality parameters of the peripheral areas

Table 2.3(a)

Name of the Districts and Block Development areas		pH	TDS (mg/L)	EC (mS/cm)	TH (mg/L)	F <sup>-</sup> (mg/L)	Cl <sup>-</sup> (mg/L)	NO <sub>3</sub> <sup>-</sup> (mg/L)	PO <sub>4</sub> <sup>3-</sup> (mg/L)	SO <sub>4</sub> <sup>2-</sup> (mg/L)	HCO <sub>3</sub> <sup>-</sup> (mg/L)
<b>Jorhat District (Jorhat West block &amp; Titabor block)</b>	Min-Max	6.5-7.3	58.4-555	0.01-0.03	78-184	0.4-0.88	0.63-3.36	0.46-12.37	0.1-3.99	0.04-2.14	55.68-262.3
	Mean	6.9	296.08	0.02	130.27	0.58	1.72	3.74	1.3	1.04	239.27
<b>Karbi-Anlong District (Rongm ongwe block, Nilip block &amp; Bokajan block)</b>	Min-Max	6.5-7.9	109-232	0.03-0.10	54-110	0.09-0.87	0.32-4.94	0.53-5.09	0.19-1.71	0.05-0.19	108.4-238.4
	Mean	7.2	165	0.06	81.77	0.47	2.71	1.52	1.71	0.08	179.29
<b>Nagaon District (Kaliabor block)</b>	Min-Max	6.8-7.0	164-610	0.04-0.09	90-186	0.34-1.32	0.09-3.19	0.95-32.8	1.11-6.28	0.02-39.83	213.5-528.6
	Mean	6.9	364.5	0.06	151.22	0.70	0.86	14.29	2.52	2.04	338.98

Table 2.3(b)

Name of the Districts and Block Development areas		Na <sup>+</sup> (mg/L)	NH <sub>4</sub> <sup>+</sup> (mg/L)	K <sup>+</sup> (mg/L)	Ca <sup>2+</sup> (mg/L)	Mg <sup>2+</sup> (mg/L)	As (mg/L)	Fe (mg/L)
<b>Jorhat</b>  <b>District (Jorhat</b>  <b>West block &amp;</b>  <b>Titabor block)</b>	Min-	7.4-	0.01-	0.04-	0.51-	0.74-	0.02-	0.94-
	Max	119.64	3.43	6.56	35.8	17.44	0.11	4.2
	Mean	56.73	1.83	2.83	21.76	10.625	0.058	1.85
<b>Karbi-Anlong</b>  <b>District</b>  <b>(Rongmongwe</b>  <b>block, Nilip</b>  <b>block &amp; Bokajan</b>  <b>block)</b>	Min-	8.26-	1.84-	1.6-	16.2-	3.3-	0.001-	0.86-
	Max	45.67	7.41	4.58	25.07	9.77	0.01	1.5
	Mean	15.54	3.09	2.33	17.34	5.13	0.003	0.95
<b>Nagaon</b>  <b>District(Kaliabor</b>  <b>block)</b>	Min-	11.06-	0.64-	2.5-3.9	24.56-	5.06-	0.001-	0.9-1.5
	Max	15.06	2.46		29.66	13.12	0.005	
	Mean	12.4	1.26	3.06	26.44	7.79	0.002	1.1

From the Table 2.1 and Table 2.3(a), it is observed that pH of all water samples collected from all eight development block of Golaghat district and its peripheral areas were within the permissible limit (6.5-8.5) (WHO 2011). Generally, the acidic (pH<7) character of the water samples are mainly due to the dissolution of carbon dioxide and organic soil and plant humus originated acids like fulvic and humic acids [24]. The EC and TDS values were also within the WHO recommended values.

Dufor and Becker classified the water to four classes on the basis of TH soft (if TH is 0-60), moderately hard (if TH is 61-120), hard (if TH is 121-180) and very hard (if TH is >180) [25]. According to this classification 86.4% water of Podumoni development block; 73.3% of Kakodonga development block; 33.3% of Morangi development block; 16.8% of Gamariguri development block and 12.5% of Sorupathar development block water samples belong to hard type water. In Dergaon, Sorupathar and Podumoni development block 13%, 12% and 5% water samples were found very hard type. Moderately hard type groundwater samples were found as

33.3%, 33.4%, 16.6% and 10% of the collected water samples in Kathalguri, Morangi, Gamariguri and Bokakhat development blocks. Similarly, TDS, EC and TH of samples collected from the peripheral areas of Golaghat district are also within the WHO recommended values.

The concentration of other dissolved anions such as  $\text{Cl}^-$ ,  $\text{NO}_3^-$ ,  $\text{SO}_4^{2-}$ ,  $\text{PO}_4^{3-}$ , and  $\text{HCO}_3^-$  in groundwater of Golaghat district varies with mean value 3.43, 1.58, 0.25, 3.42 and 104.1 mg/L in Dergaon development block; 2.71, 1.52, 1.71, 0.08 and 179.29 mg/L in Kathalguri development block; 0.86, 14.29, 2.52, 2.04 and 338.98 mg/L in Podumoni development block; 2.13, 2.73, 0.37, 0.96 and 239.79 mg/L in Kakodonga development block; 2.09, 12, 0.74, 1.834 and 46.12 mg/L in Morangi development block; 1.91, 10.11, 1.95, 0.47 and 319.5 mg/L in Gamariguri development block; 5.75, 3.06, 1.97, 0.76 and 279.5 mg/L in Sorupathar development block and 10.68, 5.04, 0.67, 7.99 and 181.17 mg/L in Bokakhat development block.  $\text{HCO}_3^-$  is the dominant anions in all collected groundwater samples of Golaghat district.

Among the cations in studied samples (in Table 2.2), except the concentration of Fe (total), the concentration of  $\text{Na}^+$ ,  $\text{NH}_4^+$ ,  $\text{K}^+$ ,  $\text{Ca}^{2+}$  and  $\text{Mg}^{2+}$  were within the ranges of WHO/BIS with mean values 10.96, 0.36, 0.56, 5.65 and 2.77 in Dergaon development block; 25.24, 3.09, 5.9, 23.03 and 6.86 in Kathalguri development block; 75.28, 3.5, 5.23, 30.71 and 12.66 in Podumoni development block; 31.9, 1.97, 3.21, 23.72 and 10.48 in Kakodonga development block; 32.22, 3.91, 2.31, 41.94 and 9.51 in Morangi development block; 84.18, 2.69, 4.35, 26.83 and 9.13 in Gamariguri development block; 65.61, 3.34, 3.07, 28.00 and 10.59 in Sorupathar development block and 13.12, 2.08, 3.21, 24.53 and 6.89 in Bokakhat development block respectively. The abundance order of  $\text{Na}^+$ ,  $\text{NH}_4^+$ ,  $\text{K}^+$ ,  $\text{Ca}^{2+}$  and  $\text{Mg}^{2+}$  in groundwater samples in Golaghat district was  $\text{Na}^+ > \text{Ca}^{2+} > \text{Mg}^{2+} > \text{K}^+ > \text{NH}_4^+$ .

Again it is seen that, 97% of water samples of the all development blocks contains iron more than WHO/BIS permissible limit (1.0 mg/L) [6,23]. The maximum iron concentration is 4.8 mg/L in Podumoni development block followed by 4.5 mg/L in Sorupathar development block than 4.4 mg/L in Dergaon development block than 4.01 mg/L in Kathalguri development block than 3.8 mg/L in Bokakhat development block than 3.2 mg/L in Gamariguri development block than 2.3 mg/L in Kakodonga development block and finally 1.67 mg/L in Morangi development block.

The variation of fluoride concentration in eight development block shown in the Table 2.4 as 0.07-0.45 mg/L in Dergaon, 0.09-0.87 mg/L in Kathalguri, 0.16-1.69 mg/L in Podumoni, 0.10-0.54 mg/L in Kakodonga, 0.08-0.46 mg/L in Morangi, 0.25-2.92 mg/L in



Gamariguri,, 0.11-1.83 mg/L in Sorupathar and 0.09-0.85 mg/L in Bokakhat development block. Maximum fluoride content recorded was 2.92 mg/L in a groundwater sample collected from Gamariguri block. 10% samples of Gamariguri block and 4% samples of Podumoni block have fluoride concentration more than WHO/BIS permissible limit (1.5 mg/L). Similarly, 14.3% groundwater samples of Sorupathar block have fluoride concentration more than 1.5 mg/L. Some groundwater samples, 28% of Podumoni development block, 30% of Gamariguri development block and 14.3% of Sorupathar development block were also found to have fluoride contamination in the range 1.0-1.5 mg/L. On the other hand collected groundwater samples of Dergaon, Kathalguri, Kakodonga, Morangi and Bokakhat development blocks were not objectionable for drinking purpose in terms of fluoride. Distribution of fluoride in different blocks are shown in Figure 2.3.

**Table 2.4: Concentration of fluoride in groundwater samples of Golaghat district**

<b>Block</b>	<b>Range (mg/L)</b>	<b>Mean (mg/L)</b>	<b>Below desirable limit (%)</b>	<b>Within WHO limit (%)</b>	<b>Above permissible limit (%)</b>
<b>Dergaon</b>	0.07-0.45	0.28	100	0	0
<b>Kathalguri</b>	0.09-0.87	0.47	100	0	0
<b>Podumoni</b>	0.16-1.69	0.76	68	28	4
<b>Kakodonga</b>	0.10-0.54	0.34	100	0	0
<b>Morangi</b>	0.08-0.46	0.23	100	0	0
<b>Gamariguri</b>	0.25-2.92	0.95	60	30	10
<b>Sorupathar</b>	0.11-1.83	0.78	71.4	14.3	14.3
<b>Bokakhat</b>	0.09-0.85	0.33	100	0	0

The concentration of arsenic in six blocks out of eight blocks is more than that of the permissible limit (WHO/BIS). In Golaghat district, maximum arsenic was found in Gamariguri block (0.460 mg/L). In Podumoni, Kakodonga, Gamariguri, Kathalguri, Sorupathar and Morangi development blocks groundwater samples were found contaminated with arsenic by 68%, 65%, 46.7%, 21.05%, 7.14% and 3.7% with the ranges of (0.001-0.450),

(0.001-0.186), (0.001-0.460), (0.001-0.077), (0.001-0.175) and (0.001-0.444) respectively.

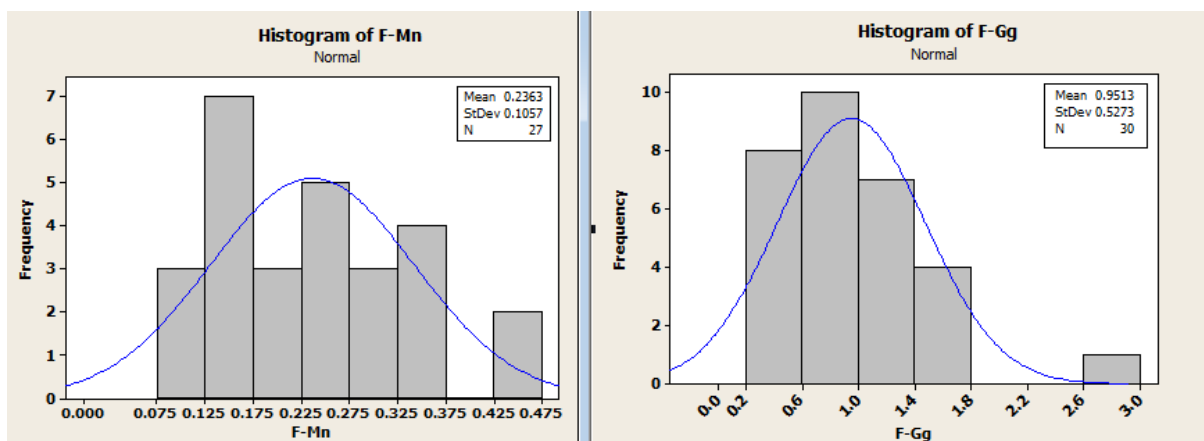
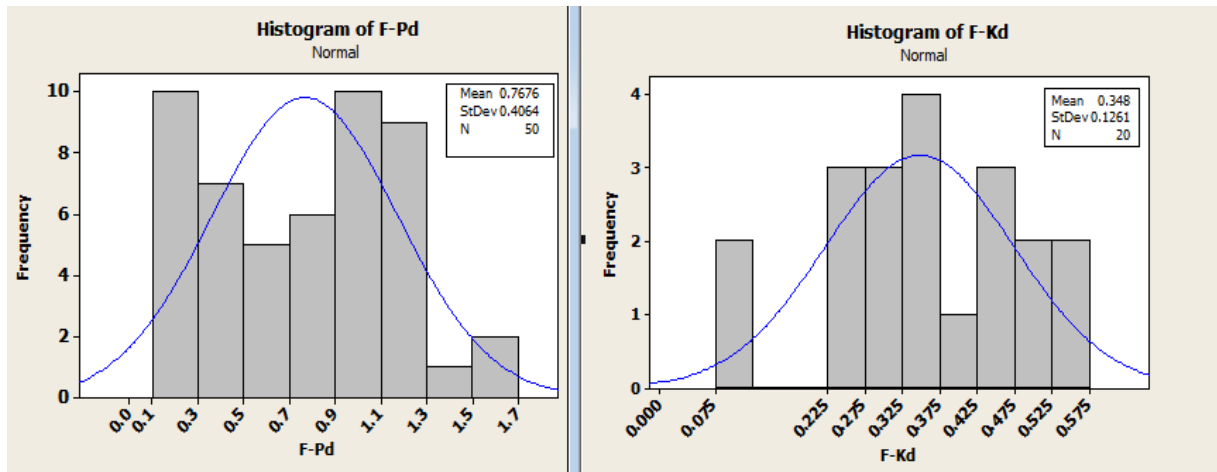
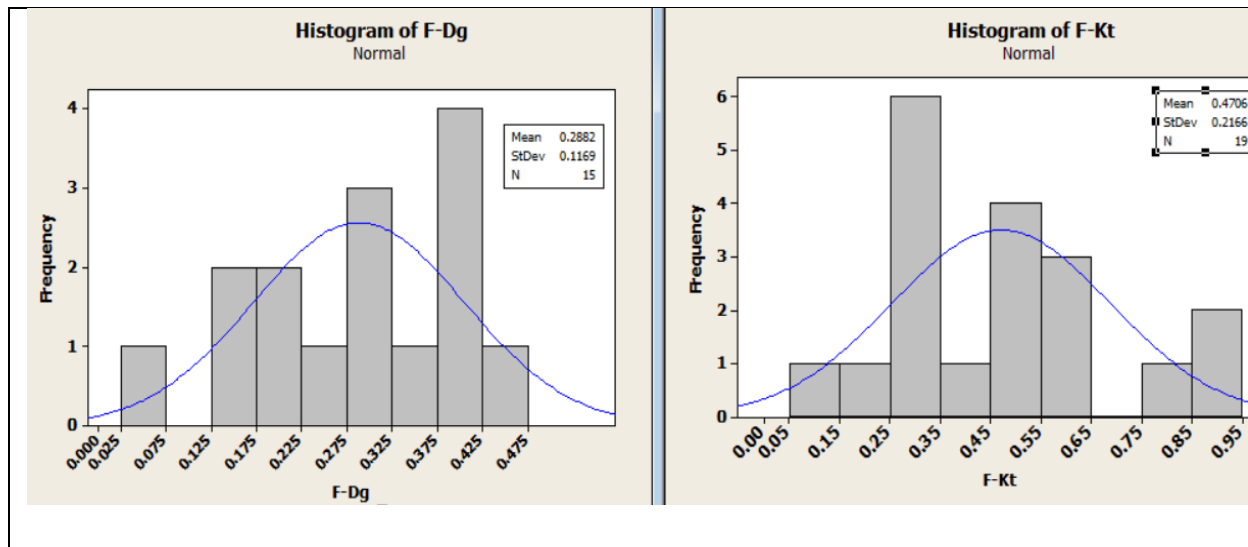
Many water samples given in Table 2.5, have As within the concentration of 0.01-0.05 mg/L.

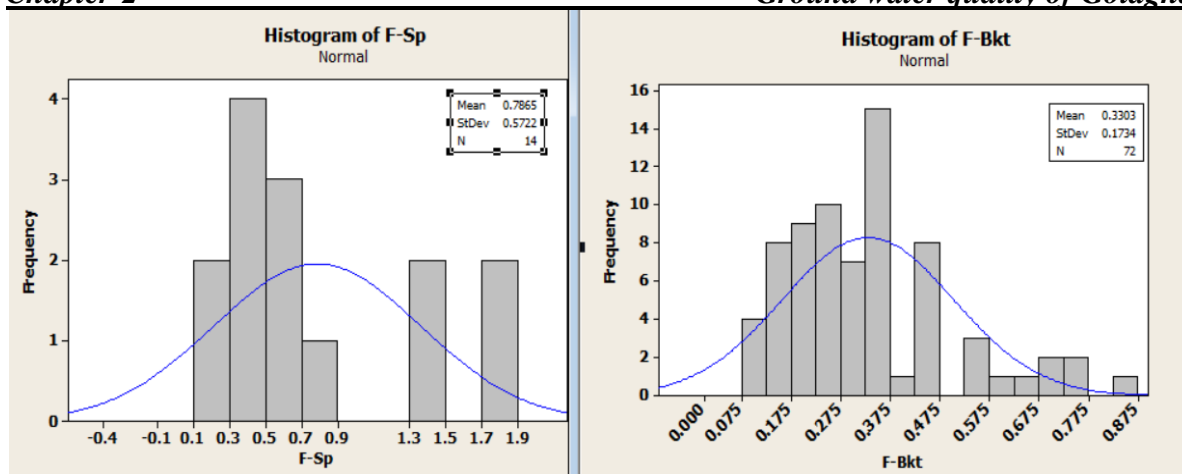
Therefore, it is observed that Podumoni, Kakodonga and Gamariguri are highly arsenic affected development block in Golaghat district. Distribution of arsenic in different blocks are shown in Figure 2.4.

**Table 2.5: Concentration of arsenic in groundwater samples of Golaghat district**

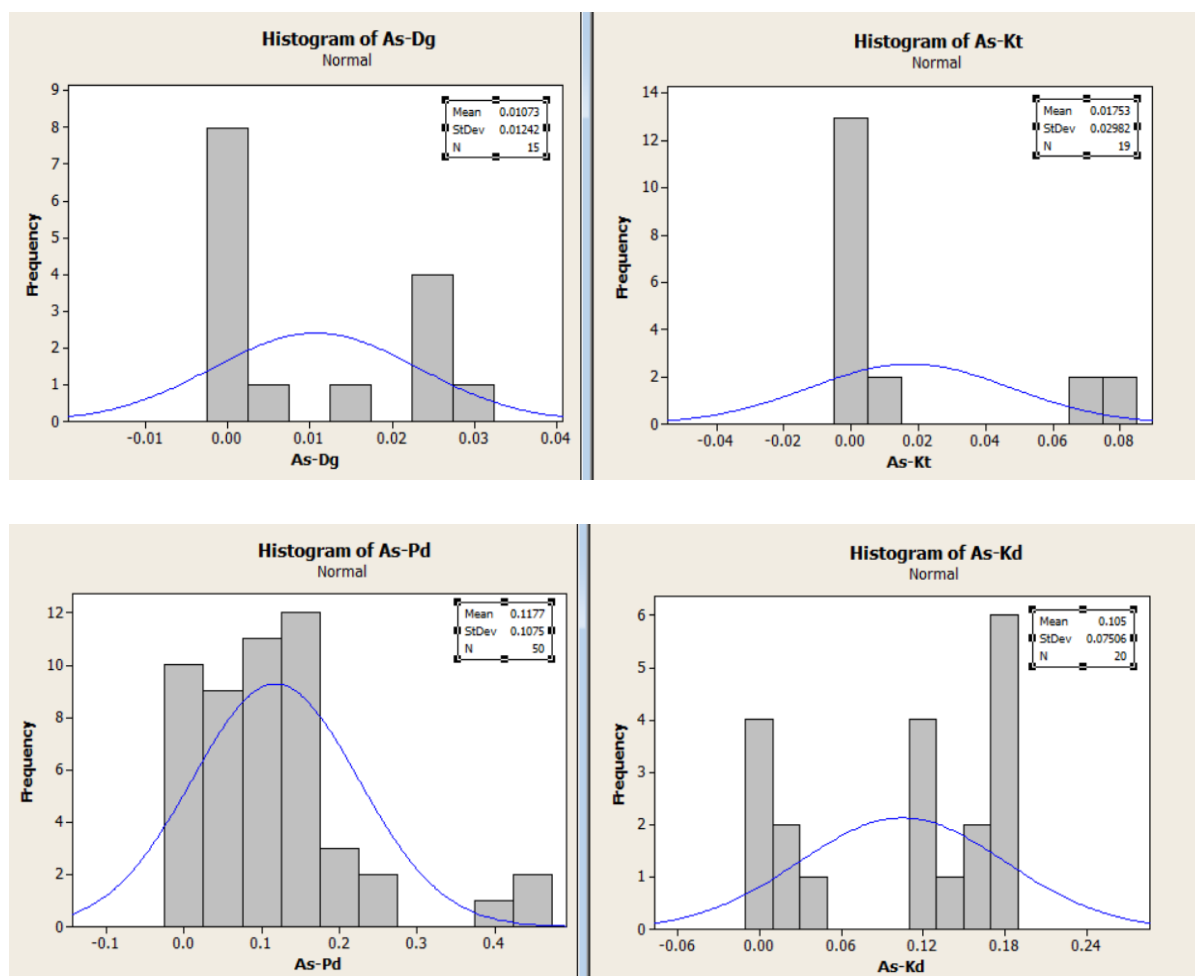
<b>Block</b>	<b>Range (mg/L)</b>	<b>Mean (mg/L)</b>	<b>Below desirable limit (%)</b>	<b>Within WHO limit (%)</b>	<b>Above permissible limit (%)</b>
<b>Dergaon</b>	0.001-0.028	0.010	60	40	0
<b>Kathalguri</b>	0.001-0.077	0.017	78.95	0	21.05
<b>Podumoni</b>	0.001-0.450	0.117	16	16	68
<b>Kakodonga</b>	0.001-0.186	0.105	20	15	65
<b>Morangi</b>	0.001-0.444	0.026	77.8	18.5	3.7
<b>Gamariguri</b>	0.001-0.460	0.082	30	23.33	46.7
<b>Sorupathar</b>	0.001-0.175	0.002	64.29	28.57	7.14
<b>Bokakhat</b>	0.001-0.024	0.002	72	28	0

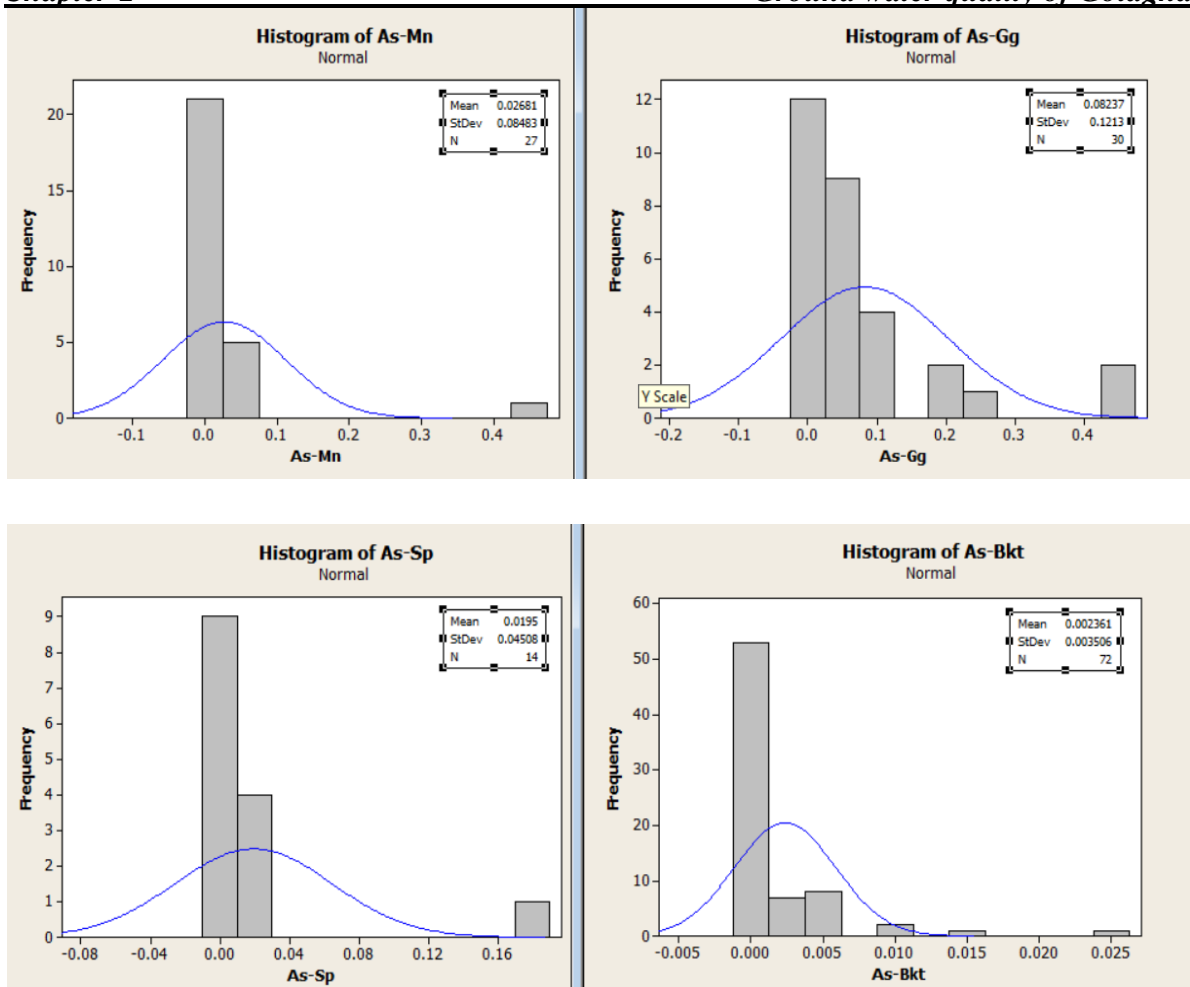
In case of peripheral areas of Golaghat district, it is seen from the Table 2.3(a) and 2.3(b) the concentration of various cations and anions including fluoride were within the WHO/BIS limit; but the concentration of arsenic was greater than the WHO/BIS limit in case of 55% samples collected from the portion of Jorhat district mainly from Titabor block development area only i.e. the eastern part of Golaghat district. It is seen that these locations of Jorhat district are adjoining area to arsenic affected development blocks Podumoni and Gamariguri of Golaghat district. Other groundwater samples collected from the adjoining areas of Golaghat district, i.e., Karbi-Anglong and Nagaon districts are not contaminated by arsenic. Distribution of fluoride and arsenic in different districts of peripheral areas of Golaghat district are shown in Figure 2.5.



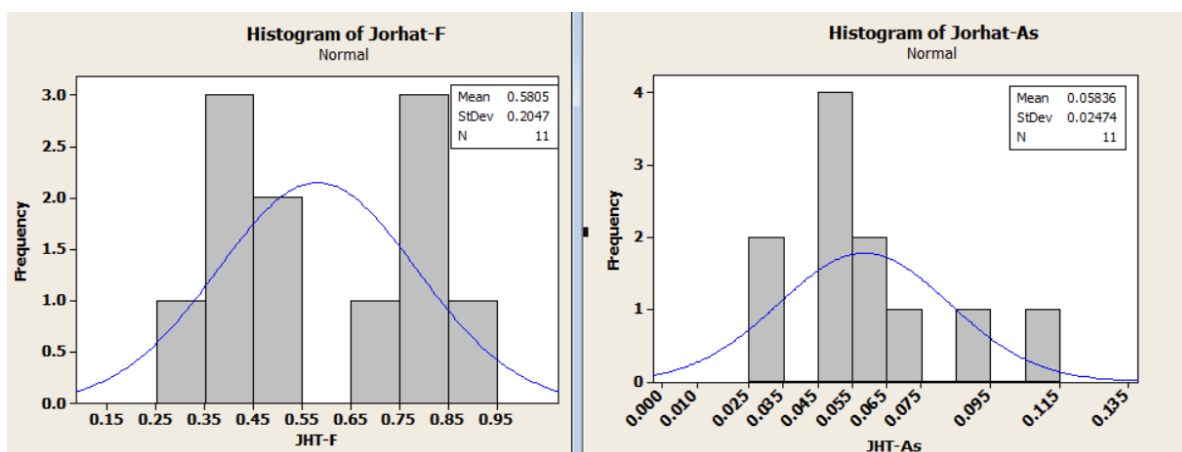


**Fig 2.3:** Graphical representation of block wise distribution of fluoride in Dergaon as F-Dg, in Kathalguri as F-Kt, in Podumoni as F-Pd, in Kakodonga as F-Kd, in Morangi as F-Mn, in Gamariguri as F-Gg, in Sorupathar as F-Sp and in Bokakhat as F-Bkt





**Fig 2.4:** Graphical representation of block wise distribution of arsenic in Dergaon as As-Dg, in Kathalguri as As-Kt, in Podumoni as As-Pd, in Kakodonga as As-Kd, in Morangi as As-Mn, in Gamariguri as As-Gg, in Sorupathar as As-Sp and in Bokakhat as As-Bkt



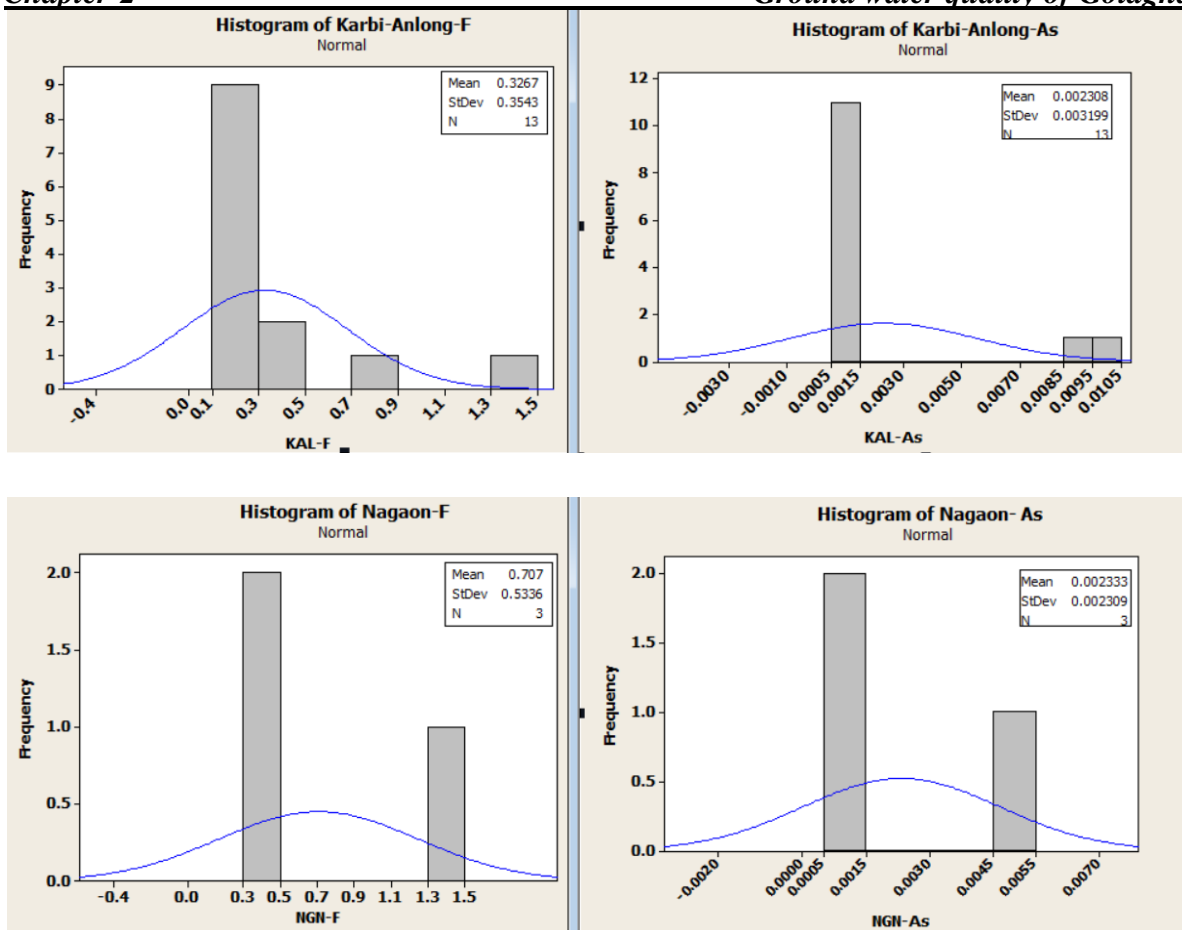


**Fig 2.5:** Graphical representation of distribution of fluoride and arsenic in peripheral areas of Golaghat district(Jorhat, Karbi-Anlong and Nagaon district) as JHT-F, JHT-As, KAL-F, KAL-As and NGN-F, NGN-As.

### Statistical analysis

In the course of statistical analysis, the correlation among the water quality parameters of groundwater samples collected from Golaghat district of Assam were determined further by using Pearson correlation (Table 2.6). In this study, It is seen that TDS bears a linear positive correlation with  $\text{Na}^+$  ( $r=0.84$ ),  $\text{HCO}_3^-$  ( $r=0.79$ ),  $\text{EC}$  ( $r=0.75$ ),  $\text{Mg}^{2+}$  ( $r=0.72$ ),  $\text{NH}_4^+$  ( $r=0.61$ ),  $\text{PO}_4^{3-}$  ( $r=0.60$ ),  $\text{Fe}$  ( $r=0.60$ ),  $\text{NO}_3^-$  ( $r=0.51$ ),  $\text{F}^-$  ( $r=0.13$ ),  $\text{As}$  ( $r=0.40$ ) and  $\text{Ca}^{2+}$  ( $r=0.44$ ). Similarly,  $\text{HCO}_3^-$  bears positive correlation with  $\text{As}$  ( $r=0.15$ ),  $\text{Na}^+$  ( $r=0.63$ ),  $\text{NH}_4^+$  ( $r=0.51$ ),  $\text{K}^+$  ( $r=0.18$ ),  $\text{Ca}^{2+}$  ( $r=0.47$ ),  $\text{Mg}^{2+}$  ( $r=0.55$ ) and  $\text{Fe}$  ( $r=0.42$ ). A significant positive correlation was found between  $\text{As}$  and  $\text{F}^-$  ( $r=0.23$ ),  $\text{Na}^+$  ( $0.33$ ),  $\text{Mg}^{2+}$  ( $0.44$ ),  $\text{Fe}$  ( $0.28$ ),  $\text{PO}_4^{3-}$  ( $0.26$ ) and  $\text{NO}_3^-$  ( $0.61$ ). Positive correlations between  $\text{Fe}$  and  $\text{F}^-$  ( $0.54$ ),  $\text{NO}_3^-$  ( $0.13$ ),  $\text{TH}$  ( $0.10$ ),  $\text{PO}_4^{3-}$  ( $0.40$ ),  $\text{As}$  ( $0.28$ ),  $\text{Na}^+$  ( $0.50$ ),  $\text{NH}_4^+$  ( $0.34$ ),  $\text{K}^+$  ( $0.25$ ),  $\text{Ca}^{2+}$  ( $0.13$ ), and  $\text{Mg}^{2+}$  ( $0.41$ ) were

also found in the collected groundwater samples. Besides these, the Pearson correlation matrices showed significant positive correlation among the various parameters of the collected groundwater samples such as TH- $\text{Ca}^{2+}$  (0.54), TH- $\text{Mg}^{2+}$  (0.51), TH- $\text{HCO}_3^-$  (0.30), TH- $\text{Cl}^-$  (0.03) and TH- $\text{SO}_4^{2-}$  (0.04), which showed that, the groundwater hardness depends on  $\text{Ca}^{2+}$ ,  $\text{Mg}^{2+}$ ,  $\text{HCO}_3^-$ ,  $\text{Cl}^-$  and  $\text{SO}_4^{2-}$ .

In case of fluoride it is seen that, although there is no strong positive correlation with other; but some positive correlation was found between  $\text{F}^-$  and  $\text{Na}^+$  (0.17),  $\text{K}^+$  (0.27),  $\text{Mg}^{2+}$  (0.298),  $\text{PO}_4^{3-}$  (0.18) and pH (0.15). The positive correlation between  $\text{F}^-$  and  $\text{Na}^+$  in some parts of Nagaon and Karbi-Anglong districts was also reported [26,27]. A positive correlation between pH and  $\text{F}^-$  was also reported by Gupta and Saikia [26,28]. From the positive correlation between  $\text{F}^-$  and  $\text{PO}_4^{3-}$  (0.18), it might be expected that  $\text{F}^-$  come to contaminate the groundwater from human activities of use of phosphate fertilisers and pesticides [29].

The positive correlation between As and Fe ( $r=0.28$ ) in groundwater of Golaghat district might be expected to come from the dissolution of As-Fe bearing minerals [4,11] and the immediate source material is likely to be ferric arsenate, with or without ferric arsenite, derived from the mineral arsenopyrite that was geologically transported to the Bengal delta and Assam valley [30]. Because arsenic originates in Himalayan head waters [31] and the two Himalayan rivers which build the Bengal delta, the Ganga and Brahmaputra drain to the Bay of Bengal by carrying the largest sediment load. Similarly, as the Brahmaputra river flows through the heart of Assam to Bengal, thus arsenic occurrence in Assam may be due to heavy deposition of sediments [4].

	TH	pH	HCO <sub>3</sub> <sup>-</sup>	TDS	EC	F <sup>-</sup>	Cl <sup>-</sup>	NO <sub>3</sub> <sup>-</sup>	PO <sub>4</sub> <sup>3-</sup>	SO <sub>4</sub> <sup>2-</sup>	As	Na <sup>+</sup>	NH <sub>4</sub> <sup>+</sup>	K <sup>+</sup>	Ca <sup>2+</sup>	Mg <sup>2+</sup>	Fe
TH	1.00																
pH	.09	1.00															
HCO <sub>3</sub> <sup>-</sup>	.30	-.05	1.00														
TDS	.31	-.03	.79	1.00													
EC	.37	.07	.47	.75	1.00												
F <sup>-</sup>	.10	.15	-.07	.13	.24	1.00											
Cl <sup>-</sup>	.03	.18	-.15	-.25	-.10	-.34	1.00										
NO <sub>3</sub> <sup>-</sup>	.19	-.26	.23	.51	.43	-.05	-.06	1.00									
PO <sub>4</sub> <sup>3-</sup>	-.13	-.14	.39	.60	.47	.18	-.37	.20	1.00								
SO <sub>4</sub> <sup>2-</sup>	.04	-.17	-.33	-.52	-.24	-.31	.09	-.37	-.24	1.00							
As	-.06	-.14	.15	.40	.39	.23	-.23	.61	.26	-.32	1.00						
Na <sup>+</sup>	.15	-.06	.63	.84	.89	.17	-.19	.35	.72	-.36	.33	1.00					
NH <sub>4</sub> <sup>+</sup>	.03	-.09	.51	.61	.35	.07	-.10	.09	.54	-.35	.05	.54	1.00				
K <sup>+</sup>	-.19	.02	.18	-.01	-.33	.27	-.15	-.23	-.14	-.28	-.16	-.23	.31	1.00			
Ca <sup>2+</sup>	.54	-.03	.47	.44	-.03	-.18	-.18	.31	-.08	-.22	.03	-.01	.14	.12	1.00		
Mg <sup>2+</sup>	.51	-.20	.55	.72	.65	.29	-.14	.43	.27	-.26	.44	.59	.27	.05	.38	1.00	
Fe	.10	.46	.42	.60	.47	.54	-.18	.13	.40	-.60	.28	.50	.34	.25	.13	.41	1.00



### Principal Component Analysis

The Principal Component Analysis (PCA) of the collected water samples shows the results of the PC loadings with a varimax rotation, as well as the eigenvalues, % variance and % cumulative variances. PCA was performed on the normalized data set (17 parameters) of groundwater of Golaghat district by using varimax with Kaiser normalization rotation method [32] to identify the sources affecting the quality of groundwater. The Scree plot (Fig 2.5(A)) indicates the number of Principal Component (PC)s having the eigen values more than 1 and taken in order to understand the underlying data structure [21,33,34]. Six major PCs were extracted which accounted 83.63% variance of the original data structure. The selected PCs can give more information than a single original variables. [14,35]. The result of the PCs loading with a varimax rotation as well as eigen values, % of variance and cumulative variance % are given in the Table 2.7. About 58.75 % variance of the total variance was represented in the first three loading factors in the groundwater samples (Fig 2.5(B)).

PC-1 accounts for 35.02 % of the total variance, showing strong positive loading ( $>0.50$ ) on TDS,  $\text{Na}^+$ , EC,  $\text{HCO}_3^-$ , Fe,  $\text{PO}_4^{3-}$ ,  $\text{NH}_4^+$ ; while moderate positive loading (0.50-0.30) on  $\text{Mg}^{2+}$  and Fe. Again showing weak positive loading on As and  $\text{NO}_3^-$ . Since the PC-1 indicated the major contribution for TDS,  $\text{Na}^+$ , EC,  $\text{HCO}_3^-$ , Fe,  $\text{PO}_4^{3-}$  and  $\text{NH}_4^+$  so these seven parameters of groundwater of Golaghat district are correlated and vary together. The high loading factor of TDS and conductivity are due to the active participation of dissolved ions in the groundwater quality. The major variables constituting PC-1 ( $\text{Mg}^{2+}$ ,  $\text{HCO}_3^-$  and  $\text{Na}^+$ ) is related to the hydro chemical variables originating from mineralization of groundwater. However, due to the absence of industrial activity, the positive loading of TDS,  $\text{HCO}_3^-$ ,  $\text{Na}^+$ , EC,  $\text{Mg}^{2+}$ ,  $\text{NH}_4^+$ , Fe and  $\text{PO}_4^{3-}$  accounted PC-1 as geogenic sources of study area.

PC-2 accounted 12.56% of the total variance and it is mainly participated by TH,  $\text{Ca}^{2+}$  and  $\text{Mg}^{2+}$  with strong positive loading; TDS and  $\text{HCO}_3^-$  with moderate positive loading and weak positive loading on EC and  $\text{NO}_3^-$ . TH,  $\text{Ca}^{2+}$  and  $\text{Mg}^{2+}$  presented positive scores, thus PC-2 could be ascribed as geogenic factor [21].

Out of the total variance, 11.15% is explained by PC-3 and is mainly carried by  $\text{NO}_3^-$  and As with strong positive loading; TDS and  $\text{Mg}^{2+}$  with moderate positive and weak positive loading on  $\text{Na}^+$ ,  $\text{PO}_4^{3-}$ , EC, Fe and  $\text{Ca}^{2+}$ . Although, the released of As and Fe was reported from the natural source under the reducing groundwater environment [36]; some authors reported that As may be released from human activities like mining [7].  $\text{Na}^+$  and  $\text{PO}_4^{3-}$  might

be come from the fertilizer used in agricultural field, so PC-3 showed mixed sources of both geogenic and anthropogenic of study area. 9.27% of the total variance of water quality is exhibited by  $K^+$  with a strong positive loading under PC-4. Due to weathering of igneous rock like potassium feldspars,  $K^+$  can be increased in natural water [17].  $Ca^{2+}$  and  $NH_4^+$  with moderate and weak positive loading on  $HCO_3^-$  and Fe. PC-5 explained 8.71 % of the total variance of water quality in groundwater with a high positive loading on Fe and pH;  $F^-$  and  $Cl^-$  with moderate positive loading and EC and TH with weak positive loading. With high positive loading on  $F^-$ ; moderate positive loading on  $Mg^{2+}$  and Fe; weak positive loading on  $Na^+$ ,  $PO_4^{3-}$ , EC, As and  $K^+$ ; PC-6 explained 6.89 % of the total variance of water quality in groundwater. The positive loading of  $Na^+$  and  $F^-$  under PC-1, PC-3, PC-4 and PC-5 corroborates with the result of Pearson correlation.

Table 2.7: Rotated component matrix for data of groundwater samples

Variables	Components					
	1	2	3	4	5	6
Na <sup>+</sup>	.894	.077	.229	-.274	.095	.126
TDS	.814	.389	.373	.064	.090	.074
PO <sub>4</sub> <sup>3-</sup>	.807	-.235	.114	-.082	-.122	.232
NH <sub>4</sub> <sup>+</sup>	.786	.008	-.061	.350	-.020	-.040
HCO <sub>3</sub>	.714	.462	.076	.241	-.004	-.103
EC	.680	.237	.283	-.481	.231	.183
TH	.034	.894	-.074	-.266	.123	.066
Ca <sup>2+</sup>	.039	.788	.190	.396	-.101	-.161
Mg <sup>2+</sup>	.437	.599	.355	-.088	-.012	.306
NO <sub>3</sub> <sup>-</sup>	.172	.233	.849	-.103	-.133	-.113
As	.135	-.044	.836	-.119	-.043	.259
SO <sub>4</sub> <sup>2-</sup>	-.314	-.008	-.540	-.485	-.424	-.050
K <sup>+</sup>	-.009	.003	-.174	.850	.075	.239
pH	-.086	.006	-.179	-.009	.876	-.037
Fe	.464	.099	.222	.220	.649	.372
F <sup>-</sup>	.038	-.025	.078	.054	.352	.856
Cl <sup>-</sup>	-.178	-.050	-.068	-.193	.363	-.689
% of variance	35.023	12.568	11.156	9.270	8.717	6.898
Cumulative %	35.023	47.591	58.747	68.017	76.734	83.632

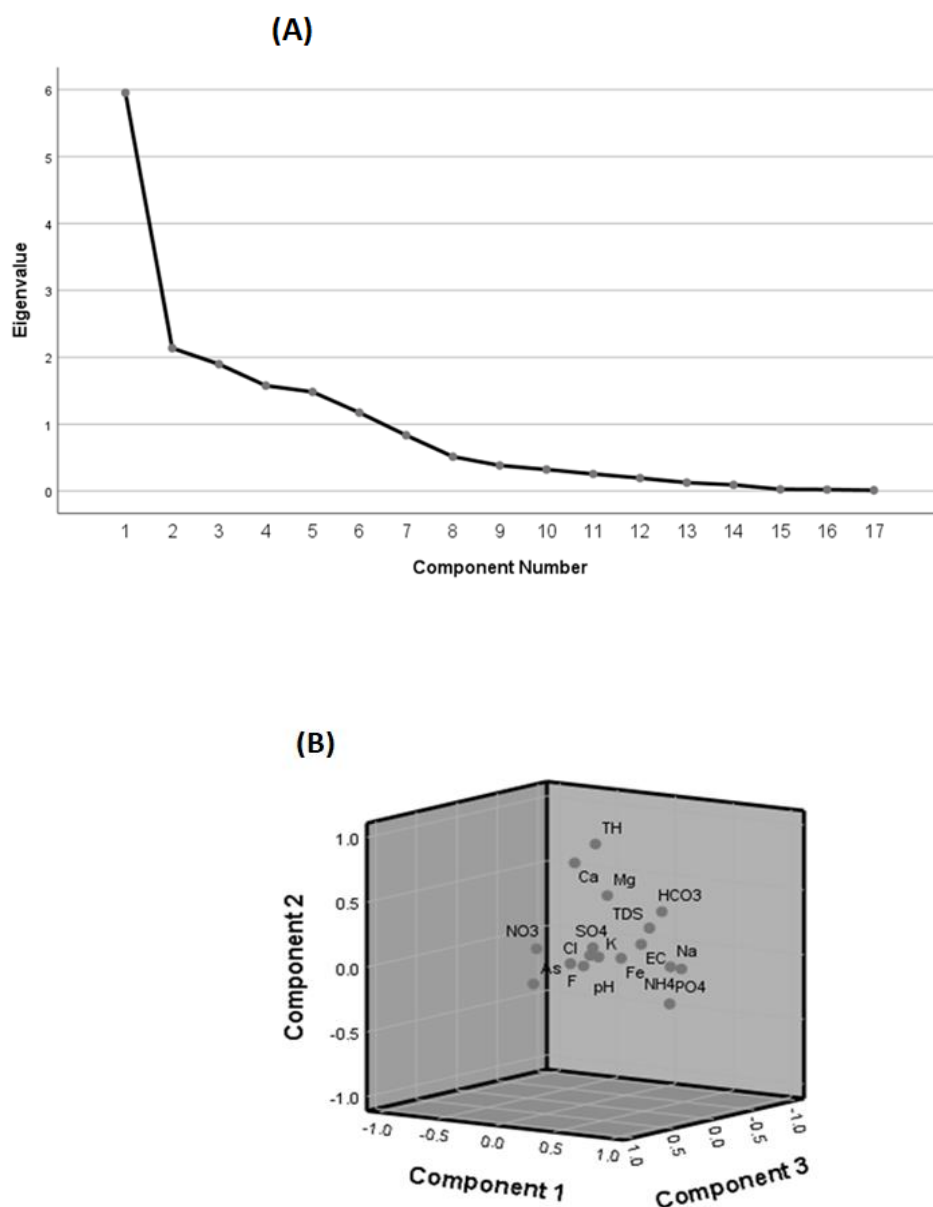


**Fig 2.6: Principal component analysis by (A) Scree plot of the eigenvalues and (B) component plot in rotated space**

### Piper classification

Piper trilinear diagrams [22] (Fig. 2.7) were prepared by using the hydrochemical data of collected groundwater samples from Golaghat district. It is seen that, most of the samples are scattered in zones B and D with respect to cations; only 6% water samples are in zone A of the lower-left triangle, which indicate that some groundwater samples are of calcium type, some of sodium type water and most are of mixed type. From the lower-right triangle of the

Fig.2.7, we can say that, since most groundwater samples are plotted in the zone E, so bicarbonate-type water is predominant. The predominant hydrochemical types are  $\text{HCO}_3^-$ - $\text{Ca}^{2+}$ ,  $\text{HCO}_3^-$ - $\text{Na}^+$  and mixed  $\text{HCO}_3^-$ - $\text{Ca}^{2+}$ - $\text{Na}^+$ - $\text{Mg}^{2+}$  types. The quadrilateral or diamond shape of the Fig.2.7. quadrilateral or diamond shape revealed that 49.8% of GW samples fall in the area 5 and another 49.8% fall in the area 8 of the diagram. So, from the Piper diagram, it can be confirmed that groundwater of golaghat district is dominated by  $\text{Mg}^{2+}$  and  $\text{Na}^+$ . The weak acids represented by  $\text{HCO}_3^-$  exceeds the strong acids represented by  $\text{SO}_4^{2-}$  and  $\text{Cl}^-$ . Again, 0.4% water samples of the area 9 in the Fig. 2.6, indicates no dominant type of water class i.e., no one cation-anion pair exceeds 50 percent, thereby indicating magnesium and sodium bicarbonate type of water [21].

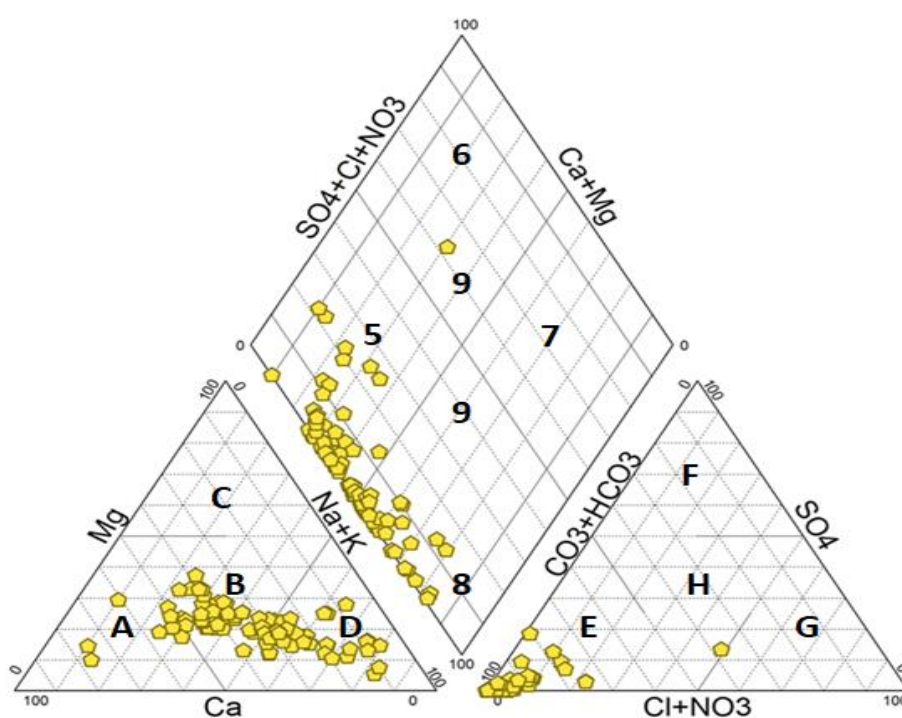


**Fig 2.7: Piper diagram of groundwater samples of Golaghat district**

## 2.4 Conclusion

The present values of pH, TDS,  $\text{HCO}_3^-$ , TH,  $\text{Na}^+$ ,  $\text{NH}_4^+$ ,  $\text{K}^+$ ,  $\text{Ca}^{2+}$  and  $\text{Mg}^{2+}$  of examined groundwater samples of Golaghat district are within the permissible limit; but with respect to fluoride and arsenic groundwater of study area is not fit for drinking at all compared to WHO/BIS safe limit. Six out of eight development blocks of Golaghat district

are highly contaminated by As, which is several fold higher than that of WHO/BIS safe limit (0.05mg/L). Highest concentration of As was found in Gamariguri block (0.460 mg/L). In Podumoni, Kakodonga, Gamariguri, Kathalguri, Sorupathar and Morangi development blocks groundwater samples were found contaminated with As by 68%, 65%, 46.7%, 21.05%, 7.14% and 3.7% respectively. Groundwater samples of two development blocks (Gamariguri and Sorupathar) are affected by fluoride and Podumoni block is partially fluoride affected area as 28% groundwater samples have concentration more than 1.0 mg/L. Although, high level of As and  $F^-$  in groundwater is mostly due to natural activities; but it may sometimes be due to some human activities, such as mining (As) and use of phosphate pesticides. In case of groundwater quality of peripheral area of Golaghat district is free from fluoride contamination; but the East-South part of Golaghat district (i.e., Jorhat district) is affected by arsenic. Concentration of Fe is also very high (0.8-4.8 mg/L) in entire Golaghat district and since As and Fe is correlated positively, so As might be originated from dissolution of As-Fe bearing minerals [4,11] and the immediate source mineral is likely to be ferric arsenate (with or without ferric arsenite). From the Piper trilinear diagram analysis, it is found that bicarbonate-type water is predominant. The predominant hydrochemical types are  $HCO_3^-$ - $Ca^{2+}$ ,  $HCO_3^-$ - $Na^+$  and mixed  $HCO_3^-$ - $Ca^{2+}$ - $Na^+$ - $Mg^{2+}$  types. Principal component analysis showed that the groundwater quality of Golaghat district of Assam is influenced by both natural and anthropogenic sources.

So, pre-treatment of groundwater of Golaghat district is necessary for the use of it for drinking purpose. Public should be made understand the chronic arsenic and fluoride toxic effects for long term use of such water by arranging awareness camp. Assessment of groundwater quality of these areas at a particular interval of time and implementation of remedial measures is very important however this is beyond the scope of present research activity therefore should be taken up during future possible studies.

The concentration of fluoride of maximum groundwater samples of Golaghat district, mainly for Dergaon, Kathalguri, Kakodonga, Morangi and Bokakhat development block area, are less than 0.5 mg/L. It may be due to the absence of fluoride containing minerals or may be due to heavy rainfall which diluted the fluoride concentration. Below the fluoride concentration range 0.5-1.0 mg/L causes dental caries [37] mainly among children. As for dental health we need sufficient amount of fluoride, so remineralization of fluoride is important. It can be done by fluoridation of water, milk, salt and toothpaste [38]. In future

work dental health assessment mainly for the children of the Golaghat district to take necessary action by supplying fluorinated water is very important.

## **References**

- [1] Sengupta A. (1999) In workshop on groundwater pollution and protection. Central Groundwater Board, Science City, Calcutta. 69-7, 1999.
- [2] Sushella A.K. (2001) A treatise on Fluorosis, Fluorosis Research and Rural Development Foundation, New Delhi. 15, 2001.
- [3] Dutta R. K., Saikia G., Das B., Bezboruah C., Das H. B., and Dube S. N. (2006) Fluoride contamination in groundwater of Central Assam, India. Asian Journal of Water Environment and Pollution. 2(3), 93–100.
- [4] Singh A.K. (2004) Arsenic contamination in groundwater of North eastern India. In Proceedings of 11th national symposium on hydrology with focal theme on water quality (pp. 255–262). Roorkee: National Institute of Hydrology.
- [5] World Health Organization (WHO) (2017) Guidelines for Drinking-water Quality: Fourth Edition Incorporating the First Addendum.
- [6] WHO (1993) Guidelines for drinking water quality. Geneva: World Health Organization <http://www.lenntech.com/WHO's-drinking-water-standards.htm>. Accessed 28 Feb 2010.
- [7] Alarcon-Herreraa M. T., Martin-Alarconb D.A., Gutierrezc M., Reynoso-Cuevasg L., Martin-Dominguezd A., Olmos-Marqueze M.A., and Bundschuhf J. (2020) Co-occurrence, possible origin, and health-risk assessment of arsenic and fluoride in drinking water sources in Mexico: Geographical data visualization. Science of the Total Environment. 698-134168, <https://doi.org/10.1016/j.scitotenv.2019.134168>.
- [8] Jimenez-Cordova M.I., Sanchez-Pena L.C., Barrera-Hernandez A., Gonzalez-Horta C., Barbier, O.C., and Del Razo L.M. (2019) Fluoride exposure is associated with altered metabolism of arsenic in an adult Mexican population. Sci. Total Environ. 684, 621–628.
- [9] Limon-Pacheco J.H., Jimenez-Cordova M.I., Cardenas-Gonzalez M., Sanchez Retana I.M., Gonsebatt M.E., and Del Razo L.M. (2018) Potential co-exposure to arsenic and

- fluoride and biomonitoring equivalents for Mexican children. *Ann. Glob. Heal.* 84, 257–273.
- [10] Wasserman G.A., Liu X., LoIacono N.J., Kline J., Factor-Litvak P., Van Geen A., Mey J.L., Levy D., Abramson R., Schwartz A., and Graziano J.H. (2014) A cross-sectional study of well water arsenic and child IQ in Maine school children. *Environ. Heal. A Glob. Access Sci. Source* 13. <https://doi.org/10.1186/1476-069X-13-23>.
- [11] Chetia M., Chatterjee S., Banerjee S., Nath M.J., Singh L., and Srivastava R.B. (2011) Groundwater arsenic contamination in Brahmaputra river basin: A water quality assessment in Golaghat (Assam), India. *Environ Monit Assess.* 173, 371–85.
- [12] Groundwater Information Booklet (2008) Golaghat District, Assam, Ministry of Water Resources, Guwahati. [http://cgwb.gov.in/District\\_Profile/Assam/.pdf](http://cgwb.gov.in/District_Profile/Assam/.pdf). Accessed 28 Feb 2010.
- [13] APHA 1998, APHA, Awwa (American Public Health Association) (1998) Standard methods for the examination of water and wastewater. American Public Health Association, Washington DC.
- [14] Viswanathan V.C. (2015) Effect of river restoration and hydrological changes on surface water quality – River reach-scale to catchment-scale study. Ph D. Thesis-presented to the Faculty of Science of the University of Neuchâtel to satisfy the requirements of the degree of Doctor of Philosophy in Science.
- [15] Liu F., Song X., Yang L., Zhang Y., Han D., Ma Y., and Bu H. (2015) Identifying the origin and geochemical evolution of groundwater using hydrochemistry and stable isotopes in the Subei Lake basin, Ordos energy base, Northwestern China. *Hydrol. Earth Syst. Sci.* 19, 551–565.
- [16] Eatson A. D., Clesceri L. S., Rice E. W., and Greenberg A. E. (2005) Standard methods for the examination of water and wastewater (21st ed., pp. 4–138). Centennial Edition. USA.
- [17] Usman U. N., Toriman M. E., Juahir H., Abdullahi M. G., Rabiou A.A., and Isiyaka H. (2014) Assessment of Groundwater Quality Using Multivariate Statistical Techniques in Terengganu. *Science and Technology.* 4, 3, 42–49 DOI:10.5923/j.scit.20140403.02.
- [18] Molla M. A., Saha N., Salam S. A., and Rakib-uz-Zaman M. (2019) Surface and groundwater quality assessment based on multivariate statistical techniques in the vicinity of Mohanpur, Bangladesh. *Int J Env Health Eng.* 4, 18.



- [19] Shrestha S., and Kazama F. (2007) Assessment of surface water quality using multivariate statistical techniques: a case study of the Fuji river basin, Japan. *Environmental Modelling and Software*. 22, 464–475.
- [20] Kumar K.S., Babu S.H., Rao P.E., Selvakumar S., Thivya C., Muralidharan S., and Jeyabal G. (2017). Evaluation of water quality and hydrogeochemistry of surface and groundwater, Tiruvallur district, Tamil Nadu, India. *Appl Water Sci*. 7, 2533–2544. <https://doi.org/10.1007/s13201-016-0447-7>.
- [21] Khound N. J., and Bhattacharyya, K. G. (2018) Assessment of water quality in and around Jia Bharali river basin, North Brahmaputra Plain, India, using multivariate statistical technique, *Applied Water Science*. 8, 221.
- [22] Piper A. M. (1944) A graphical procedure in the geochemical interpretation of water analysis. *Trans Am Geophys Union*. 25, 914–923.
- [23] Bureau of Indian Standards (BIS) (1991). 10500:1991, Second Revision ICS No. 13.060.20. [http://www.bis.org.in/sf/fad/FAD25\(2047\)C.pdf](http://www.bis.org.in/sf/fad/FAD25(2047)C.pdf). Accessed 6 Jan 2010.
- [24] Garcia M.G., Del Hidalgo V.M., and Blesa M.A. (2001) Geochemistry of groundwater in the alluvial plain of Tucuman province, Argentina. *Hydrogeol J*. 9, 597–610.
- [25] Dufor C. N., and Becker, E. (1964) Public Water Supplies of the 100 Largest Cities of the United States. U.S. Govt. Print. Off, 1964.
- [26] Saikia M. M., and Sarma H. P. (2011) Fluoride geochemistry of Kollong river basin, Assam, India. *Scholars Research Library-Archives of Applied Science Research*. 3, 3, 367-372.
- [27] Chakraborti D., Chanda C. R., Samanta G., Chaudhury U. K., Mukherjee S. C., Pal A. B., Sharma B., Mahanta K. J., Ahmed H. A., and Sing B. (2000) *Curr Sci*., 78, 1421-1423.
- [28] Gupta S., Benerjee S., Saha R., Datta J. K., and Mondal N. (2006) Fluoride geochemistry of groundwater in Nalhati-1 block of the Birbhum district, West Bengal, India. *Fluoride*. 39, 318-320.
- [29] Navarro O., Gonzalez J., Junez-Ferreira H.E., Bautista C.F., and Cardona A. (2017) Correlation of arsenic and fluoride in the groundwater for human consumption in a semiarid region of Mexico. *Procedia Eng*. 186, 333–340. <https://doi.org/10.1016/j.proeng.2017.03.259>.

- [30] Singh A. K. (2006). Review article-Chemistry of arsenic in groundwater of Ganges–Brahmaputra river basin. *Current Science*. 91, 599–605.
- [31] Chetia M., Singh S. K., Bora K., Kalita H., Saikia L. B., and Goawami D. C. (2008) Groundwater arsenic contamination in three blocks of Golaghat district of Assam. *Journal of Indian Water Works Association*. 40(2), 150–154.
- [32] Kaiser H. F. (1960) The application of electronic computers to factor analysis. *Educ Psychol Meas*. 20, 141–151.
- [33] Simeonov V., Stratis J. A., Samara C., Zachariadis G., Voutsas D., and Anthemidis A. (2003) Assessment of the surface water quality in Northern Greece. *Water Res*. 37, 4119-24.
- [34] Jackson J. E. (1991) *A user's guide to principal components*. New York: Wiley.
- [35] Kim J. O., and Mueller, C. W. (1987) *Factor Analysis: Statistical Methods and Practical Issues*, Sage University Paper Series on Quantitative Applications in the Social Sciences, series no 07–014. Sage Publications, Beverly Hills.
- [36] Chapagain S. K, Shrestha S., Nakamura T., Pandey V. P., and Kazama F. (2009). Arsenic occurrence in Groundwater of Kathmandu Valley, Nepal. *Desalination and Water Treatment*. 4, 248-254.
- [37] World Health Organization (WHO) (2011) *Guidelines for drinkingwater quality*, 4th edn. World Health Organization, Geneva.
- [38] Jones S., Burt B.A., Petersen P.E., and Lennon M.A. (2005) The effective use of fluorides in public health. *Bull World Health Organ*. 83(9), 670-6.

## **CHAPTER – 3**

**Mitigation approach of fluoride and arsenic- present state of art globally. Global solutions *vis a vis* local conditions the need for local solutions**

**3.1 Introduction**

Industrialization along with the urbanization results in rapid deterioration of water quality. Although there are many contaminants in water, fluoride and arsenic are most important. The reason of fluoride and arsenic (As) contamination of groundwater are both natural and anthropogenic activities (discussed in the chapter 1). Fluoride and arsenic enter into our health mainly by drinking water. Daily consumption of drinking water having fluoride concentrations more than 1.5 mg/L and with arsenic concentration more than 0.01 mg/L is toxic for health. The health effects for elevated concentration of fluoride and arsenic were discussed in the chapter 1. Arsenite [As (III)] and arsenate [As (V)] are the forms of arsenic found in water. The present scenario in Assam, India as well as in the World with reference to fluoride and arsenic were also discussed in the chapter 1. From the chapter 2, it is seen that the entire Golaghat district of Assam is badly affected by arsenic and three out of eight development blocks are affected by fluoride. Due to toxic effect of fluoride and arsenic, removal of these contaminants from drinking water is very essential. So developing technologies to get rid of fluoride and arsenic from groundwater has become a major topic of research in recent years.

**3.2 Existing processes for the removal of fluoride and arsenic from water**

A variety of methods have been developed for the purpose of removal of fluoride and arsenic from contaminated water. The most effective technologies used such as coagulation and precipitation using chemicals like calcium hydroxide, aluminium hydroxide, aluminum sulfate, Nalgonda technique, magnesium oxide-coated nanoparticles [1,2,3,4], adsorption [5,6], ion-exchange methods through the use of strong basic anion-exchange resin containing quaternary ammonium functional groups [7,8,9,10,11], reverse osmosis based membrane filtration, nanofiltration [11,12,13].

**3.2.1 Precipitation-Coagulation**

In this method, soluble chemicals are added in water to form the precipitation of fluoride/arsenic, then the precipitate is removed by sedimentation or filtration [14]. The three main mechanisms of this Coagulation / Precipitation [15] method are :

Precipitation: formation of the insoluble compounds with added chemicals.

Co-precipitation: soluble fluoride/arsenic are incorporated into a growing metal hydroxide phase.

Adsorption: to the external surfaces of the insoluble metal hydroxide soluble arsenic binds electrostatically.

### **For removal of fluoride**

In periodic addition of chemicals for precipitation, a certain amount of waste produce every day. Chemicals having lime are either used alone or with aluminium or magnesium salts in addition with coagulation aids. Most commonly used practice for the treatment of fluoride contaminated water is Nalgonda technique, which can be used at community water works level [16]. Lime (5% of alum), bleaching powder (optional) and alum ( $\text{Al}_2(\text{SO}_4)_3 \cdot 18\text{H}_2\text{O}$ ) are added in Nalgonda technique in sequence to water. Therefore, due to these coagulation and sedimentation takes place. In Precipitation-Coagulation process, a much larger dose of chemicals are required and a large amount of sludge produces which pauses disposal problems and requires large amount of chemicals that must be added daily [17].

### **For removal of arsenic**

Although all these mechanisms have contributions towards metal removal, precipitation does not show important role in case of arsenic removal. After coagulation and simple sedimentation it has been seen from various studies that hydrous metallic oxides together with sorbed arsenic remain suspended in colloidal form. So, sand filtration or microfiltration is necessary [18]. The most efficient treatment process for coagulation of arsenic from water is done with iron and aluminium salts and lime softening [3,4]. Prior oxidation of As(III) to As(V) is essential to improve the efficiency of the above method.

### **3.2.2 Membrane based processes**

To remove fluoride and arsenic from water, membrane based processes like nanofiltration (NF), reverse osmosis (RO), and electro dialysis are also used [19,20]. Reverse osmosis gives extremely high purity water. It is a physical process and exactly reverse of the natural osmosis as it applies for assurance on the feed water to pass through the semipermeable membrane [21]. On the basis of size and electrical charge RO membrane eliminate ions. Nanofiltration has same phenomenon as that of reverse osmosis but it requires low pressure unlike reverse osmosis. In RO the membrane have smaller pores and offer more resistance to the passage of both solvents and solutes unlike NF. As a result, both pressure and energy required in NF is less and thus faster. By using a nanofiltration pilot plant Tahaikt and others, 2006 carried out fluoride removal operation on under groundwater. The impact of

various parameters such as initial fluoride concentration, pressure and time were studied by the authors. As Fluoride is a very small ion it is strongly hydrated, it is more strongly retained on nanofiltration membrane than other monovalent anions because of its high charge density and the consequent steric effect. This technique can remove 95% As(V) at an applied pressure of less than 1.1MPa; but it removes only 75% As(III) [13]. NF membrane containing poly amide layer is very efficient to remove As(V) by 90-100%, while it is very poor in removing As (III) which is less than 10% [11]. The effectiveness of membrane process for arsenic removal is sensitive to a variety of components in the untreated water and their characteristics. Because of its high cost, production of high amount of waste etc, this technique is not efficient. It also removes other inorganic useful ions such as  $\text{Ca}^{2+}$ ,  $\text{Na}^{+}$  etc. which is necessary to be present in our drinking water at a permissible range [11].

Electro-dialysis (ED) is another membrane technology which is similar to RO, except direct current potential is used instead of high pressure. The water quality obtained from electro-dialysis is comparable to RO. When electric field is applied as driving force for the removal of ionic components from aqueous solutions through ion exchange membranes, it is called electro-dialysis. Kabay et al., 2008 studied that the separation performance increases with applied potential. It works in any pH value. In North Africa ED technology is used in large scale water treatment of high fluoride brackish water [24]. However, for the treatment of water ED method need high capital cost, require special equipment, electrical energy and specially trained operators and hence not suitable for rural application.

### **3.2.3 Ion-Exchange method**

Fluoride and arsenic (mainly for arsenate) can be removed from water by the mechanism of exchange of ions by passing water through the column of basic anion resin in either chloride or hydroxyl form. Some example of such type of resins are: Deacedite FF (IP), Amberlite XE-75, Lewatit MH-59 etc. When the chloride resins get saturated with fluoride/arsenate, they can be regenerated to their original form by using both hydrogen chloride and sodium chloride followed by washing with distilled water [11] and new chloride ions replace the fluoride/arsenate ions. However, for the regeneration of resin the required amount of regenerant is very large. The waste produced is also very large and the resins are very expensive [25].

### 3.2.4 Subterranean Arsenic Removal (SAR) Technology

It is a relatively new technique for groundwater treatment. In this technique subterranean water is pumped out aerated and repumped to earth which oxidizes arsenite to arsenate and ferrous to ferric. A natural adsorption process of arsenate to ferric takes place after the above oxidation reaction. The kinetics of subterranean oxidation of  $\text{As}^{3+}$  to  $\text{As}^{5+}$  and  $\text{Fe}^{2+}$  to  $\text{Fe}^{3+}$  is very slow, and if not properly monitored it may lead to As release to the surface water. Secondly costly submersible pumps are needed [26].

### 3.2.5 Adsorption

Adsorption is the adhesion or accumulation of molecules of gas, liquid or dissolved solid by physical/chemical forces to the surface of an adsorbent. From review of literature it is seen that, adsorption process is the most effective method for the removal or elimination of fluoride and arsenic from water in terms of low cost of the adsorbent, easy operation, high adsorption capacity and high availability of raw materials for adsorbent preparation. Adsorption of fluoride and arsenic may be physical or chemical. In case of physical adsorption interaction between adsorbent and fluoride/arsenic will be weak van-der-Waals forces, whereas in chemical adsorption there will be strong solute-adsorbent bonding. By using high-valency metals to functionalized sorbents, elimination of fluoride/arsenic by adsorption process has been widely studied in recent years [27].

Adsorption on any solid adsorbent normally occurs through three phases [12,28].

- (i) External mass transfer: the diffusion or transport of fluoride/arsenic ions to the surface of the adsorbent from bulk solution across the boundary layer surrounding the adsorbent particle.
- (ii) Adsorption of fluoride/arsenic ions on to particle surfaces.
- (iii) Intra particle diffusion: the adsorbed fluoride/arsenic ions probably interchanged with the structural elements inside adsorbent particles depending on the chemistry of solids, or the adsorbed fluoride/arsenic ions are moved to the internal surfaces for porous materials.

Fluoride/arsenic removal efficiency of an adsorbent depends upon some important characteristics of the adsorbent such as adsorption regenerability, particle and pore size, adsorption capacity, compatibility availability of the raw materials and cost. Again removal efficiency of the adsorbent always depends on initial fluoride concentration, adsorbent dose, temperature, contact time and pH [29,30].

**Table 3.1: The comparison of various technologies for the removal of fluoride and arsenic**

Technology	Advantage	Disadvantage	References
Coagulation/ precipitation:	Commercially available chemical, effective over a wider range of pH.	Expensive, require skilled operators, concentration of aluminum increases in water, sedimentation and filtration needed, produces high amount of sludges; low removal of arsenic; co-ions affect efficiency, pre-oxidation of As (III) to As (V) for arsenic removal may be required.	[17]
Membrane based filtration:	High removal capacity; remove other contaminates.	High capital cost, high-tech operation and maintenance, produces high amount of rejected water which is toxic.	[11]
Ion-exchange:	High removal capacity.	Costly, affected by co-ions (sulfate, phosphate, chloride, bicarbonate etc.), highly pH dependent, create toxic liquid waste. High-tech operation and maintenance; regeneration creates sludge disposal problem; As(III) is difficult to remove; life of resins is low	[25]
Subterranean Arsenic Removal (SAR) Technology.	In this technique both iron and arsenic can be removed. Benefit is no sludge handling necessary and sludge volume is minimal.	The kinetics of subterranean oxidation of $\text{As}^{3+}$ to $\text{As}^{5+}$ and $\text{Fe}^{2+}$ to $\text{Fe}^{3+}$ is very slow, and is not properly monitored it may lead to As release to the surface water. Secondly, costly submersible pumps are needed.	[26]



Adsorption:	Greater accessibility; inexpensive, simple operation and adsorbents are highly available.	Efficiency depends on pH, some ions interfere fluoride adsorption.	[29,30]
-------------	---	--	---------

From the above Table 3.1, it is seen that out of all of these methods the adsorption process is found to be the inexpensive and most effective method for the elimination of fluoride and arsenic from water [31,32,33,34]. Most of the technologies are pH dependent. In case of arsenic, As (V) is easy to be eliminated than that of As (III) and so pre-oxidation of As (III) to As (V) is important [35,36]. Yet the effectiveness of adsorption process for arsenic treatment requires further lower operating and maintenance costs. Although adsorption is best for the treatment of water and waste water in terms of convenience, profitability, design and significant arsenic removal efficiency [37], yet there are scopes of further improvement.

### **3.2.5.a Adsorbents for fluoride removal/elimination**

A wide variety of adsorbents for the elimination of fluoride from water have been used. Adsorptive materials like activated carbons [38,39,40,41,42], red soil, charcoal, fly ash [43,44,45], activated and impregnated alumina [46,47,48], bauxite [49,50,51], quartz [28], hematite [52,53], polymeric resins [54], activated rice husk [55,56,57], brick powder [58], pumice stone [59,60], modified ferric oxide/hydroxide [61,62,63], zeolite [64,65], seed extracts of *Moringa oleifera* [51], granular ceramics [66], hydroxyapatite (HAP) [55,67], zirconium and cerium modified materials [12,68,69], modified cellulose [70,71], clays [72,73] and magnesium-modified sorbent [74,75] have been used with various efficiencies for removing fluoride from water but the adsorption capacities of some adsorbents decreases with decreasing fluoride concentration and some of them can work only at an extreme pH value e.g. activated carbon prepared from Mangrove plant leaf powder, Almond tree bark powder, Pineapple peel powder, Chiku leaf powder, Toor plant leaf powder and Coconut coir pith, which are only efficient for fluoride elimination at  $\text{pH} < 3.0$  [76].

**Metal oxide/hydroxide**

Many researchers showed that, different metal oxides and hydroxides have adsorption capacity towards heavy metals, anions and hazardous elements in water [77].

Hydrous titanium dioxide having high surface area is a good adsorbent for fluoride [78]. Gel like titanium hydroxide-derived adsorbent from titanium oxysulphate ( $\text{TiO}(\text{SO}_4)$ ) was prepared for adsorption of fluoride [78]. Titanium hydroxide-derived adsorbent could remove fluoride ions even at low concentration and had selectivity for fluoride ions with coexisting chloride, nitrate and sulfate ions. It could eliminate fluoride to below 0.8 mg/L from solution with initial concentration of 50 mg/L [79].

Fluoride and arsenate removal efficiency of iron oxyhydroxide ( $\text{FeO}_x\text{H}_y$ ), iron and aluminum binary oxide ( $\text{FeAlO}_x\text{H}_y$ ) and aluminum oxyhydroxide ( $\text{AlO}_x\text{H}_y$ ) were analyzed [80] by batch adsorption experiment. Results showed that  $\text{FeO}_x\text{H}_y$  have high affinity towards arsenate (94.8%) but little towards fluoride (18.4%) from the solution containing both arsenate and fluoride.  $\text{AlO}_x\text{H}_y$  alone also showed some limited efficiency (29.4%) in the removal of fluoride.

Chai and others [63], showed that sulfate-doped  $\text{Fe}_3\text{O}_4/\text{Al}_2\text{O}_3$  nanoparticles also good sorbent for fluoride ion in the pH range 4.0 to 10.0. This nano adsorbent had high selectivity for fluoride as other competing anions, except phosphate, did not inhibit fluoride removal capacity. According to the authors, the mechanism of adsorption of fluoride was the creation of inner-sphere fluoride complex by ion exchange of sulfate by fluoride.

Mohapatra and others [81] used magnesium-doped nano ferrihydrite for the elimination of fluoride, authors showed that fluoride removal capacity increases with increasing Mg content.

Kang and others [82], showed that fluoride removal efficiency of calcined Mg/Fe layered double hydroxides depends on Mg/Fe molar ratio and calcinations temperature, when they used calcined Mg/Fe layered double hydroxides, for simultaneous removal of fluoride and arsenate from aqueous solution. Maximum fluoride adsorption capacity is showed by Mg/Fe layered double hydroxides at 400°C calcined temperature.

**Alumina and aluminum based materials**

Farrah and his co-workers [83], studied the interaction of fluoride ion with amorphous aluminum hydroxide, gibbsite (naturally occurring aluminum hydroxide) and aluminum oxide over a range of pH values from 3 to 8 and fluoride concentrations from 1.9-19mg/L.

Due to high surface area, activated alumina shows high adsorption property [84]. Shimelis et al. [85], showed that activated alumina obtained by heating is more effective adsorbent. Adsorption of fluoride onto alumina is a complex process [86] and depends upon the surface morphology of the adsorbent, temperature, concentration and pH of the fluoride solution. Due to the formation of aluminum sulfate with sulfate ions present in the fluoride solution, there is an inhibition of the adsorption of fluoride by sulfate ion. When alumina particles are incorporated into the chitosan polymeric matrix, then such alumina composite materials shows more efficiency in fluoride adsorption than that of activated alumina [50].

By mixing of Fe(II), Al(III) and Ce(IV) salt solutions in the molar ratio of 1:4:1 under alkaline condition [61], prepared a good adsorbent for fluoride. They also observed the adverse effect of high concentration of phosphate and arsenate in the adsorption efficiency of fluoride.

Again, the fluoride removal efficiency of alum-impregnated activated alumina was found to be 92.6% [87]. Such type of activated alumina are- alumina plus manganese dioxide, alumina plus magnesium oxide [47], alumina plus iron oxide [88], alumina plus calcium mineral [12], bauxite [89], red mud of which major components are aluminium and iron oxides [90].

### **Geomaterials**

Some cheap geomaterials also used as fluoride adsorbent [91]. In 1967, Bower and Hatcher, first published the fluoride adsorption property of minerals and soils [91]. The composition of soil is quartz, feldspar, illite and goethite. Many researchers have taken soil also as fluoride adsorbent [92].

Fluorspar, quartz, iron activated quartz and calcite were used by Fan and his co-workers [28], for the adsorption of radioisotope fluoride ( $^{18}\text{F}$ ). The authors stated that fluorspar can remove 25% of  $^{18}\text{F}$ , calcite can remove 12% and quartz can remove only 5.6%; but the iron activated quartz can remove 20% of  $^{18}\text{F}$ .

Clay has prominent adsorption property and can be used for the adsorption of fluoride and arsenic due to availability, cheap, environmental stability, high surface area and ion exchange property. The structure of clay plays a key role in determining the charge on the clay surface and type of exchange that can take place with ions in solution [92]. Guo and Tian [93] reported that fluoride and arsenic can be removed from water by using anionic clay hydrocalumite by precipitation and adsorption. Guo and Reardon [94] used mechanochemically synthesized anionic clay-meixnerite and calcined meixnerite to

investigate their fluoride removal capacity from water. The authors informed that calcined meixnerite has more fluoride removal capacity than uncalcined meixnerite. Kamble et al. [95] used modified bentonite clay (La- bentonite, Mg- bentonite and Mn- bentonite) for the removal of fluoride from water. The authors stated that fluoride adsorption capacity of La-bentonite showed 10% higher than that of unmodified bentonite. As the adsorption capacity of La-bentonite was high at  $\text{pH} > 5$ , so it indicates that exchange of fluoride ions with hydroxyl ions present on the surface of adsorbent takes place.

A type of volcanic stone known as Pumice, also has adsorption property. It is an effective and cheap material having a large surface area [96,97]. The fluoride adsorption capacities of surface modified pumice with magnesium chloride and with hydrogen peroxide are more than that of untreated pumice.

Zeolites also have been used to water treatment. It shows both adsorption and ion exchange properties. Rahmani et al. [64] reported from their experiments that, untreated zeolite has very low fluoride adsorption capacity ( $< 20\%$ ). Samatya et al. [98] said that at all pH values, the surface charges of zeolites is negative, due to which it has higher attraction towards cations is more than that of anions. Therefore, for increasing the adsorption capacity, multi-valent metallic cations were used by many researchers to obtain modified zeolite surface [99]. Sun et al. [100] used ferric ion from  $\text{FeCl}_3$  solution to treat stilbite zeolite, Zhang et al. [101] used calcium ion from calcium chloride to modify natural zeolite.

Sajidu et al. [102] reported that bauxite is a good adsorbent of which 2.5 g can remove fluoride up to 93.8% from 200 mL of 8 mg/L fluoride solution. The major component of bauxite are gibbsite ( $\text{Al}(\text{OH})_3$ ) and kaolinite ( $\text{Al}_2\text{Si}_2\text{O}_5(\text{OH})_4$ ).

### **Carbonaceous materials**

In recent years, the carbonaceous materials are widely used in the adsorption processes as well as for other industrial purposes. Physical and chemical are the two activation methods by which activated carbon can be prepared from any carbonaceous material having high concentration of carbon. The choice of method for the preparation of activated carbon depends on the density of the starting materials [103]. During the last 10 years, use of activated carbon for remediation of environmental pollution is increasing very sharply. Since these are renewable, easily available and low cost materials therefore many agricultural wastes such as coconut shell, coffee bean husks, chestnut wood [91], peels of various fruits such as jack fruit [104], orange [105], sugarcane [106] Moringa oleifera seeds

[107], Mango leaves [108], Rice husk [109], Rice straw [110], Saw dust [111] were used for the preparation of activated carbon. During carbonization i.e., thermal decomposition of carbonaceous materials, carbon precursor is formed in which all the volatile materials including the hetero atoms are removed. In physical adsorption, the resulting char obtained from the above step, are treated with zirconium, titanium, iron, calcium etc. to enhance defluoridation efficiency [112]. Alagumuthu et al. [39] stated that, unactivated cashew nut shell carbon has low adsorption efficiency than that of zirconium treated cashew nut shell carbon. Ganvir and Das [55] reported about the high fluoride removal capacity of aluminum hydroxide coated rice husk ash.

### **3.2.5.b Adsorbent for arsenic**

Various adsorbents are used for the removal of arsenic from water. Materials that have arsenic adsorption capacities are: activated alumina, activated carbon, iron media (iron oxide coated sand, granular ferric hydroxide, iron pyrites) and some natural mineral based adsorbent [90].

#### **Metal oxide/hydroxide**

Granular Ferric Hydroxide(GFH) process was developed at the Technical University of Berlin. GFH is a type of porous iron material and Simms et al, [113] stated that, GFH has arsenic adsorption capacity. The most significant disadvantage of this technology is the high cost. Chen et al. [114] reported that arsenic can be removed by zero-valent iron (ZVI)-based system. From the pilot studies the authors said that, arsenic removal by a system of ZVI plus iron-modified granular activated carbon showed significant efficiency.

#### **Alumina and aluminum based materials**

Activated Alumina (AA) is a porous granular material and can be obtained from dehydration of  $\text{Al}(\text{OH})_3$  at high temperature [115]. AA can adsorb arsenic from water on the available binding sites present on the oxide surface of AA. The arsenic absorption efficiency is also affected by other competing anions present in arsenic contaminated water. Arsenate ( $\text{H}_2\text{AsO}_4$ ) can be easily removed from water by AA than that of arsenite ( $\text{H}_3\text{AsO}_3$ ), because at below pH 9, the overall molecular charge of arsenite ( $\text{H}_3\text{AsO}_3$ ) is neutral. Hence it is necessary to oxidize arsenite to arsenate before effective treatment of arsenic contaminated water.

Zeolite have been used to water treatment. Due to large surface area and large pore sizes, zeolite act as good sorbents for several metallic and radioactive cations [116]. As zeolites are microporous and hydrated aluminosilicates of alkali and alkaline earth cations [117], they can remove contaminant from water by both adsorption and ion exchange properties. With silicon, aluminum, and oxygen, zeolites form their framework and cations, water and other molecules are present within their pores. The structure of zeolites are well-defined and it does not change when zeolites lose and gain water reversibly and exchange the constituent cations. There are more than 30 natural zeolites. Vakharkar [116], stated that a natural zeolite Chabazite shows high adsorption affinity towards arsenic.

The soil which contain high level of iron and clay also shows arsenic remediation property and this property increases with increasing the level of iron content [118]. Zhang and Selim investigated As (V) adsorption-desorption kinetics on Olivier loam, sharkey clay and Windsor sand.

For arsenic remediation, a variety of treated and coated sands are used [119,120,121,122]. Iron oxide coated sand have more pores and high surface area [123] and can remove both arsenite (As(III)) and arsenate (As(V)); however As(V) can be removed more easily than that of As(III) [124]. Adsorption capacity of such surface modified sand is influenced by pH of adsorbate solution.

Clay minerals are hydrous aluminum silicates and sometimes it contain iron, magnesium and other cations [90]. Clay can exhibit both adsorption and ion exchange properties. Kaolinite, illite and montmorillonite are examples of typical clay minerals. Influence of pH and competing anions present on adsorption of arsenate and arsenite on clay minerals were studied by Manning and Goldberg [118]. In 2004, Gillman [125] used a clay material Hydrotalcite. Fufa et al. [126] used silicon, aluminum, iron and titanium oxides containing a natural clay material containing termite mound (TM) for the removal of As(III) and As(V) from drinking water [125,126]. Mishra et al. [127] stated that, in comparison of As (V) adsorption on natural minerals followed the order:

Bauxite > nickel laterite > iron ore slime > manganese ore.

Many researchers studied about the removal of As (III) and As (V) from water by using clay minerals [118,128,129].

**Carbonaceous materials**

Activated carbon is a carbonaceous material having large surface area and highly porous structure with a broad range of pore sizes. Activated carbon is one of the most widely used adsorbent to remove organic and inorganic contaminants from water [103]. For the preparation of activated carbon, many agricultural wastes such as coconut shell, coffee bean husks, chestnut wood [130], peel of various fruits such as jack fruit [104], orange [105], sugarcane [106], *Moringaoleifera* seed [107], *Ipomoea carnea* stem [131], *Mucuna prurines* plant [132] have been used because they are renewable and low cost materials with a high carbon and low ash content. Given below a list of various prospective feed stocks proposed by various workers for the preparation of activated carbons [90]. Activated carbons are prepared by carbonization employing a slow heating in the absence of air below 600°C due to which the volatile components are removed and followed by physical or chemical activation is followed. Treatment with oxidizing agent such as CO<sub>2</sub>, O<sub>2</sub> or steam at elevated temperature i.e. physical activation or with mineral acids, bases and salts i.e. chemical activation completes the surface activation process [133]. In this stage, the char obtained from carbonization, is further surface activated by reacting with an acid like phosphoric acid [134], nitric acid or a strong base like potassium hydroxide or a salt such as zinc chloride [135] to develop functional groups like as hydroxyl, carboxyl, carbonyl and lactonic. The activeness of surface of carbon depends upon the activation condition and the temperature used for carbonization of the materials. Activation refines the pore structures. Mesopores and micropores are formed and the surface areas increases up to 2000 m<sup>2</sup>/g [103].

**Table 3.2: List of Carbon feedstocks**

Bones	Lignin Lamp black
Bagasse	Lignite Leather waste
Bark	Municipal waste
Beat-sugar sludges	Molasses
Blood	Nut shells
Blue dust	News paper
Coal	Olive stones
Coffee beans	Petroleum acid sludge
Coconut shell	Pulp mill waste
Coconut coir	Palm tree cobs
Cereals	Peel of jack fruit, orange, banana,
Cotton seeds hulls	Rubber waste
Corn cobs	Rice husk
Distillery waste	Refinery waste
Fertilizer waste slurry	Scrap tires
Fish	Sunflower seeds
Fruits pits	Tea leaves
Graphite	Wheat straw
Jute stick	Wood
Ipomoea carnea	Stem
Mucuna prurines	Stem and leaves



Commercial activated carbon prepared from coal has high arsenic adsorption efficiency. Sometimes for arsenic remediation, activated carbons impregnated with metallic silver or copper [136]. Chidambaram et al. [43] stated that untreated raw carbon have very small absorbing capacity than treated carbon.

Gu et al. [137] developed a type of activated carbon which contains iron and named as granular activated carbon (GAC). Ferric ions were impregnated in GAC by using aqueous ferrous chloride and NaOCl. Adsorption capacity of As(V) takes place in the wide pH range 4.4-11.0 and it decreases at pH > 9.0.

Chuang, et al. [138] studied the arsenic adsorption capacity of activated carbon prepared from oats hulls and they reported that, the As(V) adsorption efficiency of that activated carbon decreased from 3.09 to 1.57 mg As g<sup>-1</sup> when the initial pH increased from 5 to 8.

**References:**

- [1] Waghmare S. S., and Arfin T. (2015) Fluoride Removal from Water By Calcium Materials: A State-Of-The-Art Review. Intl J of Innovative Res in Sci, Engg and Technol, 4(9):2347-6710.
- [2] Minju N., Swaroop K. V., Haribabu K., Sivasubramanian V., and Kumar P. S. (2013) 'Removal of fluoride from aqueous media by magnesium oxide-coated nanoparticles', Desalination and water treatment. 53(11), 2905-2914.
- [3] Sancha A.M. (1999) Removal of arsenic from drinking water supplies. Proceedings, IWSA XXII World Congress and Exhibition, Buenos Aires, Argentina.
- [4] Hering J.G., and Chiu V.Q. (1998) The Chemistry of Arsenic: Treatment and Implications of Arsenic Speciation and Occurrence. AWWA Inorganic Contaminants Workshop, San Antonio, TX, February 23-24, 1998.
- [5] Loganathan P., Vigneswaran S., Kandasamy J., and Naidu R. (2013) Defluoridation of drinking water using adsorption processes. J Hazard Mater, 248–249, 1–19.
- [6] Ahmann D., Aaron D., Redman D., and Macalady L. (2002) Natural organic matter affects arsenic speciation and sorption onto hematite. Environ Sci. Technol. 26, 2889-2896.
- [7] Gandhia M.R., Kalaivania G., and Meenakshia S. (2011) Sorption of chromate and fluoride onto duolite a 171 anion exchange resin – a comparative study. Pollution, 32:2034-2040.
- [8] Sanjeev K. and Sapna, J. (2013). History, introduction, and kinetics of ion exchange materials. Journal of Chemistry. 2013: 1-13.
- [9] Alguacil F. (2003) A kinetic study of cadmium (II) adsorption on Lewatit TP260 resin. Journal of Chemical Research, **3**: 144-146.
- [10] Mbugua G., Mbuvi H. and Muthengia J. (2014). Rice husk ash derived zeolite blended with water hyacinth ash for enhanced adsorption of cadmium ions. Current World Environment, **9**: 280-286.
- [11] Jana P. (2012) Removal of arsenic(III) from water with a new solid-supported thiol Thesis and Dissertations--Chemistry.
- [12] Mohapatra M., Anand S., Mishra B.K., Giles D.E., and Singh P. (2009) Review of fluoride removal from drinking water. J. Environ. Manage. 91:67–77.
- [13] Sato Y., Kang M., Kamei T., and Magara Y. (2002) Water Research 36, 3371.

- [14] Harrison P.T.C. (2005) Fluoride in water: A UK perspective. *J. Fluor. Chem.* 126:1448–1456. doi: 10.1016/j.jfluchem.2005.09.009.
- [15] Edwards M. (1994) Chemistry of arsenic removal during coagulation and Fe–Mn oxidation, *J. Am. Water Works Assoc.* 86 (9) 64–78.
- [16] Meenakshi R.C., Maheshwari J. (2006) Fluoride in drinking water and its removal. *J. Hazard. Mater.* 137:456–463. doi: 10.1016/j.jhazmat.2006.02.024.
- [17] Ayoob S., Gupta A. and Bhat V. (2008) A conceptual overview on sustainable technologies for defluoridation of drinking water and removal mechanisms. *Critical Reviews in Environmental Science and Technology*, **38**: 401–470.
- [18] Feenstra L., Erkel J. van, Vasak L. (2007) Arsenic in groundwater: Overview and evaluation of removal methods. *igrac, International Ground Water Resources Assessment Centre, Report nr.SP 2007-2*.
- [19] Weng Y.H., Chaung-Hsieh L.H., Lee H.H., Li K.C., Huang C.P. (2005) Removal of arsenic and humic substances (HSs) by electro-ultrafiltration (EUF), *J. Hazard. Mater.* 122 (1–2) 171–176.
- [20] Gholami M.M., Mokhtari M.A., Aameri A., Alizadeh Fard M.R. (2006) Application of reverse osmosis technology for arsenic removal from drinking water. *Desalination*, 200 (1–3) 725–727.
- [21] Ndiaye P.I., Moulin P., Dominguez L., Millet J.C., Charbit F. (2005) Removal of fluoride from electronic industrial effluent by RO membrane separation. *Desalination*. 173:25–32. doi: 10.1016/j.desal.2004.07.042.
- [22] Tahai M., Achary I., Menkouchi Sahli M.A., Amor Z., Taky M., Alami A., Boughriba A., Hafsi M., Elmidaoui A. (2006) Defluoridation of Moroccan groundwater by electrodialysis: Continuous operation. *Desalination*. 189:215–220.
- [23] Kabay N., Arar O., Samatya S., Yüksel U., Yüksel M. (2008) Separation of fluoride from aqueous solution by electrodialysis: Effect of process parameters and other ionic species. *J. Hazard. Mater.* 153:107–113. doi: 10.1016/j.jhazmat.2007.08.024.
- [24] Zakia A., Bernard B., Nabil M., Mohamed T., Stephan N., and Azzedine E. (2001) Fluoride removal from brackish water by electrodialysis. *Desalination*. 133, 215 - 233.
- [25] Kumar S., and Gopal K.A. (2000) Review on Fluorosis and its Preventive Strategies. *Indian J. Environmental Protection*. 20(6):430-6.
- [26] Pandit A.B., Kumar J.K. (2019) Drinking water treatment for developing countries:

- physical, chemical and biological pollutants. Published by-Royal Society of Chemistry. ISBN-978-1-78801-019-1.
- [27] Onyango M.S., Kojima Y., Aoyi O., Bernardo E.C., and Matsuda H. (2004) Adsorption equilibrium modeling and solution chemistry dependence of fluoride removal from water by trivalent-cation-exchanged zeolite F-9. *J. Colloid Interface Sci.* 279:341–350.
- [28] Fan X., Parker D.J., and Smith M.D. (2003) Adsorption kinetics of fluoride on low cost materials. *Water Res.* 37: 4929–4937.
- [29] Rao C.R.N. (2003) Fluoride and Environment—A Review; Proceedings of the Third International Conference on Environment and Health; Chennai, India. 15–17 December, 2003 pp. 386–399.
- [30] Tomar V., Kumar D. (2013) A critical study on efficiency of different materials for fluoride removal from aqueous media. *Chem. Cent. J.* 7:1–15.
- [31] Gupta V.K., Lmran A., and Sain V.K. (2007) Defluoridation of wastewaters using waste carbon slurry. *Water Res.* 41 (15) 3307-3316.
- [32] Hu C. Y., Lo S. L., Kuan W. H., and Lee Y. D. (2005) Removal of fluoride from semiconductor wastewater by electrocoagulation-flotation. *Water Res.* 39, 895-901.
- [33] Kumar E., Bhatnagar A., Ji M., Jung W., Lee S.H., Kim S.J., Lee G., Song H., Choi J.Y., Yang J.S., and Jeon B.H. (2009) Defluoridation from aqueous solutions by granular ferric hydroxide (GFS), *Water Res.* 43: 490-498.
- [34] Ku Y., and Chiou H.M. (2002) The adsorption of fluoride ion from aqueous solution by activated alumina. *Water Air Soil Pollut.* 133:349–360. doi: 10.1023/A:1012929900113.
- [35] Jain C. K., and Singh R. D. (2012) Technological options for the removal of arsenic with special reference to South East Asia. *Journal of Environmental Management*, vol. 107, no. 1, pp. 1–18.
- [36] Glocheux Y., Pasarín M. M., Albadarín A. B., Allen S. J., and Walker G. M. (2013) Removal of arsenic from groundwater by adsorption onto an acidified laterite by-product. *Chemical Engineering Journal*, vol. 228, pp. 565–574.
- [37] Lanas S. G., Valiente M., Aneggi E., Trovarelli A., Tolazzi M., and Melchior A. (2016) Efficient fluoride adsorption by mesoporous hierarchical alumina microspheres, *RSC Adv.* 6, 42288.

- [38] Alagumuthu G., and Rajan M. (2010) Kinetic and equilibrium studies on fluoride removal by zirconium (IV): Impregnated groundnut shell carbon. *Hem. Ind.* 64:295–304. doi: 10.2298/HEMIND100307017A.
- [39] Alagumuthu G., Veeraputhiran V., and Venkataraman R. (2011) Fluoride sorption using *Cynodon dactylon* based activated carbon. *Hem. Ind.* 65:23–35. doi: 10.2298/HEMIND100712052A.
- [40] Daifullah A.A., Yakout S.M., and Elreefy S.A. (2007) Adsorption of fluoride in aqueous solutions using KMnO<sub>4</sub>-modified activated carbon derived from steam pyrolysis of rice straw. *J. Hazard. Mater.* 147:633–643. doi: 10.1016/j.jhazmat.2007.01.062.
- [41] Hernández-Montoya V., Ramírez-Montoya L.A., Bonilla-Petriciolet A., and Montes-Morán M.A. (2012) Optimizing the removal of fluoride from water using new carbons obtained by modification of nut shell with a calcium solution from egg shell. *Biochem. Eng. J.* 62:1–7.
- [42] Mohan D., Singh K.P., and Singh V.K. (2008) Wastewater treatment using low cost activated carbons derived from agricultural byproducts—A case study. *J. Hazard. Mater.* 152:1045–1053.
- [43] Chidambaram C., Ramanathan A.L., and Vasudevan S. (2003) Fluoride removal studies in water using natural materials. *Water SA.* 29:339–343.
- [44] Nath S.K., and Dutta R.K. (2010) Fluoride removal from water using crushed limestone. *Indian J. Chem. Technol.* 17:120–125.
- [45] Geethamani C.K., Ramesh S.T., Gandhimathi R., and Nidheesh (2013) Alkali-treated fly ash for the removal of fluoride from aqueous solutions. *Desalination and water treatment.* 52(19-21), 3466-3476.
- [46] Malay K.D., and Salim A.J. (2011) Comparative study of batch adsorption of fluoride using commercial and natural adsorbent. *Res. J. Chem. Sci.* 1:68–75.
- [47] Maliyekkal S.M., Shukla S., Philip L., and Nambi I.M. (2007) Enhanced fluoride removal from drinking water by magnesia-amended activated alumina granules. *Chem. Eng. J.* 140:183–192. doi: 10.1016/j.cej.2007.09.049.
- [48] Tripathy S.S., and Raichur A.M. (2008) Abatement of fluoride from water using manganese dioxide-coated activated alumina. *J. Hazard. Mater.* 153:1043–1051.
- [49] Lavecchia R., Medici F., Piga L., Rinaldi G., Zuorro A. (2012) Fluoride removal from water by adsorption on a high alumina content bauxite. *Chem. Eng. Trans.* 26:225–230.

- [50] Viswanathan N., and Meenakshi S. (2009) Role of metal ion incorporation in ion exchange resin on the selectivity of fluoride. *J. Hazard. Mater.* 162:920–930. doi: 10.1016/j.jhazmat.2008.05.118.
- [51] Vivek Vardhan C.M., and Karthikeyan J. (2011) Removal of fluoride from water using low-cost materials. *Int. Water Technol. J.* 1:120–131.
- [52] Shan Y., and Guo H. (2013) Fluoride adsorption on modified natural siderite: Optimization and performance. *Chem. Eng. J.* 223:183–191.
- [53] Teutli-Sequeira A., Martínez-Miranda V., Solache-Ríos M., Linares-Hernández Í. (2013) Aluminum and lanthanum effects in natural materials on the adsorption of fluoride ions. *J. Fluor. Chem.* 148:6–13. doi: 10.1016/j.jfluchem.2013.01.015.
- [54] Viswanathan N., Prabhu S.M., and Meenakshi S. (2013) Development of amine functionalized co-polymeric resins for selective fluoride sorption. *J. Fluor. Chem.* 153:143–150. doi: 10.1016/j.jfluchem.2013.04.002.
- [55] Ganvir V., and Das K. (2011) Removal of fluoride from drinking water using aluminum hydroxide coated rice husk ash. *J. Hazard. Mater.* 185:1287–1294. doi: 10.1016/j.jhazmat.2010.10.044.
- [56] Sarmah S., Saikia J., Bordoloi D., Goswamee R. L. (2017) Title: Surface Modification of Paddy Husk Ash by Hydroxyl-Alumina Coating to Develop an Efficient Water Defluoridation Media and the Immobilization of the Sludge by Lime-Silica Reaction. *J. Environ. Chem. Eng.* DOI: <http://dx.doi.org/10.1016/j.jece.2017.08.032>.
- [57] Saikia J., Sarmaha S. Ahmed T.H., Kalita P.J., and Goswamee R.L. (2017) Removal of toxic fluoride ion from water using low cost ceramic nodules prepared from some locally available raw materials of Assam, India. *Journal of Environmental Chemical Engineering* 5, 2488–2497.
- [58] Yadav A.K., Kaushik C.P., Haritash A.K., Kansal A., and Rani N. (2006) Defluoridation of groundwater using brick powder as an adsorbent. *J. Hazard. Mater.* 128:289–293. doi: 10.1016/j.jhazmat.2005.08.006.
- [59] Asgari G., Roshani B., and Ghanizadeh G. (2012) The investigation of kinetic and isotherm of fluoride adsorption onto functionalize pumice stone. *J. Hazard. Mater.* 217–218:123–132.
- [60] Salifu A., Petrusevski B., Ghebremichael K., Modestus L., Buamah R., Aubry C., and Amy G.L. (2013) Aluminum (hydr)oxide coated pumice for fluoride removal from drinking water: Synthesis, equilibrium, kinetics and mechanism. *Chem. Eng. J.* 228:63–74. doi: 10.1016/j.cej.2013.04.075.

- [61] Wu H.-X., Wang T.-J., Chen L., Jin Y., Zhang Y., and Dou X.-M. (2011) Granulation of Fe–Al–Ce hydroxide nano-adsorbent by immobilization in porous polyvinyl alcohol for fluoride removal in drinking water. *Powder Technol.* 209:92–97. doi: 10.1016/j.powtec.2011.02.013.
- [62] García-Sánchez J.J., Solache-Ríos M., Martínez-Miranda V., and Solís Morelos C. (2013) Removal of fluoride ions from drinking water and fluoride solutions by aluminum modified iron oxides in a column system. *J. Colloid Interface Sci.* 407:410–415.
- [63] Chai L., Wang Y., Zhao N., Yang W., and You X. (2013) Sulfate-doped Fe<sub>3</sub>O<sub>4</sub>/Al<sub>2</sub>O<sub>3</sub> nanoparticles as a novel adsorbent for fluoride removal from drinking water. *Water Res.* 47:4040–4049.
- [64] Rahmani A., Nouri J., Kamal Ghadiri S., Mahvi A.H., and Zare M. M.R. (2010) Adsorption of fluoride from water by Al<sup>3+</sup> and Fe<sup>3+</sup> pretreated natural Iranian zeolites. *Int. J. Environ. Res.* 4:607–614.
- [65] Erdem, E., Karapinar, N., Donat, R. (2004) ‘The removal of heavy metal cations by natural zeolites’, *J. Colloid Interface Sci.* 280, 309–314.
- [66] Chen N., Zhang Z., Feng C., Li M., Zhu D., and Sugiura N. (2011) Studies on fluoride adsorption of iron-impregnated granular ceramics from aqueous solution. *Mater. Chem. Phys.* 125:293–298.
- [67] Mourabet M., El Rhilassi A., El Boujaady H., Bennani-Ziatni M., El Hamri R., and Taitai A. (2012) Removal of fluoride from aqueous solution by adsorption on Apatitic tricalcium phosphate using Box–Behnken design and desirability function. *Appl. Surf. Sci.* 258:4402–4410.
- [68] Dou X., Mohan D., Pittman C.U., Jr., and Yang S. (2012) Remediating fluoride from water using hydrous zirconium oxide. *Chem. Eng. J.* 198–199:236–245. doi: 10.1016/j.cej.2012.05.084.
- [69] Swain S.K., Patnaik T., Singha V.K., Jha U., Patel R.K., and Dey R.K. (2011) Kinetics, equilibrium and thermodynamic aspects of removal of fluoride from drinking water using meso-structured zirconium phosphate. *Chem. Eng. J.* 171:1218–1226. doi: 10.1016/j.cej.2011.05.030.
- [70] Zhao Y., Li X., Liu L., and Chen F. (2008) Fluoride removal by Fe(III)-loaded ligand exchange cotton cellulose adsorbent from drinking water. *Carbohydr. Polym.* 72:144–150.
- [71] Yu X., Tong S., Ge M., and Zuo J. (2013) Removal of fluoride from drinking water

- by cellulose@hydroxyapatite nanocomposites. *Carbohydr. Polym.* 92:269–275. doi: 10.1016/j.carbpol.2012.09.045.
- [72] Çengelöglu Y., Kir E., and Ersöz M. (2002) Removal of fluoride from aqueous solution by using red mud. *Sep. Purif. Technol.* 28:81–86. doi: 10.1016/S1383-5866(02)00016-3.
- [73] Gogoi P.K., and Baruah R. (2008) Fluoride removal from water by adsorption on acid activated kaolinite clay. *Indian J. Chem. Technol.* 15:500–503.
- [74] Zhang T., Li Q., Xiao H., Mei Z., Lu H., and Zhou Y. (2013) Enhanced fluoride removal from water by non-thermal plasma modified CeO<sub>2</sub>/Mg–Fe layered double hydroxides. *Appl. Clay Sci.* 72:117–123. doi: 10.1016/j.clay.2012.12.003.
- [75] Sasaki K., Fukumoto N., Moriyama S., Yu Q., and Hirajima T. (2012) Chemical regeneration of magnesium oxide used as a sorbent for fluoride. *Sep. Purif. Technol.* 98:24–30. doi: 10.1016/j.seppur.2012.07.028.
- [76] Khan S.A., Ali, N., and Srivastava Y. (2015) Comparative Study of Defluoridation from Water using Waste Materials as Adsorbents—A Review. *IJiet*, 6:159-164.
- [77] Huang Y.H., Shih Y.J., and Chang C.C. (2011) Adsorption of fluoride by waste iron oxide: The effects of solution pH, major coexisting anions, and adsorbent calcination temperature. *J. Hazard. Mater.* 186:1355–1359. doi: 10.1016/j.jhazmat.2010.12.025.
- [78] Ishihara T., Shuto Y., Ueshima S., Ngee H.L., Nishiguchi H., and Takita Y. (2002) Titanium hydroxide as a new inorganic fluoride ion exchanger. *J. Ceram. Soc. Jpn.* 110:801–803. doi: 10.2109/jcersj.110.801.
- [79] Wajima T., Umata Y., Narita S., and Sugawara K. (2009) Adsorption behavior of fluoride ions using a titanium hydroxide-derived adsorbent. *Desalination*. 249:323–330. doi: 10.1016/j.desal.2009.06.038.
- [80] Liu R., Gong W., Lan H., Yang T., Liu H., and Qu J. (2012) Simultaneous removal of arsenate and fluoride by iron and aluminum binary oxide: Competitive adsorption effects. *Sep. Purif. Technol.* 92:100–105. doi: 10.1016/j.seppur.2012.03.020.
- [81] Mohapatra M., Hariprasad D., Mohapatra L., Anand S., and Mishra B.K. (2012) Mg-doped nano ferrihydrite—A new adsorbent for fluoride removal from aqueous solutions. *Appl. Surf. Sci.* 258:4228–4236. doi: 10.1016/j.apsusc.2011.12.047.
- [82] Kang D., Yu X., Tong S., Ge M., Zuo J., Cao C., and Song W. (2013) Performance and mechanism of Mg/Fe layered double hydroxides for fluoride and arsenate removal from aqueous solution. *Chem. Eng. J.* 228:731–740. doi: 10.1016/j.cej.2013.05.041.



- [83] Farrah H., Slavek J., and Pickering W.F. (1987) Fluoride interactions with hydrous aluminium oxides and alumina. *Aust. J. Soil Res.* 25, 55–69.
- [84] Leyva Ramos. R., Ovalle-Turrubiarres J., Sanchez-Castillo M.A. (1999) Adsorption of fluoride from aqueous solution on aluminum-impregnated carbon. *Carbon*. 37:609–617.
- [85] Shimelis B., Zewge F., and Chandravanshi B.S. (2006) Removal of excess fluoride from water by aluminum hydroxide. *Bull. Chem. Soc. Ethiopia* 20, 17–34.
- [86] Stewart T. (2009) Removal of Fluoride from Drinking Water: Analysis of Alumina Based Sorption. Institute of Biogeochemistry and Pollutant Dynamics, Department Environmental Sciences, ETH; Zürich, Switzerland: 2009. pp. 6–19. Term Paper.
- [87] Tripathy S.S., Bersillon J.-L., and Gopal K. (2006) Removal of fluoride from drinking water by adsorption onto alum-impregnated activated alumina. *Sep. Purif. Technol.* 50, 310–317.
- [88] Biswas K., Saha S.K., and Ghosh U.C. (2007) Adsorption of fluoride from aqueous solution by a synthetic iron(III)–aluminum(III) mixed oxide. *Ind. Eng. Chem. Res.* 46, 5346–5356.
- [89] Das N., Pattanaik P., and Das R. (2005) Defluoridation of drinking water using activated titanium rich bauxite. *J. Colloid Interface Sci.* 292, 1–10.
- [90] Mohan S.V., Ramanaiah S.V., Rajkumar B., and Sarma P.N. (2007) Removal of fluoride from aqueous phase by biosorption onto algal biosorbent *Spirogyra* Sp.-102: sorption mechanism elucidation. *J. Hazard. Mater.* 141, 465–474.
- [91] Wang Y., and Reardon E.J. (2001) Activation and regeneration of a soil sorbent for defluoridation of drinking water. *Appl. Geochem.* 16:531–539.
- [92] Bower C.A., and Hatcher J.T. (1967) Adsorption of fluoride by soils and minerals. *J. Soil Sci.* 3, 151–154.
- [93] Guo Q., and Tian J. (2013) Removal of fluoride and arsenate from aqueous solution by hydrocalumite via precipitation and anion exchange. *Chem. Eng. J.* 231:121–131. doi: 10.1016/j.cej.2013.07.025.
- [94] Guo Q., and Reardon E.J. (2012) Fluoride removal from water by meixnerite and its calcination product. *Appl. Clay Sci.* 56:7–15. doi: 10.1016/j.clay.2011.11.013.
- [95] Kamble S.P., Dixit P., Rayalu S.S., and Labhsetwar N.K. (2009) Defluoridation of drinking water using chemically modified bentonite clay. *Desalination*. 249:687–693. doi: 10.1016/j.desal.2009.01.031.

- [96] Malakootian M., Moosazadeh M., Yousefi N., and Fatehizadeh A. (2011) Fluoride removal from aqueous solution by pumice: Case study on Kuhbonan water. *Afr. J. Environ. Sci. Technol.* 5:299–306.
- [97] Sepehr M.N., Sivasankar V., Zarrabi M., and Senthil Kumar M. (2013) Surface modification of pumice enhancing its fluoride adsorption capacity: An insight into kinetic and thermodynamic studies. *Chem. Eng. J.* 228:192–204. doi: 10.1016/j.cej.2013.04.089.
- [98] Samatya S., Yüksel U., Yüksel M., Kabay N. (2007) Removal of fluoride from water by metal ions ( $\text{Al}^{3+}$ ,  $\text{La}^{3+}$  and  $\text{ZrO}^{2+}$ ) loaded natural zeolite. *Sep. Sci. Technol.* 42:2033–2047. doi: 10.1080/01496390701310421.
- [99] Wang S., and Peng P. (2010) Natural zeolites as effective adsorbents in water and wastewater treatment. *Chem. Eng. J.* 156:11–24.
- [100] Sun Y., Fang Q., Dong J., Cheng X., and Xu J. (2011) Removal of fluoride from drinking water by natural stilbite zeolite modified with Fe(III) Desalination. 277:121–127. doi: 10.1016/j.desal.2011.04.013.
- [101] Zhang Z., Tan Y., and Zhong M. (2011) Defluorination of wastewater by calcium chloride modified natural zeolite. *Desalination.* 276:246–252. doi: 10.1016/j.desal.2011.03.057.
- [102] Sajidu S.M.I., Masamba W.R.L., Thole B., and Mwatseteza J.F. (2008) Groundwater fluoride levels in villages of Southern Malawi and removal studies using bauxite. *Int. J. Phys. Sci.* 3:1–11.
- [103] Mohammad-Khah A., and Ansari R. (2009) Activated charcoal: Preparation, characterization and applications: A review article. *Int. J. ChemTech Res.* 1:859–864.
- [104] Hameed B.H. (2009) Removal of cationic dye from aqueous solution using jackfruit peel as non-conventional low-cost adsorbent. *J Hazard Mater*, 162:344–350.
- [105] Gandhi N., Sirisha D., and Sekhar K.B.C. (2016) Adsorption of fluoride ( $\text{F}^-$ ) from aqueous solution by using pineapple (*Ananascomosus*) peel and orange (*Citrus sinensis*) peel powders. *International Journal of Environmental Bioremediation & Biodegradation*, 4(2):55-67.
- [106] Roy P., Mondal N.K., Bhattacharya S., Das B., and Das K. (2013) Removal of arsenic(III) and arsenic(V) on chemically modified low-cost adsorbent: batch and column operations. *Applied Water Science.* 3(1), 293–309.

- [107] Khusaibi T.M.A., Dumaran J.J., Devi M.G., Rao L.N., and Feroz, S. (2015) Treatment of Dairy Wastewater using Orange and Banana Peels. *Journal of Chemical and Pharmaceutical Research*, 7(4):1385-1391.
- [108] Madhu R., Sankar K. v., Chen S. M., and Selvan R. K. (2014). Eco –Friendly synthesis of activated carbon from dead mango leaves for the ultrahigh sensitive detection of toxic heavy metal ions and energy storage applications. *RSC Advances*, 4: 1225-1233.
- [109] Guo X., and Chen F. (2005) Removal of arsenic by bead cellulose loaded with iron oxyhydroxide from groundwater, *Environmental Science & Technology*, 39(14), 6808–6818.
- [110] Wang S.L., Tzon Y.M., Lu Y.H., and Sheng G. (2007) Removal of 3-chlorophenol from water using rice-straw-based caebon. *Journal of Hazard Mater.* 147: 313-318.
- [111] Ismadji S., Sudaryanto Y., Hartono S.B., Setiawan L. E. K., and Ayucitra, A. (2005) Activated carbon from char obtained from vacuum pyrolysis of teak sawdust: pore structure development and characterization. *Bioresour Technol*, 96(12): 1364-1369.
- [112] Habuda-Stanic M., Ravancic M.E., and Flanagan A. (2014) A review on adsorption of fluoride from aqueous solution, *Materials (Basel)*. 7(9), 6317-6366  
doi: 10.3390/ma7096317.
- [113] Simms J. and Azizian F. (1997) Pilot Plant Trials on the Removal of Arsenic from Potable Water Using Activated Alumina,” *Proceedings AWWA Water Quality Technology Conference*, November 9-12.
- [114] Chen W, Parette R and Cannon FS (2012): Pilot–scale studies of arsenic removal with granular activated carbon and zero–valent iron, *Environmental Engineering Science*, 29(9), 897–901.
- [115] Chen, A. S. C.; Snoeyink, V. L.; Fiessinger, F. (1987) *Environmental Science & Technology*. 21, 83.
- [116] Vakharkar Ashutosh S. (2005) Adsorption studies for arsenic removal using modified chabazite Graduate Theses and Dissertations. <http://scholarcommons.usf.edu/etd/891>.
- [117] Mampton F.A. (1997) *Mineralogy and Geology of Natural Zeolites*, Southern Printing, Blacksburg, VA.
- [118] Manning B.A., and Goldberg S. (1997) Arsenic(III) and arsenic(V) adsorption on three California soils. *Soil Sci.* 162 (12) 886–895.

- [119] Petrusevski B., Sharma S.K., Kruis F., Omeruglu P., and Schippers J.C. (2002) Family filter with iron-coated sand: solution for arsenic removal in rural areas. *Water Sci. Technol.: Water Supply* 2 (5–6) 127–133.
- [120] Nguyen T.V., Vigneswaran S., Ngo H.H., Pokhrel D., and Viraraghavan T. (2006) Specific treatment technologies for removing arsenic from water, *Eng. Life Sci.* 6 (1) 86–90.
- [121] Ramakrishna D.M., Viraraghavan T., and Jin Y.-C. (2006) Coated sand for arsenic removal: investigation of coating parameters using factorial design approach, *Pract. Periodical Hazard. Toxic Radioactive Waste Manage.* 10 (4) 198–206.
- [122] Thirunavukkarasu O.S., Viraraghavan T., Subramanian K.S., and Tanjore S. (2002) Organic arsenic removal from drinking water, *Urban Water* 4 (4) 415–421.
- [123] Lo S.-L., Jeng H.-T., and Lai C.-H. (1997) Characteristics and adsorption properties of iron-coated sand, *Water Sci. Tech.* 35 63–70.
- [124] Bagla P., and Kaiser J. (1996) India's spreading health crisis global arsenic effects. *Science* 274, 174–175.
- [125] Gillman G.P. (2006) A simple technology for arsenic removal from drinking water using hydrotalcite, *Sci. Total Environ.* 366, 926–931.
- [126] Fufa F., Alemayehu E. and Lennartz B. (2014) Sorptive removal of arsenate using termite mound, *Journal of Environmental Management.* 132, 188–196.
- [127] Mishra S.P., Mohapatra D., Mishra D., Chattopadhyay P., Roy Chaudhury G., and Das R.P. (2014) Arsenic adsorption on natural minerals. *Journal of Materials and Environmental Science.* 5(2), 350–359.
- [128] Chakravarty S., Dureja V., Bhattacharyya G., Maity S., Bhattacharjee S. (2002) Removal of arsenic from groundwater using low cost ferruginous manganese ore. *Water Res.* 36 (3) 625–632.
- [129] Arai Y., Sparks D.L., and Davis J.A. (2005) Arsenate adsorption mechanisms at the allophane–water interface, *Environ. Sci. Technol.* 39 (8) 2537–2544.
- [130] Prahas D., Kartika Y., Indraswati N. and Ismadji S. (2008) Activated carbon from jackfruit peel waste by H<sub>3</sub>PO<sub>4</sub> chemical activation: Pore structure and surface chemistry characterization, *Chemical Engineering Journal.*, 140, 32–42.
- [131] Saikia J., Sarmaha S., Saikia P., and Goswamee R.L. (2018) Harmful weed to prospective adsorbent: low-temperature-carbonized *Ipomoea carnea* stem carbon coated with aluminum oxyhydroxide nanoparticles for defluoridation. *Environmental Science and Pollution Research.* <https://doi.org/10.1007/s11356-018-3572-z>.

- [132] Pongener C., Kibami D., Rao K.S., Goswamee R.L., and Sinha D. (2017) Adsorption studies of fluoride by activated carbon prepared from *Mucuna prurines* plant. J. Water Chem. Technol. 39, 108-115. doi: 10.3103/s1063455X17020096.
- [133] Pollard S.J.T., Fowler G.D., Sollars C.J., and Perry R. (1992) Low cost adsorbents for waste and waste water treatment: a review, Sci. Total Environ. 116 31–52.
- [134] Hesas R.H., Niya A.A., Daud W.M.W., and Sahu J.N. (2013) Preparation and characterization of activated carbon from apple waste by microwave-assisted phosphoric acid activation: application in methylene blue adsorption. Bio Resources, 8(2):2950-2966.
- [135] Pongener C., Kibami D., Rao K.S., Goswamee R.L., and Sinha D. (2015) Synthesis and Characterization of Activated Carbon from the Biowaste of the Plant *Manihot Esculenta*. Chemical Science Transactions, 4(1):59-68.
- [136] Rajakovic L.V. (1992) Sorption of arsenic onto activated carbon impregnated with metallic silver and copper, Sep. Sci. Technol. 27 (11) 1423–1433.
- [137] Gu Z., Fang J., and Deng B. (2005) Preparation and evaluation of GAC-based iron-containing adsorbents for arsenic removal, Environmental Science & Technology, 39(10), 3833–3843.
- [138] Chuang C.L., Fan M., Xu M., Brown R.C., Sung S., Saha B., and Huang C.P. (2005) Adsorption of arsenic(V) by activated carbon prepared from oat hulls, Chemosphere 61 (4) 478–483.

## **CHAPTER - 4**

### **PREPARATION OF FLUORIDE AND ARSENIC ADSORBENTS (CBP AND IOCS) FROM LOCALLY AVAILABLE RAW MATERIALS AND THEIR CHARACTERIZATION**

A part of this chapter has been published as **Gogoi C., Saikia, J., Sarmah, S. Sinha, D., and Goswamee, R.L. Removal of Fluoride from Water by Locally Available Sand Modified with a Coating of Iron Oxides.** Water Air Soil Pollut **229**, 118, 2018. Doi:10.1007/s11270-018-3754-9

From the chapter 2, it is seen that, ground water of Golaghat district is highly contaminated by arsenic. It is also found that some of the borewells in Bosagaon of Podumoni block, Matikhula village of Gomariguri block are affected by both fluoride and arsenic. From the study of various existing techniques for the removal of fluoride and arsenic (already discussed in the chapter 3), it is seen that adsorption method is the best technique. Although there are so many adsorbents for fluoride and arsenic; but most of the adsorbents are not appropriate for rural areas due to high financial and technological constraints. Therefore, it is important to search for methods mainly based on easily available materials which are cost effective, benign and can exhibit high adsorption efficiency towards both fluoride and arsenic present in ground water.

From that perspective, in this study it was tried to develop some low-cost adsorbents from locally available materials especially available in and around Golaghat district. Mainly two adsorbents were developed -(a) biocarbon (CBP)-which is a waste carbonised ash of banana obtained during domestic preparation of edible alkali from dried trunks of Musa Balbisiana plant and (b) sand (IOCS)-which is obtained by surface modifying some particular sands available in Kaliani river of Golaghat district (also known as Kanaighat sand). Both the adsorbents were characterized and investigated for their efficacy as adsorbents for the removal of arsenic and fluoride from aqueous system. The studies were conducted on a series of batch mode adsorption experiments to assess the potentiality of the adsorbents for the removal of fluoride and arsenic from the contaminated water.

## **4.2 Activated carbon as adsorbent**

Recently carbon has become a magnificent element in materials science and the present era is the era of carbon. Accordingly, in recent years activated carbon is the most widely used material as best porous adsorbent to adsorb contaminants from water and air. Activated carbon (AC) is an amorphous form of carbon, whose reactivity is higher than commonly available charcoal. Activated carbon has a large surface area which ranges typically from 500 to 2000 m<sup>2</sup>g<sup>-1</sup> and a high degree of internal porosity (micropores) with pore diameters smaller than 2 nm [1]. These very fine pores gives the basis of its remarkable adsorption properties [2] and fast adsorption kinetics [3]. AC exhibits high adsorption capacity towards low molecular weight compounds [4].

For the removal of contaminants such as fluoride, arsenic, lead, mercury, cadmium etc. present in water, activated carbon have been used most widely. There are several reports of using AC for the removal of trace elements, ions, fluorides inorganic pollutants, organic pollutants dissolved in aqueous media [5,6,7]. The adsorption efficiency of activated carbon is a function of different physico-chemical parameters of the AC, such as surface area, pore size distribution, surface functional groups, adsorbent modification procedure etc. [8,9,10,11]. Again the textural and surface properties of carbon materials highly dependent on the nature and the origin of the carbonaceous materials (whether it is obtained from animal, plant or minerals) and the methods of their preparation [12,13].

Carbon-oxygen surface functional groups of activated carbon are very important which control the surface characteristics such as acidic, basic and physico-chemical properties and the chemical reactivity of these materials. The types of carbon-oxygen surface functional groups [14] are shown in Fig 4.1. On the treatment of carbon with oxygen at temperature 400°C or by reacting with oxidizing solution at room temperature, acidic surface groups are formed [15]. These acidic surface functional groups are carboxylic, phenolic and lactonic due to the presence of which carbon surface become hydrophilic and polar in character [16] and in absence of these functional groups the untreated raw carbon can adsorb only very small amount of anions like fluoride [17].

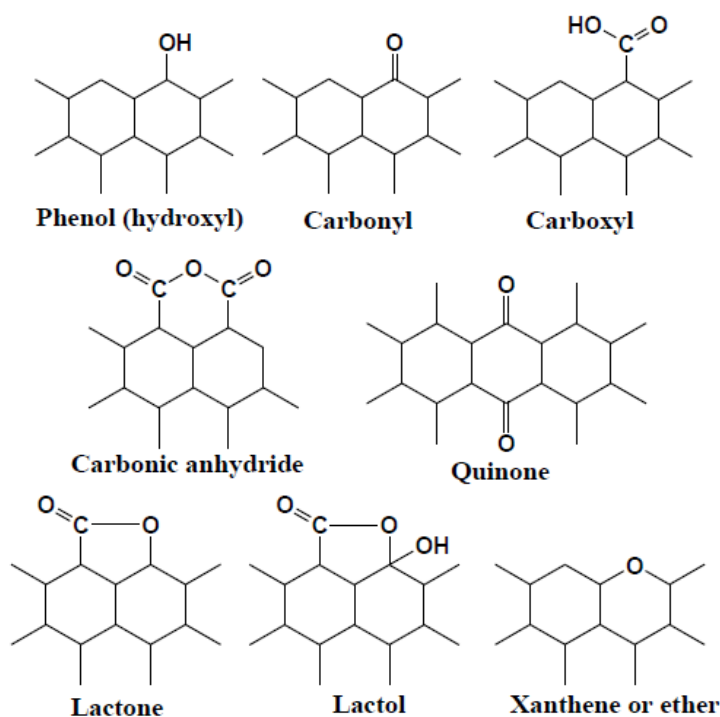


**Fig 4.1: Some important functional groups present on the surface of carbon [18]**



Activated carbons can be prepared by physical or gas activation (PhA) (activation with oxidizing agents such as CO<sub>2</sub> or steam) and chemical activation (ChA) (activation with mineral salts) depends upon the starting carbonaceous material and desired carbon density.

**Physical or gas activation (PhA):** In this process the raw material is carbonized first at 400-500°C which converts the carbonaceous raw materials to carbon by escaping the volatile compounds and then the carbon is exposed to oxidizing gases like carbon dioxide, carbon monoxide or steam at 800-1000°C or and with air at low temperature [19,20].

**Chemical activation (ChA):** In ChA, before carbonization, the raw material is impregnated with an activating agent, an acid like phosphoric acid [21], nitric acid [22] or a strong base like potassium hydroxide [23], or a salt such as zinc chloride [24] and then carbonization with conventional heating in an electrical furnace in presence of inert atmosphere at temperatures ranging from 400°C to 800°C, or carbonization with microwave heating [25,26]. Microwave heating is a time consuming and energy saving process.

From the literature review it is seen that the unactivated raw carbon can adsorb very small amount of adsorbate [17]. This can be explained as the formation of very small and limited surface area during carbonization due to the blocking of its pores largely with resins and products of incomplete combustion. Various pores such as open pores, closed pores, blind pores and transport pores are present in a porous solid. Based upon their dimension they are classified by IUPAC nomenclature as Microporous having pore width less than 2nm, Mesoporous having pore width between 2 and 50nm and Macroporous having pore width greater than 50nm [27,28,29]. An activated carbon surface also possess all these types of pores (Fig 4.2).

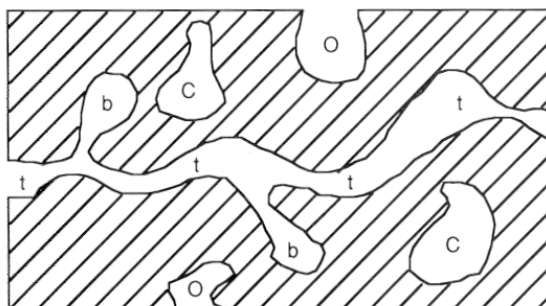


**Fig 4.2: Various pores present in a porous solid O- open pores; C- closed pores; t- transport pores; b-blind pores.**

So activation of carbon is very essential which remove the unwanted materials to open the pores, to increase surface area and to produce the surface functional groups [1] for which activated carbon shows significant adsorption capacity. Apart from this, AC is a hydrophobic adsorbent so because of good solvation of metal ions in aqueous solution activated carbon shows poor adsorbability towards metal ions from polar aqueous solution. Different surface functional groups present in activated carbon are given in the Fig 4.3.

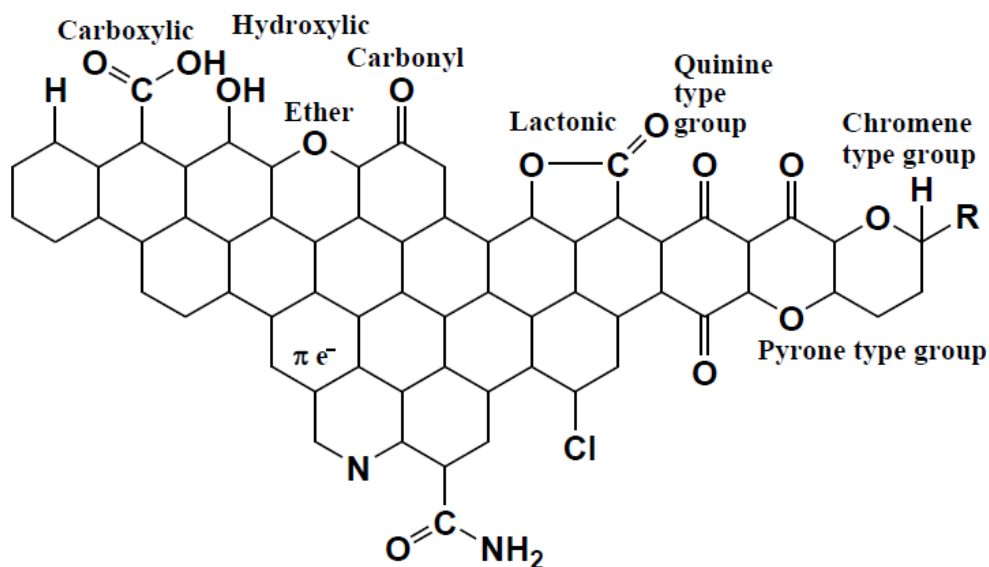


**Fig 4.3: Different surface functional groups present on carbon [18]**

#### **4.2.1 Carbon of banana plant-as adsorbent**

In this study, for the removal of fluoride and arsenic from contaminated water, the banana plant *Musa balbisiana* for preparing activated carbon was selected. In Assam, *Musa balbisiana* is locally known as *Athiya Kol/Bhim Kol*. *Musa balbisiana* is an indigenous variety of banana in Assam. This banana plant is very common in the kitchen garden of each Assamese family. Since the time immemorial the various ethnic groups of Brahmaputra valley of Assam, have been consuming not only the ripe fruits of this plant, but also the stem and male buds as food nutrients. Another important use of *Musa balbisiana* is as medicine in the name of *Kolkhar* or edible banana alkali. *Kolkhar* is a type of food additive derived from the stem of *Musa balbisiana* and is very popular Assamese food additive. From ancient times without even much knowledge of its chemistry, Assamese people have been using *Kolkhar* as antacid to improve the digestive system. Again, *Kolkhar* was also used for washing clothes and hair instead of soap and shampoo. Even Assamese people used to have their kitchen fire

**Chapter-4**                      **Preparation & characterization of adsorbents of fluoride & arsenic**

place as a mini factory cum storage place of versatile activated carbon where *Musa balbisiana* peel are hanged over for drying for any future contingency need of edible alkali (Fig 4.4). From the literature review it is seen that, many researchers reported about the chemical constituent and uses of Kolkhar, bhimkol or *Musa balbisiana*, liquid extract of banana trunk [30,31,32,33,34,35,36,37,38]. From the experiments on Kolkhar, Kalita and Kandar, (2014) reported that Kolkhar contain less sodium and high potassium, so it can be used as salt substitute to reduce such type of diseases which are associated with intake of higher amount of sodium in our table salt.



**Fig 4.4: Assamese traditional kitchen fire place containing dry banana peel and stem for the preparation of *Kolkhar***

The reason for selecting this banana plant, *Musa balbisiana* as raw materials for fluoride and arsenic adsorption is that, at the time of preparation of Kolkhar by Assamese traditional method, a huge amount of carbon is produced as byproduct and treated as waste product and hence this waste biocarbon is selected as adsorbent to see if it could be used for noble applications.

The plant taxonomic details of *Musa balbisiana* is given below [73]-



**Fig 4.5: *Musa balbisiana* plant**

#### **Scientific classification of *Musa balbisiana***

Kingdom: Plantae

Division: Angiospermae

Class: Scitaminae

Order: Zingiberales

Family: Musaceae

Genus: *Musa*

Species: *M. balbisiana* Colla

#### **4.3 Sand as adsorbent**

River sand naturally occurs on the surface of the river. Sand is a collection of finely divided rock and various mineral grains. Sand itself is not a mineral. It is a sediment like clay, gravel and slit. ISO 14688-1[39] grades sands in three types. The particle size of fine sand is in the range of 0.063mm to 0.2mm, medium sand is in the range of 0.2mm to 0.63mm and coarse sand is in the range of 0.63mm to 2.0mm. Silica ( $\text{SiO}_2$ ) in the form of quartz-is the most common constituent of sand. The composition of minerals of sand varies from place to

place, because it depends upon the local rock sources and conditions. Again, depending on the natural sources from which sand is formed, it is classified into three types: river sand, pit sand and sea sand. Pit sand is obtained by formation of pits in soil. The grains of pit sand are sharp and angular and free from salts. River sand is obtained from the banks or beds of rivers. Due to mutual attrition under the action of water current river sands are fine rounded grains. Sea sand is obtained from sea shores. The porosity of sand depends upon not only its size and shape but also the moisture and clay components present in it. If the sand is too fine, the porosity will be low.

Sand has some weak natural adsorption property. The adsorption properties of the sand however can be modified by surface modification. Ferric ion coated quartz sand surface shows higher fluoride adsorption capacity than uncoated quartz sand [40], because ferric ions acted as a bridge between quartz and fluoride.

#### **4.3.1 Selection of *Kanaighat* sand as local raw material for preparation of adsorbent**

Since to make the water affordable after defluoridation and dearsenication especially to that economically weaker village residents it is preferred that adsorbents should preferably be made up from local raw materials, accordingly in this study, naturally occurring sand from Kaliani river of Kanaighat and Labanghat area (Latitude 26.583986 deg N, Longitude 93.754945 deg E) of Golaghat district of Assam, India was collected. There are several reasons for selecting these sands as in Kanaighat area, since already a rich sand supply infrastructure exists there. Which if proper technologically developed further may one day give rise to establishment of advanced adsorbent materials producing plant catering to the needs of the population of the neighbouring areas for water treatment purposes especially for the fluoride and arsenic removal at an economical price.

Origin of the Kaliani river on whose banks these two places Labanghat and Kanaighat are situated lies in the neighbouring Karbi-Anglong district of Golaghat district which meanders through the hills comprising oldest Archean gneissic rocks [41]. It flows through the pediment zones of the border areas of Golaghat district and meets Dhunseri river at Labanghat area of Golaghat district. Like any other sand this is also a naturally occurring granular material, consisting of small grains or particles of mineral and rock fragments.

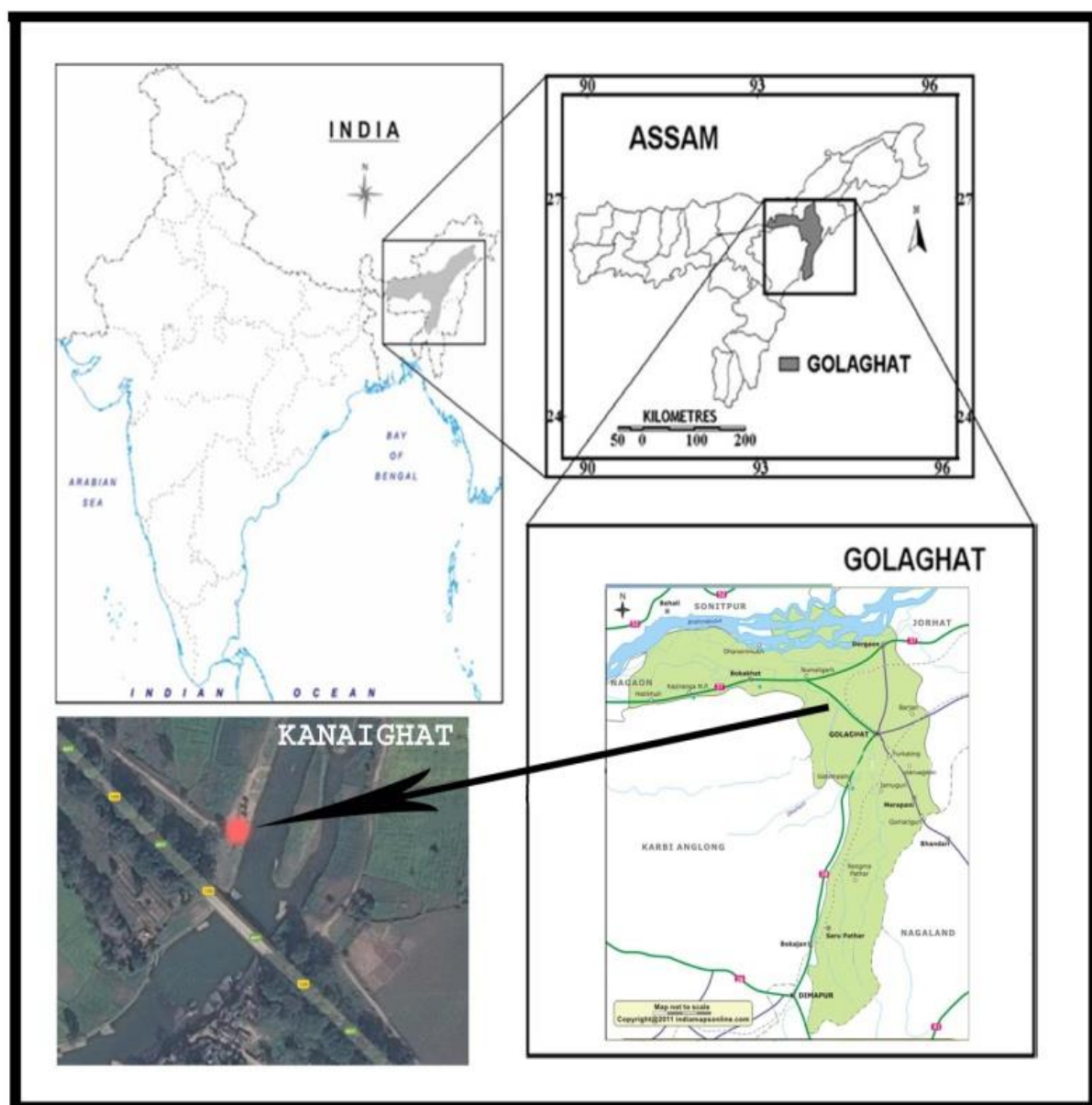


Fig 4.6: Site map of sand collection area



**Fig 4.7: Photo of Kanaighat sandbar on the banks of river Kaliani**

The preparation and characterization studies of two adsorbents from the above two selected locally available raw materials are described below in the following sections i.e., section A and section B.



## SECTION A

## PREPARATION AND CHARACTERIZATION OF CARBON OF BANANA PLANT (CBP)

## 4.4 Experimental

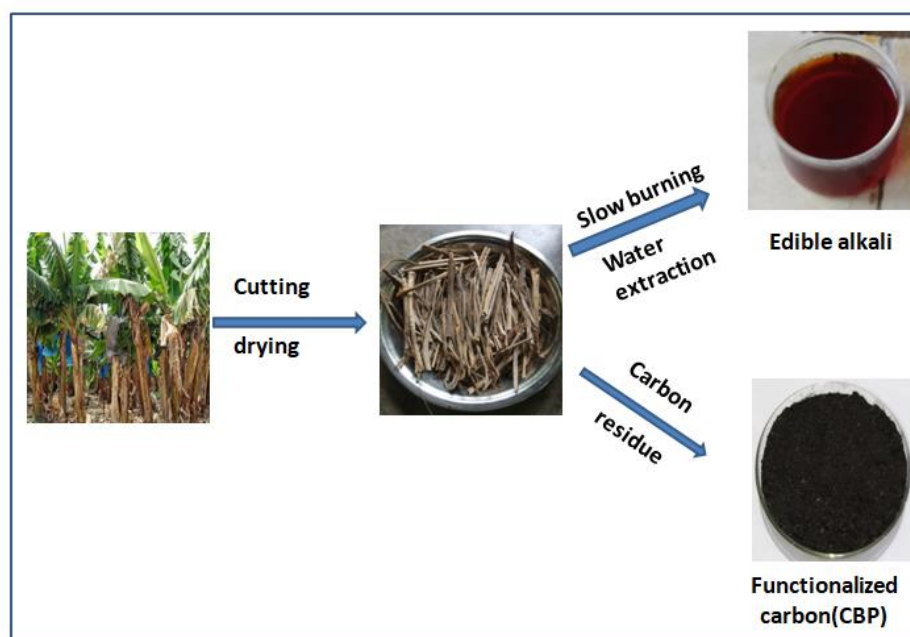
4.4.1 Preparation of the adsorbent (carbon from Banana plant, *Musa balbisiana*)

Fig4.8: Graphical abstract of preparation of CBP

For this study, the green stems of *Musa balbisiana* plant were collected from Boruah Gaon region of Golaghat district of Assam, India. Collected stems were cleaned, cut into small pieces and dried strongly in October sun for several days. Drying of 25 Kg of green mass yielded around 3.0 Kg of dried mass. The hard sun dried mass of stems of *Musa balbisiana* was slowly burnt; from the ashes of burnt biomass the alkali was extracted by solvent extraction with water at pH 10. The insoluble carbon portion was separated by filtration and dried carefully at 60°C. The carbon powder obtained as residue over the filtration barrier in the process was a byproduct which due to exposure to high *in-situ* alkalinity develops a base mediated surface functional group formation. Finally ground the



**Chapter-4**                      ***Preparation & characterization of adsorbents of fluoride & arsenic***  
dried Carbon of banana plant in a planetary micro pulverizer at 600 RPM for 5 minutes and stored in the name of CBP as our study material.

#### **4.4.2 Physico-chemical characterization of CBP**

Various parameters such as moisture content, volatile compound present, water soluble matter, ash content, acid soluble matter, fixed carbon, pH and conductivity were determined as per ASTM standards. Bulk density of the adsorbent CBP was also determined [42]. Carbon, hydrogen and nitrogen content of CBP were measured by using the CHN analyzer (Model-2400, Perkin Elmer). Zeta potential, zero point charge, oxygen containing functional group present, pore volume and surface area were also determined. Surface morphology, elemental composition, surface functional group present, thermal stability etc of CBP were also determined.

##### **a) Moisture content of CBP**

A pre-heated (at 110°C in an oven for 1 hour) silica crucible was allowed to cool at room temperature and the weight of the crucible (B g) was taken. Almost one gram of CBP was taken in the crucible and weighted (C g). The crucible with CBP was dried in a drier continuously and the dried sample was continuously reweighed at 10 min. interval until a constant weight (D g) was obtained. The ratio of change in original weight expressed in percentage gives the moisture content [43].

$$\text{Moisture content (\%)} = \frac{C-D}{C-B} \times 100 \quad \text{----- (4)}$$

##### **b) Volatile matter of CBP**

A silica crucible was preheated in a furnace at 900°C for 10 min. cooled in a desiccator and the weight of the crucible (B g) was taken. Almost one gram of CBP was taken in the crucible and weighed (C g). The crucible with CBP was heated in the furnace at about 900°C for 10 min and then cooled in a desiccators and reweighed (D g). The loss in weight gives the volatile matter [44].

$$\text{Volatile matter (\%)} = \frac{C-D}{C-B} \times 100 \quad \text{----- (5)}$$

**c) Water soluble matter of CBP**

Almost 1g of CBP (B g) was added to 100 ml distilled water and shaken thoroughly for about 30 min. and filtered through a pre-weighed Whatman filter paper (C g). The residue was dried, cooled and weighed with the filter paper (D g). The loss in weight gives water soluble matter present [45].

$$\text{Water soluble matter (\%)} = \frac{D-C}{B} \times 100 \quad \text{----- (6)}$$

**d) Ash content of CBP**

A silica crucible was preheated in a furnace at 900°C for 1 hour and cooled in a desiccator and then weight of the crucible (B g) was taken. Almost one gram of CBP was taken in the crucible and weighed (C g). The crucible with CBP was heated with lid on at about 900°C for 1 hour and then cooled in a desiccator and reweighed (D g). The loss in weight gives the ash content [46].

$$\text{Ash content (\%)} = \frac{C-D}{C-B} \times 100 \quad \text{----- (7)}$$

**e) Acid soluble matter of CBP**

Acid soluble matter of CBP was determined by following the “Test method of activated carbon” [47]. A thin slurry of 1g CBP was prepared by mixing with small amount of water in an evaporating dish and then repeatedly digested with 5-10 mL of conc. HCl. Then it was diluted with 100 mL water and filtered using a previously weighed sintered crucible. The weight of the remaining part of the sample was calculated after drying for a constant weight at 110°C.

$$\text{Acid insoluble matter (\%)} = \frac{D-C}{B} \times 100 \quad \text{----- (8)}$$

Where, B=mass of the sample taken=1g; C=mass of crucible; D=mass of the crucible and the remaining sample after heating.

**f) Fixed Carbon of CBP**

The quantity of fixed carbon in percentage is obtained by subtracting the sum of percentage composition of volatile matter, moisture content, acid soluble, water soluble and

**Chapter-4** *Preparation & characterization of adsorbents of fluoride & arsenic*  
ash content from 100 percent. Fixed carbon from the sample were obtained using the following relation [48].

$$\text{Fixed carbon (\%)} = 100 - (\text{volatile matter} + \text{ash content} + \text{moisture content}) \text{ ----- (9)}$$

#### **g) Bulk density of CBP**

Bulk density is defined as weight per unit volume of material. Weight of empty cylinder and weight of cylinder with carbon sample were taken. Then the carbon sample was transferred into the aluminium plate and oven dried at a temperature of 105°C for 60mins. After drying the weight of the dry sample was measured.

$$\text{DB} = (m_2 - m_1) / v \text{ ----- (10)}$$

$m_1$  = mass of measuring cylinder in grams

$m_2$  = mass of measuring cylinder + its contents

$v$  = volume of the measuring cylinder in litre

#### **h) The pH and conductivity of the adsorbent CBP**

For this study, 1 g of the carbon sample (CBP) in 100 mL of distilled water were taken in a beaker and the mixture was stirred for 1 hour [49]. The sample was allowed to stabilize for some time and there after the pH and conductivity were measured.

#### **i) Zeta potential of CBP**

Zeta Potential of CBP was measured by using Zetasizer instrument of model-Nano ZS, Malvern, UK. Zeta Potential is the potential difference between the dispersion medium and the stationary layer of fluid attached to the surface of the dispersed particle. It is a measure of the magnitude of the electrostatic or charge repulsion / attraction among particles and is one of the fundamental parameters which causes of dispersion, aggregation or flocculation and can be applied to improve the formulation of dispersions, emulsions and suspensions.

#### **j) Zero point charge (pH<sub>zpc</sub>) of CBP**

The PZC (point of zero charge/zero charge point/zero point charge) of CBP was determined by measuring pH [50]. PZC is the pH when the surface charge of the compound is zero [51]. For this experiment 50 ml of 0.01M NaCl solutions of different pH were taken into a series of Erlenmeyer flasks. Their pH values were adjusted in range between 2 and 12 by

#### **Chapter-4                      Preparation & characterization of adsorbents of fluoride & arsenic**

using 0.01M HCl and 0.01M NaOH solution. These pH values of the solutions are noted as pH-initial. 0.35 g of carbon sample CBP was added into each flasks and after continuous shaking for 48 h, pH of the solutions were measured as pH-final. PZC of CBP is the point when  $pH_{init} = pH_{final}$ . The  $pH_{zpc}$  was determined by plotting  $pH_{initial}$  vs  $pH_{init} - pH_{final}$ .

#### **k) Oxygen containing functional groups (Boehm's titration) present in CBP**

The functional groups bearing oxygen atoms present on the surface of CBP were determined by the Boehm titration method [52]. For it 1.0 g of the activated carbons was taken with 15 mL solutions of each of  $NaHCO_3$  (0.1 M),  $Na_2CO_3$  (0.05 M) and NaOH (0.1 M) separately for determination of acidic groups and 0.1 M HCl for the determination basic groups /sites respectively and shaken at room temperature for 48 hours at 180 rpm. After filtration, the filtrates of the mixtures were back titrated with HCl (0.1 M) for acidic and NaOH (0.1 M) for basic groups by using pH indicators. The numbers of acidic sites of various types were calculated under the consideration that NaOH neutralizes carboxylic, phenolic and lactonic groups and that  $Na_2CO_3$ -carboxylic and lactonic and  $NaHCO_3$  only carboxylic groups. The difference between the groups titrated with  $Na_2CO_3$  and those titrated with  $NaHCO_3$  is considered to be lactones and the difference between the groups titrated with NaOH and those titrated with  $Na_2CO_3$  is considered to be phenol [42]. The number of surface basic sites were calculated from the amount of hydrochloric acid, which reacted with the carbon.

#### **l) Pore volume and surface area of CBP (BET method)**

The study of physical adsorption of nitrogen gas on CBP was carried out at 77.3 K by using an Autosorb-iQ Station 1 (Quantachrome, USA) for determination of the specific surface area and pore volume applying Brunauer–Emmett–Teller (BET) equation. Specific surface area was the total surface area of a solid per unit of mass. In this experiment, the volume of gas adsorbed which is correlated to the total surface area of the particles including pores on the surface of CBP was measured at the boiling point of nitrogen (77.3K) by using the BET equation (equation 11) [53]. Prior to gas adsorption measurements, the carbon was degassed at 200°C for 3 h.

$$\frac{P}{V(P_0 - P)} = \frac{1}{V_m C} + \frac{C-1}{V_m C} \times \frac{P}{P_0} \quad \text{----- (11)}$$

#### **Chapter-4                      Preparation & characterization of adsorbents of fluoride & arsenic**

where  $V$  is the specific amount adsorbed at the relative pressure  $p/p_o$  and  $V_m$  is the specific monolayer capacity. By plotting  $\frac{P}{V(P_o-P)}$  vs  $p/p_o$ , the BET constant  $C$  and  $V_m$  can be found from the gradient and intercept and by using cross sectional area surface area can be calculated.

$$V_m = \frac{1}{\text{gradient} - \text{intercept}}$$

$$C = 1 + \frac{\text{gradient}}{\text{intercept}}$$

The surface area is determined by the following equation

$$S_{\text{BET}} = (N A V_m / V_M m_s) \times 10^{-20}$$

Where,  $S_{\text{BET}}$  is the surface area ( $\text{m}^2\text{g}^{-1}$ )

$N$  is the Avogadro's number ( $6.023 \times 10^{23}$  molecules/mole)

$A$  is the area occupied by an adsorbate molecule ( $16.2 \text{ \AA}$  for nitrogen)

$V_m$  is the quantity of gas adsorbed for monolayer coverage of surface ( $\text{cm}^3$ )

$m_s$  is the mass of the solid analyzed (g)

$V_M$  is the molar volume of gas ( $22,414 \text{ cm}^3\text{mol}^{-1}$ )

For nitrogen as adsorptive gas, the above equation becomes

$$S_{\text{BET}} = 4.35 V_M / m_s$$

#### **m) Field Emission Scanning Electron Microscopy (FESEM) study of CBP**

The Carbon of Banana Plant (CBP) was also characterized by using Field Emission Scanning Electron Microscope (FESEM), Energy Dispersive X-ray Spectroscopy (EDX) (SEM-JEOL JMS 6390 LV instrument). SEM image gives the morphology and structural characteristics of the materials. EDX analysis was carried out in order to find the elemental composition. The scanning electron microscope scans a sample with a focused beam of electrons to produce high magnified images of sample's surface topography. The two-dimensional images are produced from the signals that comes from interactions of the electron beam with atoms at various depths within the sample. In addition to surface evaluation, it also

**Chapter-4**                      ***Preparation & characterization of adsorbents of fluoride & arsenic***  
measures elemental composition in or on the surface of the sample, when used with the EDS feature.

**n) FT-IR study of CBP**

The chemical functionality of CBP was qualitatively identified by Fourier Transform Infra Red spectroscopy method. FT-IR analysis was carried out by using FT-IR instrument (model- IR Affinity-1, Shimadzu, Japan) by preparing KBr pellet. When infrared radiation passes through the sample, the absorbed radiation is converted into rotational and vibrational energy by the sample molecules. Different types of bonds of different functional groups present in the sample absorb infrared radiation of different wavelengths. The FTIR spectrometer generate a graph from the resulting signal in the form of absorbance spectra of different surface functional group present [53].

**o) Thermo Gravimetric Analysis (TGA) of CBP**

Thermal analysis of CBP was carried out to know about the changes in weight in relation to time and temperature i.e., thermal stability in order to know about the decomposition pattern of CBP at different temperature by using DTA-TGA equipment Q-600 (M/S TA Instruments, USA). TGA were done by taking alumina as a reference at a heating rate of 20°C/minute under argon atmosphere.

**p) Powder X-ray Diffraction (PXRD) study of CBP**

Powder X-ray Diffraction (PXRD) analysis was done by using X-Ray Diffractometer (Model Ultima IV, Rigaku, Japan) to know the crystallographic structure, crystallite size (grain size) and preferred orientation in the adsorbent CBP. With the help of PXRD unknown substance can be identified by comparing the diffraction data with database maintained by the International Centre for Diffraction Data.

**4.5 Results and discussion**

The proximate and elemental analysis of functionalised Carbon of Banana Plant (CBP) are shown in Table 4.1.

**Table 4.1: Physico-chemical parameters of CBP**

Serial Number	Parameters	Value
1	pH	8.0
2	Conductance	0.36 mS
3	Ash Content	26 % w/w
4	Moisture Content	6.19 % w/w
5	Volatile Compound Present	41.17 % w/w
6	Water Soluble Matter	0.9% w/w
7	Acid soluble Matter	30.47 % W/W
8	Fixed Carbon	26.64 % W/W
9	Bulk Density	0.33 g/mL
10	Average Zeta Potential	-18.9 mV
11	The Particle Size (Diameter)	1420 nm
12	BET Surface Area	42.99 m <sup>2</sup> /g
13	Pore Volume	0.15 cc/g
14	Pore Radius	1.67 nm
15	pH ZPC	9.6
16	Carbon	49.62 % w/w
17	Hydrogen	1.82 % w/w
18	Nitrogen	0.67 % w/w
19	Oxygen*	21.89 % w/w

N.B. Oxygen\* = 100% - (C% + H% + N% + ash%)

High value of ash content (26% w/w) indicate that the pores present on the surface are not well preserved. As most of the spaces are occupied by the ash, it affects the adsorption efficiency of CBP.

In CBP, the moderate value of moisture content (6.19 % w/w) indicate the moderate adsorption capacity as comparatively low moisture content indicate higher adsorption capacity (Pongener, 2015). CBP contain high amount of volatile compound (41.17 % w/w) and acid soluble matter (30.469 % W/W). The low value of water soluble matter (0.9 % w/w) indicate that CBP is almost insoluble in water and hence it can be used in water treatment.

pH and Conductivity of CBP are 8.0 and 0.36 mS respectively. As for most application of carbon, pH range is 6-8 is acceptable [54,55], so CBP is satisfactory in application of water treatment. Conductivity depends on total dissolved solids (TDS) in water.

It is found that the average zeta potential is -18.9 mV. It indicates the incipient instability of CBP dispersions. Normally, a value of >30 whether it may be +ve or -ve indicates good stability of dispersions due to repulsion of the particles. The negative symbol of the zeta potential value means that the net charge of the scattering object including up to the slipping plane is negative.

ZPC of CBP is 9.6. It means at 9.6 pH of adsorbate solution, CBP shows net charge zero and hence at this pH it can't act as adsorbent. At lower pH than ZPC value 9.6, due to the donation of more  $H^+$  to the adsorbent surface by the adsorbate solution, the adsorbent surface becomes positively charged and hence can attract anions [56]. The values of initial pH and final pH in determining of ZPC of CBP are given in Table 4.2 and the corresponding plot is given in Fig 4.1



**Table 4.2:** pH of 0.01M NaCl solution before and after treatment with CBP

Initial pH ( $pH_i$ )	Final pH ( $pH_f$ )	$pH_i - pH_f$
3.5	9.5	-6.0
4.5	9.8	-5.3
5.5	9.7	-4.2
6.5	9.5	-3.0
7.5	9.7	-2.2
9.5	9.8	-0.3
11.1	9.8	1.3

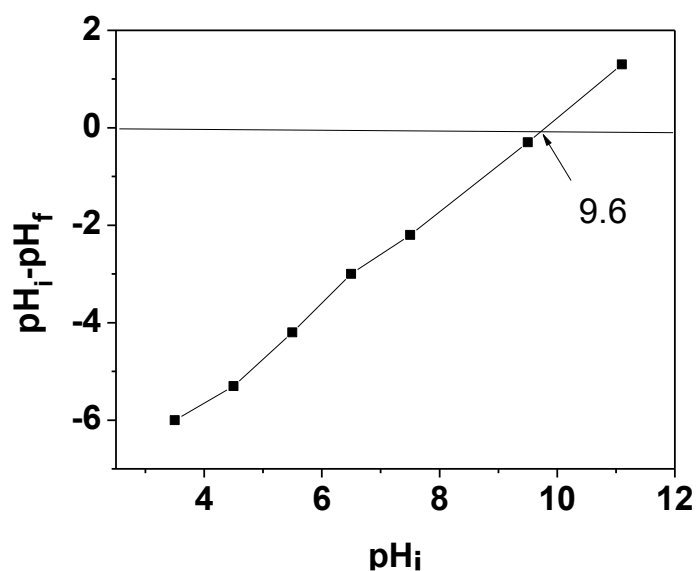


**Fig 4.9:** Plot of  $pH_i$  vs  $pH_i - pH_f$

From Boehm titration, the amount of surface functional group having oxygen such as carboxylic group, lactonic group, phenolic group and surface basicity were calculated and

**Chapter-4** *Preparation & characterization of adsorbents of fluoride & arsenic*  
given in Table 4.3. It is seen that the amount of total basic groups is greater than the total acidic groups (due to carboxylic groups, lactonic groups and phenolic groups).

**Table 4.3: Surface acidic groups and basic groups present in CBP, measured by Boehm titration method**

Adsorbent	Total Surface Acidity mmol/g	Amount of Carboxylic group mmol/g	Amount of Lactonic group mmol/g	Amount of Phenolic group mmol/g	Amount of surface Basicity mmol/g
0.2g CBP	4.35	1.25	2.45	0.65	4.4

From nitrogen adsorption study, BET surface area of CBP was calculated and it was found as 42.99 m<sup>2</sup>/g and the pore volume as 0.15 cc/g. Surface area of CBP is very small.

#### Scanning electron microscopy (FESEM) characterization of CBP

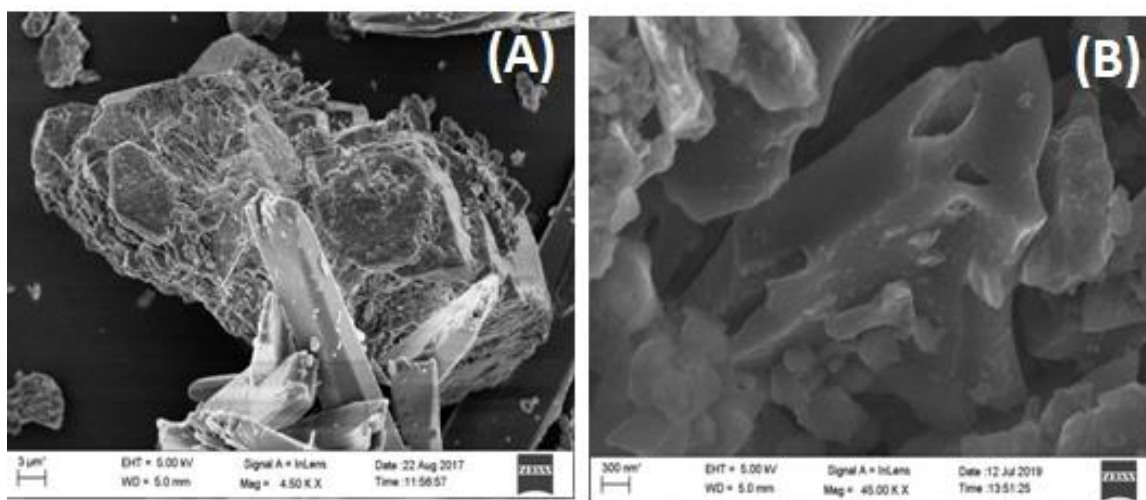


**Fig 4.10: (A) and (B) are FESEM images (A & B) of CBP**

From the various magnifying FESEM images of CBP (Fig 4.10), we can know about the surface morphology. In case of CBP, some holes and cave type openings were found on the surface. It also showed complex disorganized rough surface structures having pores of different sizes and shapes. From EDX spectra the chemical composition of CBP was obtained.

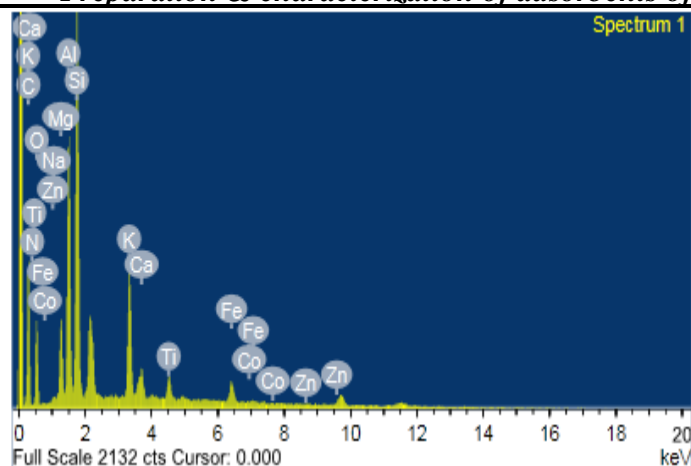


Fig 4.11: EDX spectra for elemental composition of CBP

Table 4.4: Elemental composition of CBP from EDX spectra

Element	C	N	O	Na	Mg	Al	Si	K	Ca	Co	Ti	Fe	Zn	Toal
Weight %	38.4	0.62	24.60	0.17	2.72	8.17	9.23	6.49	4.47	0.12	1.78	3.06	0.19	100.00
Atomic %	54.2	0.75	26.04	0.12	1.9	5.14	5.56	2.81	1.88	0.03	0.63	0.93	0.04	100.00

## FT-IR study

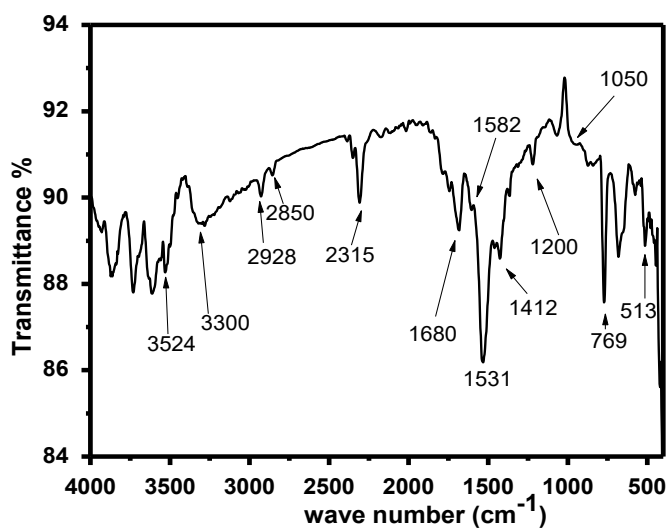


Fig 4.12: FTIR spectra of CBP

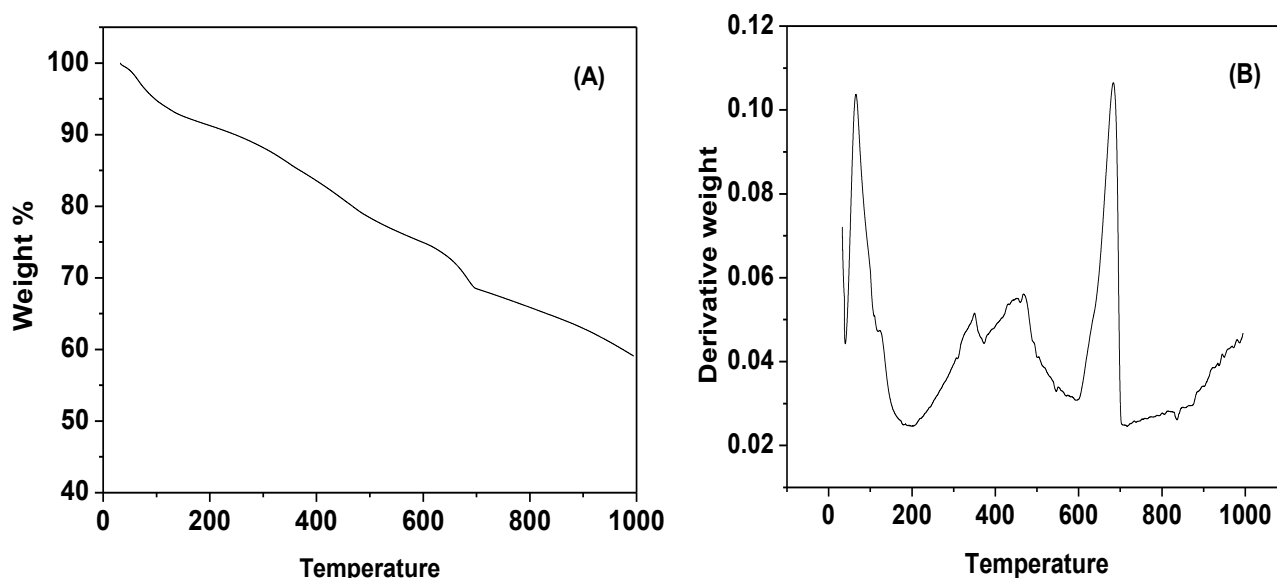
The FTIR spectra of CBP is shown in Figure 4.11. Table 4.5 summarizes the assignment of the main bands obtained.

**Table 4.5: Wave numbers and assignment of the principal bands in the FTIR spectra of CBP**

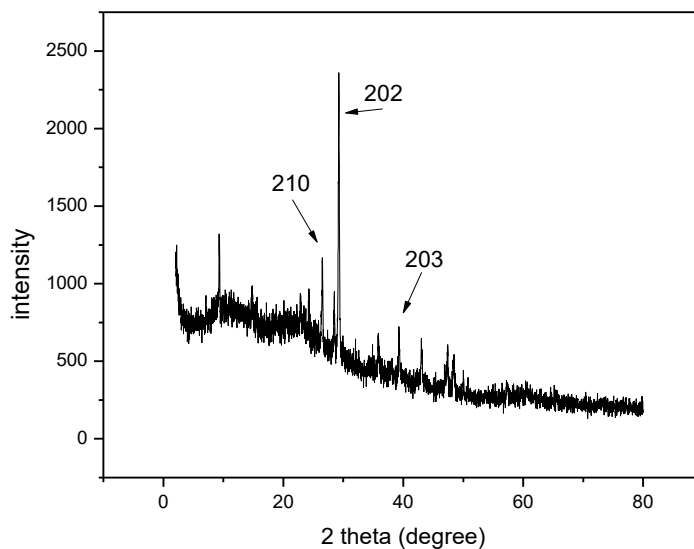
Wave Number (cm <sup>-1</sup> )	Assignments	References
3524-3300	O-H stretching vibrations (inter molecular hydrogen bonded)	[21]
2920	C-H asymmetric stretching	[21]
1680	C=O stretching	[57]
1582	C=O stretching vibration of lactone and carbonyl group	[21]
1412	C-H asymmetric bending of alkene	[21]
1200	C-O in carboxylic acid, alcohols, phenols	[21]
769-513	C-C stretching	[42]

Fourier transform infra red (FTIR) transmission spectra of CBP showed hydroxyl functional groups including hydrogen bonding (O-H stretching) peaks at 3524–3300 cm<sup>-1</sup> due to O-H stretching vibrations of the phenolic groups, at 1680 cm<sup>-1</sup> due to C=O stretching , at 1582 cm<sup>-1</sup> due to C=O stretching vibration of lactone and carbonyl group, at 1422 cm<sup>-1</sup> due to C-H asymmetric bending, at 1200-1050 cm<sup>-1</sup> due to C-O stretching in carboxylic acid sand alcohols and phenols at 769-513 cm<sup>-1</sup> due to C-C stretching. The presence of broad band around 3400–2400 cm<sup>-1</sup> and peak at 1680cm<sup>-1</sup> indicates the presence of carboxylic acid [58,59]. The peaks in the regions of 3600 – 3800 cm<sup>-1</sup> are the typical for activated carbon [60].

## Thermo Gravimetric Analysis (TGA)

**Fig 4.13: Thermogram of CBP**

TGA studies reveal the stability of CBP under high temperature. From the Fig 4.12, it was seen that initially a weight loss occurs at 96°C, with a percent mass loss of 6.0% which was expected to be due to the presence of molecules like water and other volatile matter. Again some weight loss was observed at around 462°C, with a percent mass loss of 20% which was expected to be due to the loss of carbon monoxide. Another weight loss at 688°C, with a percent mass loss of 31% was observed which may be due to the loss of carbon dioxide. Because from some reference of thermal decomposition of calcium oxalate, it was seen that at temperatures ranging 400 – 530 °C, it losses carbon monoxide and at temperatures ranging 600 – 810 °C, losses carbon dioxide [61]. At temperature 1000°C CBP showed a percent mass loss of 40% with 60% remaining as unburnt.

**Powder X-ray Diffraction (PXRD) study****Fig 4.14: XRD Spectra of CBP**

From the XRD pattern (Fig 2) formation of crystalline phase of the compound Calcium Aluminium Oxide Carbonate Hydrate [ $\text{Ca}_6\text{Al}_2\text{O}_6(\text{CO}_3) \cdot 32 \text{H}_2\text{O}$ ], PDF Card No. 00-041-0215, with a hexagonal structure was confirmed with distinct lattice planes (202), (210) & (203) at  $2\theta = 3.026, 3.282$  &  $2.358$  and 100%, 65% & 50% intensity.

## Section B

### PREPARATION AND CHARACTERIZATION OF IRON OXIDE COATED SAND (IOCS)

#### 4.6 Experimental

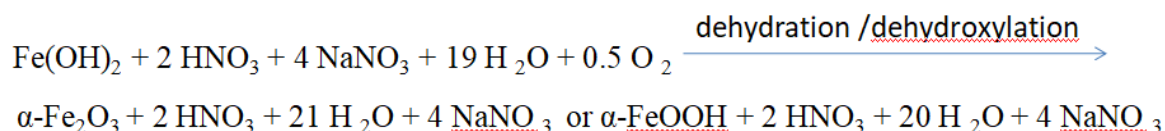
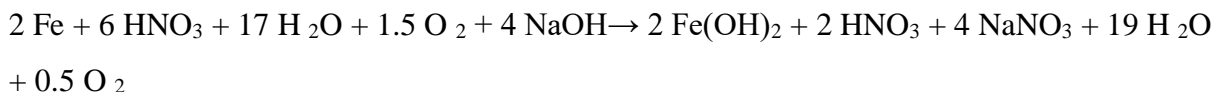
##### 4.6.1 Preparation of the adsorbent Iron Oxide Coated Sand, IOCS by surface modification of Kanaighat sand

Locally available *Kanaighat sand* (KS) was collected from the Kanaighat area. The collected sand sample was mixed thoroughly by quartering and coning, sieved through mesh to obtain 650-800 micrometer mean sized sand particle. This sand was modified by coating of iron oxide on the surface of sand grain. At first, the sand was washed repeatedly to remove unwanted clay or other particles. It was then soaked in 0.1 N  $\text{HNO}_3$  acid solution overnight and thereafter rinsed with deionized distilled water repeatedly and dried at  $100^\circ\text{C}$  for 20 hr. For iron oxide coating over the surface of the sand particle, a solution containing a mixture of 80 mL of 2 M  $\text{Fe}(\text{NO}_3)_3 \cdot 9\text{H}_2\text{O}$  and 1 mL of 10 M NaOH was poured over 200 g dried sand placed in a heat resistant dish. After gentle agitation, the mixture was heated for 5 hr at  $110^\circ\text{C}$  and then at  $550^\circ\text{C}$  for 4 hr. Upon cooling, the coated sand was washed with deionized distilled water till the black colored fraction was washed away and dried in hot air oven at  $100^\circ\text{C}$ . After cooling, again the solution containing the same mixture of  $\text{Fe}(\text{NO}_3)_3 \cdot 9\text{H}_2\text{O}$  and NaOH was poured over the dry sand and heated for 36 hr at  $110^\circ\text{C}$  and the activated sand prepared was named as Iron Oxide Coated Sand (IOCS).

The prepared iron oxide coated sand (IOCS) was taken for adsorption of fluoride and arsenic. Some other report of Iron oxide coating to develop adsorbents for water decontamination from various pollutants such as arsenic [62], metal ions [63,64], synthetic dyes and pharmaceutical and personal care products are also reported [65]. They perform as good adsorbent due to the large surface area to volume ratio and high reactivity. Similar behaviour is reported for various metal oxide nano particles also. However, among these nano oxidic adsorbents, iron oxides [66] are more attractive because of their environmental benignity, cost and high reactivity toward target pollutants. Various forms of iron oxides, oxyhydroxides and hydroxides, all are collectively called as 'iron oxides' [67].

#### **Chapter-4                      Preparation & characterization of adsorbents of fluoride & arsenic**

The mechanism of formation of iron oxide in IOCS by  $\text{FeNO}_3 \cdot n\text{H}_2\text{O}$  solution used to generate the coating can be explained by the following chemical equation [62]:



On strong heating after evaporation of water the residual solution becomes concentrated and causing Fe-oxide to precipitate on the surface of KS. Due to constant 36 hours heating at  $110^\circ\text{C}$ , the synthesized IOCS becomes progressively less hygroscopic. From FTIR and PXRD analysis also, the formation of Fe-oxide coating can be confirmed.

#### **4.6.2 Physico-chemical characterization of the adsorbent (IOCS) prepared**

##### **a) Chemical composition of raw *Kanaighat* sand and iron content of prepared IOCS**

The chemical analysis of the raw *Kanaighat* Sand (KS) was carried out by conventional titrimetric and gravimetric methods involving initial fusion of the material at  $1000^\circ\text{C}$  in  $\text{Na}_2\text{CO}_3$  mixture. By this method various amount of metal (Fe, Al, Ca and Mg) oxide present in KS were determined. Amount of iron in coated iron oxide on the surface of IOCS was also determined by the same conventional titrimetric and gravimetric methods.

##### **b) pH and conductivity of the IOCS**

For this study, 1 g of IOCS in 100 mL of distilled water were taken in a beaker and the mixture was stirred for 1 hour [49]. The samples was allowed to stabilize for some time and there after the pH and conductivity were measured.

##### **c) Zeta Potential of the adsorbent IOCS**

Zeta Potential of IOCS was measured by using Zetasizer instrument of model-Nano ZS, Malvern, UK.



**d) Zero point charge ( $\text{pH}_{\text{zpc}}$ ) of IOCS**

As the isoelectric point (IEP) and zero point charge/point of zero charge (PZC) for iron oxide, oxyhydroxide and hydroxide has no significant difference [68], so by measuring the zeta potential at various pH, zero point charge/point of zero charge (PZC) of IOCS was determined.

**e) Pore volume and BET surface area IOCS**

The study of physical adsorption of nitrogen gas on IOCS was carried out at 77.3 K by using an Autosorb-iQ Station 1 (Quantachrome, USA) for determination of the specific surface area and pore volume applying Brunauer–Emmett–Teller (BET) equation (11).

**f) Scanning Electron Microscopy (SEM) study of IOCS**

The Iron Oxide Coated Sand (IOCS) was also characterized using Field Emission Scanning Electron Microscope (FESEM), Energy Dispersive Spectroscopy (EDS) using SEM-JEOL JMS 6390 LV instrument. SEM images in different magnification and EDS spectra give opportunity to study the surface morphology and elemental composition in or on the surface of the sample IOCS.

**g) FT-IR study of IOCS**

The functional group analysis of IOCS was carried out by Fourier Transform Infra Red spectroscopic method in the range of  $400\text{--}4000\text{ cm}^{-1}$ . FT-IR analysis was carried out by using FT-IR instrument (model- IR Affinity-1, Shimadzu, Japan) by preparing KBr pellet.

**h) Thermo Gravimetric Analysis (TGA) of IOCS**

Thermal analysis of IOCS was carried out to know about the thermal stability i.e., about the decomposition pattern of IOCS at different temperature by using DTA-TGA equipment Q-600 (M/S TA Instruments, USA).

**i) Powder X-ray Diffraction (PXRD) study and IOCS**

Powder X-ray Diffraction (PXRD) analysis was done by using X-Ray Diffractometer (Model Ultima IV, Rigaku, Japan) using  $\text{CuK}\alpha$  radiation and maintained a scan rate of 2 degree/minute to characterize the crystallographic structure of IOCS.

## 4.7 Results and discussion

### Chemical Composition of Kanaighat Sand and percentage of iron in IOCS

The main oxidic component in the raw KS is silica (90%), Table 4.6 shows the oxidic chemical composition of the sand.

**Table 4.6: Composition of Kanaighat Sand**

Composition	Silica	Fe <sub>2</sub> O <sub>3</sub>	Al <sub>2</sub> O <sub>3</sub>	CaO	MgO	Loss on Ignition	Total
(% W/W)	90.01%	0.79%	4.00%	2.79%	1.99%	0.36%	99.95%

The amount of iron oxide on the surface of prepared IOCS sample was determined by subtracting the difference of percentages of it from IOCS and KS after determining the same by chemical analysis method. IOCS was found to contain 15 % iron oxide W/W which is an almost 14.2% W/W rise of iron oxide content.

### Zero point charge (pH<sub>zpc</sub>)

The observed values of zeta potential of IOCS with different pH are given in Table 4.7 and the corresponding plot is given in Fig 4.14. It is seen that at pH 7.8, the zeta potential of IOCS is zero. From this plot the zero point charge (pH<sub>zpc</sub>) is determined as 7.8. It means at higher pH than pH<sub>zpc</sub> value (7.8), IOCS can act as adsorbent for anionic species. Because at lower pH than pH<sub>zpc</sub>, adsorbate solution donate more H<sup>+</sup> to the adsorbent surface, due to which the adsorbent surface becomes positively charged and hence can attract anions [56].

Table 4.7: Values of zeta potential with corresponding pH values

pH	Zeta potential
1.5	16.36
3.8	8.23
7.8	-0.06
10	-16.16
11.2	-20.04

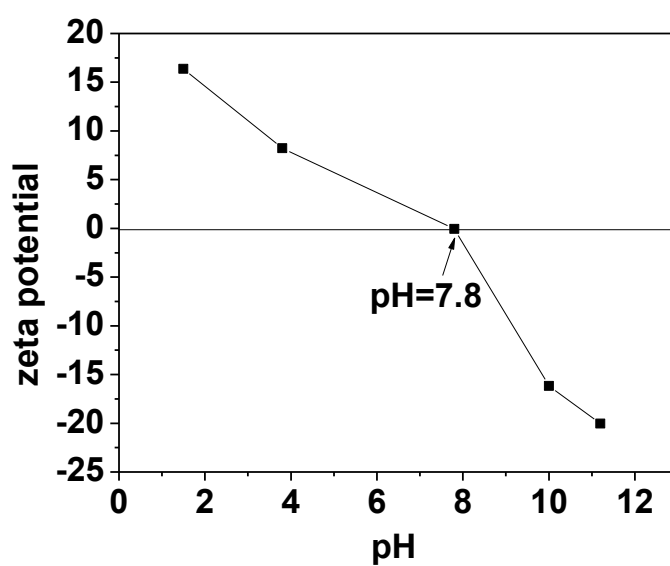


Fig 4.15: Plot of Zeta potential vs pH of IOCS

#### Characterisation of BET surface area

From nitrogen gas adsorption study, BET surface area, pore volume and pore radius were calculated and are given in Table 4.8.

Table 4.8: Values of BET surface area, pore size of KS and IOCS

Sand	BET Surface area	Pore size
KS (Kanaighat sand)	6.97 m <sup>2</sup> /g	17.75 Å
IOCS (Iron oxide coated sand)	16.54 m <sup>2</sup> /g	17.79 Å

## Scanning electron microscopy (SEM) study of KS and IOCS surface

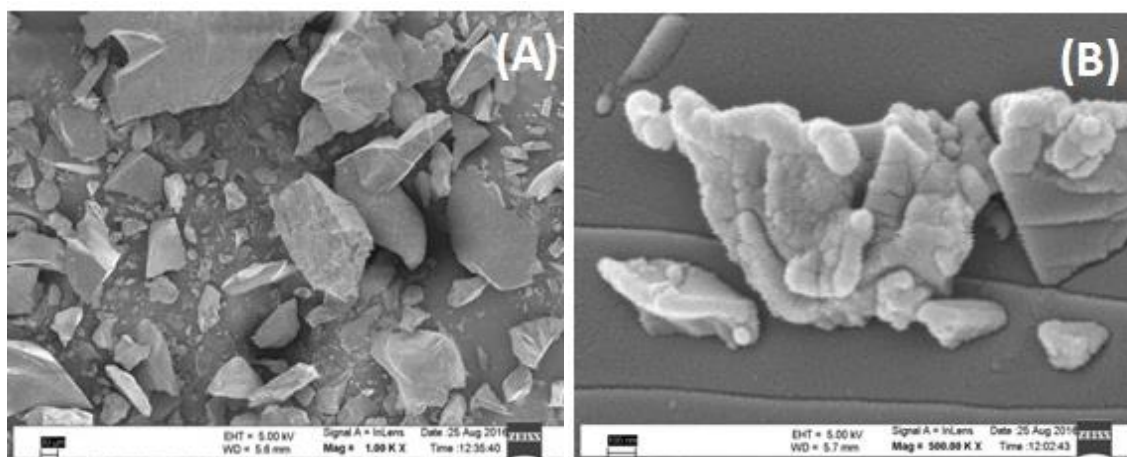
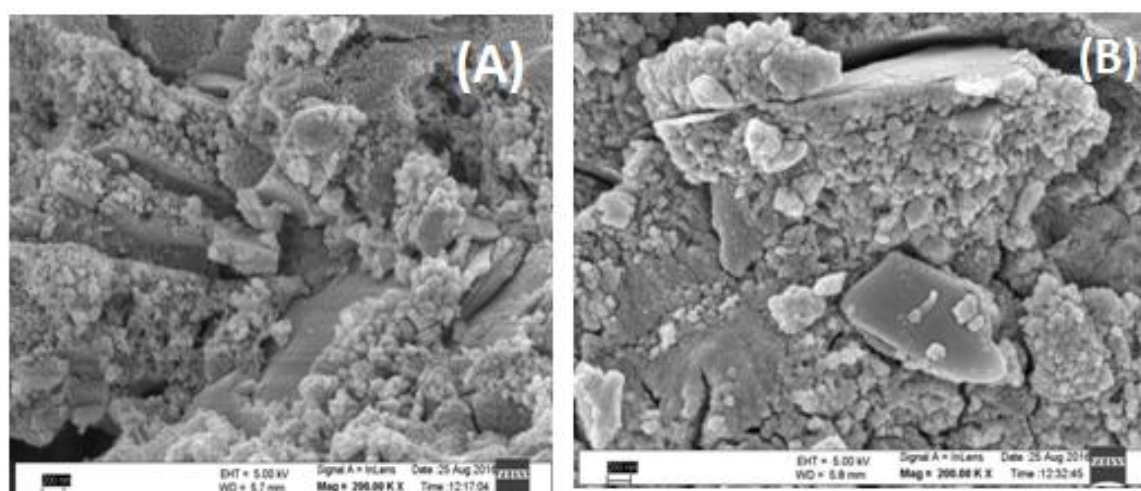
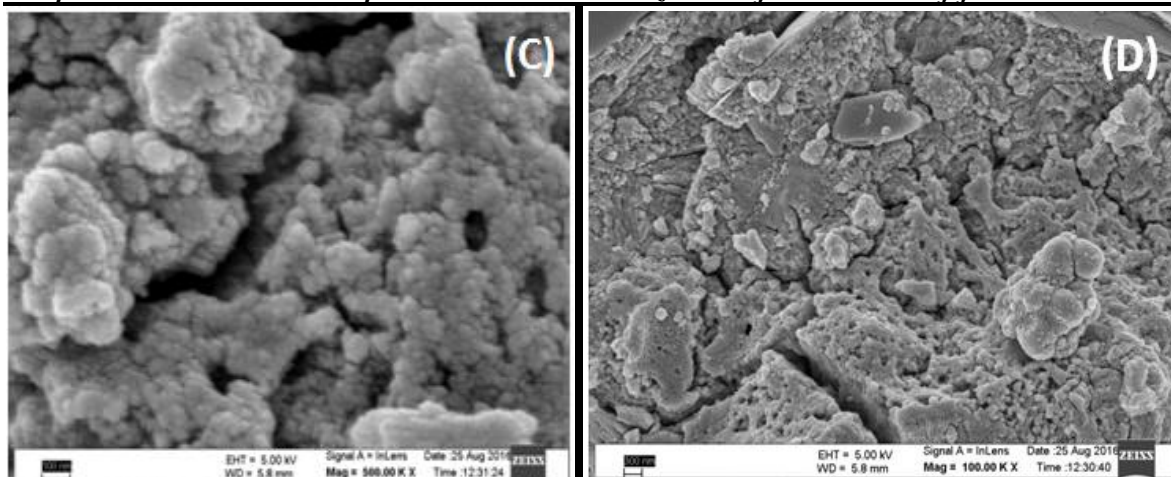
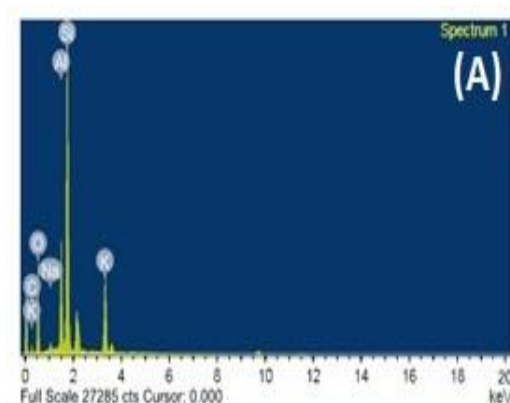


Fig 4.16: (A) &amp; (B) are FESEM images of raw Kanaighat sand (KS)

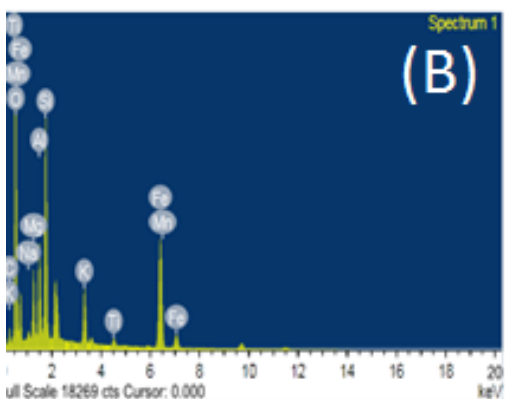




**Fig 4.17:** (A), (B), (C) & (D) are FESEM images of Iron Oxide Coated Sand (IOCS)



Elem...	Weight%	Atomic%
C K	9.22	15.17
O K	42.62	52.61
Na K	0.95	0.82
Al K	8.36	6.12
Si K	28.60	20.11
K K	10.24	5.17
Totals	100.00	



Elem...	Weight%	Atomic%
C K	7.90	13.60
O K	47.18	61.01
Na K	0.77	0.69
Mg K	4.08	3.47
Al K	4.73	3.63
Si K	10.68	7.87
K K	3.45	1.83
Ti K	0.69	0.30
Mn K	0.21	0.08
Fe K	20.31	7.53
Totals	100.00	

**Fig 4.18:** EDX Spectrum of (A) KS and (B) IOCS

From the SEM photograph it was seen that, the surface of the raw sand KS was very rough and edgy as shown in Fig 4.14. However, a small amount of perfectly ovular grains are also available in the heterogenous mixture, while the iron coated sand (IOCS) has a uniformly coated surface. In the FESEM image of IOCS (Fig 4.15), formation of coating of nano iron oxide spheres over sand surface was clearly observed. The surface of the sand was covered with almost spherical swollen looking nano iron oxide particles. The surface elemental

**Chapter-4**      ***Preparation & characterization of adsorbents of fluoride & arsenic***  
characterisation by EDX analysis of both KS and IOCS are shown in Fig 4.16. Fig 4.16 (B) showed the presence of 20.31 weight% iron in IOCS.

#### FTIR Study of KS and IOCS

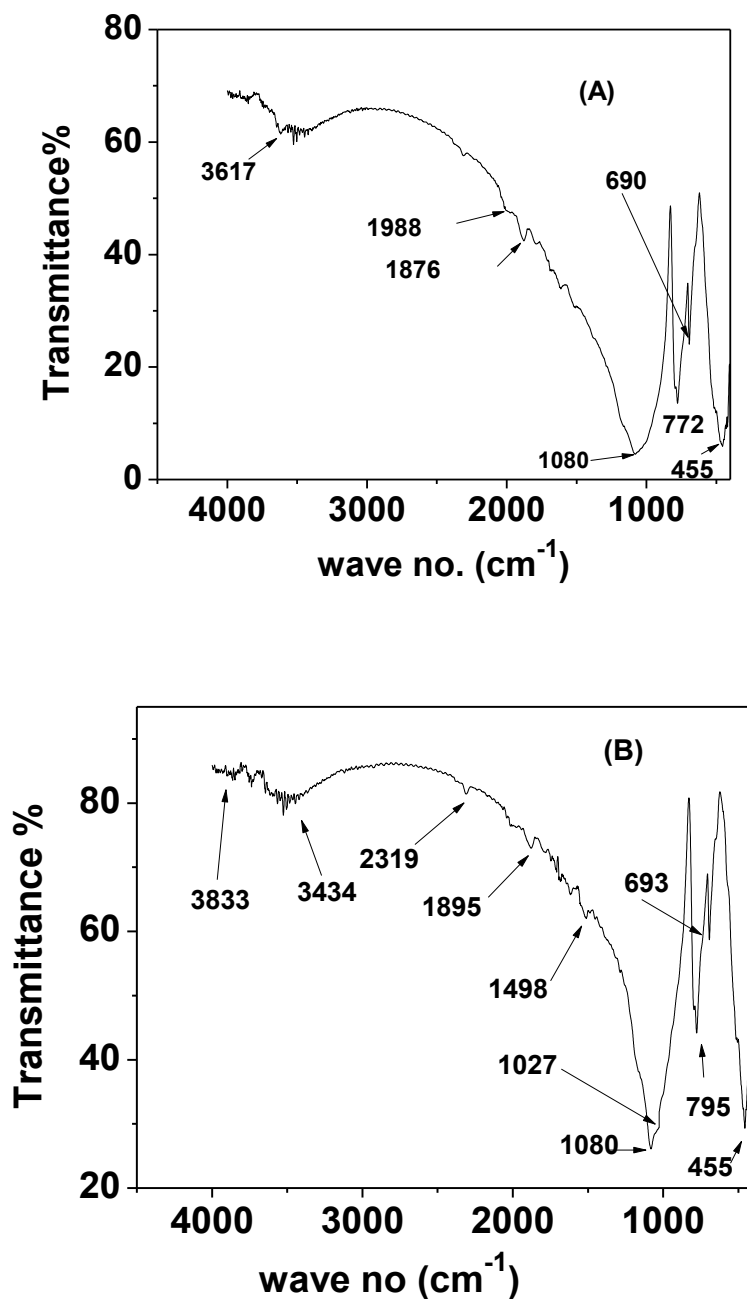


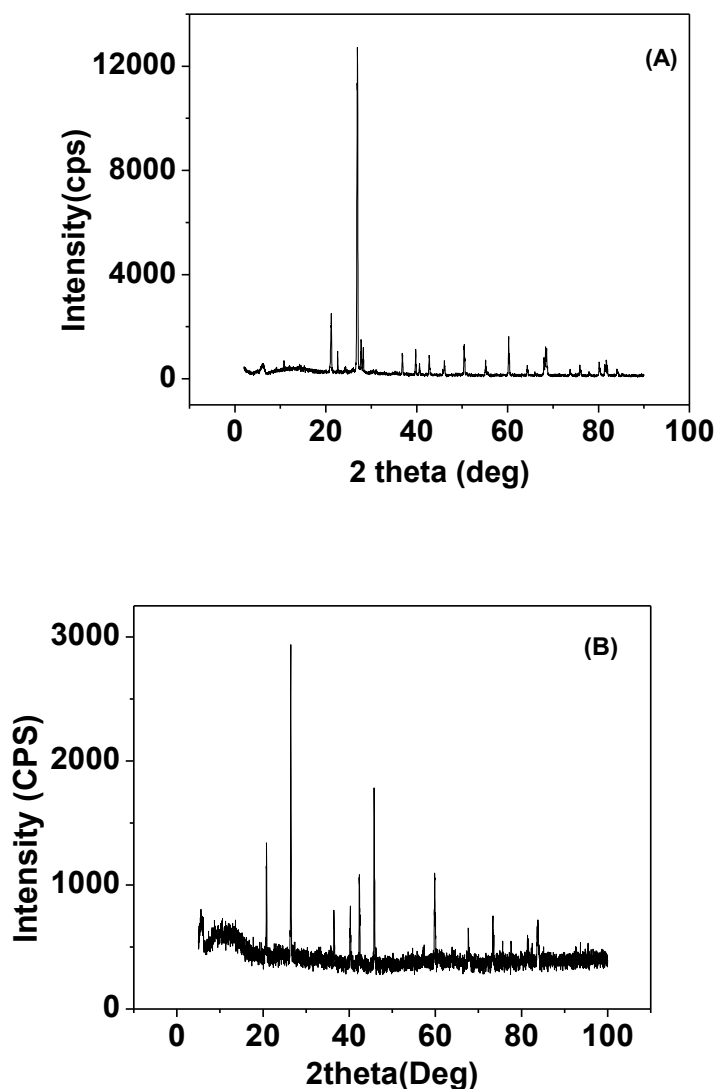
Fig 4.19: FTIR Spectra of (A) KS and (B) IOCS

**Table 4.9: Wave numbers and assignment of the principal bands in the FTIR spectra of KS and IOCS**

Wave Number (cm <sup>-1</sup> )	Assignments
3430	O-H stretching vibrations of SiOH group
1080	Si-O stretching
770	Si-O bend
450-460	Fe-O stretching
690	O-Si-O bend

FTIR spectra Fig.4.17 of KS (A), and IOCS (B) show peaks at 3430–3423 cm<sup>-1</sup> due to -OH stretching vibrations of the SiOH group and at  $\approx 1080$  cm<sup>-1</sup> for Si–O stretching vibration [69]. The band at 450-460 cm<sup>-1</sup> is due to Fe-O stretching vibration. Most of the peaks at 3620, 1100-1000, 770 and 690 cm<sup>-1</sup> can be attributed to the presence of quartz in the sample [70]. The similarity of FTIR spectra of silica and goethite coated silica was also described by Ying et al, [71]. The absorption bands at 795 and 455 cm<sup>-1</sup>, suggests that goethite was coated on the silica surface. The appearance of the 1080 cm<sup>-1</sup> peak in the difference spectrum may indicate enhanced asymmetric stretching of SiO<sub>4</sub>.

## Study of XRD Spectra of KS (A) and IOCS (B)

**Fig 4.20: XRD Spectra of KS (A) and IOCS (B)**

From the XRD analysis (Fig 4.18) formation of orthorhombic FeOOH particles on the sand surface (PDF-26-0792) was confirmed with distinct planes (110, 200 & 310) at 2 theta = 26.99, 36.47 & 59.94 on modification with ferric salt



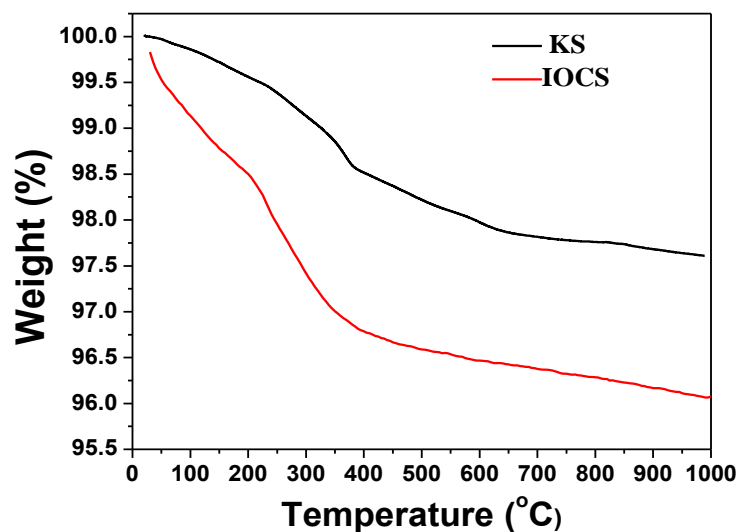


Fig 4.21: TGA curve of KS and IOCS

From TGA it is seen that, the coated iron oxide compound is thermally stable as a very small amount of weight loss is observed which is due to the evaporation of physically bound water [71,72].

#### 4.8 Conclusions

Carbon of banana plant (CBP) is prepared from a highly available indigenous variety of banana plant *Musa balbisiana*. This carbon due to exposure to high alkalinity during alkali extraction undergoes a base mediated surface functionalisation. From the FESEM and FT-IR analysis, it is seen that CBP is a porous adsorbent having oxygen containing surface functional group. Its total surface acidity is 4.35 mmol/g and total surface basicity is 4.40 mmol/g. Since  $pH_{zpc}$  is 9.6, so CBP can be used as adsorbent for both fluoride and arsenic from aqueous solution at below pH 9.6, i.e., within the pH range of drinking water.

The Kanaighat Sand (KS) having 90% silica had very rough and edgy surface; but synthesized iron oxide coated sand no such edgy rough surface. The presence of nano sized ovular grains of iron oxide on the sand surface of KS is very distinct in the FESEM image of IOCS. As zero point charge of IOCS is 7.8, so IOCS can be used as adsorbent for both fluoride and arsenic from aqueous solution at below pH 7.8.

- [1] Mohammad-Khah A., and Ansari R. (2009) Activated Charcoal: Preparation, characterization and Applications : A review article International Journal of ChemTech. 1(4) 859-864, 2009.
- [2] Alhamed Y.A. (2006) Activated carbon from Dates' stone by  $ZnCl_2$  activation. Eng Sci 17:75–98.
- [3] Prahas D., Kartika Y., Indraswati N. and Ismadji S. (2008) Activated carbon from jackfruit peel waste by  $H_3PO_4$  chemical activation: Pore structure and surface chemistry characterization, Chemical Engineering Journal. 140, 32–42.
- [4] Sivarajasekar N., and Baskar R. (2015) Biosorption of basic violet 10 onto activated Gossypium hirsutum seeds: Batch and fixed-bed column studies. Chinese Journal of Chemical Engineering. 23 (10), 1610-1619.
- [5] Mukherjee S., Kumar S., Misra A.K., and Acharya P.C. (2006) Removal of aqueous nickel (II) using laterite as a low-cost adsorbent. Water Environ Res. 78:2268–2275.
- [6] Bhatnagar A., and Minocha A. (2006) Conventional and non-conventional adsorbents for removal of pollutants from water - a review. Indian J.Chem. Technol. 13:203–217.
- [7] Ioannidou O., and Zabaniotou A. (2007) Agricultural residues as precursors for activated carbon production - a review. Renew Sustain Energy Rev. 11:1966–2005.
- [8] Gomez-Serrano V., Macias-Garcia A., and Espinosa-Mansilla. (1998) Adsorption of  $Hg^{2+}$ ,  $Cd^{2+}$  and  $Pb^{2+}$  from aqueous solution on heat-treated and sulphurized activated carbon, Water Res. 32(1), 1-4.
- [9] Bansal R.C., Donet J.B., and Stoeckli F. (1988) Active Carbon. Marcel Dekker: New York. ISBN: 0-8247-7842-1.
- [10] Kairvelu K., Thamaraiselvi K., and Namazivayam C. (2001) Removal of heavy metals from industrial wastewaters by adsorption onto activated carbon prepared from agricultural solid waste. Bioresour. Technol. 76(1), 63-65.
- [11] Ansari R., and Sadegh M. (2007) Application of Activated Carbon for Removal of Arsenic ions from aqueous solutions. E- Journal of chemistry. 4(1), 103-108.
- [12] Abe I., Iwasaki S., Tokimoto T., Kawasaki N., Nakamura T., and Tanada S. (2004) J. Colloid Interface Sci. 275, 35.
- [13] Olivares-Marin C.M., Gonzalez A.F., Garcia V.M., and Serrano G. (2006) Preparation of activated carbon from cherry stones by chemical activation with  $ZnCl_2$ . Appl Surf Sci. 252:5967-5971.

- [14] Konoshita K. (1988) Carbon, electrochemical and physical properties. John Wiley & Sons, Chichester, New York, Brisbane, Toronto 1988. 533 Seiten. <https://doi.org/10.1002/bbpc.198800269>.
- [15] Lopez-Ramon M.V., Stoeckli F., Moreno-Castilla C., and Carrasco-Marin F. (1999) On the characterization of acidic and basic surface sites on carbons by various techniques. Carbon. 37: 1215-1221.
- [16] Viswanathn G., Jaswanth A., Gopalakrishnan S., Ilango, S.S., and Aditya G. (2009) Determining the optimal fluoride concentration in drinking water for fluoride endemic regions in South India. Sci. Total Environ. 407, 5298–5307.
- [17] Chidambaram S., Ramanathan A.L., and Vasudevan S. (2003) Fluoride removal studies in water using natural materials. Water SA. 29:339-343.
- [18] Saikia J. (2019) Synthesis and coating of nano particle loaded carbon on ceramic barriers prepared from local resources for treatment of contaminated water - Thesis, CSIR-NEIST Jorhat.
- [19] Laine J., Calafat A., and Labady M. (1989) Preparation and characterization of activated carbons from coconut shell impregnated with phosphoric acid. Carbon. 27(2),191-195.
- [20] Dąbrowski A. (2001) Adsorption from theory to practice. Advances in Colloid and Interface Science. 93, 135-224.
- [21] Hesas R.H., Niya A.A., Daud W.M.W., and Sahu J.N. (2013) Preparation and characterization of activated carbon from apple waste by microwave-assisted phosphoric acid activation: application in methylene blue adsorption. Bio Resources. 8(2):2950-2966.
- [22] Pongener C., Kibami D., Rao K.S., Goswamee R.L., and Sinha D. (2015) Synthesis and Characterization of Activated Carbon from the Biowaste of the Plant Manihot Esculenta. Chemical Science Transactions. 4(1):59-68.
- [23] Singh P., Raizada P., Pathania D., Sharma G., and Sharma P. (2013) Microwave induced KOH activation of guava peel carbon as an adsorbent for congo red dye removal from aqueous phase. Indian Journal of Chemical Technology. 20:305-311.
- [24] Ahiduzzaman Md., Islam A.K.M.S. (2016) Preparation of porous bio-char and activated Carbon from rice husk by leaching ash and chemical activation. Springer plus 5(1):1248.
- [25] Deng H., Li G., Yang H., and Tang J. (2010) Preparation of activated carbons from

- cotton stalk by microwave assisted KOH and K<sub>2</sub>CO<sub>3</sub> activation. Chem Eng J. 163:373–381.
- [26] Zhang G., Zhang L., Deng H., and Sun P. (2011) Preparation and characterization of sodium carboxymethyl cellulose from cotton stalk using microwave heating. J Chem Technol Biotechnol. 86:584–589.
- [27] Marsh H., and Rodriguez-Reinoso F. (2006) Activated carbon, Elsevier Science & Technology Books, Amsterdam.
- [28] Guo J., and Lua A.C. (2000) Preparation of activated carbons from oil-palm-stone chars by microwave induced carbon dioxide activation. Carbon. 38(14), 1985-1993.
- [29] Chen W., Sun X.D., Cai Q., and Li H.D. (2007) Facile synthesis of thick ordered mesoporous TiO<sub>2</sub> film for dye-sensitized solar cell use, Electrochemistry Communications. 9, 382-385, DOI: 10.3969/j.issn.0438–1157.2013.09.036.
- [30] Kalita P., and Kandar C.C. (2014) Kolakhar- a traditional herbal soda of Assam, J Adv Pharm Res Biosci. 2(5): 122-123.
- [31] Neog S.R., and Deka D.C. (2013) Salt substitute from banana plant (Musa- balbisiana Colla), Journal of Chemical and Pharmaceutical Research. 5(6):155-159.
- [32] Hemanta M.R., Mane V.K., and Bhagwat A. (2014) Analysis of Traditional Food Additive Kolakhar for its Physico-Chemical Parameters and Antimicrobial Activity, J Food Process Technol. 5:11.
- [33] Debandya M. (2010) Banana and its by product utilization: an overview. Journal of Scientific and Industrial Research. 69: 323-329.
- [34] Hussain A. (2010) In vitro screening of the leaves of musa paradisiaca for anthelmintic activity. The Journal of Animal & Plant Sciences. 20: 5-8.
- [35] Preeti J. (2011) Antibacterial and antioxidant activities of local seeded banana fruits. African Journal of Pharmacy and Pharmacology. 5: 1398-1403.
- [36] Kadirvel K. (2010) Investigations on Anti-Diabetic Medicinal Plants Used by Tribal Inhabitants of Nalamankadai, Chitteri Reserve Forest, Dharmapuri. Ethnobotanical Leaflets. 14: 236-247.
- [37] Arawande J.O., and Komolafe E.A. (2010) Antioxidative Potentials of Banana and Plantain Peel Extracts on Crude Palm Oil. Ethnobotanical Leaflets. 14: 559-569.
- [38] Adinarayana K.P.S., and Babu A.P. (2011) Anti-oxidant activity and cytotoxicity of ethanolic extracts from rhizome of Musa acuminata. Natural Science. 3: 291-294.
- [39] ISO 14688-1: Geotechnical investigation and testing-Identification and classification of soil, 2017[E].

- [40] Fan X., Parker D.J., Smith M.D. Adsorption kinetics of fluoride on low cost materials. Water Res. 2003;37:4929–4937.
- [41] Ground Water Information Booklet (GWIB) Karbi Anglong District, Assam, 2013.
- [42] Ekpete O.A., and Horsfall M. Jr. (2011) Preparation and characterization of activated carbon derived from fluted pumpkin stem waste. Res J Chem Sci. 1(13):10-17.
- [43] Annual book of ASTM standards (2004) Standard test method for moisture in activated carbon. Philadelphia PA, United State of America. ASTM D 2867-2895.
- [44] Annual book of ASTM standards (2003) Standard test method for volatile matter content of activated carbon. Philadelphia PA, United State of America. ASTM D 5832-5895.
- [45] Annual book of ASTM standards (2009) Standard test method for water soluble of activated carbon. Philadelphia PA, United State of America. ASTM D 5029-5098.
- [46] Annual book of ASTM standards (1999) Standard test method for total ash content of activated carbon. Philadelphia PA, United State of America. ASTM D 2866-2894.
- [47] Test Methods for Activated Carbon. (1986) European Council of Chemical Manufacturer's Federations, CFFIC
- [48] Bhomick P. (2019) A study on applications of activated carbon prepared from biomass material. Thesis. Nagaland University.
- [49] Annual book of ASTM standards (2011) Standard test for pH of activated carbon Philadelphia PA, United State of America ASTM D 3838-3850.
- [50] Saikia J., Sarmah S., Ahme T.H., Kalita P.J., and Goswamee, R.L. (2017) Removal of toxic fluoride ion from water using low cost ceramic nodules prepared from some locally available raw materials of Assam, India. Journal of Environmental Chemical Engineering. 5:2488–2497.
- [51] Kosmulski M. (2009). pH dependent surface charging and points of zero charge. IV. Update and new approach. J colloid Interface Sci. 337, 439-448.
- [52] Boehm, H.P., Diehl, E., Heck, W., Sappok, R. (1964) Angew Chem Int Ed, 3(10):669-677.
- [53] Bansal R.C., and Goyal M. (2005) Activated carbon adsorption. CRC Press, New York. <http://dx.doi.org/10.1201/9781420028812>.
- [54] Ahmed M., Marshall W.E., Rao R.M. (2000). Granular activated carbons from agricultural by-products; preparation properties and application in cane sugar refining. Bulletin of Louisiana state university Agricultural centre.

- [55] Okieimen F.E., Okieimen C.O., and Wuana R.A. (2007) Preparation and characterization of activated carbon from rice husks. *J Chem Soc.* 32:126-136.
- [56] Menendez-Diaz J.A., and Martln-Gullonb I. (2006) In: Activated carbon surfaces in environmental remediation, *Interface Sci Technol.* 7.
- [57] Garcia M.D., Garzon F.J.L., and Mendoza M.J.P. (2002) On the Characterization of Chemical Surface Groups of Carbon Materials. *Journal of Colloid and Interface Science.* 2481:16–122.
- [58] Guo Y., and Rockstraw D.A. (2006) Physical and chemical properties of carbons synthesized from xylan, cellulose, and Kraft lignin by H<sub>3</sub>PO<sub>4</sub> activation. *Carbon.* 44:1464–1475.
- [59] Boonamnuavitaya V., Sae-ung S., and Tanthapanichakoon W. (2003) Preparation of activated carbons from coffee residue for the adsorption of formaldehyde. *Sep Purif Technol.* 42:159–168.
- [60] Barkauskas J., Dervinyte M. (2004) An investigation of the functional groups on the surface of activated carbons. *J Serb ChemSoc.* 69(5):363–375.
- [61] Haines P.J. (2002) Principles of Thermal Analysis and Calorimetry. The Royal Society of Chemistry.
- [62] Thirunavukkarasu O.S., Viraraghavan T., and Subramanian K. S. (2002) Arsenic removal from drinking water using ironoxide coated sand. *Water, Air, and Soil Pollution.* 142, 95 –111.
- [63] Saha P.D., Chakraborty S., and Chowdhury S, (2012) Batch and continuous (fixed-bed column) biosorption of crystal violet by *Artocarpus heterophyllus* (jackfruit) leaf powder, *Colloids and Surfaces B: Biointerfaces* 92, 262–270.
- [64] Wan S. L., He F., Wu J. Y., Wan W. B., Gu Y. W., and Gao B. (2016) Rapid and highly selective removal of lead from water using grapheme oxide-hydrated manganese oxide nanocomposites. *Journal of Hazardous Materials.* 314, 32 –40.
- [65] Kalkan N.A., Aksoy S., Aksoy E.A., and Hasirci N. (2012) Preparation of chitosan-coated magnetite nanoparticles and application for immobilization of laccase. *Journal of Applied Polymer Science.* 123, 707 –716.
- [66] Kiczka M., Wiederhold J.G., Frommer J., Voegelin A., Kraemer S.M., Bourdon B., and Kretzschmar R. (2011). Iron speciation and isotope fractionation during silicate weathering and soil formation in an alpine glacier forefield chronosequence. *Geochimica et Cosmochimica Acta.* 75, 5559–5573.

- [67] Cornell R.M., and Schwertmann U. (1996) *The iron oxides*, Weinheim (Germany), VCH Publishers. 573
- [68] Kosmulski M. (2003) A literature survey of the differences between the reported isoelectric points and their discussion. *Colloids and Surfaces A: Physicochemical and Engineering Aspects*. 222, 113 –118.
- [69] Umlong I.M., Das B., Devi R.R., Borah K., Saikia L.B., Raul P. K., and Singh S.B.L. (2012) Defluoridation from aqueous solution using stone dust and activated alumina at a fixed ratio. *Applied Water Science*. 2, 29 –36.
- [70] Shukla S.C. (2008) Development, safety evaluation and comparative studies of low cost adsorbent technology for arsenic removal from drinking water- Thesis, Industrial Toxicology Research Centre, Lucknow, India.
- [71] Ying X., and Lisa A. (2005) Synthesis and characterization of iron oxide-coated silica and its effect on metal adsorption. *Journal of Colloid and Interface Science*. 282, 11 – 19.
- [72] Ford R.G., and Bertsch P.M. (1999) Distinguishing between surface and bulk dehydration-dehydroxylation reactions in synthetic goethites by high-resolution thermogravimetric analysis. *Clays and Clay Minerals*. 47(3), 32–337.
- [73] Borborah K., Borthakur S.K., and Tanti B. (2016) *Musa balbisiana* colla-texonomy, traditional knowledge and economic potentialities of the plant in Assam, India. *Indian Journal of Traditional Knowledge* 15(1), 116-120.

## **CHAPTER - 5**

### **REMOVAL OF FLUORIDE FROM CONTAMINATED WATER BY USING TWO LOCALLY AVAILABLE MODIFIED MATERIALS:**

#### **SECTION A-CBP & SECTION B-IOCS**



Removal of fluoride from water is an important issue. From the literature it was observed (discussed in chapter-3) that, there are different fluoride removal methods like coagulation/precipitation, membrane filtration (reverse osmosis; nanofiltration; electro-dialysis), ion-exchange and adsorption. Although, coagulation/precipitation, membrane filtration and ion-exchange methods can remove fluoride from contaminated water efficiently but due to high expenses and need of skilled operator, these techniques are not effective for common people of developing countries like India. So, adsorption method is considered as suitable and efficient for the removal of fluoride from contaminated water in terms of low cost of the adsorbent, high adsorption capacity and high availability of raw materials of adsorbent.

In chapter 4, two adsorbents were prepared from locally available materials. This chapter is taken for the study of fluoride removal capacity of these two prepared fluoride adsorbents:

1. **Carbon of Banana Plant (CBP).** It was obtained as waste materials at the time of preparation of banana alkali (*Kolkhar*) by Assamese traditional method and taken as an adsorbent for the adsorption of fluoride from contaminated water.
2. **Surface modified “Kanaighat Sand” (IOCS).** This naturally occurring river sand was collected from Kanaighat area of Golaghat district of Assam. A mixture of 2M  $\text{Fe}(\text{NO}_3)_3 \cdot 9\text{H}_2\text{O}$  and 1mL of 10M NaOH solution was used for the iron oxide coating over the surface of sand grain. This iron oxide coated sand is named as IOCS.

## **5.2 Materials and methods**

### **5.2.1 Preparation of standard fluoride stock solution**

By dissolving 2.178 g NaF (Merck, Germany) in double distilled water in a 1000 mL of volumetric flask, 1000 mg  $\text{L}^{-1}$  of a standard fluoride solution was prepared. The solution was further diluted to 100 mg  $\text{L}^{-1}$ . All solutions for adsorption and analysis were prepared by appropriate dilution of the prepared fluoride stock solution of 100 mg  $\text{L}^{-1}$ .

### **5.2.2 Determination of fluoride concentration**

Orion 4 star (pH/ISE) selective ion electrode was utilized for the determination of concentration of fluoride ion. The fluoride sensitive electrode was calibrated by using 1, 5, 10, 50 and 100 mg/L fluoride solutions. TISAB III (Total Ionic Strength Adjustment Buffer) was used as a buffer for fluoride measurement. This is a ready to use bottled solution added for

adjusting the ionic strength of fluoride bearing aqueous solutions and is manufactured by various reputed chemical firms. It also complexes with ions like  $\text{Fe}^{3+}$  so that they don't harm or affect the estimation of fluoride by Ion Sensitive Electrode. The results of ISE were further cross checked regularly by Ion Chromatography (Model 881 Compact IC pro Metrohm and column Metrosep C4-150/4.0).

### **5.2.3 Batch mode adsorption study**

All experiments were carried out by batch adsorption method. The effect of adsorbent dose, agitation time, pH, competitive anions and temperature on the efficiency of fluoride removal of CBP and IOCS were investigated at temperature 30°C by using 25 mL of fluoride solutions in conical flasks. After shaking at 180 RPM, the suspensions of each conical flask were allowed to settle down and filtered using a Whatman 42 grade filter paper. The filtrate was collected and subjected to fluoride estimation by using ion selective electrode. Percentage removal (E) and removal capacity ( $q_e$ ) was calculated using equation (1) and (2) from the chapter 1 respectively.

## **5.3 Results and discussion**

### **SECTION A: CBP AS AN ADSORBENT**

#### **5.3.A.1 Results and discussions of fluoride adsorption studies using CBP**

##### **a) Effect of adsorbent dose**

The effect of various amount of adsorbent on defluoridation was studied by taking initial fluoride concentration of 5.00 mg/L and at pH 6.1 with different adsorbent doses of 0.05, 0.1, 0.15, 0.2, 0.25, 0.35, 0.4 and 0.45 g respectively. Fig.5 reveals that the percentage removal of fluoride increases with increasing amount of CBP and 69% of fluoride was adsorbed with 0.45 g in 25 mL of solution in 3 hours shaking and at temperature 30°C. The increase in fluoride removal is attributed to the increase in surface area and the availability of more active binding sites with the increase of amount of adsorbent [1]. Since the percentage of fluoride removal capacity of CBP is increased from 20.22%-66.4% at a constant rate of increase of adsorbents from 0.05 g to 0.35 g CBP and begins to start a declining trend of the rate of removal percentage when the amount of CBP reached 0.45 g. Therefore, 0.35 g was chosen as the optimum value of the adsorbent CBP for maximum removal of fluoride.

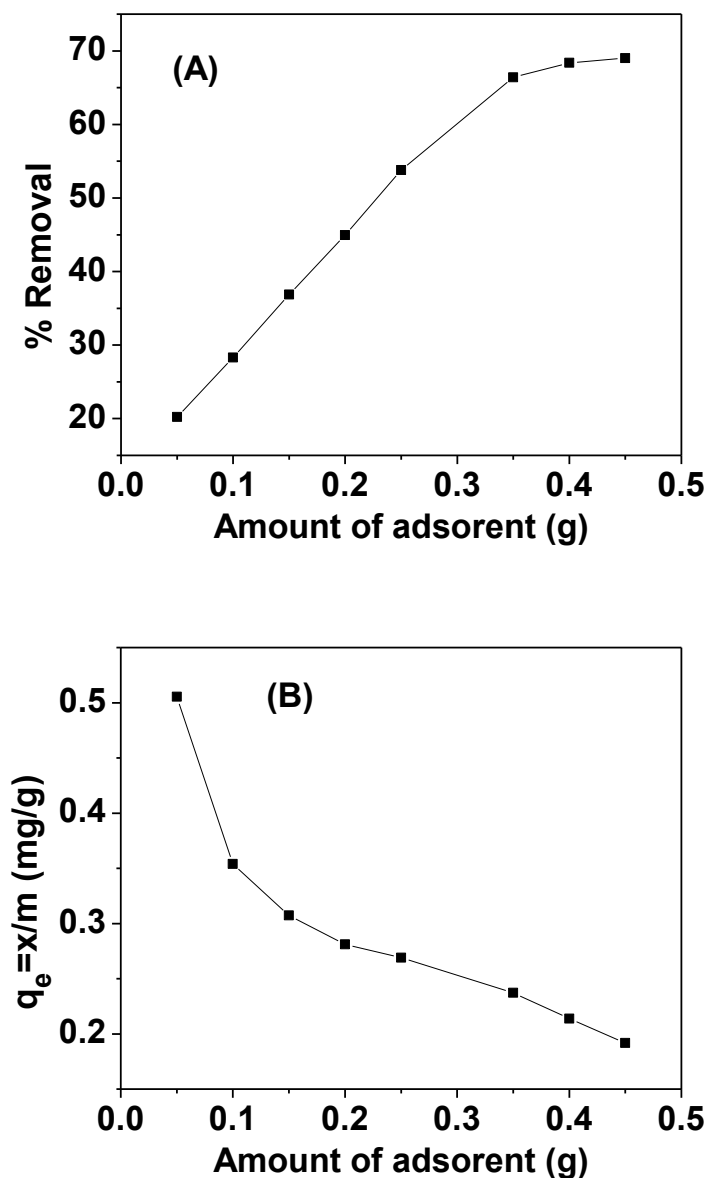


**Fig 5.1: Effect of adsorbents dose on the (A) percent removal of fluoride (B) removal capacity ( $q_e$ ) at 30°C at the pH of 6.1 and 3 hours of stirring.**

#### **b) Effect of initial concentration of fluoride solution**

The initial concentration of fluoride solution affect on adsorption process. A given amount of CBP can adsorb a certain amount of fluoride to establish equilibrium. Fluoride solutions of different concentration (3.00-50.00 mg/L) with 0.35 g of CBP were taken in a set of experimental flasks. From the Fig 5.2, highest % removal by CBP showed at 5.35 mg/L fluoride solution and gradually decreases with increasing fluoride concentration. This is because at higher concentration the available sites on the surface of adsorbent for adsorption

become fewer in comparison to lower concentration. Removal capacity  $q_e$ , in mg/g increases gradually with increasing concentration of adsorbate. Since, maximum fluoride removal percentage is shown by 5.35 mg/L fluoride solution, so the optimum fluoride concentration is chosen as 5.00 mg/L to carry out the further experiments.

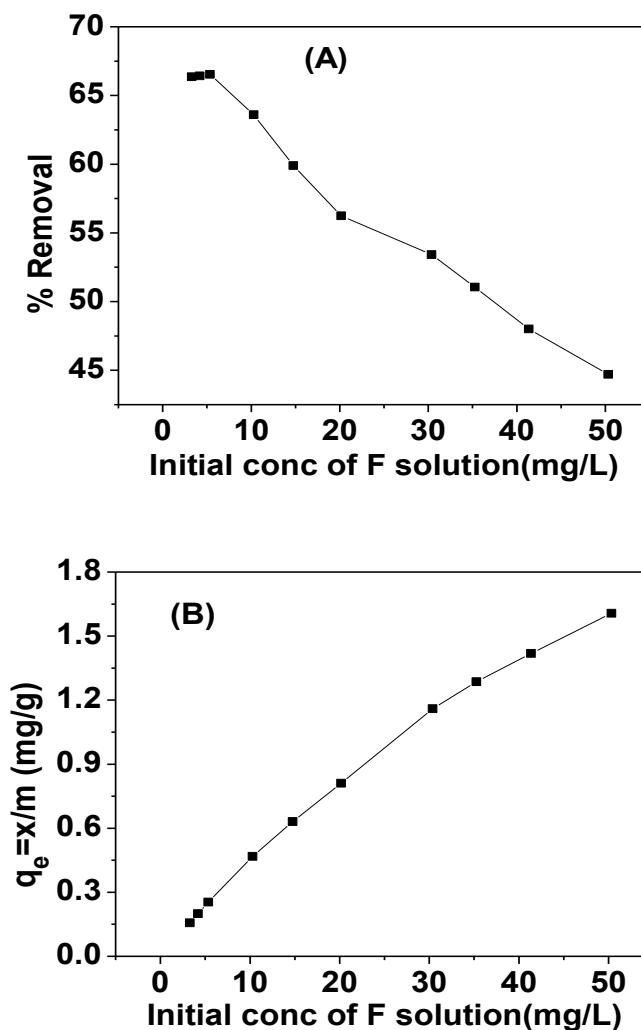


**Fig 5.2: Effect of initial concentration of fluoride solution on defluoridation by CBP at 30°C in a pH of 6.1 with 3 hours stirring**

### c) Effect of pH of fluoride solution on defluoridation

Adsorption of a species from aqueous solution is influenced by pH of the solution. The surface properties of carbon are affected by pH of the solution [2,3]. Because pH changes the charges of surface functional groups of adsorbent and change the ionization and species of the adsorbate [4]. The pH affect on fluoride removal percentage was studied by using 0.35 g of adsorbent in each 25 mL of 5.00 mg/L fluoride solution of pH range 3-10.8. Fig.5.3 shows

that the fluoride adsorption capacity of CBP decreases with increasing pH. The maximum fluoride removal capacity of the adsorbent CBP is in acidic conditions, which may be due to the formation of weak hydrofluoric acid or combined effect of both chemical and electrostatic interaction between the oxide surface of the adsorbent and fluoride ion. Decrease of fluoride removal capacity in alkaline medium can be explained due to competition of fluoride and hydroxide ions on the active sites of CBP [5,6].

Since maximum fluoride adsorption capacity is shown by CBP adsorbent at highly acidic medium, it is practically not meaningful to carry out the experiment in that condition as in the event of a practical process such a pH is not a suitable. So the pH value 6.1, which is original pH of the fluoride solution is taken as optimum pH.

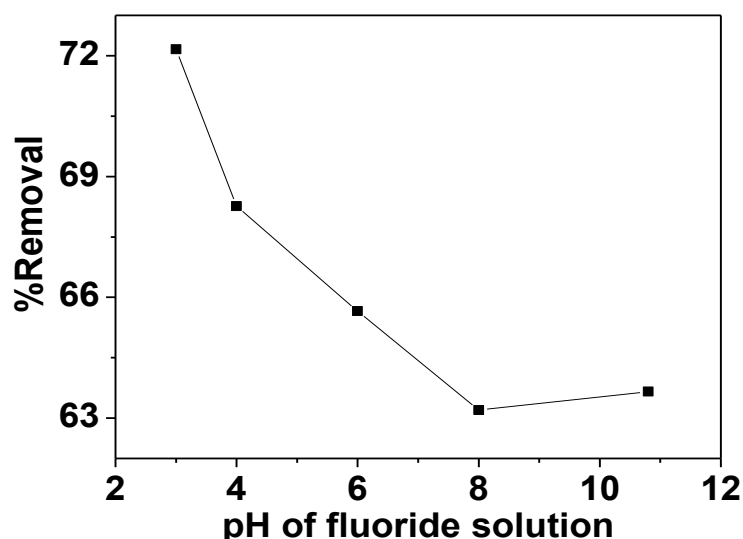
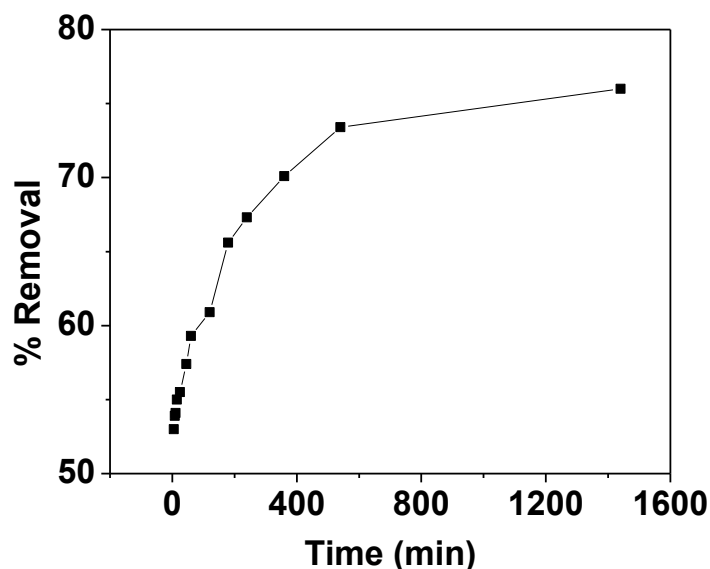


Fig 5.3: Graph of effect of pH of fluoride solution on defluoridation by CBP

#### d) Effect of contact time

The contact time between adsorbent surface and adsorbate affect on adsorption process. A given amount of CBP can adsorb a certain amount of fluoride at a given time to establish equilibrium. For the investigation of maximum adsorption efficiency, effect of contact time between fluoride solution and adsorbent CBP was studied. This experiment was carried out at pH 6 by taking 0.35 g adsorbent per 25 mL of 5 mg/L fluoride solution at different contact times from 5-1440 min. Fig. 5.4 shows that percentage of fluoride removal efficiency rapidly increases with increasing contact time up to 180 minute and then rate of

increasing of adsorption decreases gradually. The fast adsorption rate at the initial stage may be explained by large availability of the number of active binding sites on the adsorbent surface and after a lapse of time, due to repulsion between the adsorbed solute species on the surface of the adsorbent and the bulk phase, adsorption i.e., percent removal efficiency decreases. Therefore, 180 minute is chosen as the optimum time for carrying out of the experiment.



**Fig 5.4 :Effect of contact time on the adsorption of fluoride at 30°C in a pH of 6.1 with adsorbent dose of 14 g/L**

#### **e) Adsorption isotherms study**

An adsorption isotherm is an equation which represents the relation between the amount of adsorbate adsorbed on the surface of the adsorbent and the equilibrium concentration of the adsorbate in the solution at a given temperature. Adsorption isotherm study gives information on the efficiency of the adsorbent at a particular temperature. In this study spiked fluoride solution of different concentration (3-50 mg/L and pH=6.1) were taken and stirred for 3 hours with 0.35 g adsorbent CBP at constant temperature 30°C. Three most commonly used Langmuir, Freundlich and Temkin adsorption isotherm models were taken to study the adsorption occurring in the experimental set up.

**Langmuir adsorption isotherm**

Langmuir adsorption isotherm explains quantitatively the formation of monolayer on the surface of the adsorbent containing a large number of identical sites. From the slope and intercept of the linear plot of  $C_e/q_e$  against  $C_e$ , (from equation 7 of chapter 1) in Fig. 5.5(A) the Langmuir maximum adsorption capacity  $q_m$  and equilibrium constant  $b$  are calculated. The separation factor or equilibrium parameter  $R_L$  also calculated from the equation 8 of chapter 1.

**Freundlich adsorption isotherm**

Freundlich isotherm generally explains the adsorption behaviour of heterogeneous surface. Freundlich adsorption constant i.e., the adsorption capacity of adsorbent  $K_f$  and intensity of adsorption  $n$  are calculated (from equation 9 of chapter 1) from the linear plot of  $\log q_e$  versus  $\log C_e$ , in Fig. 5.5 (B).

**Temkin adsorption isotherm**

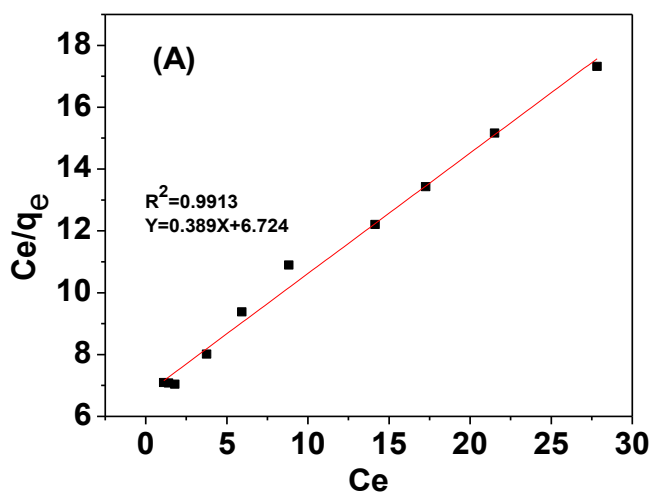
Temkin and Pyzhev considered the effects of indirect adsorbent-adsorbate interactions on adsorption isotherms and assumed that the free energy of adsorption is a function of the surface coverage [7,8,9]. The Temkin isotherm constant  $A_T$  (L/g) and  $B_T$  (where  $B_T = RT/b_T$ , where  $b_T$  is the Temkin constant and  $R$  is the gas constant) are calculated from the intercept and the slope of the plot of  $q_e$  against  $\ln C_e$  from Fig 5.5(C) which is drawn with the help of equation 10 of chapter 1.

The corresponding Langmuir, Freundlich and Temkin parameters along with correlation coefficients are given in Table 5.1. From the table, it is seen that the Langmuir maximum adsorption capacity  $q_m$  is  $2.57 \text{ mg g}^{-1}$  and the equilibrium constant  $b$  is  $0.06 \text{ L mg}^{-1}$ . The value of dimensionless constant separation factor or equilibrium parameter  $R_L$  gives the acceptability of the Langmuir model. In our study, the value of Langmuir isotherm, the separation factor or equilibrium parameter,  $R_L$  lay in the range  $0 < R_L < 1$  (in Fig. 5.5(D)), indicates that the fluoride adsorption on CBP is favourable under the conditions of experiments and takes place as monolayer adsorption on the surface that is homogenous in adsorption affinity [10]. The value of Freundlich adsorption constant i.e., the adsorption capacity of adsorbent  $K_f$  is  $0.16 \text{ mg}^{1-1/n} \text{ L}^{1/n} \text{ g}^{-1}$ . The value of  $n$  ( $=1.4$ ) at equilibrium lies in between 1 and 10 indicates the favourable adsorption. From the correlation coefficients ( $R^2$ ), it can be said that, Temkin isotherm model of adsorption may also be significant in this case. The order of favourability of fluoride adsorption on CBP, in terms of  $R^2$  is Freundlich

( $R^2=0.9915$ ) > Langmuir ( $R^2=0.9913$ ) > Temkin ( $R^2=0.9578$ ). It can be concluded that the Freundlich isotherm model is more fitted than the Langmuir isotherm model for the experimental data because of the highest value of correlation coefficient. Based upon the Langmuir model, the maximum fluoride adsorption capacity of CBP is 2.57 mg/g.

**Table 5.1: Langmuir, Freundlich, and Temkin parameters along with correlation coefficients**

Langmuir Isotherm		Freundlich Isotherm		Temkin Isotherm	
b (Lmg <sup>-1</sup> )	0.06	K <sub>f</sub> (mg <sup>1-1/n</sup> L <sup>1/n</sup> g <sup>-1</sup> )	0.16	A <sub>T</sub> (L g <sup>-1</sup> )	0.97
q <sub>m</sub> (mg g <sup>-1</sup> )	2.57	N	1.4	B <sub>T</sub> (Jmol <sup>-1</sup> )	0.45
R <sup>2</sup>	0.9913	R <sup>2</sup>	0.9915	R <sup>2</sup>	0.957
R <sub>L</sub>	0.258-0.841				





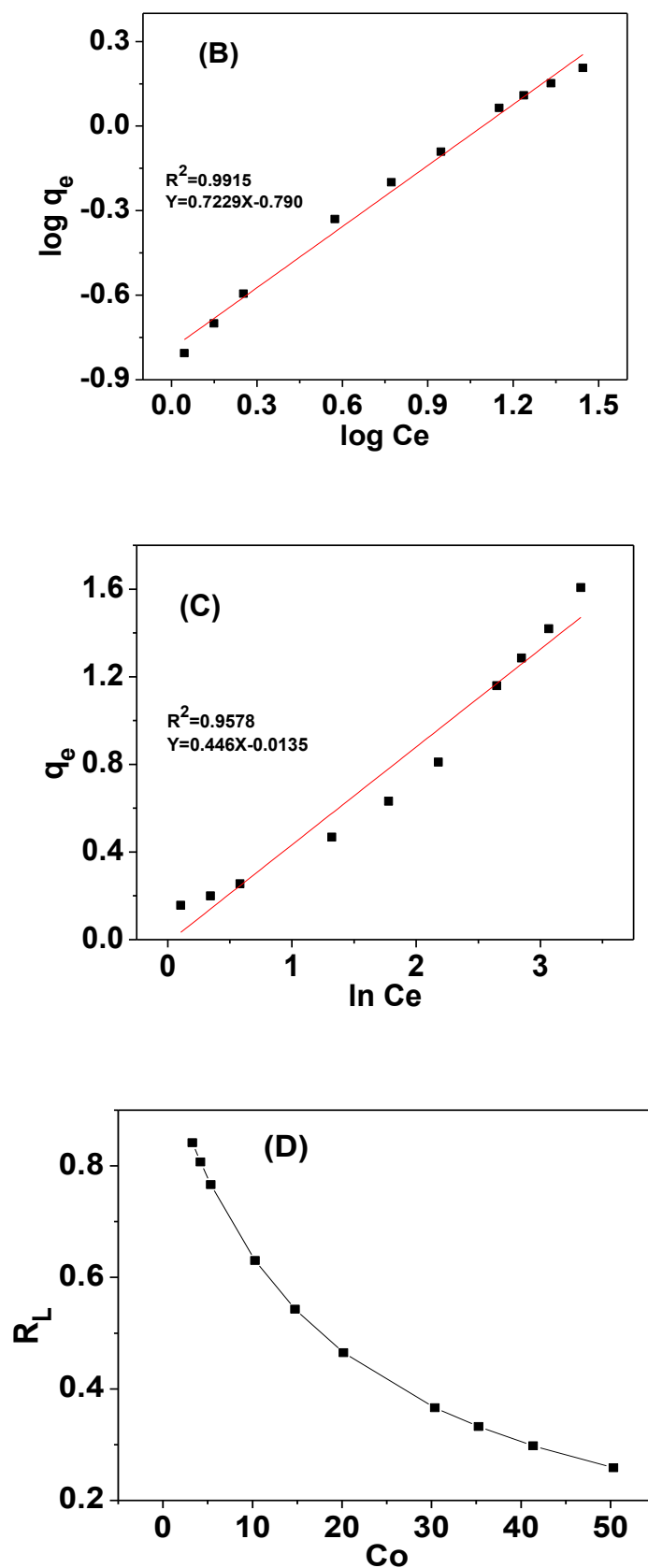


Fig 5.5: (A) Langmuir, (B) Freundlich, (C) Temkin adsorption isotherm of CBP and (D) graph of  $R_L$  vs  $C_0$

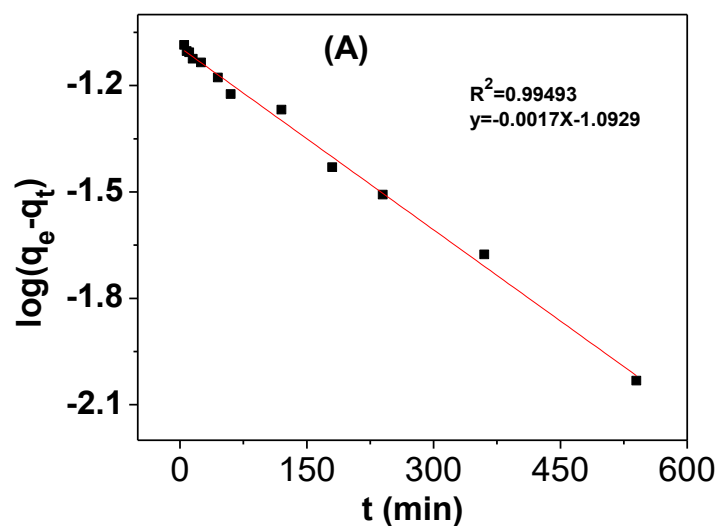
**f) Adsorption Kinetic Study**

Kinetics studies give significant evidence to understand the adsorption dynamics. In this study pseudo first order kinetics, pseudo second order kinetics, intra particle diffusion and Elovich models (equations 3, 4, 5 & 6 of chapter 1) were used to interpret the kinetics of fluoride adsorption on CBP. The adsorption reaction was carried out at optimum conditions.

Adsorption kinetic model parameters are tabulated in Table 5.2. Pseudo first order rate constant,  $k_1$  ( $=0.004 \text{ min}^{-1}$ ) and first order adsorption capacity i.e amount of adsorption at equilibrium  $q_e$  ( $=0.08 \text{ cal mg/g}$ ) were calculated from the Fig. 5.6(A). The low value of  $k_1$  indicates the slow rate of adsorption. Second order rate constant,  $k_2$  ( $=0.23 \text{ g mg}^{-1} \text{ min}^{-1}$ ) and second order adsorption capacity,  $q_e$  ( $=0.27 \text{ cal mg/g}$ ) were determined by plotting  $t/q_t$  against  $t$  in Fig. 5.6(B). Since, larger the  $k_2$  value slower is the adsorption rate, so from the calculated value of  $k_2=0.23 \text{ g mg}^{-1} \text{ min}^{-1}$  indicates higher rate of adsorption. In case if Elovich kinetic model, from the plot of  $q_t$  versus  $\ln t$  in Fig. 5.6(C) the value of initial adsorption rate  $a$  ( $=305.57 \text{ mg g}^{-1} \text{ min}^{-1}$ ) and the desorption constant  $b$  ( $=64.1 \text{ g/mg}$ ) were calculated. In Intra Particle Diffusion model, the rate of intra particle diffusion controls adsorption kinetics. From the plot of  $q_t$  versus  $t^{1/2}$  in Fig. 5.6(d),  $k_d$  ( $=0.003 \text{ mg g}^{-1} \text{ min}^{-1/2}$ ) and  $C$  ( $=0.18$ ) were calculated. Intra particle diffusion constant,  $k_d$  is obtained as  $0.003 \text{ mg g}^{-1} \text{ min}^{-1/2}$ , which means a lesser significance of this process. Since, from the Fig. 5.6(A, B, C and D) it is seen that,  $R^2$  values of all kinetic models are almost near to 1. However, the pseudo second order kinetic model was the best fitting model ( $R^2=0.999$ ) for fluoride adsorption on CBP. The value of chi-square ( $\chi^2$ ) was found to be least for pseudo second order kinetic model, which also again prove the best fitting of pseudo second order kinetic model. It was also observed that there was a linear relationship between  $q_t$  and  $t^{1/2}$  as evidenced by the  $R^2$  value. Thus, from the table, we can conclude that there may be other processes operating simultaneously with pseudo second order kinetics, controls the rate of adsorption [11,12].

**Table 5.2: Comparison of pseudo first order, pseudo second order, intra particle diffusion and Elovich model rate constants and calculated  $q_e$  values using CBP as adsorbent**

Pseudo first order		Pseudo second order		Elovich		Intraparticle diffusion	
$k_1$ ( $\text{min}^{-1}$ )	0.004	$k_2$ ( $\text{g mg}^{-1} \text{min}^{-1}$ )	0.23	$b$ ( $\text{g mg}^{-1}$ )	64.1	$k_d$ ( $\text{mg g}^{-1} \text{min}^{-1/2}$ )	0.003
$q_{e\text{cal}}$ ( $\text{mg g}^{-1}$ )	0.08	$q_{e\text{cal}}$ ( $\text{mg g}^{-1}$ )	0.27	$a$ ( $\text{mg g}^{-1} \text{min}^{-1}$ )	305.57	C	0.18
$R^2$	0.995	$R^2$	0.999	$R^2$	0.938	$R^2$	0.9905
$\chi^2$	$4.29 \times 10^{-4}$	$\chi^2$	$3.67 \times 10^{-6}$	$\chi^2$	$5.09 \times 10^{-5}$	$\chi^2$	$8.09 \times 10^{-5}$



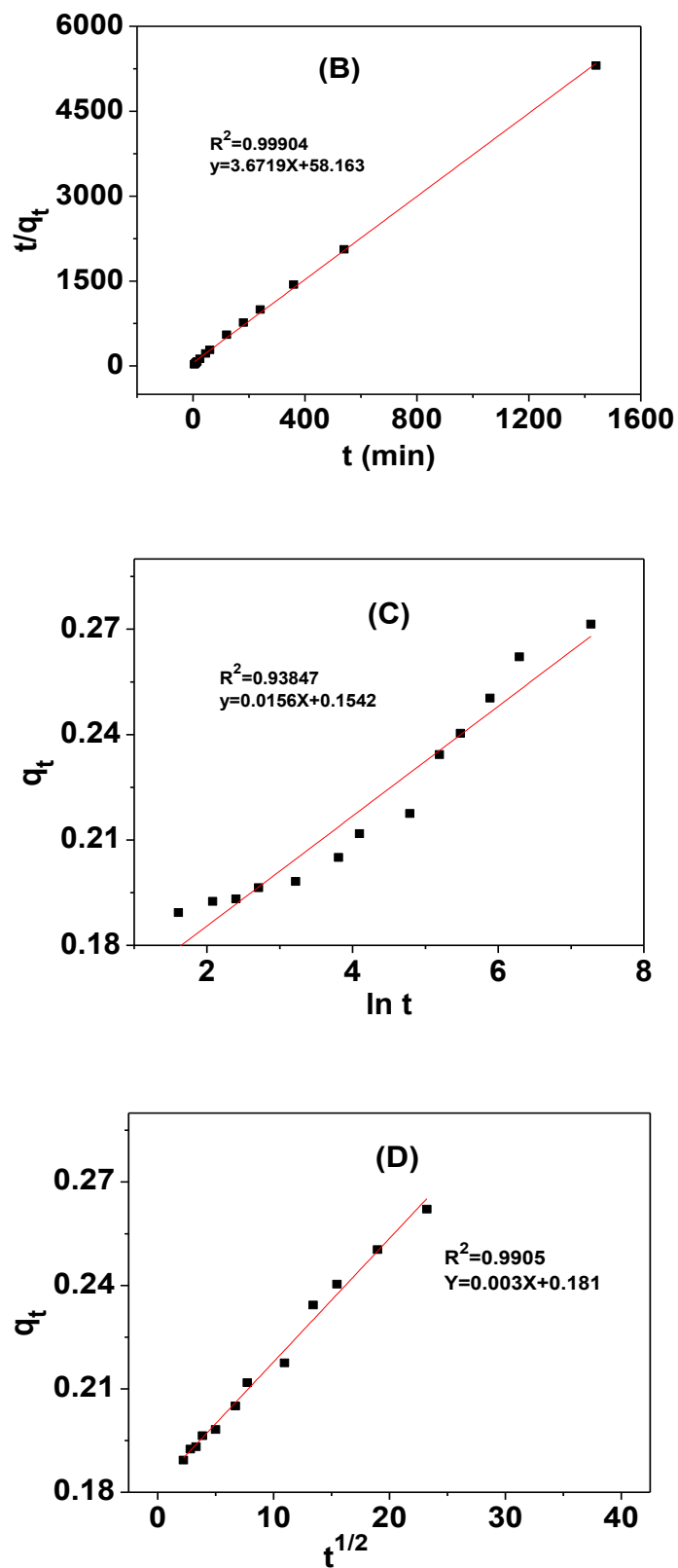
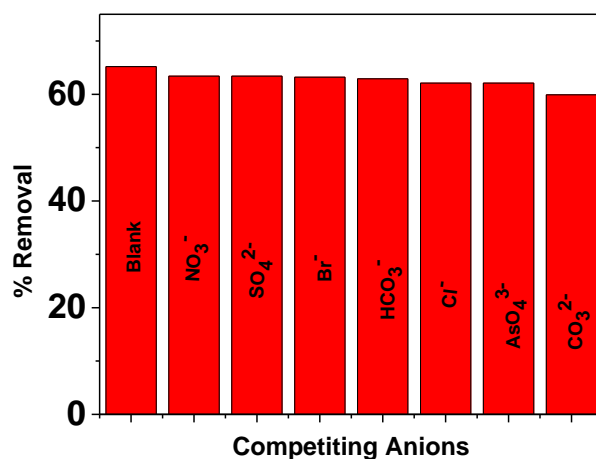


Fig 5.6: Graph (A), (B), (C) and (D) are the psuedo first order, psuedo second order, Elovich model and intra particle diffusion of kinetics study

**g) Effect of competitive anions on defluoridation**

In general, sulphate, chloride, bromide, nitrate, phosphate, carbonate and bicarbonate are present in water. These anions compete with fluoride ions during adsorption. Since, ground water in many places are simultaneously contaminated by both Arsenic and Fluoride e.g. certain wells in Barua Gaon area of Golaghat district of Assam, India as found by the present group of investigators in a separate study, so the effect of the arsenate ion with other anions on the removal of fluoride was also investigated at the temperature 30°C and at 180 RPM by batch mode experiment and using 5.00 mg/L fluoride synthetic solution in the presence of 50 mg/L each co-existing anion. It has been observed that nitrate ions have lowest negative effect on the removal of fluoride (Fig.11). The decreasing order of effect of co-ions with respect to fluoride adsorption capacity is as given below

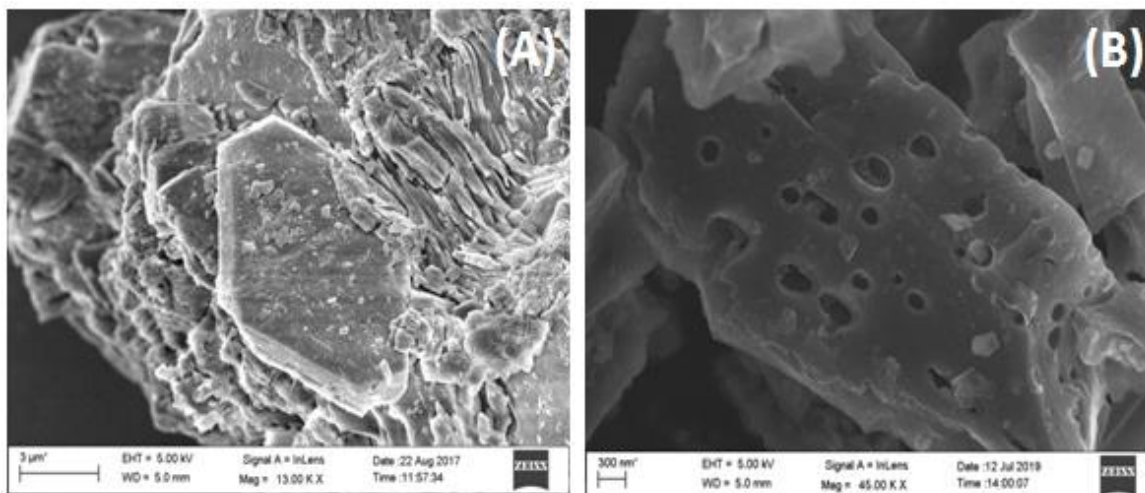
Nitrate < sulphate < bromide < bicarbonate < chloride < arsenate < carbonate.



**Fig 5.7: Bar diagram showing the effect of competitive anions on defluoridation**

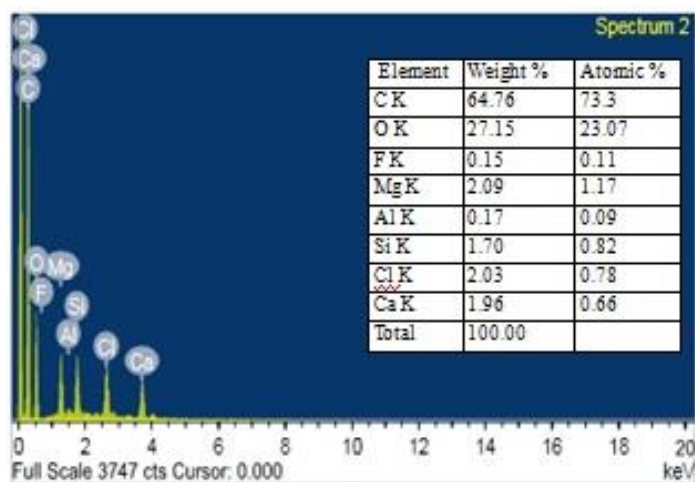
## 5.3.A.2: Studies on CBP after adsorption of fluoride

## a) Study of FESEM images &amp; EDX spectra



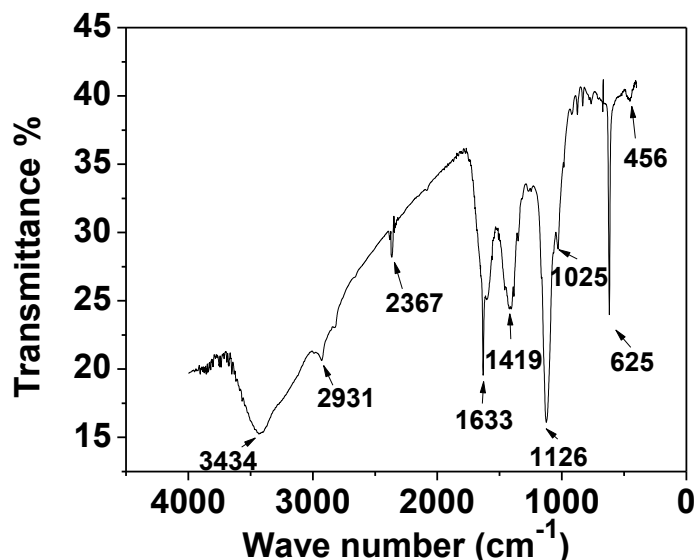
**Fig 5.8: Various magnification FESEM photograph (A & B) of CBP after adsorption of fluoride**

After fluoride adsorption, the SEM images of CBP in different magnification were taken and shown in the Fig 5.8. It is seen that, the surface of CBP after adsorption of fluoride is different from the SEM images of raw CBP (Fig 4.9 of chapter 4). This significant deformation in the structural organization of the CBP is due to adsorption of fluoride in its surface. This adsorption behavior is further supported by EDX analysis and FTIR study.



**Fig 5.9: EDX spectra of CBP after adsorption of fluoride**

Thus, the EDX analysis provides the direct evidence for the adsorption of fluoride on the surface of the adsorbent CBP.

**b) Study of FT-IR spectra**

**Fig 5.10: FT-IR spectra of CBP after adsorption of fluoride**

After adsorption of fluoride, to study the interaction between fluoride ion and the active sites present on the surface of CBP, FTIR spectroscopy was carried out and the spectra is given in the Fig 5.10. A close examination of the Fig 4.11 reveals the slight shift of asymmetric bending vibration, asymmetric stretching vibration of C-H of alkene from 1412 cm<sup>-1</sup> (Fig 4.11 from chapter 4) and 2928 cm<sup>-1</sup> to 1419 cm<sup>-1</sup> and 2931 cm<sup>-1</sup> respectively. The disappearance of C=O stretching vibration frequency (1582 cm<sup>-1</sup> in Fig 4.11, chapter 4) in the FTIR spectra of CBP after adsorption of fluoride shows that fluoride ion binds with carboxylate group.

So from the above SEM images, EDX spectra and FT-IR spectrum is attributed to the adsorption of fluoride on the adsorbent carbon of banana plant (CBP).

**5.3.A.3: Mechanism of adsorption of fluoride**

The carbon of banana plant (CBP) ash is naturally functionalized by -OH, -COOH, and -C=O groups during the process of edible alkali extraction. The mechanism of fluoride adsorption of CBP can be explained with the help of description of Gandhi et al. [13]. The hetero atoms O and H undergo protonation and they release a lone pairs of electrons. These lone pair electrons develop a positive charge and they participate in the adsorption of fluoride.

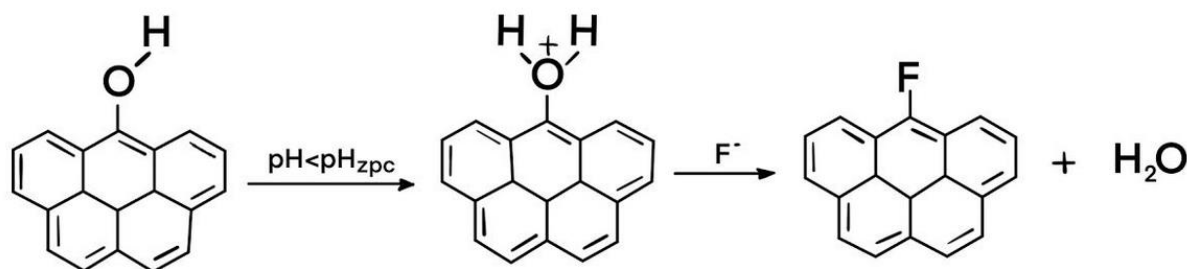
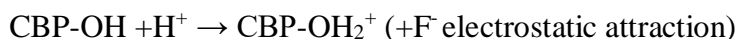


**Fig 5.11: A plausible mechanism of fluoride adsorption onto CBP**

## SECTION B: IOCS AS AN ADSORBENT

### 5.3.B.1 Results and discussions of fluoride adsorption studies using IOCS

#### a) Effect of adsorbent dose

The effect of various amount of adsorbent on defluoridation was studied by taking initial fluoride concentration of 10.00 mg/L and pH 6.1 with different adsorbent doses of 0.05, 0.1, 0.15, 0.2 and 0.25 g respectively. Fig 5.12(a) reveals that the percentage removal of fluoride increases with increasing amount of IOCS and nearly 89% of fluoride was adsorbed with 0.25 g of adsorbent added in 25 mL of solution in a 3 hours of shaking time and at temperature 30°C. The increase in fluoride removal was attributed to the increase in surface area and the availability of more active binding sites with the increase of amount of adsorbent [1]. Since at first, the rate of increase of fluoride removal capacity was increased (from 50%-75%) with the amount of adsorbent from 0.05 g to 0.1 g IOCS and then it again increased up to 89% when the amount of adsorbent dose was 0.25 g. Therefore, 0.25 g is chosen as the optimum value of the adsorbent IOCS for maximum removal of fluoride.

#### b) Effect of contact time

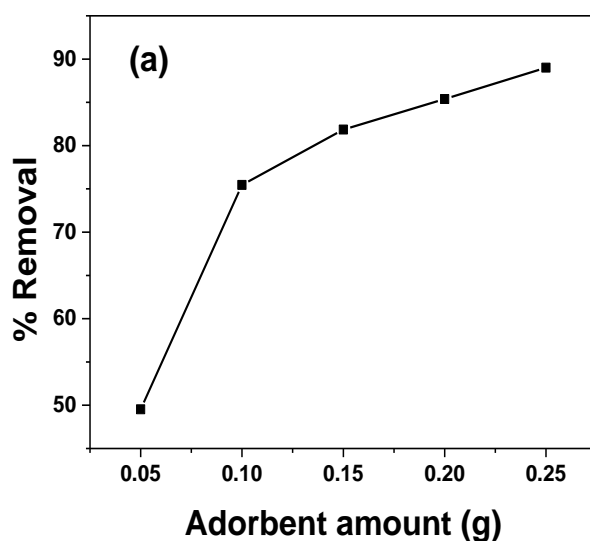
The contact time between adsorbent surface and adsorbate plays an important role in adsorption process. A given amount of adsorbent can adsorb a certain amount of adsorbate at a given time to establish equilibrium. For the investigation of maximum sorption efficiency,



the effect of contact time between fluoride solution and adsorbent IOCS was studied. This experiment was carried out at pH 6.1 by taking 0.25 g adsorbent per 25 mL of 10 mg/L fluoride solution at different contact times from 2-240 min. Fig 5.12(b) shows that percentage of fluoride removal efficiency rapidly increases with increasing contact time. It was 38.5% at 2 minute and 85.5% at 45 minute and then rate of increasing of adsorption decreases gradually. The fast adsorption rate at the initial stage may be explained by large availability of the number of active binding sites on the adsorbent surface as well as the concentration of fluoride ion in the solution is maximum due to which the driving force for adsorption of fluoride on the surface of adsorbent is maximum. After a lapse of time, due to repulsion between the adsorbed solute species on the surface of the adsorbent and the bulk phase, adsorption i.e., % removal efficiency decreases. Therefore 45 minute is chosen as the optimum time for carrying out of the experiments.

### c) Effect of initial concentration of fluoride solution

The effect of initial concentration of fluoride solution 5 to  $\approx 55$  mg/L with 0.25g of IOCS were taken in a set of experimental flasks. From the Fig 5.12(c), it is seen that initially, fluoride removal capacity (mg/g) of IOCS increases gradually and closes to 1.95 mg/g at the fluoride concentration of 26.7 mg/L and it remains the same up to the fluoride concentration of 55 mg/L. This is because at higher concentration the available sites on the surface of adsorbent for adsorption become fewer in comparison to lower concentration. Since maximum fluoride removal capacity was shown by 26.7 mg/L fluoride solution and it was very high fluoride concentration, so the optimum fluoride concentration was chosen as 10 mg/L to carry out the experiment.



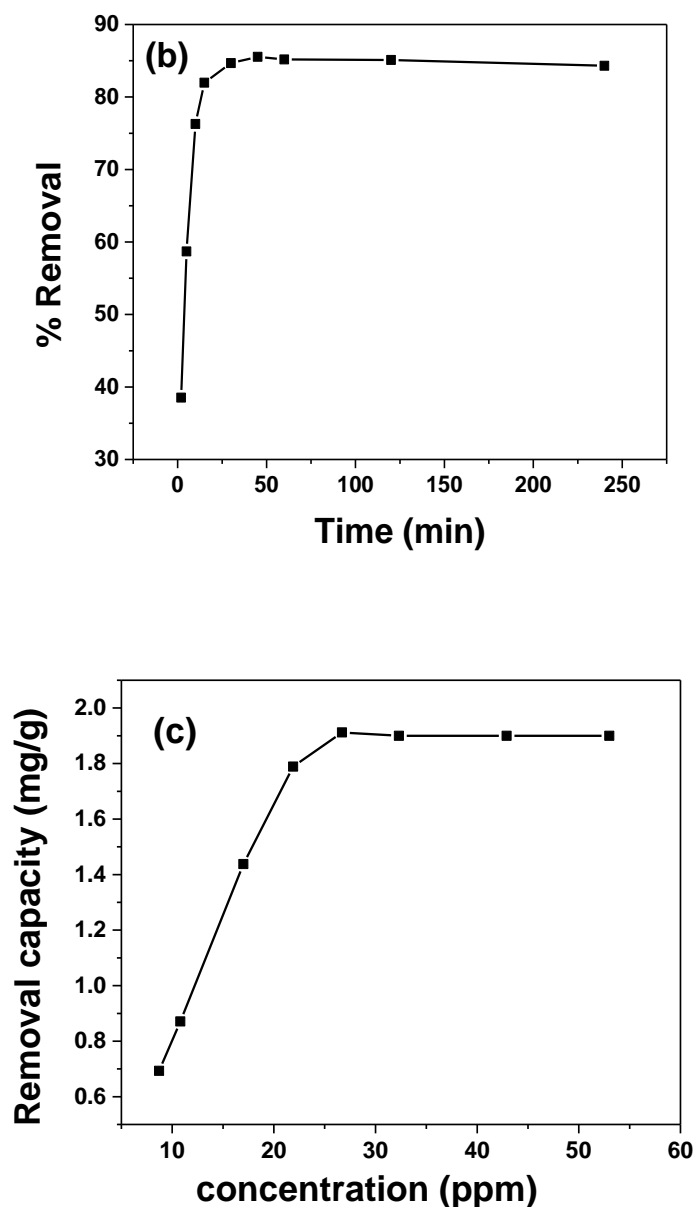


**Fig 5.12:** (a)- Effect of adsorbent dose on the adsorption of fluoride at 30°C in a pH of 6.1 with 3 hour stirring, (b)- Effect of contact time on the adsorption of fluoride at 30°C in a pH of 6.1 with an adsorbent of 10 g/L, (c)- Effect of initial concentration of fluoride solution on defluoridation at 30°C in a pH of 6.1 with an adsorbent of 10 g/L.

#### **d) Effect of pH on defluoridation**

The removal of a species from aqueous solution by adsorption process is influenced by pH of the solution, because pH can alter the surface charge of an adsorbent. [2,3,14,15]. The pH affect on fluoride removal percentage was studied by using 0.25 g of adsorbent in each 25 mL of 10.00 mg/L fluoride solution of pH range 2.5-9.5. pH adjustment were carried out using 0.1 M NaOH and 0.1 M HCl. Fig 5.13 shows that the adsorption of fluoride on IOCS

increases from 87.5% at pH=2.5 to the maximum 89.14% at pH 6.1 and thereafter decreases with further increase in pH. The maximum adsorption at acidic pH may be due to the formation of weak hydrofluoric acid or combined effect of both chemical and electrostatic interaction between the oxide surface of the adsorbent and fluoride ion. Decrease of fluoride removal capacity in alkaline medium can be explained due to competition of fluoride and hydroxide ions on the active sites of IOCS [5,6,9].

The optimum pH is taken as 6.1 to carry out further experiments because at this pH of fluoride solution, IOCS showed maximum fluoride adsorption capacity.

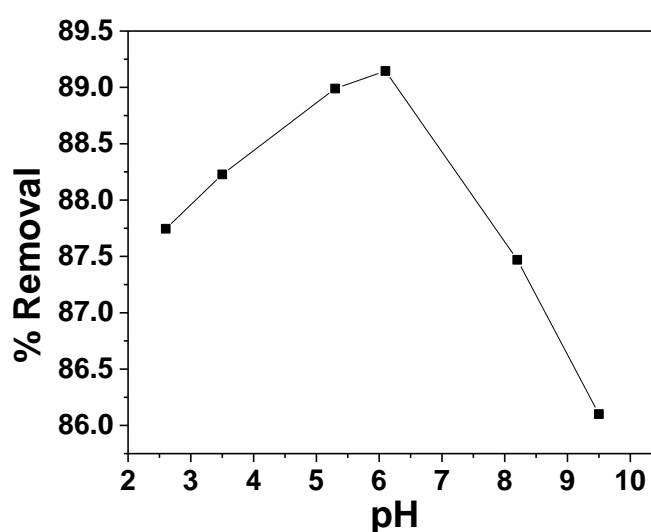


**Fig 5.13: Effect of pH of fluoride solution on % removal of fluoride by IOCS at 30°C**

#### **e) Adsorption isotherms Study**

Adsorption isotherms are used to determine the amount of adsorbate that can be hold on the surface of the adsorbent as a function of adsorbate concentration in the liquid phase at a fixed temperature and at equilibrium condition. In this study spiked fluoride solution of different concentration (8-53 mg/L and pH=6.1) were taken and stirred for 3 hours with 0.25 g adsorbent IOCS at constant temperature 30°C. The resulting isotherm data obtained from this experiment (given in Table 5.3) was interpreted using most commonly used Langmuir, Freundlich and Temkin isotherm models.

#### **Langmuir adsorption isotherm**

Langmuir adsorption isotherm explains quantitatively the formation of monolayer on the surface of the adsorbent containing a large number of identical sites.

From the slope and intercept of the linear plot of  $C_e/q_e$  against  $C_e$ , (from equation 7 of chapter 1) in Fig 5.14(a) the value of Langmuir constant  $q_m$ , i.e., monolayer surface coverage (mg/g) also called as adsorption capacity, and Langmuir constant  $b$  were calculated.

### Freundlich adsorption isotherm

Freundlich isotherm generally explain the adsorption behaviour of heterogeneous surface and it agrees with the Langmuir isotherm equation and experimental data in some extent of concentration range. Freundlich adsorption constant i.e., the adsorption capacity of adsorbent  $K_f$  and intensity of adsorption  $n$  were calculated (equation 9 of chapter 1) from the linear plot of  $\log q_e$  versus  $\log C_e$  in Fig 5.14(b).

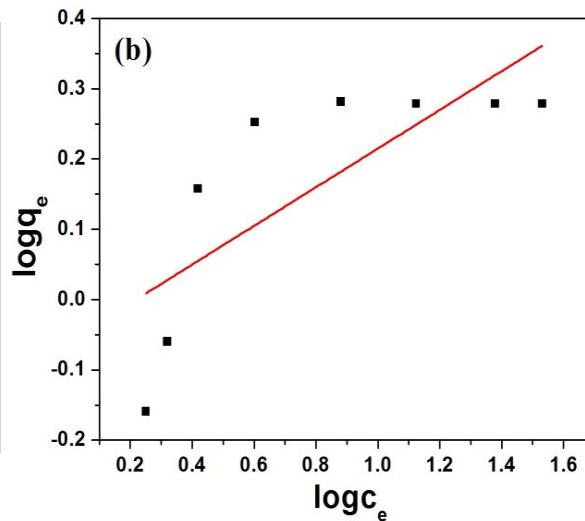
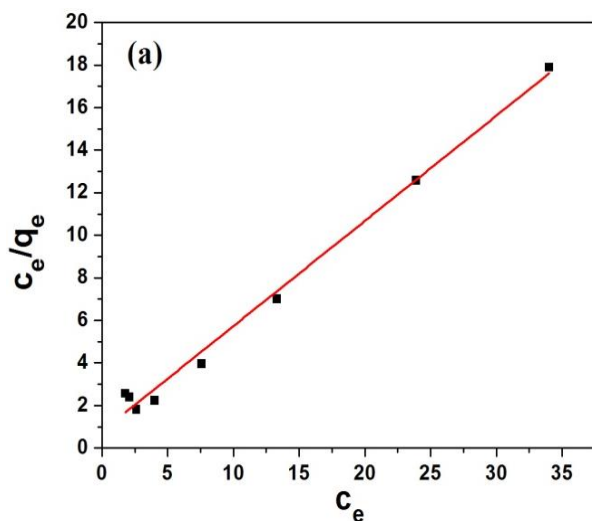
### Temkin adsorption isotherm

The Temkin isotherm describes adsorbent-adsorbate interaction on the adsorption process. The Temkin isotherm constant  $A_T$  (L/g) and  $B_T$  (where  $B_T = RT/b_T$ ,  $b_T$  is the Temkin constant and  $R$  is the gas constant) are calculated from the intercept and the slope of the plot of  $q_e$  against  $\ln C_e$  from Fig 5.14(c).

The corresponding Langmuir, Freundlich, and Temkin parameters along with correlation coefficients are given in Table 5.3). From the Table, it is seen that the Langmuir maximum adsorption capacity  $q_m$  (mg g<sup>-1</sup>) is 2.04 and the equilibrium constant  $b$  (Lmg<sup>-1</sup>) is 0.62. The separation factor or equilibrium parameter  $R_L$  [where  $R_L = 1/(1+bC_0)$ ] also calculated and its value gives the acceptability of the Langmuir model to fit the data. The value of  $R_L$  indicates the shape of the isotherm to be either unfavorable ( $R_L > 1$ ), linear ( $R_L = 1$ ), favorable ( $0 < R_L < 1$ ) or irreversible ( $R_L = 0$ ) [16]. In our study (Fig 5.14(d)), the value of  $R_L$  lay in the range  $0 < R_L < 1$ , indicating the fluoride adsorption on IOCS is favorable under the conditions of experiments and takes place as monolayer adsorption on the surface that is homogenous in adsorption affinity [10]. The value of Freundlich adsorption constant i.e., the adsorption capacity of adsorbent  $K_f$  in mg<sup>1-1/n</sup> L<sup>1/n</sup>g<sup>-1</sup> is 1.15. The value of  $n$  is 3.63 at equilibrium, which lies in between 1 and 10 indicating the favourable adsorption; but from the correlation coefficients ( $R^2$  value), it can be said that, Freundlich and Temkin isotherm models ( $R^2=0.5281$  and  $0.5902$ ) of adsorption are not fitted and the best fitted isotherm model is Langmuir adsorption isotherm model ( $R^2=0.990$ ). The estimated maximum fluoride adsorption capacity of IOCS is 2.04 mg/g.

Table 5.3: Langmuir, Freundlich, and Temkin parameters along with correlation coefficients

Isotherm	R <sup>2</sup>	Constant	Value
Langmuir $C_e/q_e = C_e/q_m + 1/(bq_m)$	0.990	b (L/mg)	0.62
		q <sub>m</sub> (mg/g)	2.04
		R <sub>L</sub>	0.03-0.16
Freundlich $\log q_e = \log K_f + (1/n)\log C_e$	0.5281	K <sub>f</sub> (mg/g(L/mg) <sup>1/n</sup> )	1.15
		n	3.63
Temkin $q_e = B_T \ln A_T + B_T \ln C_e$	0.5902	A <sub>T</sub> (L/g)	11.9
		B <sub>T</sub> (J/mol)	0.35



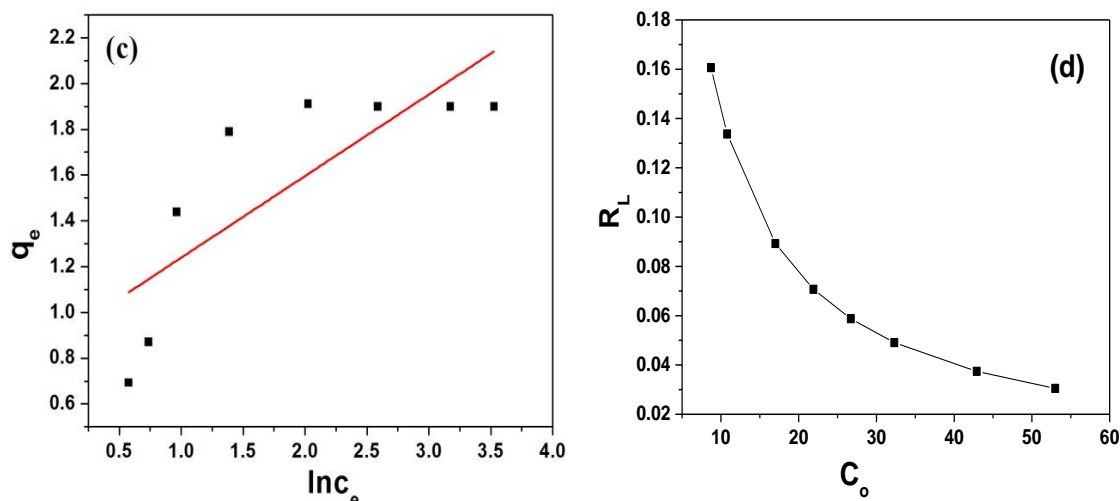


**Fig 5.14: (a) Langmuir, (b) Freundlich, (c) Temkin adsorption isotherm of IOCS and (d) graph of  $R_L$  vs  $C_0$**

#### **f) Adsorption Kinetic Study**

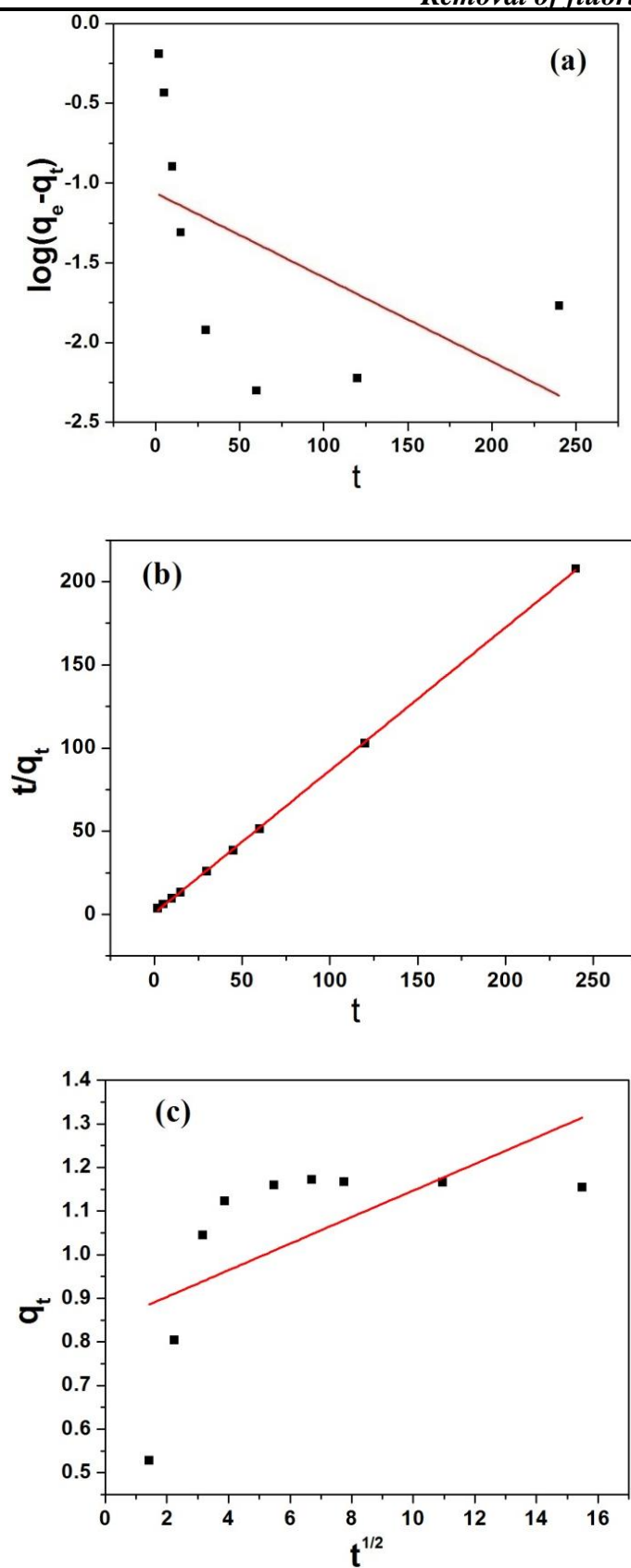
In this study pseudo first order, pseudo second order, intra particle diffusion and Elovich models were used to interpret the kinetics of fluoride adsorption on IOCS. This adsorption kinetic study was carried out in optimum condition i.e., by taking 0.25g adsorbent per 25 mL of 10 mg/L fluoride solution of pH 6.1 and for 45 minute stirring at 30°C.

The resulting data of adsorption kinetic model are tabulated in Table 5.4. Pseudo first order rate constant,  $k_1$  ( $= 0.01 \text{ min}^{-1}$ ) and first order adsorption capacity i.e amount of adsorption at equilibrium  $q_{e,cal}$  ( $=0.08\text{mg/g}$ ) were calculated from the linear plot of  $\log (q_e - q_t)$  versus  $t$  in the Fig. 5.15(a). Pseudo second order rate constant,  $k_2$  ( $=1.00 \text{ g/mgmin}$ ) and second order adsorption capacity,  $q_{e,cal}$  ( $=1.16 \text{ mg/g}$ ) were determined by plotting  $t/q_t$  against  $t$  in Fig. 5.15(b). In Intra Particle Diffusion model, the rate of intra-particle diffusion controls adsorption kinetics. From the linear equation of intra-particle diffusion model (equation number 6, chapter 1), plot of  $q_t$  versus  $t^{1/2}$  in plot [Fig 5.15(c)]. However from the linear fitting of  $q_t$  versus  $t^{1/2}$  [Fig 5.15(d)],  $k_d$  ( $=0.008 \text{ mg g}^{-1} \text{ min}^{-1/2}$ ),  $C$  ( $=1.27$ ) and the correlation coefficient ( $R^2=0.0578$ ) were calculated and these values means the poor significance of this model. In case if Elovich kinetic model, from the plot of  $q_t$  versus  $\ln t$  in Fig 5.15(d) the value of initial adsorption rate  $a$  ( $=1.09 \times 10^4 \text{ mg g}^{-1} \text{ min}^{-1}$ ) and the desorption constant  $b$  ( $=11.49 \text{ g/mg}$ ) were calculated. In the Table 5.4, the various parameters of all kinetics models are compared.

It is seen that in the experiments of kinetic study of adsorption of fluoride on IOCS did not follow the pseudo-first order equation as well as Intra Particle Diffusion model and Elovich model. From the correlation coefficient it is confirmed that adsorption data followed the pseudo-second order equation.

**Table 5.4: Comparison of the various parameters obtained in Pseudo first order, Pseudo Second order, Intra particle diffusion model and Elovich model of adsorption of fluoride onto IOCS**

Kinetics Model	Parameters	Value
<b>Pseudo First order</b>  $\log(q_e - q_t) = \log q_e - k_1(t/2.303)$	$K_1 (\text{min}^{-1})$	0.01
	$q_{e,cal}(\text{mg/g})$	0.08
	$R^2$	0.1759
<b>Pseudo Second order</b>  $t/q_t = [1/(k_2 q_e^2)] + t/q_e$	$K_2 (\text{g/mg min})$	1.00
	$q_{e,cal}(\text{mg/g})$	1.16
	$R^2$	0.9997
<b>Intra Particle diffusion</b>  $q_t = k_d t^{1/2} + C$	$K_d (\text{mg/g min}^{1/2})$	0.03
	$R^2$	0.29251
<b>Elovich</b>  $q_t = 1/b[\ln(ab)] + 1/b[\ln t]$	$b (\text{g/mg})$	8.2
	$a[\text{mg}/(\text{g min})]$	23.71
	$R^2$	0.654





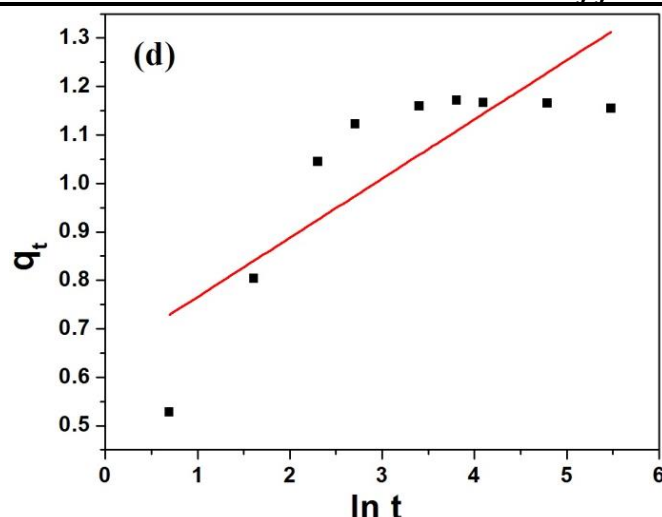


**Fig 5.15: Plots of (a) pseudo-first-order, (b) pseudo second- order, (c) Intra particle diffusion model and (d) Elovich model.**

#### **g) Thermodynamic analysis**

Temperature is an indicator for the adsorption nature on a solid surface whether it is an exothermic or endothermic process. The thermodynamic parameters of the adsorption process were determined from experimental data obtained at various temperatures using the equations (equation no. 12, 13 & 142 of chapter 1).

From the slope and intercept of the plot of  $\ln K_d$  versus  $1/T$  (Fig 5.16), the change of enthalpy  $\Delta H^0$  and change of entropy  $\Delta S^0$  were calculated. All the thermodynamic parameters ( $\Delta H^0$ ,  $\Delta S^0$  &  $\Delta G^0$ ) are given in the Table 5.5.

From the figure,  $\Delta H^0$  and  $\Delta S^0$  are calculated.

$$\Delta H^0 = \text{Slope} \times R = -436.73442 \text{ J mol}^{-1}; \quad R \text{ is the gas constant } (8.31445 \text{ J K}^{-1} \text{ mol}^{-1}).$$

$$\Delta S^0 = \text{Intercept} \times R = 1.02877 \text{ J mol}^{-1} \text{ K}^{-1}$$

$$\text{Thus, } \Delta G^0 = \Delta H^0 - T\Delta S^0 = -0.74845 \text{ kJ mol}^{-1} \text{ at } 303\text{K}$$

$$\Delta G^0 = \Delta H^0 - T\Delta S^0 = -0.75873 \text{ kJ mol}^{-1} \text{ at } 313\text{K}$$

$$\Delta G^0 = \Delta H^0 - T\Delta S^0 = -0.76903 \text{ kJ mol}^{-1} \text{ at } 323\text{K}$$

$$\Delta G^0 = \Delta H^0 - T\Delta S^0 = -0.77417 \text{ kJ mol}^{-1} \text{ at } 328\text{K}$$

Negative value of  $\Delta H^0$  reveals exothermic nature of adsorption [17]. The positive value of  $\Delta S^0$  indicates the increased randomness during the adsorption of fluoride. The negative  $\Delta G^0$  values for the adsorbent IOCS shows the spontaneous adsorption process [10,18].

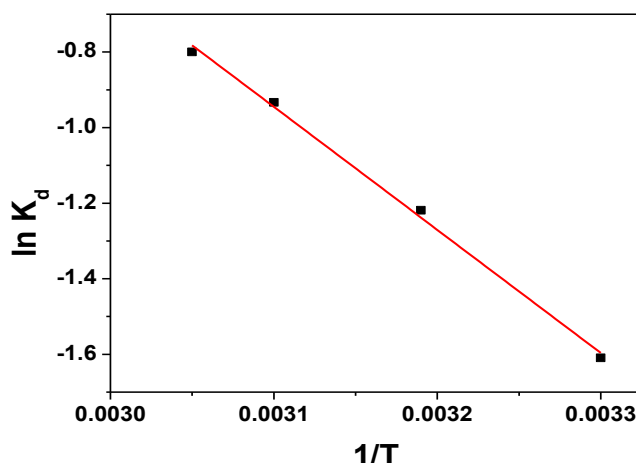


**Fig 5.16: Van't Hoff plots of fluoride adsorption onto IOCS**

**Table 5.5: Thermodynamic parameters ( $\Delta G^\circ$ ,  $\Delta H^\circ$  and  $\Delta S^\circ$ ) of fluoride adsorption on IOCS**

T (K)	$\Delta G^\circ$ (kJmol <sup>-1</sup> )	$\Delta H^\circ$ (Jmol <sup>-1</sup> )	$\Delta S^\circ$ (Jmol <sup>-1</sup> )
303	-0.74845	-436.73442	1.02877
313	-0.75873		
323	-0.76903		
328	-0.77417		

#### **h) Effect of other anions on defluoridation:**

Since besides fluoride ion, other anions such as sulphate, chloride, bromide, nitrate, arsenate, carbonate and bicarbonate also present in ground water, so influence of these anions on fluoride sorption capacity is also very important. In this experiment, fluoride sorption capacity was determined in the absence of co-existing anions and in the presence of each anion of 50 mg/L in optimum condition. From the Fig 5.17, it has been observed that nitrate ions have lesser effect on the removal of fluoride but the carbonate ions showed highest effect towards the active site and thereby decreasing the sorption capacity of fluoride. The decreasing order of effect of co-ions with respect to fluoride adsorption capacity for the adsorbent IOCS follows the order:

nitrate < bromide < chloride < bicarbonate < sulphate < arsenate < carbonate.

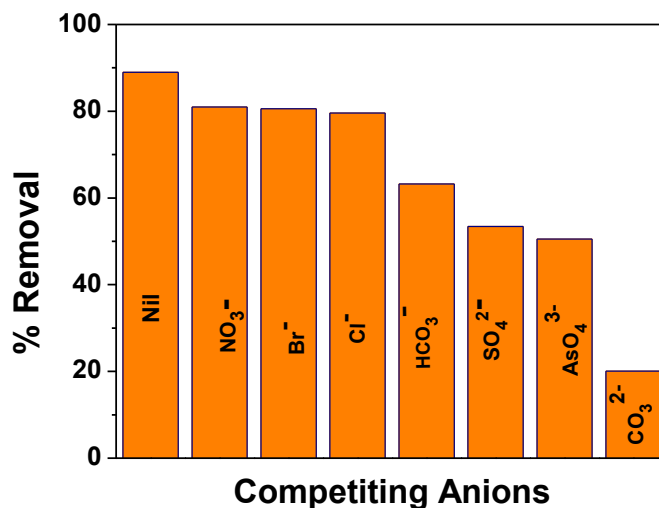


Fig 5.17: Bar diagram showing the effect of competitive anions on defluoridation

### 5.3.B.2: Studies on IOCS after adsorption of fluoride

#### a) Study of FESEM images & EDX spectra

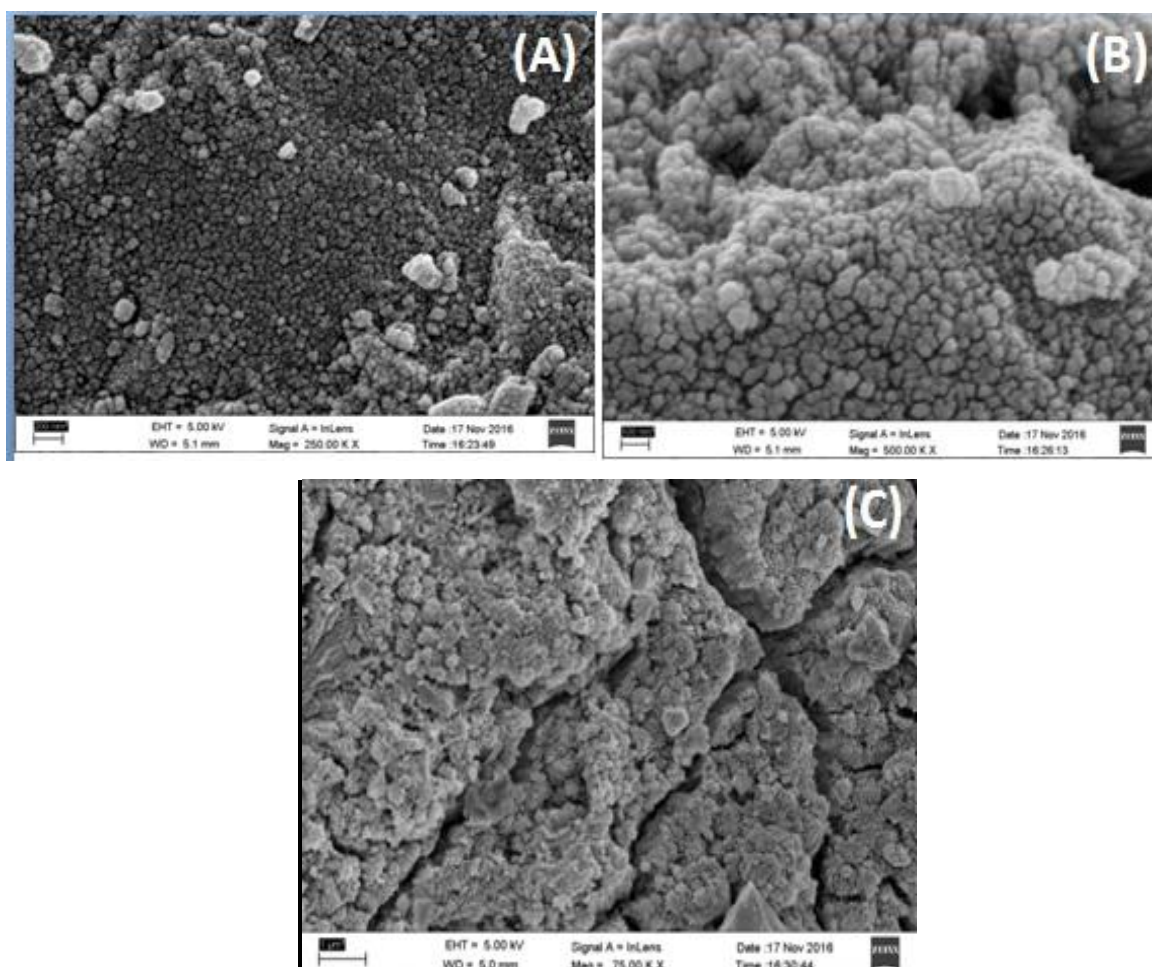
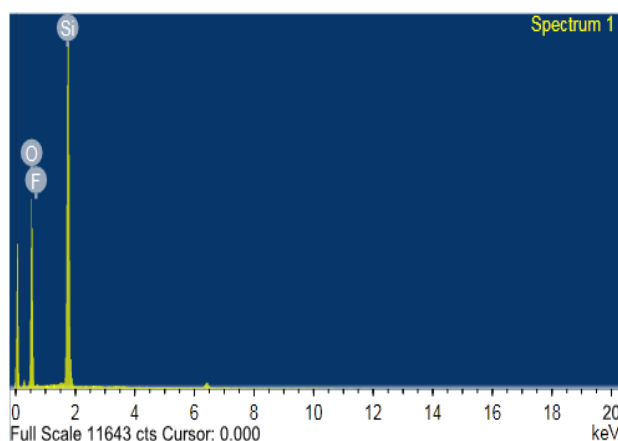


Fig 5.18: (A), (B) & (C) are FESEM photograph of IOCS after adsorption of fluoride

After fluoride adsorption, the SEM images of IOCS were taken at different magnification to observe the change in surface structure and shown in the Fig 5.18. It is seen that, the surface of IOCS after adsorption of arsenic is changed from the SEM images of raw IOCS (Fig 4.16 of chapter 4). This significant deformation in the structural organization of the IOCS indicates the adsorption of fluoride is a surface phenomenon. This adsorption behavior is further supported by EDX (Fig 5.19) analysis and FTIR (Fig 5.20) study.



Element	Weight %	Atomic %
O K	62.26	74.27
F K	0.23	0.24
Si K	37.51	25.49

**Fig 5.19: EDX spectra of Iron Oxide Coated Sand (IOCS) after adsorption of fluoride**

Presence of fluoride in the EDX spectra of IOCS after adsorption of fluoride, it is confirmed that the adsorption of fluoride on IOCS is a surface phenomenon.

#### b) Study of FTIR spectra

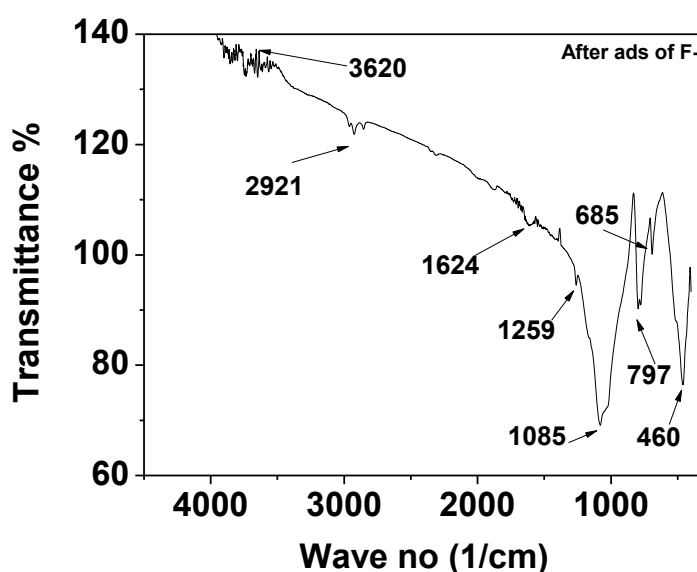


**Fig 5.20: FT-IR spectra of IOCS before and after adsorption of fluoride**

After adsorption of fluoride, to study the interaction between fluoride ion and the active sites present on the surface of IOCS, FTIR spectroscopy was carried out and the spectra is given in the Fig 5.20. From close examination, the FT-IR spectra of IOCS before adsorption [Fig 4.18(B)] with the FT-IR spectra of after adsorption of fluoride, it is seen that the appearance of the various vibration bands of Si-OH, Si-O, Fe-O etc in both spectrum are same. As, fluoride-containing compound absorbs IR in the range  $1400\text{--}1000\text{ cm}^{-1}$  [19], the absorption band at  $1259\text{ cm}^{-1}$  in spectra of after adsorption of fluoride on IOCS can be attributed to the presence of fluoride in our compound. There was an overall decrease in the % transmittance of IR intensity in fluoride treated IOCS adsorbents which is due to the exchange of -OH from its surface with fluoride ions [20].

So from the above SEM images, EDS spectra and FT-IR spectrum attributed to the adsorption of fluoride on the adsorbent iron oxide coated sand (IOCS).

#### 5.4: Conclusions:

Present study has shown that the both adsorbent obtained from locally available materials have good fluoride adsorption property.

CBP is a very simple carbon which is naturally functionalized, obtained at the time of preparation of banana alkali by Assamese traditional method, is a good adsorbent of fluoride. Various results obtained in the study on adsorbent dose, adsorption isotherm, effect of pH and effect of co-ions shows that the carbon of banana plant (CBP) have good fluoride removal capacity which is 66.4% on treatment of an optimum dose of 0.35 g CBP in 25 mL of 5mg/L fluoride aqueous solution. The maximum fluoride removal capacity of CBP was at pH 2-3. Sorption kinetic data lead us that CBP follow the pseudo second order equation and Langmuir adsorption isotherm model. Defluoridation capacity of the adsorbent is also affected by other anions. The decreasing order of effect of co-ions with respect to fluoride adsorption capacity for the adsorbent follows the nitrate < sulfate < bromide < bicarbonate < chloride < arsenate < carbonate. Thus CBP which is otherwise a waste material can be expected to be a successful cheaper adsorbent of fluoride for common people in the rural areas. Apart from the above the high negative surface charge bearing CBP may also find other prospective rural applications like pesticide carrier, controlled release fertilizer or cleaning of oily waste water etc.

IOCS which is iron oxide coated surface modified Kanaighat sand is a very effective adsorbent material for efficient adsorption of fluoride from aqueous medium. Various results obtained in the study on adsorbent dose, adsorption isotherm, effect of pH and effect of co-

ions shows that the iron oxide coated sand (IOCS) have excellent fluoride removal capacity of 89.5% removal on treatment of an optimum dose of 0.25 g IOCS in 25 mL of 17mg/L fluoride aqueous solution. The adsorption capacity increase with the increasing pH of the adsorbate up to 6.1 and then it decreases again with further increase of pH. Sorption kinetic data revealed that the adsorption kinetics for IOCS followed the pseudo second order equation. The equilibrium data was fitted to Langmuir adsorption models. Defluoridation capacity of the adsorbent is also affected by other anions. The decreasing order of effect of co-ions with respect to fluoride adsorption capacity for the adsorbent follows the order nitrate < bromide < chloride < bicarbonate < sulphate < arsenate < carbonate.

## **Reerences**

- [1] Das B., Mondal N.K. (2011) Calcareous soil as a new adsorbent to remove lead from aqueous solution: equilibrium, kinetic and thermodynamic study. *Universal J Environ Res Technol.* 1:51587.
- [2] Zahra D., Mohammad A.B., Mojdeh R., and Mohammad F. (2013) Adsorption of methylene blue dye from aqueous solution by modified pumice stone: Kinetics and equilibrium studies. *Health scope.* 2(3): 136-144.
- [3] Xu D., Tan X.L., and Wang X.K. (2008). Adsorption of Pb (II) from aqueous solution to MX-80 bentonite: Effect of pH, ionic strength, foreign ions and temperature. *Appl Clay Sci.* 41:37-46.
- [4] Bhomick P.C., Supong A., Baruah M., Pongener C., and Sinha D. (2018) Pine cone biomass as an efficient precursor for the synthesis of activated biocarbon for adsorption of anionic dye from aqueous solution: isotherm, kinetic, thermodynamic and regeneration studies. *Sustainable Chemistry and Pharmacy.* 10, 41-49.
- [5] Chen N., Zhang Z., Fenga C., Zhub D., Yang Y., and Sugiura N. (2011) Preparation and characterization of porous granular ceramic containing dispersed aluminum and iron oxides as adsorbents for fluoride removal from aqueous solution. *J Hazard Mater.* 186(1):863–868.
- [6] Chen N., Feng C., and Li M. (2014) Fluoride removal on Fe-Al-impregnated granular ceramic adsorbent from aqueous solution. *Clean Technol Environ Policy.* 16(3):609–617.
- [7] Bansal R.C., and Goyal M. (2005) *Activated carbon adsorption*, CRC Press, Taylor &

- Francis Group, LLC.
- [8] Tan I.A.W., Ahmad A.L., and Hameed B.H. (2008) Adsorption of basic dye on high– surface–area activated carbon prepared from coconut husk: equilibrium, kinetic and thermodynamic studies, *Journal of Hazardous Materials*. 154(1– 3), 337–346.
- [9] Chiban M., Carja G., Lehotu G., and Sinan F. (2012) Equilibrium and thermodynamic studies for the removal of As(V) ions from aqueous solution using dried plants as adsorbents, *Arabian Journal of Chemistry*. doi: 10.1016/j.arabjc.2011.10.002.
- [10] Saikia J., Sarmaha S., Ahmed T.H., Kalita P.J., and Goswamee R.L. (2017) Removal of toxic fluoride ion from water using low cost ceramic nodules prepared from some locally available raw materials of Assam. *India Journal of Environmental Chemical Engineering*. 5: 2488–2497.
- [11] Emmanuel K.A., Ramaraju K.A., Rambabu G., and Rao A.V. (2008) Removal of fluoride from drinking water with activated carbons prepared from HNO<sub>3</sub> activation – a comparative study. *Rasayan J Chem*. 1(4):802-818.
- [12] Ozcan A.S., Erdem B., Ozcan B. (2004) Adsorption of Acid Blue 193 from aqueous solutions onto Na-bentonite and DTMA-bentonite. *J Colloid Interface Sci*. 280: 44–54.
- [13] Gandhi N., Sirisha D., and Sekhar K.B.C. (2016) Adsorption of fluoride (F-) from aqueous solution by using pineapple (*Ananascomosus*) peel and orange (*Citrus sinensis*) peel powders. *International Journal of Environmental Bioremediation & Biodegradation*. 4(2):55-67.
- [14] Kamaraj R., and Vasudevan S. (2015a) Decontamination of selenate from aqueous solution by oxidized multi-walled carbon nanotubes. *Powder Technology*. 274, 268–275.
- [15] Kamaraj R., and Vasudevan S. (2015b) Evaluation of electrocoagulation process for the removal of strontium and cesium from aqueous solution. *Chemical Engineering Research and Design*. 93, 522–530.
- [16] Hameed B. H. (2009) Removal of cationic dye from aqueous solution using jackfruit peel as non-conventional low-cost adsorbent. *Journal of Hazardous Materials*. 162, 344 –350.
- [17] Rincon-Silva N.G., Moreno-Pirajan J.C., and Giraldo L.G. (2015) Thermodynamic Study of Adsorption of Phenol, 4-Chlorophenol, and 4-Nitrophenol on Activated Carbon Obtained from Eucalyptus Seed. *Journal of Chemistry*. ID 569403, <http://dx.doi.org/10.1155/2015/569403>

- [18] Al-Rashed S. M., and Al-Gaid A. A. (2012) Kinetic and thermodynamic studies on the adsorption behavior of Rhodamine B dye on Duolite C-20 resin. *Journal of Saudi Chemical Society*. 16(2), 209–215.
- [19] Umlong I.M., Das B., Devi R. R., Borah K., Saikia L. B., Raul P. K., and Singh S.B.L. (2012) Defluoridation from aqueous solution using stone dust and activated alumina at a fixed ratio. *Applied Water Science*. 2, 29–36.
- [20] Meenakshi S., Sundaram C. S., and Sukumar R. (2008). Enhanced fluoride sorption by mechano-chemically activated kaolinites. *Journal of Hazardous Materials*. 153, 164–172.



## **CHAPTER - 6**

### **REMOVAL OF ARSENIC FROM CONTAMINATED WATER BY USING TWO LOCALLY AVAILABLE MATERIALS:**

#### **SECTION A-CBP**

**&**

#### **SECTION B-IOCS**

**6.1 Introduction**

Presence and removal of arsenic from water are two important global issue. From the literature it was observed (discussed in chapter-3) that, there are different arsenic removal methods like coagulation/precipitation, membrane filtration (reverse osmosis; nanofiltration; electro-dialysis), ion-exchange and adsorption. Although all these methods can remove arsenic from contaminated water successfully, but due to low cost, easy to handle and high availability of the materials which can be activated for removal of arsenic from contaminated water, adsorption is the most common method. Again due to high expensive nature and need of skilled operator, coagulation/precipitation, membrane filtration and ion-exchange methods are not highly effective for common people of developing countries like India.

In chapter 4, two adsorbents were prepared from locally available materials for the removal of arsenic from contaminated water. This chapter is taken for the study of arsenic removal capacity of these two prepared arsenic adsorbents:

1. **Carbon of banana plant (CBP)** and
2. **Surface modified “Kanaighat Sand” (IOCS).**

The oxidation state of arsenic plays a role in its removal. As (V) (arsenate) is considered as more easily removable than As (III) (arsenite) [1,2,3].

**6.2 Materials and methods****6.2.1 Preparation of standard arsenic stock solution**

A stock solution of arsenic [As (V)] of 5 mg/L was prepared by appropriate dilution of arsenic standard solution ( $\text{H}_3\text{AsO}_4$ , 1000 mg/L of Marck KgaA). For the adsorption study required concentration of As (V) solutions were prepared from the stock solution. To get desired pH of arsenic solution, 0.1M HCl or 0.1M NaOH solution was used. All reagents and chemicals were prepared by using ultra pure water.

**6.2.2 Determination of As (V) (arsenate,  $\text{H}_2\text{AsO}_4^-$ ) concentration**

Generally, arsenic concentration in water is determined by atomic absorption spectroscopy (AAS) method. It is based on absorption of optical radiation at specific frequency by free metallic atoms in the gaseous state. Atomic absorption spectroscopy quantifies the absorption of ground state atoms in the gaseous state. So, in AAS technique total arsenic concentration is determined as all arsenic ions present in solution is converted

into atomic state. A blank was analyzed between element-specific standard readings to verify the instrument's baseline stability. For calibration 0.005 mg/L, 0.01 mg/L, 0.02 mg/L & 0.04 mg/L arsenic solutions were prepared from standard arsenic solution for AAS. Before analysis As (V) was prereduced to As (III) according to the user guide of AAS [4]. KI solution (KI+ascorbic acid) in HCl solution of concentration 5 mol/L is used for the prereduction of As (V), for which the time required is 30 minute. Water sample of As (III) (pre-reduced) was analyzed by using Atomic Absorption Spectrophotometer (Perkin Elmer, USA) with MHS-15 (Mercury Hydride Generation system) at 193.7 analytical wave length and 0.7 –nm slit width. Radiation source was an electrode less discharge lamp for arsenic with 20-second prereaction purge time and 10-second postreaction purge time. Argon gas and sodium borohydrate were used for the hydride generation [5]. The results of AAS were further cross checked regularly by Ion Chromatography (Model 881 Compact IC pro Metrohm and column Metrosep C4-150/4.0).

### **6.2.3 Batch mode adsorption study**

By batch mode method, adsorption study was carried out. The effect of adsorbent dose, agitation time, pH, competitive anions and temperature on arsenic adsorption efficiency of CBP and IOCS were investigated at temperature 30°C by using 25 mL of arsenic solutions in conical flasks. After shaking at 180 RPM, Whatman 42 grade filter paper was used for filtration, and the remaining arsenic concentration was determined by AAS. Percentage removal (E) and removal capacity ( $q_e$ ) was calculated using equation (1) and (2) from the chapter 1.

## **6.3: Results and discussion**

### **SECTION A: CBP AS AN ADSORBENT**

#### **6.3.A.1 Results and discussions of arsenic adsorption studies using CBP**

##### **a) Effect of adsorbent dosage**

The effect of various amount of adsorbent (CBP) on adsorption of As (V) was studied by taking arsenic solution of concentration 0.5 mg/L and at pH 7 with different adsorbent dosage of 0.05, 0.1, 0.15, 0.2, 0.25, 0.3, 0.35, 0.4, and 0.45 g respectively. Fig.6.1 reveals that the percentage removal of arsenic increases with increasing amount of CBP and nearly 80.78

% of arsenic was adsorbed with 0.45 g in 25 mL of solution in 3 hours shaking and at temperature 30°C. The increase in arsenic removal is attributed to the increase in surface area and the availability of more active binding sites with the increase of amount of adsorbent [6]. Since the percentage of arsenic removal capacity of CBP is increased (from 69.46%-79.87%) at a constant rate from 0.05 g to 0.35 g CBP and decreased the rate of removal percentage when the amount of CBP is 0.45 g. Therefore 0.35g is chosen as the optimum value of the adsorbent CBP for maximum removal of arsenic.

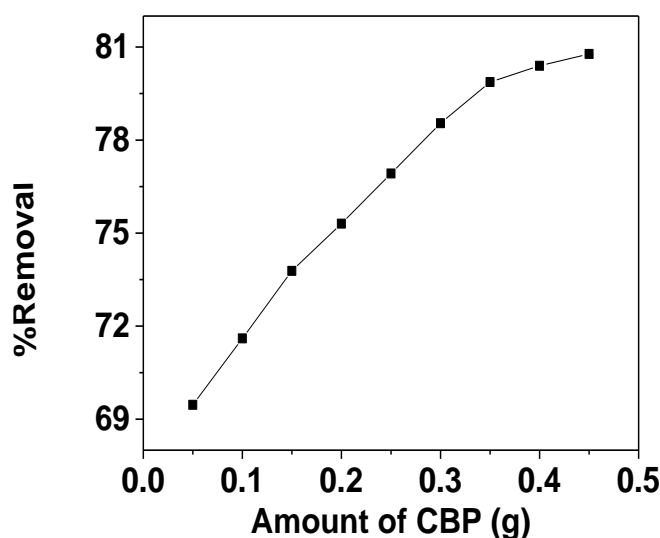


**Fig 6.1: Effect of adsorbents dosage on the %removal of arsenic at 30°C in pH- 7 with 3 hours stirring.**

#### **b) Effect of initial concentration of arsenic solution**

The concentration of arsenic solution plays a significant role in adsorption process. A given amount of adsorbent can adsorb a certain amount of adsorbate to establish equilibrium. The effect of initial concentration of arsenic solution (0.3-5 mg/L) of pH 7 with 0.35 g of CBP were taken in a set of experimental flasks. From the Fig 6.2, highest % removal by CBP showed 79.88 % at 0.525 mg/L arsenic solution. This is because at higher concentration, the available sites on the surface of adsorbent for adsorption become fewer in comparison to lower concentration. Since maximum arsenic removal percentage is shown by 0.525 mg/L arsenic solution, so the optimum arsenic concentration is chosen as 0.5 mg/L to carry out the experiment.

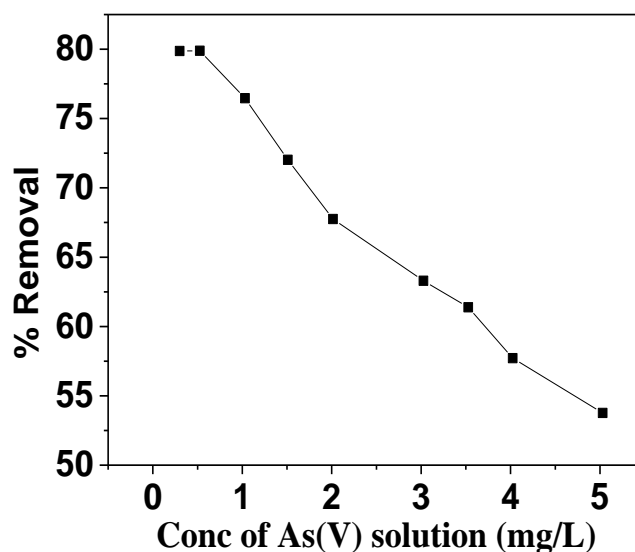


**Fig 6.2: Effect of initial concentration of arsenic solution on adsorption of arsenic by CBP at 30°C in a pH of 7 with 3 hours stirring**

### c) Effect of pH on As (V) adsorption

Adsorption of a species from aqueous solution is influenced by pH of the solution. Because pH changes over all surface charge of the adsorbent, especially the charges of surface functional group of adsorbent and change the ionization and species of the adsorbate [7,8,9]. The pH affect on arsenic removal percentage was studied by using 0.35 g of adsorbent in each 25 mL of 0.500 mg/L arsenic solution of pH rang 3-11. Fig.6.3 shows that the adsorption of arsenic on CBP increases with increasing pH from 3 to 7. The maximum arsenic % removal capacity of the adsorbent CBP is 79.96 in neutral condition, which is attributed due to the formation of surface complexation on the adsorbent at pH 7 [10,11]. At this pH, for As-V,  $\text{H}_2\text{AsO}_4^-$  species is the predominant which binds with two oxygen atoms of carboxylate groups [12,13] and releases two water molecules. Again the optimum pH = 7 can be explained due to the formation of positive charge (as pH ZPC of CBP is 9.6) and electrostatic interaction between the surface charge of the adsorbent and arsenateion. Decrease of arsenic removal capacity in alkaline medium can be explained due to repulsion between arsenate and negative charge of adsorbent surface i.e., availability of  $-\text{OH}^-$  ions [14].

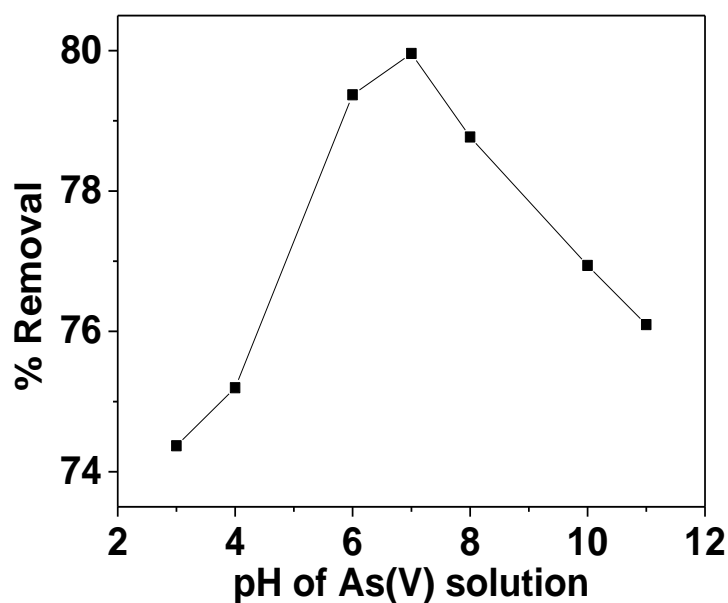


Fig 6.3: Effect of pH on adsorption of As (V)

#### d) Effect of contact time

The contact time between adsorbent surface and adsorbate also affect the adsorption process. A given amount of adsorbent can adsorb a certain amount of adsorbate at a given time to establish equilibrium. For the investigation of maximum adsorption efficiency, effect of contact time between arsenic solution and adsorbent CBP was studied. This experiment was carried out at pH 7 by taking 0.35 g adsorbent per 25 mL of 0.5 mg/L arsenic solution at different contact times from 5-1440 min. Fig. 6.4 shows that percentage of arsenic removal efficiency rapidly increases with increasing contact time up to 180 minute and then rate of increasing of adsorption decreases gradually. The fast adsorption rate at the initial stage may be explained by large availability of the number of active binding sites on the adsorbent surface and after a lapse of time, due to repulsion between the adsorbed solute species on the surface of the adsorbent and the bulk phase, adsorption i.e., % removal efficiency decreases. Therefore, 180 minute is chosen as the optimum time to carry out the experiment.

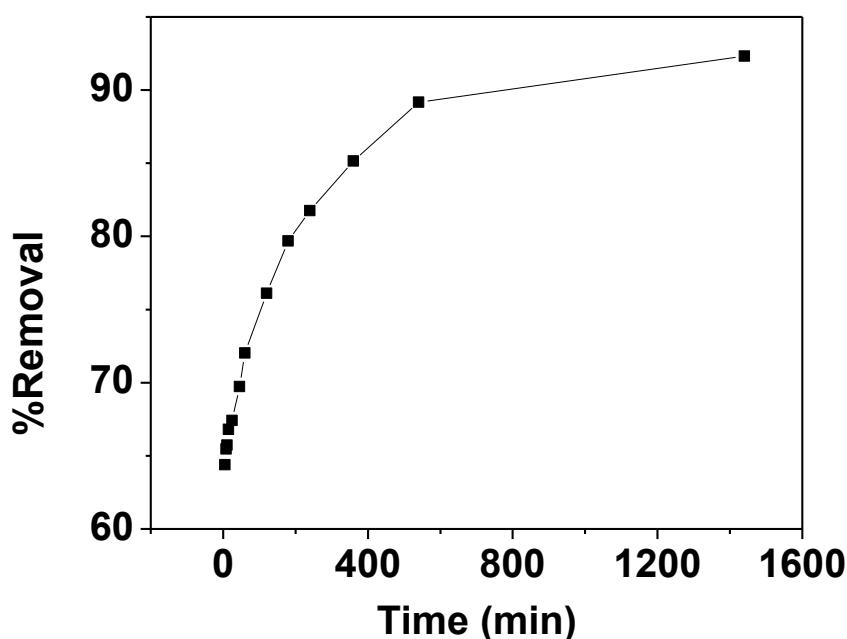


Fig 6.4: Effect of contact time on the adsorption of arsenic at 30°C

#### e) Adsorption kinetics study

The adsorption kinetics models (equations 3, 4, 5 & 6 of chapter 1) are generally used to investigate the path and steps involved in adsorption. In this study adsorption reaction was carried out by maintaining the parameters at their optimum level. The pseudo first order, pseudo second order, Elovich and intra particle diffusion models were used to interpret the kinetics of arsenic adsorption on CBP.

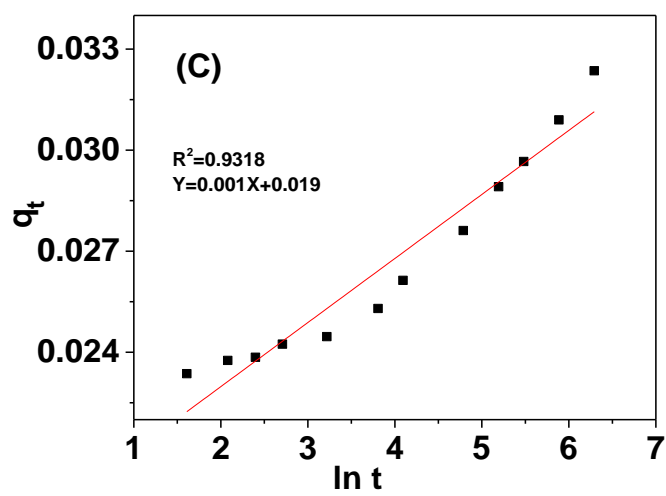
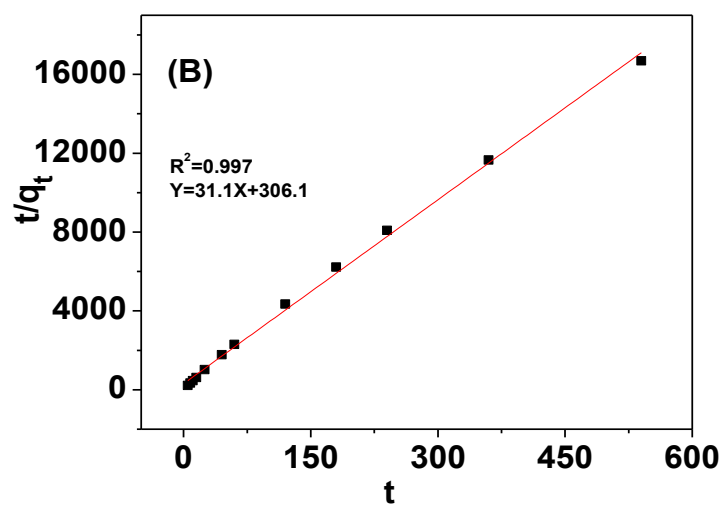
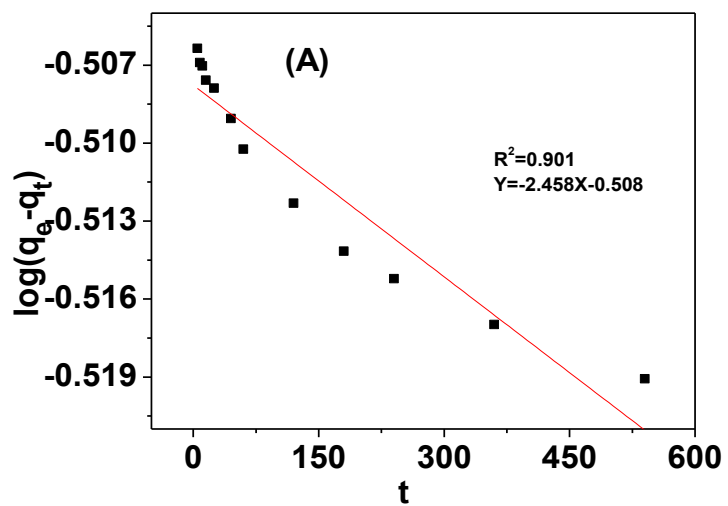
Adsorption kinetic model parameters are tabulated in Table 6.1. Pseudo first order rate constant,  $k_1$  ( $= 5.66 \text{ min}^{-1}$ ) and first order adsorption capacity i.e amount of adsorption at equilibrium  $q_e$  ( $= 0.31 \text{ mg g}^{-1}$ ) were calculated from the Fig. 6.5(A). Pseudo second order rate constant,  $k_2$  ( $= 3.2 \text{ g mg}^{-1} \text{ min}^{-1}$ ) and second order adsorption capacity,  $q_e$  ( $= 0.03 \text{ mg/g}$ ) were determined by plotting  $t/q_t$  against  $t$  in Fig. 6.5(B). In case if Elovich kinetic model, from the plot of  $q_t$  versus  $\ln t$  in Fig. 6.5(C) the value of initial adsorption rate  $a$  ( $= 1.7 \times 10^5 \text{ mg g}^{-1} \text{ min}^{-1}$ ) and the desorption constant  $b$  ( $= 1000 \text{ g/mg}$ ) were calculated. In Intra Particle Diffusion model, it was investigated that, whether the movement of arsenic species towards the pore of adsorbent CBP was possible as a rate controlling step. From the plot of  $q_t$  versus  $t^{1/2}$  in Fig. 6.6(D),  $k_d$  ( $= 0.004 \text{ mg g}^{-1} \text{ min}^{-1/2}$ ) and  $C$  ( $= 0.02$ ) were calculated. The  $R^2$  value ( $= 0.992$ ) indicates the significance of this process. Again, according to Ranjan et al. [15], the intra

particle diffusion will be the only rate controlling step if and only if the intercept line passes through the origin. But in the present study, since the intercept line does not pass through the origin, so it is confirmed that the intra particle diffusion is not the only rate controlling step. Since, from the Fig. 6.5(A, B, C & D) it is seen that,  $R^2$  values of all kinetic models are almost near to 1. The value of chi square ( $\chi^2$ ) is lowest for pseudo second order kinetic (in Table 6.1), so the pseudo second order kinetic model was found to be the best fitting model ( $R^2 = 0.997$ ) for arsenic adsorption on CBP. Again along with these, the calculated  $q_e$  value (= 0.03 mg/g) from the pseudo second order kinetic is almost equivalent with experimental  $q_e$  value (= 0.03 mg/g), which is far apart from the pseudo first order kinetic model. As the value of correlation coefficients ( $R^2$ ) of all kinetic models are greater than 0.9, so it can be said that, other processes also may be operating simultaneously with pseudo second order kinetics [16,17].

**Table 6.1: Comparison of pseudo first order, pseudo second order, intra particle diffusion and Elovich model rate constants and calculated  $q_e$  values using CBP as adsorbent**

Pseudo first order $\log (q_e - q_t) = \log q_e - k_1(t/2.303)$		Pseudo second order $t/q_t = [1/(k_2 q_e^2)] + t/q_e$		Elovich $q_t = 1/b [\ln(ab)] + 1/b [\ln t]$		Intraparticle diffusion $q_t = k_d t^{1/2} + C$	
$k_1$ ( $\text{min}^{-1}$ )	5.66	$k_2$ ( $\text{g mg}^{-1} \text{min}^{-1}$ )	3.2	$b$ ( $\text{g mg}^{-1}$ )	1000	$k_d$ ( $\text{mg g}^{-1} \text{min}^{-1/2}$ )	0.0004
$q_e$ , (cal) ( $\text{mg g}^{-1}$ )	0.31	$q_e$ , (cal) ( $\text{mg g}^{-1}$ )	0.03	$a$ ( $\text{mg g}^{-1} \text{min}^{-1}$ )	$1.7 \times 10^5$	C	0.02
$R^2$	0.901	$R^2$	0.997	$R^2$	0.932	$R^2$	0.992
$\chi^2$	$3.76 \times 10^{-4}$	$\chi^2$	$1.68 \times 10^{-7}$	$\chi^2$	$6.06 \times 10^{-7}$	$\chi^2$	$6.56 \times 10^{-7}$





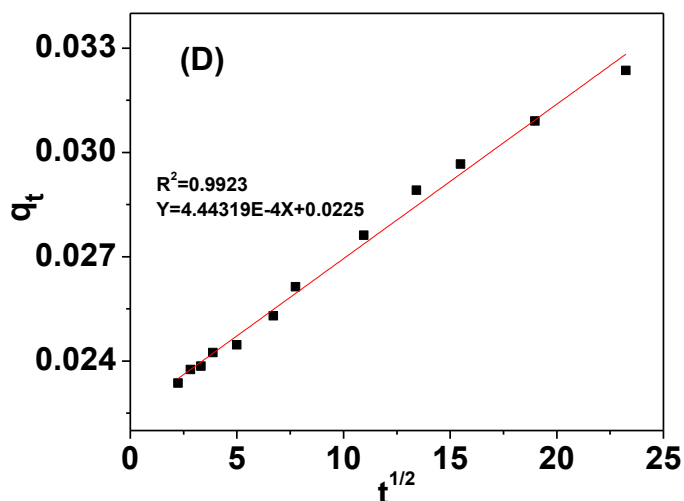


**Fig 6.5: Graph (A), (B), (C) and (D) are the Psuedo first order, psuedo second order, Elovich model and Intra Particle diffusion of kinetics study.**

#### **f) Adsorption isotherms study**

Adsorption isotherms give the information about the distribution of adsorbed molecules between the surface of the adsorbent and the liquid solutions at equilibrium. Adsorption isotherm study gives the information on the efficiency of the adsorbent at a particular temperature. Nine experiments in total were carried out to access the type of isotherm for adsorption of arsenic on the adsorbent CBP. For each experiment 0.35 g adsorbent was added to 25 mL of spiked arsenic solution of different concentration (0.298-5.03 mg/L and pH=7) and stirred for 3 hours at constant temperature 30°C. Three most commonly used models Langmuir, Freundlich and Temkin were taken to study the adsorption occurring in the set up.

#### **Langmuir adsorption isotherm**

Langmuir adsorption isotherm model describe the formation of monolayer of adsorbate molecule on the surface of the adsorbent containing a large number of identical sites [18]. From the slope and intercept of the linear plot of  $C_e/q_e$  against  $C_e$ , (from equation 7 of chapter 1) in Fig. 6.6(A), the Langmuir maximum adsorption capacity  $q_m$  and equilibrium constant  $b$  were calculated. The separation factor or equilibrium parameter  $R_L$  also calculated from the equation 8 of chapter 1.

### Freundlich adsorption isotherm

Freundlich isotherm generally explain the adsorption behaviour of heterogeneous surface. Freundlich adsorption constant i.e., the adsorption capacity of adsorbent  $K_f$  and intensity of adsorption  $n$  are calculated (from equation 9 of chapter 1) from the linear plot of  $\log q_e$  versus  $\log C_e$ , in Fig. 6.6(B). The value of  $n$  indicates the affinity of adsorbent towards the adsorbate.

### Temkin adsorption isotherm

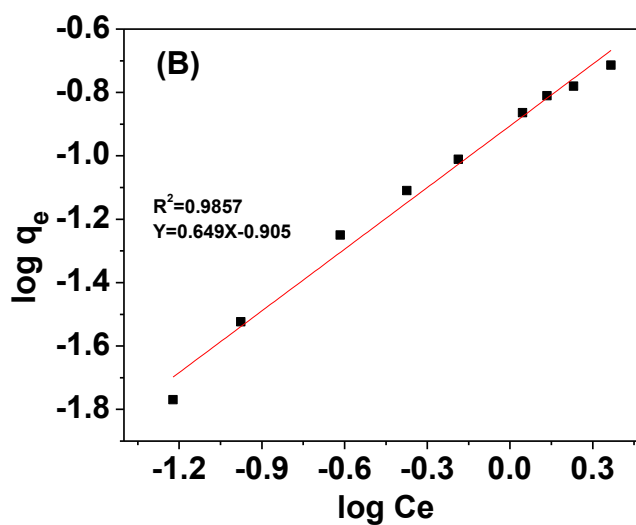
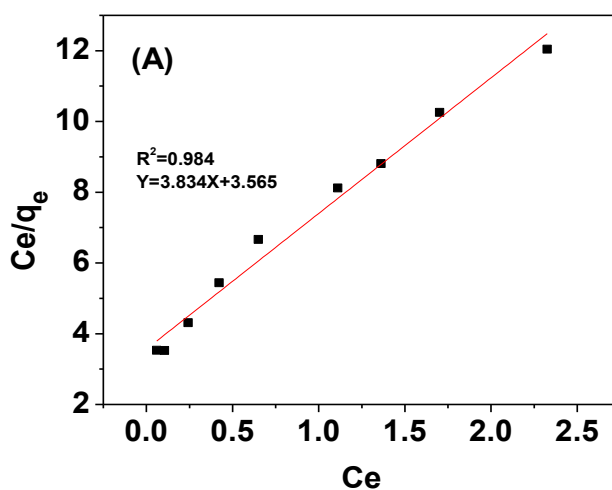
Temkin and Pyzhev assumed that, the heat of adsorption normally decreases linearly rather than logarithmically with surface coverage [19,20,21]. This isotherm model considered the effects of indirect adsorbent-adsorbate interactions on adsorption. The Temkin isotherm constant  $A_T$  (L/g) and  $B_T$  (where  $B_T = RT/b_T$ ,  $b_T$  is the Temkin constant and  $R$  is the gas constant) (from equation 10 of chapter 1) are calculated from the intercept and the slope of the plot of  $q_e$  against  $\ln C_e$  from Fig 6.6(C).

The corresponding Langmuir, Freundlich, and Temkin parameters along with correlation coefficients ( $R^2$ ) and chi square ( $\chi^2$ ) values are given in Table 6.2. From the table, it is seen that the Langmuir maximum adsorption capacity  $q_m$  is  $0.26 \text{ mg g}^{-1}$  and the equilibrium constant  $b$  is  $1.07 \text{ Lmg}^{-1}$ . The value of dimensionless constant separation factor or equilibrium parameter  $R_L$  gives the acceptability of the Langmuir model in Fig. 6.6(D) to fit the data when  $R_L$  is in between 0 and 1. In our study, the value of Langmuir isotherm, the separation factor or equilibrium parameter,  $R_L$  lay in the range  $0 < R_L < 1$ , indicates that the arsenic adsorption on CBP is favourable under the conditions of experiments and takes place as monolayer adsorption on the surface that is homogenous in adsorption affinity [22]. The value of Freundlich adsorption constant i.e., the adsorption capacity of adsorbent  $K_f$  is  $0.12 \text{ mg}^{1-1/n} \text{ L}^{1/n} \text{ g}^{-1}$ . The value of  $n$  ( $=1.54$ ) at equilibrium lies in between 1 and 10 indicates the favourable adsorption. Again, the plot of  $\log q_e$  versus  $\log C_e$  (from equation 5 of chapter 1), giving a straight line that indicates the confirmation of Freundlich adsorption isotherm. From the correlation coefficients, it can be said that, Temkin isotherm model of adsorption may also be significant in this case. The order of favourability of arsenic adsorption on CBP is Freundlich ( $R^2=0.986$ ) > Langmuir ( $R^2=0.984$ ) > Temkin ( $R^2=0.952$ ). Again as the value of chi square ( $\chi^2$ ) is lowest for Freundlich adsorption isotherm, so it can be concluded that the Freundlich isotherm model is more fitted than the Langmuir isotherm model for the

experimental data because of the highest value of correlation coefficient. Based upon the Langmuir model, the maximum arsenic adsorption capacity of CBP is 0.26 mg/g.

**Table 6.2: Langmuir, Freundlich, and Temkin parameters along with correlation coefficients**

Langmuir Isotherm		Freundlich Isotherm		Temkin Isotherm	
b (Lmg <sup>-1</sup> )	1.07	K <sub>f</sub> (mg <sup>1-1/n</sup> L <sup>1/n</sup> g <sup>-1</sup> )	0.12	A <sub>T</sub> (L g <sup>-1</sup> )	1.00
q <sub>m</sub> (mg g <sup>-1</sup> )	0.26	n	1.54	B <sub>T</sub> (Jmol <sup>-1</sup> )	0.05
R <sup>2</sup>	0.984	R <sup>2</sup>	0.986	R <sup>2</sup>	0.952
R <sub>L</sub>	0.15-0.75				
χ <sup>2</sup>	0.13804	χ <sup>2</sup>	0.00173	χ <sup>2</sup>	0.0018



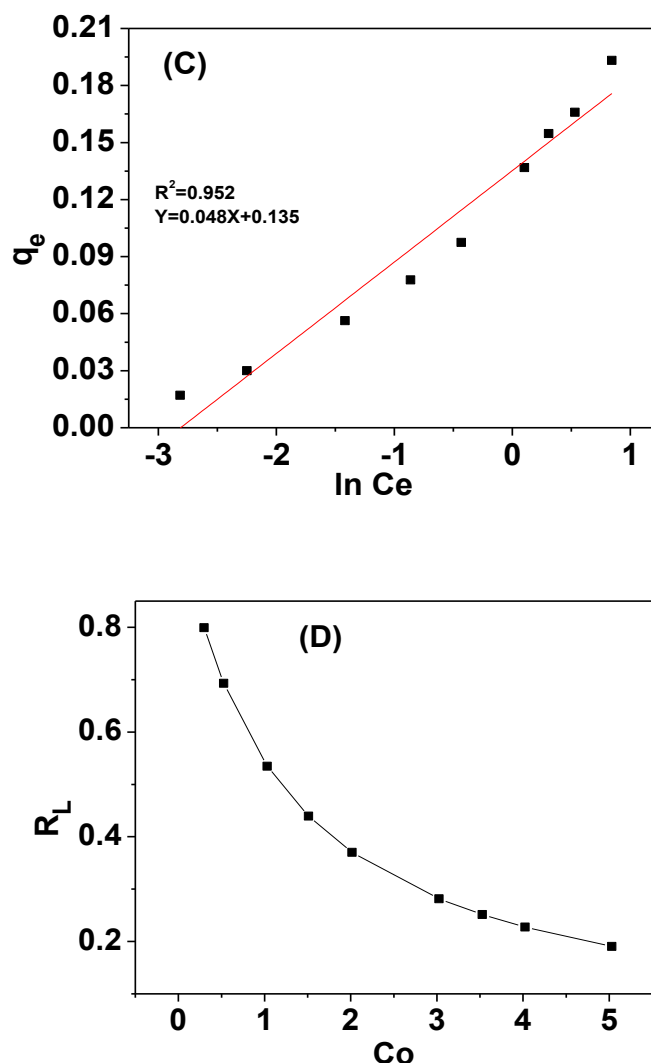


**Fig 6.6: (A) Langmuir, (B) Freundlich, (C) Temkin adsorption isotherm of CBP and (D) graph of  $R_L$  vs  $C_0$**

#### g) Effect of temperature on arsenic adsorption

Amongst the various factors, temperature is one of the important which can affect the efficiency of adsorption in a given adsorbate-adsorbent system. So for the study of influence of temperature on adsorption of arsenic onto the surface of CBP was studied at the temperatures of 20°, 25°, 30°, 40° and 50° C. For this experiment 0.35 g adsorbent per 25 mL of 0.5 mg/L arsenic solution of pH 7 was taken. From the Fig 6.7, it is seen that, percentage of arsenic removal increases with increasing temperature, i.e., adsorption of arsenic onto CBP is endothermic adsorption. Since higher temperature favours increased adsorption, so the type of adsorption is chemisorptions in nature.

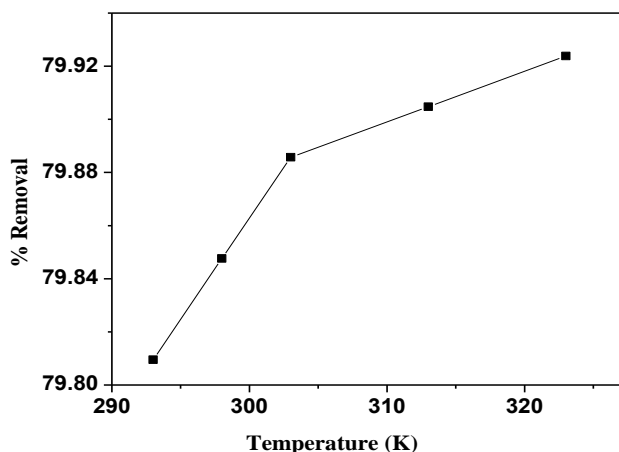


**Fig 6.7: Effect of temperature on arsenic adsorption by CBP**

#### **h) Effect of other anions on arsenic adsorption**

In presence of various anions the arsenic sorption capacity is also very important. In this experiment, arsenic sorption capacity was determined in the presence of each anion of 50 mg/L in optimum condition. From the Fig 6.8, it has been observed that chloride ions showed least effect but the carbonate ions have highest effect on the removal of As(V) towards the active site and thereby decreasing the sorption capacity of As(V). The decreasing As(V) adsorption capacity for the adsorbent CBP follows the order

Chloride < bromide < bicarbonate < fluoride < sulphate < carbonate.

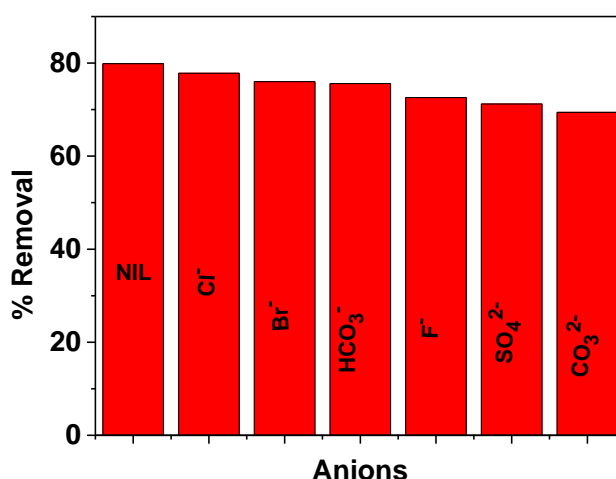


**Fig 6.8: Bar diagram showing the effect of competitive anions on the adsorption of arsenic by CBP**

**6.3.A.2: Simultaneous adsorption of fluoride and arsenic from real ground water**

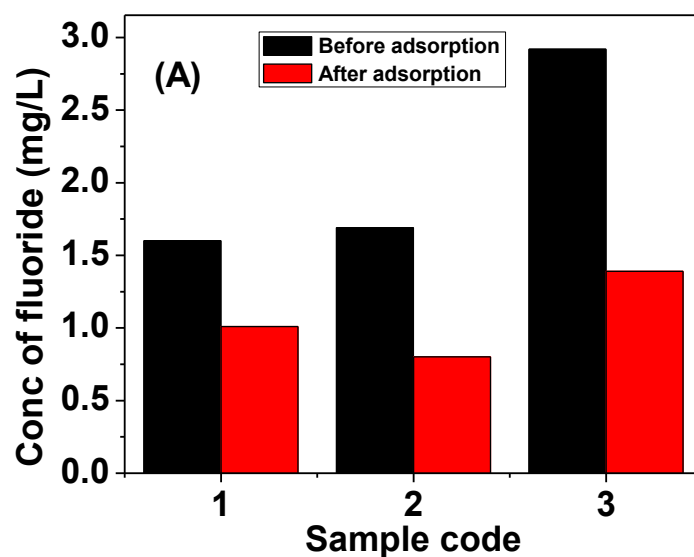
In chapter 2, it is mentioned that total 247 number of groundwater samples were collected for the assessment of groundwater quality of Golaghat district of Assam. The selected three groundwater samples (two from Padumoni block development area and one from Gamariguri block development area) were taken for the removal of both fluoride and arsenic by using carbon of banana plant (CBP). The chemical composition (already determined by ISO method) of these three natural water samples are given in the Table 6.3. 25 mL of each sample was treated with 0.35 g of CBP for 3 hours. Concentration of fluoride and arsenic in the groundwater samples before and after treatment with CBP are given in Table 6.4. It is seen that amount of both fluoride and arsenic decreases considerably and it is possible to bring the level of fluoride and arsenic below the maximum permissible limits by the BIS [23] which is for fluoride 1.5 mg/L and for arsenic 0.05 mg/L.

**Table 6.3: Chemical composition of real life ground water collected from different places of Golaghat district of Assam, India**

Parameters	Name of places and serial numbers		
	1. Bosa Kumar gaon (Padumoni block)	2. Salikihat (Padumoni block)	3. Borjan (Gamariguri block)
<b>Total alkalinity(mg/L)</b>	341	218	367
<b>TH (mg/L)</b>	116	140	44.8
<b>pH</b>	6.9	6.8	7.5
<b>Turbidity (NTU)</b>	20	50	45
<b>EC (mS/cm)</b>	0.069	0.051	0.138
<b>Sodium (mg/L)</b>	111.9	52.9	150
<b>Potassium (mg/L)</b>	2.8	2.4	2.4
<b>Chloride</b>	15	20	20
<b>Fluoride (mg/L)</b>	1.6	1.69	2.92
<b>Arsenic (mg/L)</b>	0.168	0.108	0.077
<b>Nitrate (mg/L)</b>	22	5	25
<b>Iron (mg/L)</b>	0.125	0.15	0.1

**Table 6.4:** The residual amount of fluoride and arsenic of collected real life ground water after treatment with CBP

Parameters		Name of places and serial numbers		
		1. Bosa Kumar gaon	2. Salikihat	3. Borjan
Fluoride	Concentration(mg/L) before adsorption	1.6	1.69	2.92
	Concentration(mg/L) after adsorption	1.01	0.802	1.39
	% Removed	36.88	52.54	52.39
Arsenic	Concentration(mg/L) before adsorption	0.168	0.108	0.077
	Concentration(mg/L) after adsorption	0.033	0.021	0.017
	% Removed	79.83	79.95	77.55





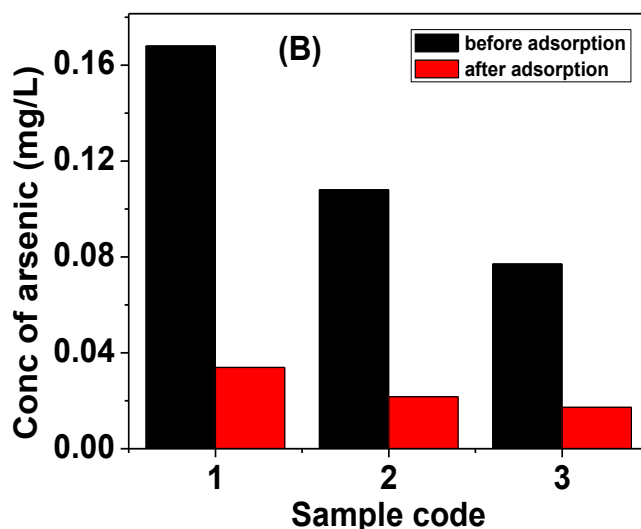


**Fig 6.9: Bar diagram of concentration of fluoride (A) and arsenic (B) in natural water before and after adsorption by CBP**

### 6.3.A.3: Characterization of CBP after arsenic adsorption

#### a) Study of FESEM images & EDX spectra

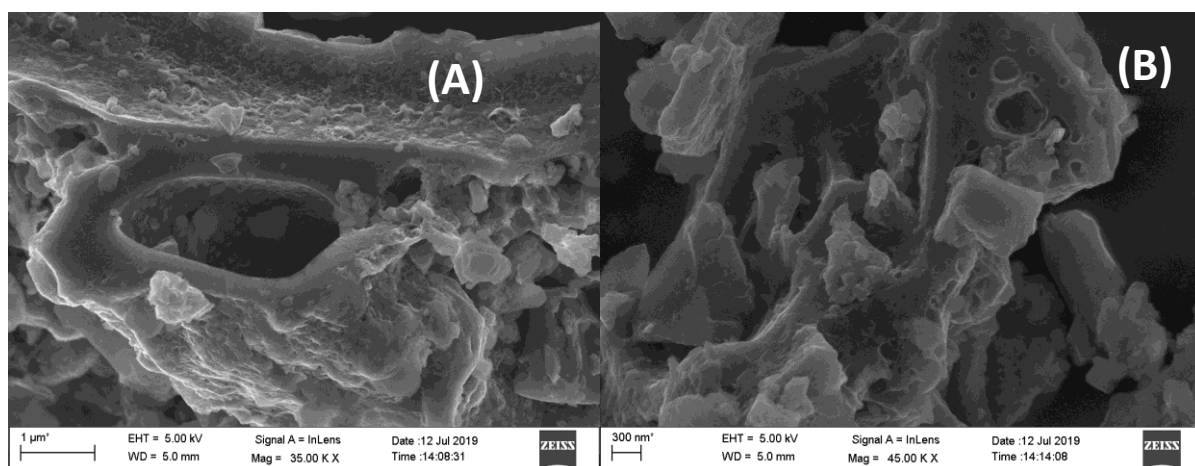


**Fig 6.10: FESEM images of CBP (A) & (B) after adsorption of arsenic at various magnification**

After arsenic adsorption, the SEM images of CBP were taken at different magnifications and shown in Fig 6.10. It is seen that the surface of CBP after adsorption of arsenic is changed from the SEM images of raw CBP (Fig 4.10 from chapter 4). There is no significant deformation in the structural organization of the platy CBP particles where the adsorption of arsenic species generally takes place, however there is a decrease of heterogenous nature of adsorbent mass e.g decrease of presence of acicular salt like crystals

are seen in the FESEM images in comparison to the FESEM images (Fig 4.9 of chapter 4) of freshly prepared adsorbents. Probably, the acicular salt crystals were dissolved out during the contact with aqueous arsenate solution. This adsorption and dissolution behavior as well as retention of As in CBP surface is further supported by EDX analysis (Fig 6.11 and Table 6.5) and FTIR study.

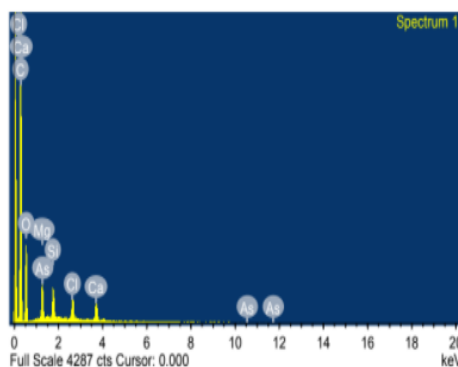


Fig 6.11: EDX spectra of CBP after adsorption of arsenic

Table 6.5: Elemental composition of CBP from EDX spectra, after adsorption of arsenic

Element	C	O	Mg	Si	Cl	Ca	As	Total
Weight%	65.15	28.87	1.78	1.41	1.23	1.44	0.12	100.00
Atomic%	73.06	24.3	0.99	0.68	0.47	0.48	0.02	100.00

#### b) Study of FT-IR spectra

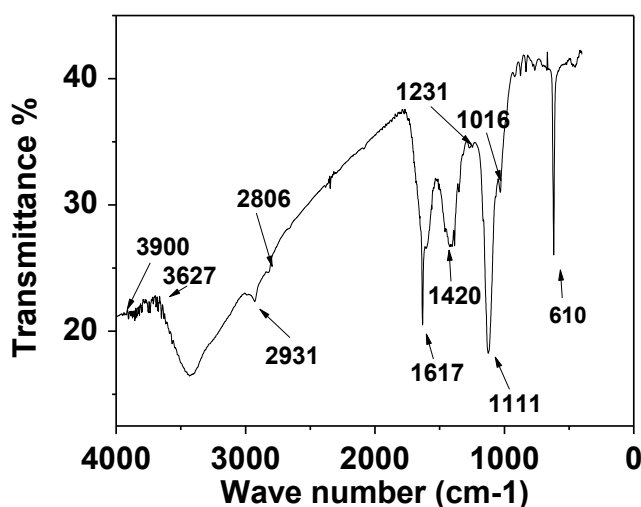


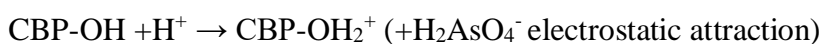
Fig 6.12: FT-IR spectra of CBP after adsorption of arsenic

After adsorption of arsenic, to study the interaction between arsenic ion and the active sites present on the surface of CBP, FTIR spectroscopy was carried out and the spectra is given in the Fig 6.12. A close examination of the Fig 6.12 reveals the slight shift of asymmetric bending vibration, asymmetric stretching vibration of C-H of alkene from 1412 (Fig 4.11 from chapter 4) and 2928 to 1420 and 2931  $\text{cm}^{-1}$  respectively. The shifting of C=O stretching vibration frequency from 1680 to 1617  $\text{cm}^{-1}$  indicates that the functional groups are mainly responsible for binding of arsenic via adsorbent [18].

So from the above SEM images, EDX spectra and FT-IR spectrum attributed to the adsorption of arsenic on the adsorbent carbon of banana plant (CBP).

#### 6.3.A.4: Mechanism of adsorption of arsenic on CBP

The carbon of banana plant (CBP) is naturally functionalized by -OH, -COOH, and -C=O groups. At lower pH, the hetero atoms O and H undergo protonation and they release a lone pairs of electrons [24]. These lone pair electrons develop a positive charge and then they participate in the adsorption of arsenic.



### SECTION B: IOCS AS AN ADSORBENT

#### 6.3.B.1: Results and discussion of Arsenic adsorption studies using IOCS

##### a) Effect of adsorbent dosage

The adsorbate concentration plays a significant role in adsorption process. A given amount of adsorbent can adsorb a certain amount of adsorbate to establish equilibrium. The effect of initial concentration of arsenic solution (0.2-2.0 mg/L) with 0.35 g of IOCS were taken in a set of experimental flasks. In the Fig 6.13, the highest 99.78 % removal by IOCS showed at 2.0 mg/L arsenic solution. Since, the percentage of arsenic removal capacity of IOCS is increased (from 96 %-98.98 %) at a constant rate from 0.2 mg/L to 0.5 mg/L of arsenic concentration and then decreased the rate of removal percentage up to the arsenic concentration 2.0 mg/L. This is because at higher concentration the available sites on the surface of adsorbent for adsorption become fewer in comparison to lower concentration. The optimum arsenic concentration is chosen as 0.5 mg/L to carry out the experiment.

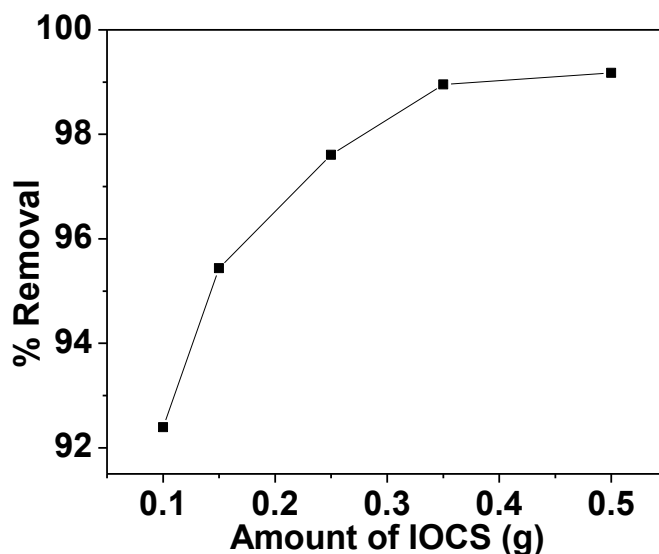


**Fig 6.13: Effect of adsorbents dose on percent removal of As (V) at 30°C in the pH of 7 with 45 minutes stirring.**

**b) Effect of initial concentration of arsenic solution**

The adsorbate concentration plays a significant role in adsorption process. A given amount of adsorbent can adsorb a certain amount of adsorbate to establish equilibrium. The effect of initial concentration of arsenic solution (0.2-2.0 mg/L) with 0.35 g of IOCS were taken in a set of experimental flasks. In the Fig 6.14, the highest 99.78 % removal by IOCS showed at 2.0 mg/L arsenic solution. Since the percentage of arsenic removal capacity of IOCS is increased (from 96 %-98.98 %) at a constant rate from 0.2 mg/L to 0.5 mg/L of arsenic concentration and then decreased the rate of removal percentage up to the arsenic concentration 2.0 mg/L. This is because at higher concentration the available sites on the surface of adsorbent for adsorption become fewer in comparison to lower concentration. The optimum arsenic concentration is chosen as 0.5 mg/L to carry out the experiment.

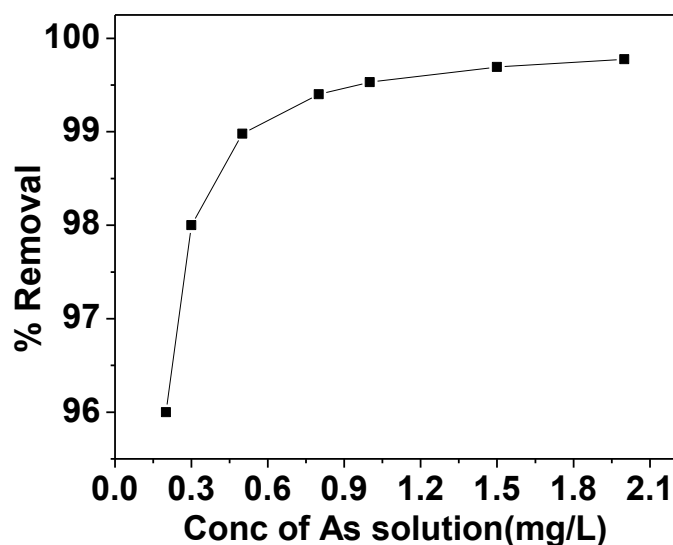


**Fig 6.14: Effect of initial concentration of arsenic solution on percent removal by IOCS at 30°C in a pH of 7 with 45 minutes stirring.**

### c) Effect of pH on As (V) adsorption

The removal of a species from aqueous solution by adsorption process is influenced by pH of the solution. Because pH changes over all surface charge of the adsorbent, especially the charges of surface functional group of adsorbent and change the ionization and species of the adsorbate [7,8]. The pH affect on arsenic removal percentage was studied by using 0.35 g of adsorbent in each 25 mL of 0.5 mg/L arsenic solution of pH range 2.8-11. Fig.6.15 shows that there is no vast change in adsorption of arsenic on IOCS from pH 2.8 to 7 although it increases from 97.8 to 98.98 and thereafter it decreases abruptly up to pH 11. The maximum arsenic % removal capacity of the adsorbent IOCS is 98.98 % in neutral condition, which is attributed due to the formation of surface complexation on the adsorbent at pH 7 [10,11]. At this pH, for As (V),  $\text{H}_2\text{AsO}_4^-$  species is the predominant. The maximum removal of As (V) at pH 7.5 was also noted by Stenkamp [25] on iron oxide coated sand using as an adsorbents. The results also show that in highly acidic medium, where the adsorbent's surfaces are highly protonated and As (V) mostly exist in the form of neutral  $\text{H}_3\text{AsO}_4$  species [26]. Again the optimum pH = 7 can be explained as a result of formation of positive charge (as pH ZPC of IOCS is 7.8) and electrostatic interaction between the surface charge of the adsorbent and arsenateion. Decrease of arsenic removal capacity in alkaline medium can be explained due to repulsion between arsenate and negative charge of adsorbent surface i.e., availability of  $-\text{OH}^-$  ions [14].

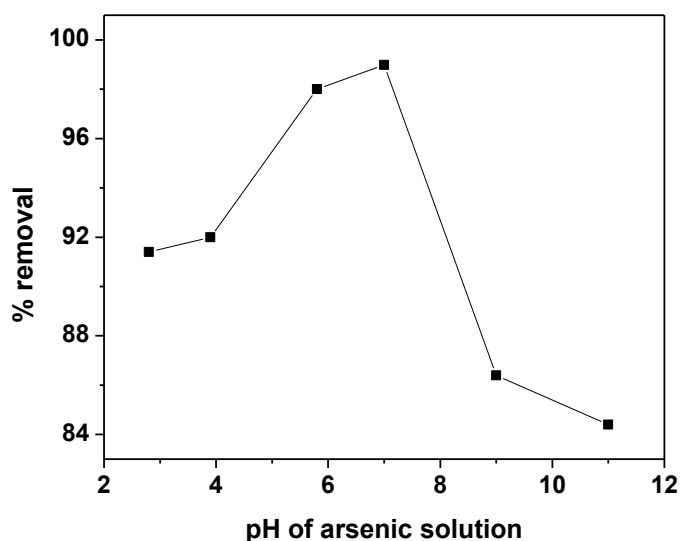


**Fig 6.15: Effect of pH of arsenic solution on percent removal of arsenic by IOCS at 30°C**

**d) Effect of contact time**

The contact time between adsorbent surface and adsorbate plays a significant role in the adsorption process. A given amount of adsorbent can adsorb a certain amount of adsorbate at a given time to establish equilibrium. For the investigation of maximum adsorption efficiency, effect of contact time between arsenic solution and adsorbent IOCS was studied. This experiment was carried out at pH 7 by taking 0.35 g adsorbent per 25 mL of 0.5 mg/L arsenic solution at different contact times from 5-180 min. Fig. 6.16 shows that percentage of arsenic removal efficiency rapidly increases with increasing contact time up to 45 minute and then rate of increasing of adsorption decreases gradually. The fast and rapid adsorption rate at the initial stage may be explained by large availability of the number of active binding sites on the adsorbent surface and after a lapse of time, due to repulsion between the adsorbed solute species on the surface of the adsorbent and the bulk phase, adsorption i.e., percent removal efficiency decreases. Therefore, 45 minute is chosen as the optimum time for carry out the experiment.

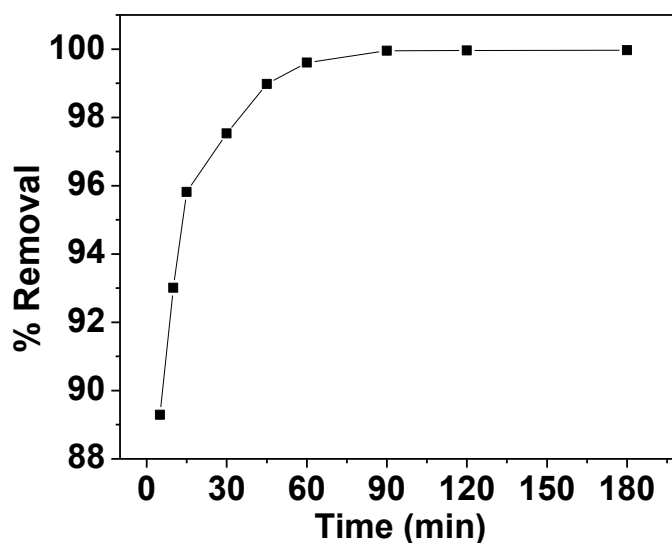


Fig 6.16: Effect of contact time on the adsorption of arsenic at 30°C

#### e) Adsorption kinetics Study

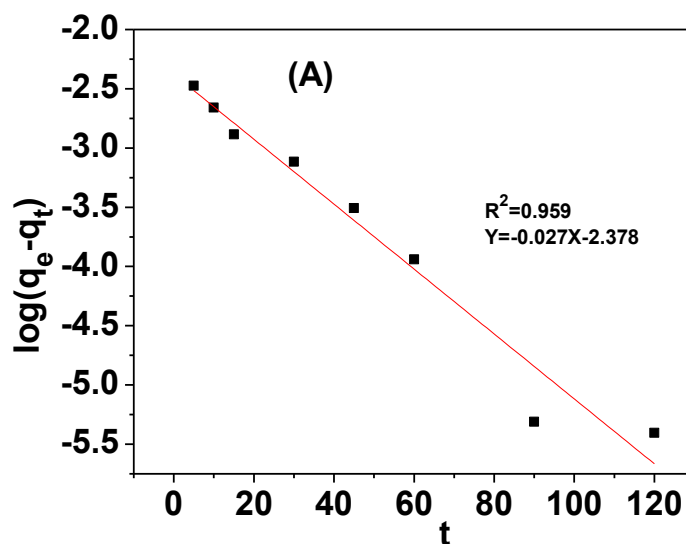
In this study pseudo first order, pseudo second order, Elovich and intra particle diffusion models (linear equations 3, 4, 5 & 6 of chapter 1) were used to interpret the kinetics of arsenic adsorption on IOCS. This adsorption kinetic study was carried out at optimum condition i.e., by taking 0.35 g adsorbent per 25 mL of 0.5 mg/L arsenic solution at pH 7 and at temperature 30°C.

The resulting data of adsorption kinetic model are tabulated in Table 6.6. Pseudo first order rate constant,  $k_1$  ( $= 0.06 \text{ min}^{-1}$ ) and first order adsorption capacity i.e amount of adsorption at equilibrium  $q_e$  ( $= 0.004 \text{ mg/g}$ ) were calculated from the Fig. 6.17(A). Pseudo second order rate constant,  $k_2$  ( $= 46.51 \text{ g mg}^{-1} \text{ min}^{-1}$ ) and second order adsorption capacity,  $q_e$  ( $= 0.03 \text{ mg/g}$ ) were determined by plotting  $t/q_t$  against  $t$  in Fig. 6.17(B).  $R^2$  value ( $R^2=0.999$ ) suggests that the adsorption data followed the Pseudo second order kinetic equation. In case if Elovich kinetic model, from the plot of  $q_t$  versus  $\ln t$  in Fig. 6.17(C) the value of initial adsorption rate  $a$  ( $= 8.79 \times 10^{26} \text{ mg g}^{-1} \text{ min}^{-1}$ ) and the desorption constant  $b$  ( $= 1111.11 \text{ g/mg}$ ) were calculated. In Intra Particle Diffusion model, the rate of intra-particle diffusion controls adsorption kinetics. From the linear equation of intra-particle diffusion model (equation number 6, chapter 1), plot of  $q_t$  versus  $t^{1/2}$  in plot (Fig 6.17(D)), it is seen that there are three portion AB, BC and CD. The initial curve portion AB is because of external mass transfer, intermediate BC portion due to intra-particle diffusion and the plateau portion CD to the equilibrium stage where intra-particle diffusion starts to slow down due to extremely low

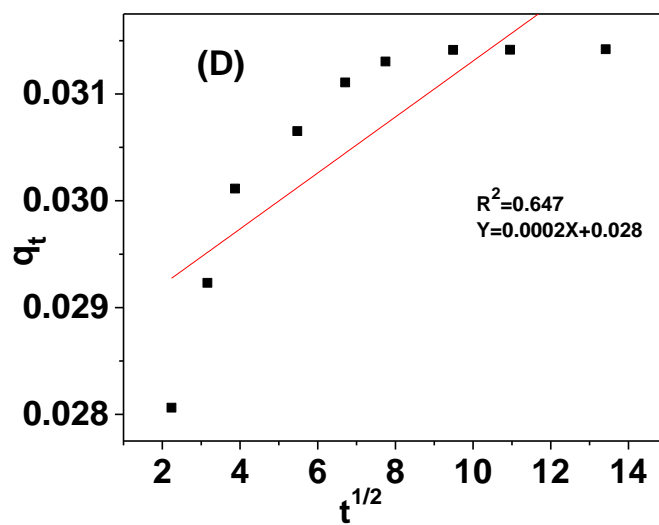
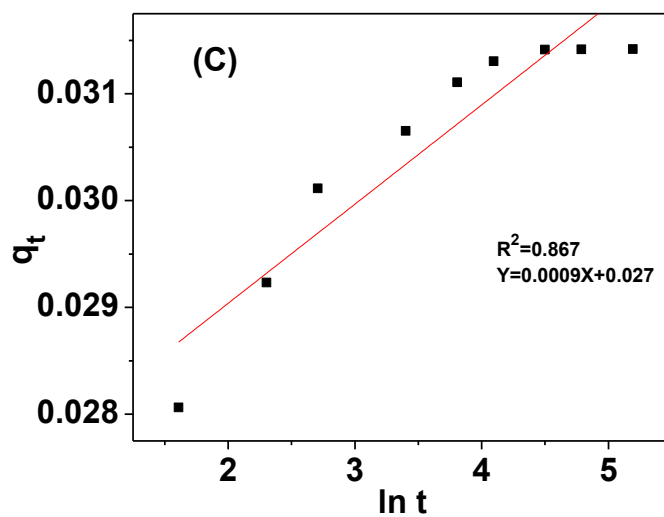
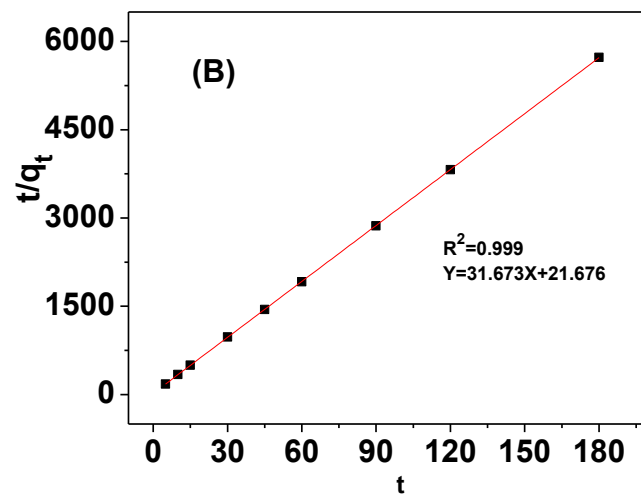
solute concentrations in the solution [27]. However, from the linear fitting of  $q_t$  versus  $t^{1/2}$  (Fig. 6.18(D)),  $k_d$  ( $=2.62 \text{ mgg}^{-1} \text{ min}^{-1/2}$ ),  $C$  ( $=0.03$ ) and the correlation coefficient ( $R^2=0.647$ ) were calculated and these values means the less significance of this model.

**Table 6.6: Comparison of pseudo first order, pseudo second order, Elovich and intra particle diffusion model rate constants and calculated  $q_e$  values using IOCS as adsorbent**

Kinetic model	$R^2$	Constant	Value
<b>Pseudo first order</b> $\log(q_e - q_t) = \log q_e - k_1(t/2.303)$	0.959	$k_1 (\text{min}^{-1})$	0.06
		$q_{e, \text{cal}} (\text{mg g}^{-1})$	0.004
<b>Pseudo second order</b> $t/q_t = [1/(k_2 q_e^2)] + t/q_e$	0.999	$k_2 (\text{g mg}^{-1} \text{ min}^{-1})$	46.51
		$q_{e, \text{cal}} (\text{mg g}^{-1})$	0.03
<b>Elovich</b> $q_t = 1/b[\ln(ab)] + 1/b[\ln t]$	0.867	$b (\text{g mg}^{-1})$	1111.11
		$a (\text{mgg}^{-1} \text{ min}^{-1})$	$8.795 \times 10^{26}$
<b>Intraparticle diffusion</b> $q_t = k_d t^{1/2} + C$	0.647	$k_d (\text{mgg}^{-1} \text{ min}^{-1/2})$	0.0002







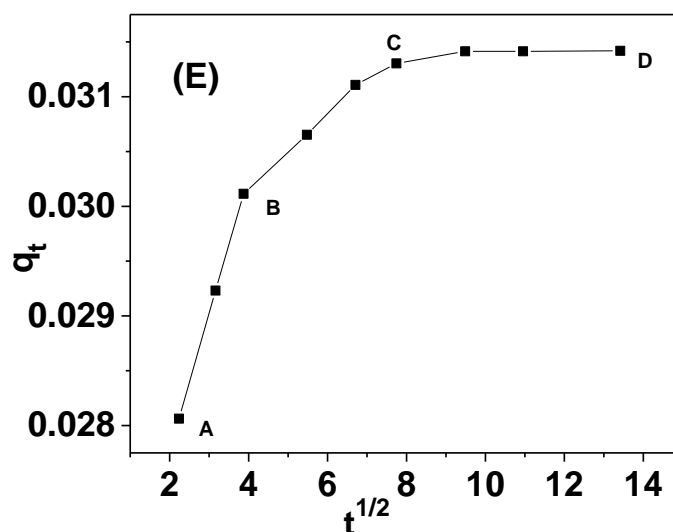


**Fig 6.17: Plot (A) pseudo-first-order kinetic model; (B) pseudo second- order kinetic model; (C) Elovich model; (D) Linear plot of intra particle diffusion model and (E) Non linear plot of intra particle diffusion model.**

#### **f) Adsorption isotherms Study**

An adsorption isotherm represents the equilibrium relationship between the adsorbate concentration in the liquid phase and that on the adsorbents surface at a given condition. Adsorption isotherm study gives information on the efficiency of the adsorbent at a particular temperature. Five experiments in total were carried out to access the type of isotherm for adsorption of arsenic on the adsorbent IOCS. For each experiment 0.35 g adsorbent was added to 25 mL of spiked arsenic solution of different concentration (0.2-2.0 mg/L and pH=7) and stirred for 45 minutes at constant temperature 30°C. Three most commonly used models Langmuir, Freundlich and Temkin were taken to study the adsorption occurring in our set up.

#### **Langmuir adsorption isotherm**

Langmuir adsorption isotherm explains quantitatively the formation of monolayer on the surface of the adsorbent containing a large number of identical sites. From the slope and intercept of the linear plot of  $C_e/q_e$  against  $C_e$ , (from equation 7 of chapter 1) in Fig. 6.18(A) the Langmuir maximum adsorption capacity  $q_m$  and equilibrium constant  $b$  are calculated. The separation factor or equilibrium parameter  $R_L$  also calculated from the equation 8 of chapter 1.

**Freundlich adsorption isotherm**

Freundlich isotherm generally explain the adsorption behaviour of heterogeneous surface and it agrees with the Langmuir isotherm equation and experimental data in some extent of concentration range. Freundlich adsorption constant i.e., the adsorption capacity of adsorbent  $K_f$  and intensity of adsorption  $n$  are calculated (from equation 9 of chapter 1) from the linear plot of  $\log q_e$  versus  $\log C_e$ , in Fig. 6.18(B). The value of  $n$  indicates the affinity of adsorbent towards the adsorbate.

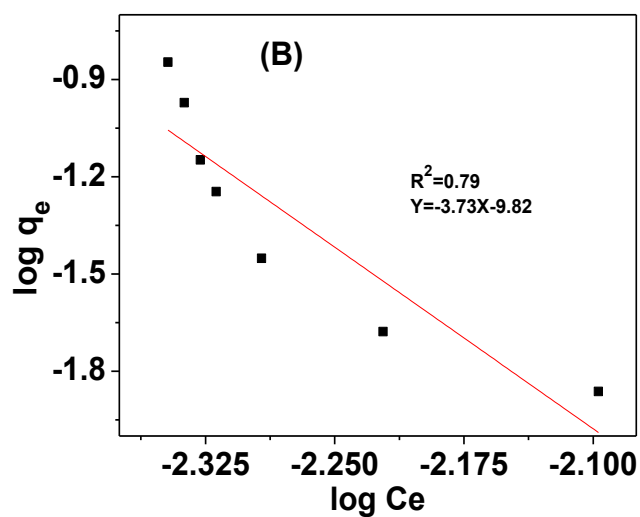
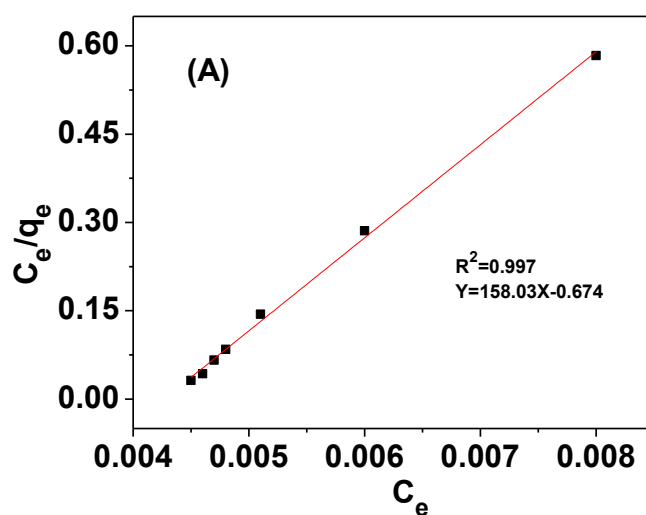
**Temkin adsorption isotherm**

Temkin and Pyzhev considered the effects of indirect adsorbate/adsorbate interactions on adsorption isotherms and assumed that the free energy of adsorption is a function of the surface coverage [19,20,21]. The Temkin isotherm constant  $A_T$  (L/g) and  $B_T$  (where  $B_T = RT/b_T$ ,  $b_T$  is the Temkin constant and  $R$  is the gas constant) are calculated from the intercept and the slope of the plot of  $q_e$  against  $\ln C_e$  from Fig 6.18(C).

The corresponding Langmuir, Freundlich, and Temkin parameters along with correlation coefficients are given in Table 6.7. From the table, it is seen that the Langmuir maximum adsorption capacity  $q_m$  is  $0.006 \text{ mg g}^{-1}$  and the equilibrium constant  $b$  is  $234.759 \text{ Lmg}^{-1}$ . The value of dimensionless constant separation factor or equilibrium parameter  $R_L$  gives the acceptability of the Langmuir model in Fig. 6.18(D) to fit the data when  $R_L$  is in between 0 and 1. In our study, the value of Langmuir isotherm, the separation factor or equilibrium parameter,  $R_L$  lay in the range  $0 < R_L < 1$ , indicates that the arsenic adsorption on IOCS is favourable under the conditions of experiments and takes place as monolayer adsorption on the surface that is homogenous in adsorption affinity [22]. In Freundlich adsorption isotherm, the value of  $n=0.26$  at equilibrium does not lie in between 1 and 10 indicates the unfavourable adsorption. Again, the plot of  $\log q_e$  versus  $\log C_e$  (from equation 5 of chapter 1), giving the information about the unfavourability of Freundlich adsorption isotherm. From the correlation coefficients, it can be said that, Temkin isotherm model of adsorption may also be significant in this case. The order of favourability of arsenic adsorption on IOCS is Langmuir ( $R^2=0.997$ ) > Freundlich ( $R^2=0.79$ ) > Temkin ( $R^2=0.478$ ). Again, the chi square test was analyzed to identify the best fitted isotherm model by using equation 10 of chapter 1. It is seen that, Langmuir isotherm have lowest ( $\chi^2$ ) value among the other adsorption isotherm models, so the Langmuir isotherm model can be concluded as the more fitted model than the Freundlich isotherm model for the experimental data.

Table 6.7: Langmuir, Freundlich, and Temkin parameters along with correlation coefficients

Langmuir Isotherm		Freundlich Isotherm		Temkin Isotherm	
b (Lmg <sup>-1</sup> )	234.759	K <sub>f</sub> (mg <sup>1-1/n</sup> L <sup>1/n</sup> g <sup>-1</sup> )	1.51x10 <sup>-10</sup>	A <sub>T</sub> (L g <sup>-1</sup> )	78342
q <sub>m</sub> (mg g <sup>-1</sup> )	0.006	n	0.26	B <sub>T</sub> (Jmol <sup>-1</sup> )	-0.170
R <sup>2</sup>	0.997	R <sup>2</sup>	0.79	R <sup>2</sup>	0.478
R <sub>L</sub>	0.02-0.002				
χ <sup>2</sup>	9.35x10 <sup>-5</sup>	χ <sup>2</sup>	0.0286	χ <sup>2</sup>	0.0116



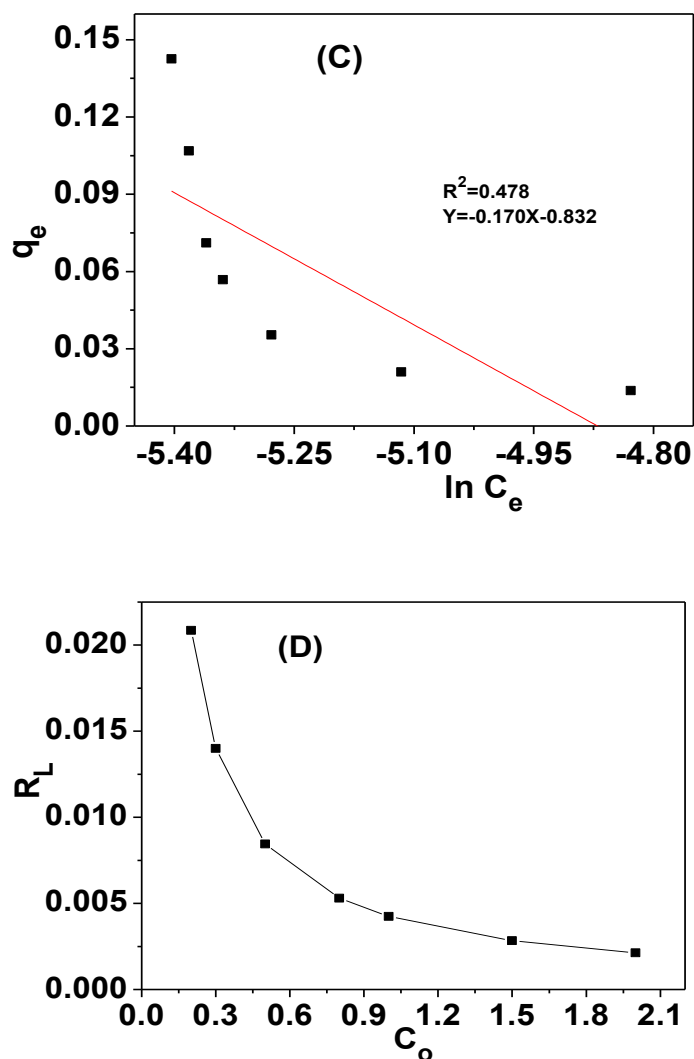


Fig 6.18: (A) Langmuir, (B) Freundlich, (C) Temkin isotherms of arsenic adsorption by IOCS and (D) graph of  $R_L$  vs  $C_o$

#### g) Effect of Temperature on arsenic adsorption

Effect of temperature on adsorption of arsenic was investigated at the temperature range of 293-323 K. From the Fig 6.19, it is seen that the arsenic adsorption efficiency increases from 293-323 K temperature. The viscosity in aqueous solution is decreased by increasing the temperature. In addition to that, the release of adsorbent molecules is increased across the external boundary layer and in the pores of adsorbent particles, hereby resulting in increased removal efficiency [28,29,30].

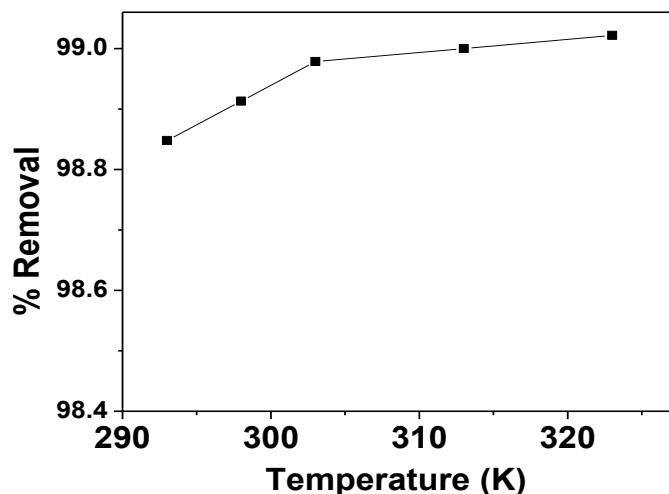


Fig 6.19: Effect of temperature on arsenic adsorption by IOCS

From the slope and intercept of the plot of  $\ln K_d$  versus  $1/T$  (Fig 6.20), the change of enthalpy  $\Delta H^0$  and the change of entropy  $\Delta S^0$  were calculated. And the calculated values of all the thermodynamic parameters are given in the Table 6.8.

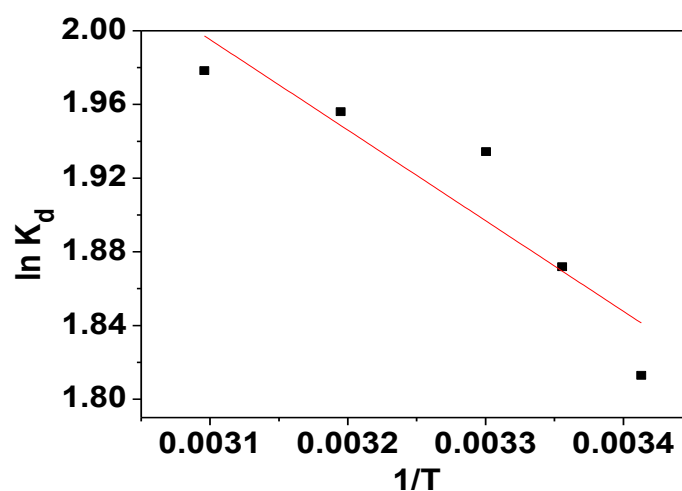


Fig 6.20: Plot of  $\ln K_d$  versus  $1/T$

Table 6.8: Thermodynamic parameters ( $\Delta G^0$ ,  $\Delta H^0$  and  $\Delta S^0$ ) of arsenic adsorption on IOCS

Parameters	Values				
T (K)	293	298	303	313	323
$\Delta G^0$ (kJmol <sup>-1</sup> )	-4.41	-4.55	-4.7	-4.99	-5.28
$\Delta H^0$ (KJmol <sup>-1</sup> )	4.087				
$\Delta S^0$ (KJmol <sup>-1</sup> )	0.029				

In Table 6.8, the positive value of  $\Delta H^\circ$  indicates that the adsorption of arsenic on IOCS is endothermic in nature and the adsorption efficiency of arsenic increases with the increase in temperature and the positive value of  $\Delta S^\circ$  indicates the increased randomness during the adsorption of arsenic and the negative  $\Delta G^\circ$  values for the adsorbent IOCS indicate the favorable and spontaneous adsorption process [22]. It is seen here that adsorption capacity increase with increasing temperature from 20°C to 50°C, so the adsorption of fluoride on CBP is an endothermic process [31].

#### h) Effect of other anions on adsorption of arsenic

Influence of the anions present in water on arsenic adsorption capacity is also very important. In this experiment, arsenic adsorption capacity was determined in the presence of each anion of 50 mg/L in optimum condition. From the Fig 6.21, it has been observed that bromide ions have less effect on the removal of arsenic but the carbonate ions showed highest effect towards the active site and thereby decreasing the sorption capacity of fluoride. The decreasing arsenic adsorption capacity for the adsorbent IOCS follows the order

bromide < chloride < fluoride < sulphate < bicarbonate < carbonate.

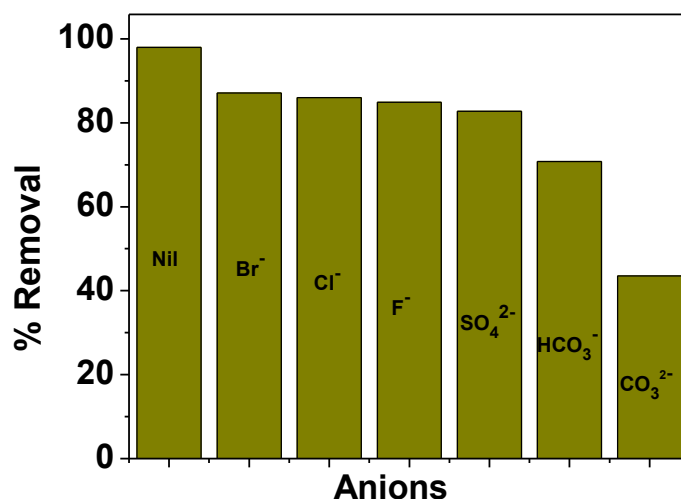


**Fig 6.21: Bar diagram showing the effect of competitive anions on adsorption of arsenic by IOCS**

### 6.3.B.2: Simultaneous adsorption of fluoride and arsenic from real ground water by IOCS

25 mL of each groundwater sample was treated with 0.35 g of IOCS for 45 minutes. Concentration of fluoride and arsenic in the groundwater samples before and after treatment with IOCS are given in Table 6.9 and Fig 6.22. It is seen that amount of both fluoride and arsenic decreases considerably and it is possible to bring the level of fluoride and arsenic below the maximum permissible limits by the BIS [23] which is for fluoride 1.5 mg/L and for arsenic 0.05 mg/L.

**Table 6.9: The amount of fluoride and arsenic of collected real life groundwater before and after treatment with NIOCS**

Parameters		Name of places and serial numbers		
		1. Bosa Kumar gaon	2. Salikihat	3. Borjan
Fluoride	Concentration(mg/L) before adsorption	1.6	1.69	2.92
	Concentration(mg/L) after adsorption	0.995	0.780	1.39
	% Removed	37.81	53.85	52.40
Arsenic	Concentration(mg/L) before adsorption	0.168	0.108	0.077
	Concentration(mg/L) after adsorption	0.006	0.001	0.003
	% Removed	96.43	99.07	96.10



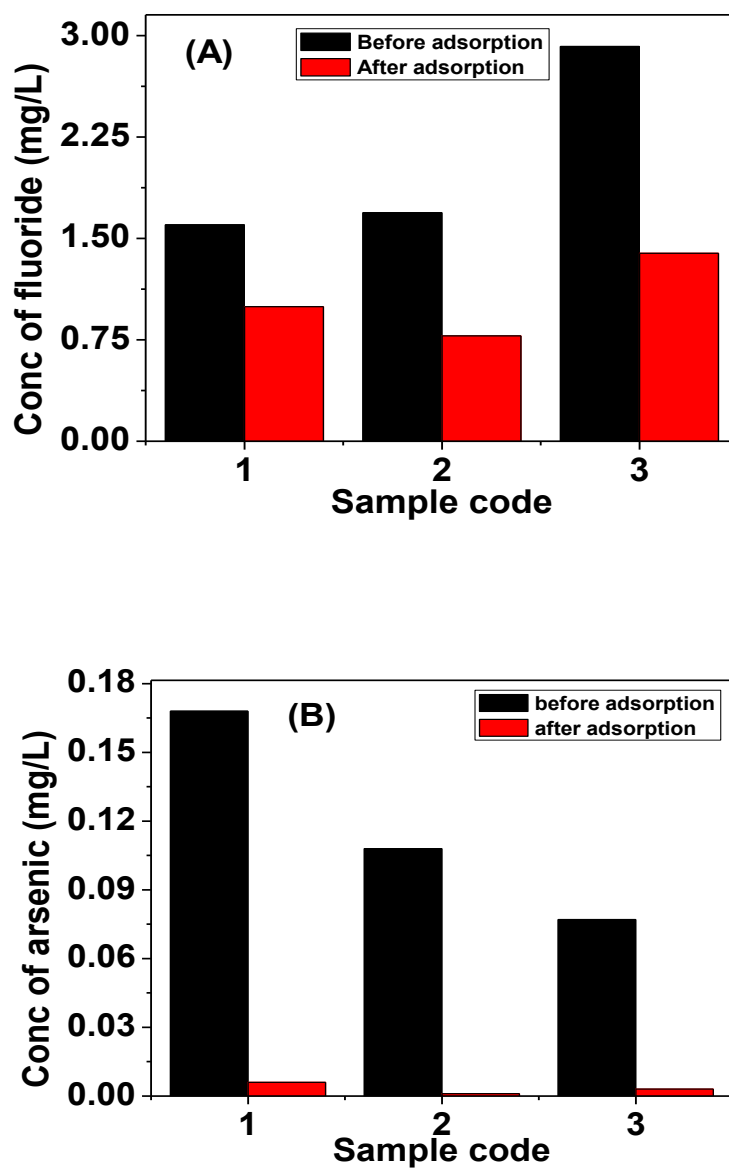


**Fig 6.22: (A) Bar diagram of concentration of fluoride before and after adsorption. (B) Bar diagram of concentration of arsenic before and after adsorption.**

## 6.3.B.3: Some study of IOCS after adsorption of arsenic

## a) Study of FESEM images &amp; EDX spectra

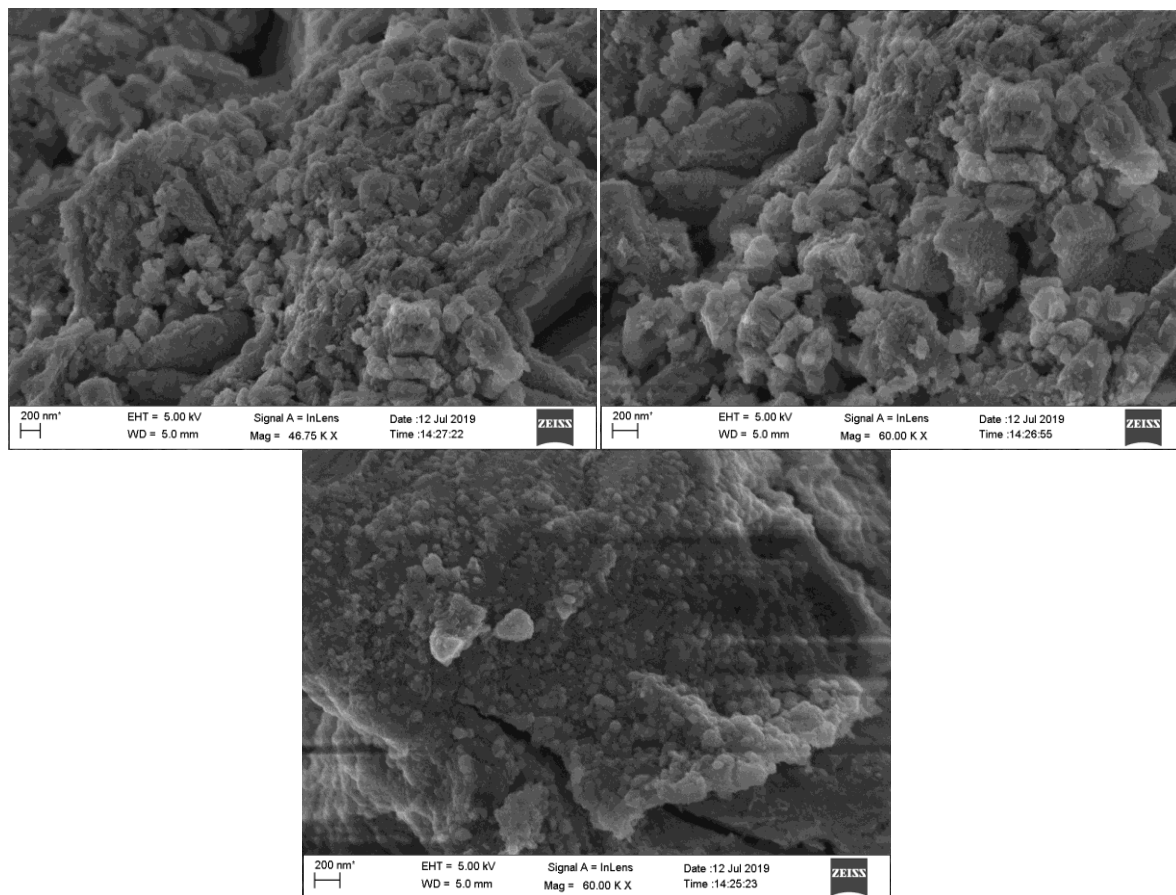


**Fig 6.23: FESEM images of IOCS after adsorption of arsenic**

After arsenic adsorption, the FESEM images of IOCS were taken at various magnifications and shown in the Fig 6.23. It is seen that, the surface of IOCS after adsorption of arsenic is changed from the FESEM images of IOCS (Fig 4.16 of chapter 4). This significant deformation in the structural organization of the IOCS indicates the adsorption of arsenic is a surface phenomenon. This adsorption behavior is also further supported by EDX (Fig 6.24 and Table 6.10) analysis and FTIR study.

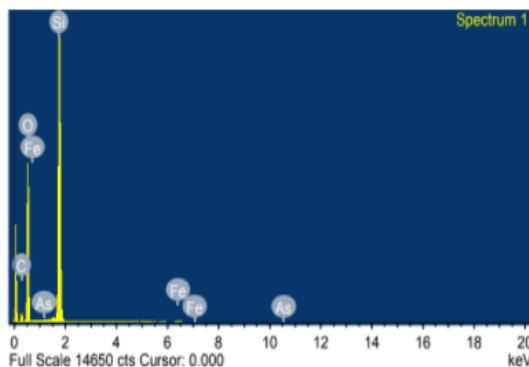


**Fig 6.24: EDX spectra of IOCS after adsorption of arsenic**

Table 6.10: Elemental composition of IOCS from EDX spectra, after adsorption of arsenic

Element	C K	O K	Si K	Fe K	As L	Total
Weight %	12.75	57.83	28.90	0.47	0.04	100.00
Atomic %	18.58	63.26	18.01	0.15	0.01	

### b) Study of FTIR Spectra

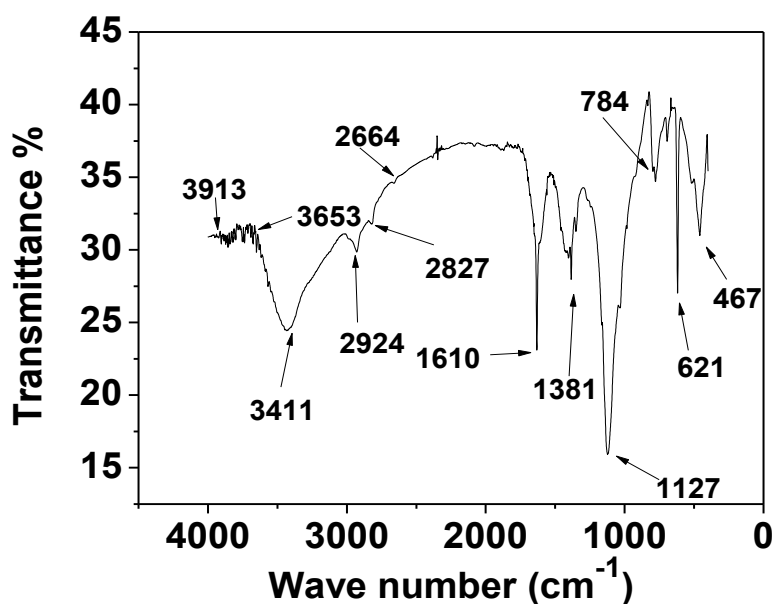


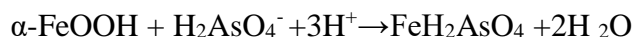
Fig 6.25: FT-IR spectra of IOCS after adsorption of arsenic

By comparing the FT-IR spectra of IOCS before adsorption Fig 4.18(B) (in chapter 4) and after adsorption of arsenic Fig 6.25, it was seen that the peaks of Si-O stretching, Si-O band, Fe-O stretching and O-Si-O band shifted from  $1080\text{ cm}^{-1}$ ,  $777\text{ cm}^{-1}$ ,  $455\text{ cm}^{-1}$  and  $690\text{ cm}^{-1}$  to  $1127\text{ cm}^{-1}$ ,  $784\text{ cm}^{-1}$ ,  $467\text{ cm}^{-1}$  and  $784\text{ cm}^{-1}$ . These shifting of peaks and appearance of strong bands in the spectrum (Fig 6.25) of the adsorbed IOCS indicate the presence of arsenic on the surface of adsorbent IOCS [32].

#### 6.3.B.4: Mechanism of As adsorption on IOCS

As the iron oxide coating on the surface of IOCS is  $\text{FeOOH}$ , so arsenic adsorption mechanism can be explained with the help of Edwards, 1994. According to Edwards the oxyanionic arsenic species arsenate adsorb at the oxyhydroxide surface by forming complexes

with the surface sites. Such specific adsorption may involve replacement of surface hydroxyl groups by the adsorbing ligand as follows [33]:



## 6.4 Conclusion

It is seen that a very simple carbon which is naturally functionalized, obtained at the time of preparation of edible banana alkali by a traditional green method practised by the Assamese people of North East Region of India from the dried stems of *Musa balbisiana*, is a good adsorbent of arsenic. This carbon of banana plant (CBP) has good arsenic removal capacity which is almost 79.9 % on treatment of an optimum dose of 0.35 g CBP in 25 mL of 0.5 mg/L arsenic aqueous solution at pH=7.0. Arsenic sorption kinetic data lead us to conclude that CBP follows the pseudo second order equation and Freundlich adsorption isotherm model. In interfering arsenic adsorption capacity, the presence of carbonate ion in Arsenate spiked synthetic water shows the highest interfering effect and chloride ion shows the least interfering effect. In case of natural ground water also CBP behaves as a good adsorbent for both fluoride and arsenic bearing water. Thus CBP, which is otherwise a waste material can be expected to be a successful cheaper green adsorbent of arsenic for common people in the rural areas. Thereby, also the scope of prospects of rural employment generation and skill modernization in North Eastern Region of India and other places in the world where the traditional practice of edible alkali generation from biomass of *Musa balbisiana* or similar species is known from time immemorial.

In case of IOCS also it is seen that, after iron oxide coating the locally available Kanaighat sand (IOCS) in Golaghat district of Assam become a good adsorbent of arsenic. Various results obtained in the study on adsorbent dose, adsorption isotherm, effect of pH and effect of co-ions shows that the IOCS have good arsenic removal capacity which is almost 98.9 % on treatment of an optimum dose of 0.35 g IOCS in 25 mL of 0.5 mg/L arsenic aqueous solution at pH=7.0. Arsenic sorption kinetic data showed that IOCS follows the pseudo second order equation and Langmuir adsorption isotherm model. Arsenic adsorption capacity of the adsorbent is also affected by other anions. The decreasing arsenic adsorption capacity for the adsorbent IOCS follows the order

bromide < chloride < fluoride < sulphate < bicarbonate < carbonate.

On using natural groundwater, IOCS also shows its good efficiency towards simultaneous adsorption of both fluoride and arsenic. Thus, IOCS can be expected to become a successful cheaper adsorbent for arsenic and fluoride from ground water for common people in the rural areas.

**References**

- [1] Ohta K., and Suzuki M. (1978) Electrothermal atomic-absorption spectrometry of arsenic and its application to environmental samples, *Talanta*, 25-160162.
- [2] Bagla P., Kaiser J. (1996) India's spreading health crisis global arsenic effects. *Science* 274,174-175.
- [3] Jain C.K., and Singh R.D. (2012) Technological options for the removal of arsenic with special reference to South East Asia. *Journal of Environmental Management*. vol. 107, no. 1, pp. 1–18.
- [4] Eatson A. D., Clesceri L. S., Rice E. W., and Greenberg A. E. (2005) Standard methods for the examination of water and wastewater (21st ed., pp. 4–138). Centennial Edition, USA.
- [5] Chetia M., Chatterjee S., Banerjee S., Nath M.J., Singh L., and Srivastava R.B. (2011) Groundwater arsenic contamination in Brahmaputra river basin: A water quality assessment in Golaghat (Assam), India. *Environ Monit Assess*. 173, 371-85.
- [6] Das B., and Mondal N.K. (2011) Calcareous soil as a new adsorbent to remove lead from aqueous solution: equilibrium, kinetic and thermodynamic study. *Universal J Environ Res Technol*. 1:51587.
- [7] Zahra D., Mohammad A.B., Mojdeh R., and Mohammad F. (2013) Adsorption of methylene blue dye from aqueous solution by modified pumice stone: Kinetics and equilibrium studies. *Health scope*. 2(3): 136-144.
- [8] Xu D., Tan X.L., and Wang X.K. (2008) Adsorption of Pb(II) from aqueous solution to MX-80 bentonite: Effect of pH, ionic strength, foreign ions and temperature. *Appl Clay Sci*. 41:37-46.
- [9] Bhomick PC., Supong A., Baruah M., Pongener C., and Sinha D. (2018) Pine cone

- biomass as an efficient precursor for the synthesis of activated biocarbon for adsorption of anionic dye from aqueous solution: isotherm, kinetic, thermodynamic and regeneration studies. *Sustainable Chemistry and Pharmacy*. 10, 41-49.
- [10] Yang L., Wu S., Paul C.J. (2007) Modification of activated carbon by polyaniline for enhanced adsorption of aqueous arsenate. *Ind Eng Chem Res*. 46:2133–2140. doi:10.1021/ie0611352.
- [11] Hao J., Han M.J., Wang C., and Meng X. (2009) Enhanced removal of arsenite from water by a mesoporous hybrid material—Thiol functionalized silica coated activated alumina. *Microporous Mesoporous Mater*. 124:1–7. doi:10.1016/j.micromeso.2009.03.021.
- [12] Schmidt G.T., Vlasova N., Zuzaan D., Kersten M., and Daus B. (2008) Adsorption mechanism of arsenate by zirconyl-functionalized activated carbon. *J Colloid Interface Sci*. 317:228–234. doi: 10.1016/j.jcis.2007.09.012.
- [13] Tiwari A., Dewangana T., and Bajpai A.K. (2008) Removal of toxic As (V) ions by adsorption onto alginate and carboxymethyl cellulose beads. *J Chin Chem Soc*. 55:952–961.
- [14] Schiewer S., and Volesky B. (2000) Biosorption process for heavy metal removal. In: Lovley DR (ed) *Environmental microbe–metal interactions*. ASM Press, Washington. pp 329–362.
- [15] Ranjan D., Talat M., and Hasan S.H. (2009) Rice polish: an alternative to conventional adsorbents for treating arsenic bearing water by upflow column method. *Ind Eng Chem Res* 48:10180–10185. doi:10.1021/ie900877/p.
- [16] Emmanuel K.A., Ramaraju K.A., Rambabu G., and Rao A.V. (2008) Removal of fluoride from drinking water with activated carbons prepared from HNO<sub>3</sub> activation – a comparative study. *Rasayan J Chem*. 1(4):802-818.
- [17] Ozcan A.S., Erdem B., and Ozcan B. (2004) Adsorption of Acid Blue 193 from aqueous solutions onto Na-bentonite and DTMA-bentonite. *J Colloid Interface Sci*. 280: 44–54.
- [18] Alam M.A., Shaikh W. A., · Alam M. O., Bhattacharya T., Chakraborty S., Show B., and Saha I. (2018) Adsorption of As (III) and As (V) from aqueous solution by modified *Cassia fistula* (golden shower) biochar, *Applied Water Science*. 8:198.
- [19] Bansal R.C. and Goyal M. (2005) *Activated carbon adsorption*, CRC Press, Taylor &

- Francis Group, LLC.
- [20] Tan I.A.W., Ahmad A.L., and Hameed B.H. (2008) Adsorption of basic dye on high– surface–area activated carbon prepared from coconut husk: equilibrium, kinetic and thermodynamic studies, *Journal of Hazardous Materials*. 154(1– 3), 337–346.
- [21] Chiban M., Zerbet M., Carja G., and Sinan F. (2012) Application of low–cost adsorbents for arsenic removal: a review, *Journal of Environmental Chemistry and Ecotoxicology*. 4(5), 91–102.
- [22] Saikia J., Sarmah S., Ahmed T.H., Kalita P.J., and Goswamee R.L. (2017) Removal of toxic fluoride ion from water using low cost ceramic nodules prepared from some locally available raw materials of Assam, India. *Journal of Environmental Chemical Engineering*. 5:2488–2497.
- [23] Bureau of Indian Standards (BIS) (1991). 10500:1991, Second Revision ICS No. 13.060.20. [http://www.bis.org.in/sf/fad/FAD25\(2047\)C.pdf](http://www.bis.org.in/sf/fad/FAD25(2047)C.pdf). Accessed 6 Jan 2010.
- [24] Gandhi N., Sirisha D., and Sekhar K.B.C. (2016) Adsorption of fluoride (F-) from aqueous solution by using pineapple (*Ananascomosus*) peel and orange (*Citrus sinensis*) peel powders. *International Journal of Environmental Bioremediation & Biodegradation*. 4(2):55-67.
- [25] Stenkamp V.S., and Benjamin M.M. (1994) Effect of iron oxide coating on sand filtration. *J.AWWA*. 86 (8) 37-50. <http://doi.org/10.1002/j.1551-8833.1994.tb06236.x>.
- [26] Shukla S.C. (2008) Development, safety evaluation and comparative studies of low cost adsorbent technology for arsenic removal from drinking water. Ph D thesis submitted to Hemwatinandan Bahuguna Garhwal University.
- [27] Daifullah A., Yakout S., and Elreefy S. (2007) Adsorption of fluoride in aqueous solutions using KMnO<sub>4</sub>-modified activated carbon derived from steam pyrolysis of rice straw. *Journal of Hazardous Materials*. 147(1-2), 633–643.
- [28] Ananta S., Saumen B., and Vijay V. (2015) Adsorption isotherm, thermodynamic and kinetic study of arsenic (III) on iron oxide coated granular activated charcoal. *Int Res J Environ Sci*. 1(4):64–77.
- [29] Al-Qodah Z., and Lafi W. (2003) Adsorption of reactive dyes using shale oil ash in fixed beds. *J Water Supply Res Technol-AQUA*. 52(3):189–198.
- [30] Rahdar S., Taghavi M., Khaksefidi R., and Ahmadi S. (2019) Adsorption of arsenic (V) from aqueous solution using modified saxaul ash: isotherm and thermodynamic study; *Applied Water Science*. (2019) 9:87; <https://doi.org/10.1007/s13201-019-0974-0>.

- [31] Rincon-Silva N.G., Moreno-Pirajan, J.C., and Giraldo L.G. (2015) Thermodynamic Study of Adsorption of Phenol, 4-Chlorophenol, and 4-Nitrophenol on Activated Carbon Obtained from Eucalyptus Seed. Journal of Chemistry. ID 569403, <http://dx.doi.org/10.1155/2015/569403>
- [32] Yuan T., Luo Q.F., Hu J.Y., Ong S.L., and Ng W.J. (2003) A study on arsenic removal from household drinking water. J. Environ. Sci. Heal A. 38:1731-1744.
- [33] Mohan D., and Pittman Jr. C. U. (2007) Arsenic removal from water/wastewater using adsorbents-A critical review. Journal of Hazardous Materials doi:10.1016/j.jhazmat.2007.01.006.



# **CHAPTER – 7**

## **Summary and Conclusions**

*This chapter represents a brief summary and conclusion of the thesis. The future scope of the study also have been highlighted in this chapter.*

Water is one of the prime necessities of life. Three fourth of the earth is water. In spite of such abundance, amount of safe water availability decreases day by day in all over the world. Although ground water contributes 0.6% of total water resources on the Earth, it is the major and preferred source of drinking water as well as agricultural and industrial use in India. Over the past few decades ground water is getting polluted due to fast growing population, urbanization, industrialization. In many areas ground water is contaminated with toxic materials as well as heavy metals. The ground water sources of various part of Assam are contaminated by arsenic and fluoride. In case of Assam, Jorhat district is highly affected by arsenic, Karbi-Anglong and Nagaon districts are highly affected by fluoride. Golaghat district of Assam is surrounded by these three districts Jorhat, Karbi-Anlong and Nagaon. So, assessment of groundwater quality of Golaghat district and its peripheral areas is very much essential with reference to fluoride and arsenic. Not only the water quality assessment, but removal of fluoride and arsenic from contaminated water is also important.

For assessment of groundwater quality, 247 water samples from the entire Golaghat district and 27 samples from the peripheral areas of the district were collected and analysed by various standard methods. Concentration of fluoride was determined by using Ion Selective Electrode and by Atomic Absorption Spectroscopy method was used for determining the concentration of arsenic. Different statistical techniques were used. From the Piper trilinear diagram analysis, it is found that bicarbonate-type water is predominant. The predominant hydrochemical types are  $\text{HCO}_3^- - \text{Ca}^{2+}$ ,  $\text{HCO}_3^- - \text{Na}^+$  and mixed  $\text{HCO}_3^- - \text{Ca}^{2+} - \text{Na}^+ - \text{Mg}^{2+}$  types. Principal component analysis showed that the both geogenic and anthropogenic sources are responsible for the groundwater quality of Golaghat district in Assam. The present values of pH, TDS,  $\text{HCO}_3^-$ , TH,  $\text{Na}^+$ ,  $\text{NH}_4^+$ ,  $\text{K}^+$ ,  $\text{Ca}^{2+}$  and  $\text{Mg}^{2+}$  of examined groundwater samples of Golaghat district are within the permissible limit; but with respect to fluoride and arsenic groundwater of study areas is not fit for drinking at all as compared to WHO/BIS safe limit. Six out of eight development blocks of Golaghat district are highly contaminated by As, which is several fold higher than that of WHO/BIS safe limit (0.05mg/L). Highest concentration of As was found in Gamariguri block (0.460 mg/L). In Podumoni, Kakodonga, Gamariguri, Kathalguri, Sorupathar and Morangi development

blocks ground water samples were found contaminated with As. Groundwater samples of two development blocks (Gamariguri and Sorupathar) are affected by fluoride and Podumoni block is going to be fluoride affected area as 28% groundwater samples have concentration more than 1.0 mg/L. Although high level of As and  $F^-$  in groundwater is mostly due to natural activities; but it may be due to some human activities, such as mining (As) and use of phosphate pesticides. In case of groundwater quality of peripheral area of Golaghat district is free from fluoride contamination; but the East-South part of Golaghat district (i.e., Jorhat district) is affected by arsenic. Concentration of Fe is also very high (0.8-4.8 mg/L) in entire Golaghat district and since As and Fe is correlated positively, so As might be come from dissolution of As-Fe bearing minerals and the immediately source material is likely to be ferric arsenate (with or without ferric arsenite). Therefore, removal of both fluoride and arsenic from groundwater of Golaghat district is very necessary. The concentration of fluoride of maximum groundwater samples of Golaghat district, mainly for Dergaon, Kathalguri, Kakodonga, Morangi and Bokakhat development block area, are less than 0.5 mg/L.

For fluoride and arsenic removal, although there are so many different methods; but adsorption method is taken as most appropriate due to high efficiency, availability of adsorbent, cost effective and easy to handling. In this study, two locally available materials were taken. One is biocarbon from banana plant and other is coarse river sand collected from Kanaighat.

The biocarbon which is used as adsorbent for fluoride and arsenic in this study, is a waste material produced at the time of preparation of edible alkali from the stem or peel of banana (*Musa Bulbisiana*), which is popularly known as *Kol-Khar* among the Assamese people of North East India. The carbon fraction obtained at the time of preparation of banana alkali, due to exposure to high alkalinity during alkali extraction undergoes a base mediated surface functionalisation. This functionalized waste bio carbon was used as an adsorbent for fluoride and arsenic from ground water and named as CBP in this study.

For another adsorbent, raw material was Kaliani river sand, collected from Kanaighat of Golaghat district. This Kanaighat sand was surface modified with iron oxide for the removal of fluoride and arsenic from water. The surface modified sand was named as Iron Coated Sand (IOCS).

In order to understand the adsorption kinetics of CBP and IOCS, various parameters such as effect of adsorbent dose, concentration of adsorbate solution, pH of adsorbate solution, contact time, temperature, presence of other anions in the fluoride and arsenic adsorption efficiency of CBP and IOCS in the present work.

From the FESEM and FT-IR analysis, it is seen that CBP is a porous adsorbent having oxygen containing surface functional group. Since  $pH_{zpc}$  is 9.6, so CBP can be used as adsorbent for both fluoride and arsenic from aqueous solution at below pH 9.6, i.e., within the pH range of drinking water.

The presence of nano sized ovular grains of iron oxide on the sand surface of KS is very distinct in the FESEM image of IOCS. Since  $pH_{zpc}$  is 7.8, so IOCS can be used as adsorbent for both fluoride and arsenic from aqueous solution within the pH range of drinking water.

The percentage removal of fluoride at pH 6.1 and temperature 30°C by 0.35 g CBP was 66.4% from 25 mL of 5.00 mg/L fluoride solution at 180 minutes. Fluoride adsorption kinetic data showed that CBP follows the pseudo second order equation and Langmuir adsorption isotherm model. In case of arsenic adsorption, 0.35 g CBP showed 79.9% removal capacity from 25 mL of 0.5 mg/L arsenic aqueous solution at pH=7.0 and the pseudo second order kinetic and Freundlich adsorption isotherm is the best fitted model than the Langmuir model.

Iron oxide coated sand (IOCS) have good fluoride removal capacity of 89.5% removal on treatment of an optimum dose of 0.25 g IOCS in 25 mL of 17 mg/L fluoride aqueous solution of pH 6.1 at 45 minutes and temperature 30°C. IOCS have excellent arsenic removal capacity which is almost 98.9 % on treatment of an optimum dose of 0.35 g in 25 mL of 0.5 mg/L arsenic aqueous solution at pH=7.0. Both fluoride and arsenic sorption kinetic data showed that IOCS follows the pseudo second order equation and Langmuir adsorption isotherm model.

Both IOCS and CBP showed good efficiency towards simultaneous adsorption of both fluoride and arsenic from contaminated groundwater. Thus both IOCS and CBP can be expected to be a successful cheaper adsorbent of arsenic and fluoride for common people in the rural areas.

**Future scope of the study**

- In future a survey of dental health assessment of people of the areas (having fluoride concentration  $<0.5$  mg/L), mainly the dental health of the children should be taken up to know whether necessary action need to be taken for supplying fluorinated water is really important.
- Assessment of groundwater quality of Golaghat district in time to time is very necessary.
- Modification of CBP and its application for the treatment of water may bring scope for rural employment generation through micro enterprise development.

# CURRICULUM VITAE

NAME

CHAMPA GOGOI

DATE OF BIRTH

1<sup>st</sup> MARCH 1973

## EDUCATIONAL QUALIFICATION

SL. No	Name of the Examination	Year of Passing	Name of Board/University	Division
1	B.Sc.	1994	Dibrugarh University	Second
2	M.Sc.	1997	Dibrugarh University	First (first class first)

## RESEARCH PUBLICATION

**Gogoi C.**, Saikia, J., Sarmah, S. Sinha, D., and Goswamee, R.L. Removal of Fluoride from Water by Locally Available Sand Modified with a Coating of Iron Oxides. *Water Air Soil Pollut* **229**, 118, 2018. (Springer, IF: 1.769)

Bhomick P.C., Supong A., Baruah M., Pongener C., **Gogoi C.**, and Sinha D. Alizarin Red S adsorption onto biomass-based activated carbon: optimization of adsorption process parameters using Taguchi experimental design. *International Journal of Environmental Science and Technology*. 2019 (Springer, IF: 2.031)

Saikia J., Allou N.B., Sarmah S., Bordoloi P., **Gogoi C.**, and Goswamee R.L. Reductant free synthesis of silver-carbon nanocomposite using low temperature carbonized *Ipomoea carnea* stem carbon and study of its antibacterial property. *J. Environ. Chem. Eng.* 6(2018)4226-4235

Saikia P., Gogoi C., and Goswamee R.L.

## Book Chapters Published

**Gogoi C.**, Sinha, D., and Goswamee, R.L. Water quality evaluation of Gomariguri Block of Golaghat district of Assam, India with reference to arsenic and fluoride. *Conservation and Preservation of Bioresources in North-East India*. Edited by Mr.

Hari Prasad Nath, Mr. Phalgun Chetia, Mr. Pankaj Kalita. 126-135, 2020, ISBN No-978-8-941574-0-3

### **Papers to be communicated**

**Gogoi C.,** Bhomick P.C., Saikia, J., Sinha, D., and Goswamee, R.L. Functionalised carbon from *Musa Balbisiana* stems - a byproduct of edible alkali preparation and a suitable adsorbent for arsenic from contaminated water.

**Gogoi C.,** Kalita P.J., Saikia P., Sinha, D., and Goswamee, R.L. Assessment of ground water quality of the Golaghat district of Assam, India and its peripheral area using multivariate statistical technique with special reference to the presence of higher levels of fluoride and arsenic.

### **CONFERENCES/SEMINARS/WORKSHOPS ATTENDED**

Presented a Paper titled, “Water quality evaluation of Gamariguri Block of Golaghat District of Assam, India with reference to Arsenic and Fluoride” in National Seminar on Conservation and Preservation of Bioresources in North-East India, June 28<sup>th</sup> -29<sup>th</sup>, 2019, Department of Chemistry, C.N.B. College, Bokakhat, Assam.

Presented a Paper titled, “Removal of Toxic Arsenic from Water by A Functionalised Locally Available Carbon Banana Peel Ash (*kol-khar sai*)” in NSCIR-2018, November 9<sup>th</sup> -10<sup>th</sup>. Organized by Department of Chemistry, Nagaland University.

Presented a Paper titled, “Removal of Toxic Fluoride from Water by A Functionalised Locally Available Carbon Banana Peel Ash (*kol-khar sai*)” in UGC sponsored National Seminar on RTERCP-2017, September 22<sup>nd</sup> -23<sup>rd</sup>, Department of Chemistry, D.R. College, Golaghat, Assam.

Presented a Paper titled, “Removal of fluoride from water by functionalized carbon obtained during extraction of edible alkali from *Musa bulbasiana* (*Bhim Kol*) Stem”. International Conference on ICETNMST-2017, January 4<sup>th</sup> -6<sup>th</sup>, Department of Chemistry, Nagaland University.

Presented a Paper titled, “Modification of Locally Available Sand by Coating with Nano

Iron Oxide for Its Possible Use in Water Defluoridation” in International Conference on Advances in Nanotechnology, 9<sup>th</sup> - 13<sup>th</sup> January 2017. Don Bosco University, Guwahati.

Presented a Paper titled, “Preparation of nano iron oxide coated Kanaighat sand,

its characterization and potential application for defluoridation from water” in International Conference on Emerging Trends in Nanomaterials Science and Technology, 4<sup>th</sup> -6<sup>th</sup> January, 2017. Organized by department o Science and Humanities, NIT, Nagaland.

Attended Workshop on “Sensitization Workshop on DST Women Scientist Scheme”.

Jointly organized by DST, New Delhi and Nagaland University at SASRD Medziphema, 4<sup>th</sup> -5<sup>th</sup>, 2019

Attended Workshop on “National Thematic Workshop on Advances in

Nanostructured Materials: Applications and Persepectives [ANMAP]”, The Assam Kaziranga University, Assam. June 1-2, 2016